

https://dspace.org/

Synthesis, characterization and catalytic properties of silicoaluminophosphate microporous molecular sieves

Ramaripa, Phuti Suzan

2014-02-06
http://hdl.handle.net10539/13681

Downloaded from a DSpace repository. https://dspace.org/

SYNTHESIS, CHARACTERIZATION AND CATALYTIC PROPERTIES OF SILICOALUMINOPHOSPHATE MICROPOROUS MOLECULAR SIEVES

BY

PHUTI SUZAN RAMARIPA

Submitted in the fulfilment of the requirements for the degree of

Masters of Science in the Faculty of Science

Department of Chemistry

University of the Witwatersrand

Private Bag x 03

Wits

2050

South Africa

Supervisors: Professor: Michael S Scurrell

Co-Supervisor: Professor Malose Peter Mokhonoana (UL)

August 2013

DECLARATION

I declare that SYNTHESIS, CHARACTERISATION, AND CATALYTIC PROPERTIES OF MICROPOROUS SILICOALUMINOPHOSPHATE MOLECULAR SIEVES is my own, unaided work under the supervision of Prof. Michael Scurrell and Prof. Malose Peter Mokhonoana. It is being submitted for the degree of Masters of Science in the University of Witwatersrand, Johannesburg. It has not been submitted for any degree or examination in any other university.

Name: Phuti Suzan Ramaripa (Mrs)

_____

(Signature of Candidate)

_____ day of _____ 20_____in _____

ABSTRACT

In this study, an attempt was made to synthesis SAPO-34 using piperidine as structure directing agent/ template. The synthesis parameters such as crystallization temperature, crystallization time, phosphorus content and silicon content, as well as Na, Fe, Co and Ni impregnation were varied. The resulting materials were characterized by a combination of physicochemical techniques such as XRD, SEM spectroscopy, NH_3-TPD and SS NMR spectroscopy. The peaks at 2θ = 9.9^0, 13.0^0, 15.0^0, 18.0^0, 21^0, 26^0, 32^0 on XRD patterns confirmed the presence of SAPO-34 phase, extra peaks at 2θ = 7.9 ^{0}, 20 ^{0}, 23 ^{0}and 26 of XRD patterns indicated the existence of SAPO-5. Most of the samples of the molecular sieves comprised SAPO-5 and SAPO-34. The SAPO-5 materials were the main domain and SAPO-34 materials were less. The two peaks that appeared in the temperature regions between the ranges 190-250 ^{0}C and 340-380 ^{0}C that were assigned for weak and medium Brønsted acid site on NH_3-TPD profiles. The SS NMR spectroscopy and XRD patterns confirmed a SAPO-34 phase with amorphous phase in a sample prepared with SiO_2/Al_2O_3 = 2.4 molar ratio at 200 ºC for 5 days. The NH_3-TPD profile and SS NMR spectroscopy for this molecular sieve confirmed the presence of weak and strong acid sites assigned to P-OH-Al and Si-OH-Al hydroxyl groups. All the molecular sieves were used in MTO reaction. The selectivity to ethylene and propylene on the molecular sieves prepared at 190 ^{0}C for 5 days is better than the selectivity to ethylene and propylene on the molecular sieve synthesized at 170 ^{0}C, 200 ^{0}C and 210 ^{0}C for 5 days. Molecular sieve prepared at 200 ^{0}C for 4 days was better in ethylene and propylene selectivity than the molecular sieve prepared at 200 ^{0}C for 2-3 days, 5-6 days. Methane and DME were the main products on most of the molecular sieves. Methane, ethylene and propylene and some impurities were the products on molecular sieve prepared with SiO_2/Al_2O_3 = 2.4 molar ratio in MTO reaction. The conversions of DME towards light olefins were extremely low. Na-SAPO reduced methane, and improved ethylene and propylene selectivity. Non-modified and Co-SAPO molecular sieves improved the selectivity towards light olefins. Piperidine can be used as a template to synthesis SAPO-34 molecular sieve within a short period of five days. SAPO-5 was synthesized instead of SAPO, and

DME was the main product instead of light olefins on the molecular sieves during MTO reactions.

DEDICATIONS

To my husband LESIBA THOMAS RAMARIPA, my daughters MASECHABA JEANETTE, PILETJIE DINA AND RAMOKONE MOITSHELA RAMARIPA my granddaughter MOTHEPANA PONTSHO RAMARIPA whose love inspiration and endless support made this dissertation possible.

This dissertation is dedicated to my late mother and father EGNES MEISIE RAMADIMETSA AND DANIEL PILETJIE TLOU RAPUDI.

ACKNOWLEDGEMENTS

I would like to thank my supervisors Prof Michael S Scurrell and Prof Peter Malose Mokhonoana for introducing me to the world of catalysis and fuel energy. I really enjoyed working under your supervision. Thank you for the excellent ideas and advises that you have provided for my dissertation. To my assistant supervisor Prof Neil Coville thank you for being patient and contribute in to the corrections of my work in the absence of my supervisor Prof Mike Scurrell due to the illness. To CATOMAT group, thank you guys for all the assistant and being such a friendly group. To Colleen Coutts thank you for being there in the arrangements of the accommodation during my visit at Wits. To the former EDP and Chemistry staff members' thank you for the support and encouragement you gave me. To Dr Phokoane Ramatsetse thank you for the SEM and PXRD data. To Mr Basil Chassaulas and Themba Tshabala thank you for the technical support. To SANERI and University of Limpopo thank you for the financial support.

TABLE CONTENTS

CONTENTS	PAGE
DECLARATION	II
ABSTRACT	III
ACKNOWLEDGEMENT	IV
LIST OF FIGURES	
LIST OF TABLE	
CHAPTER ONE – INTRODUCTION	1
1. 1 Background	1
1.1.1 Rationale of the study	1
1.1.2 Problem statement	1
1.1.3 Aim	1
1.1.4 Objectives	2
1.1.5 Research Approach	2
1.1.6 Dissertation outline	2
1.2 Literature Review	3
1.2.1 General introduction	3
1.2.2. History of Zeolites	5
1.2.3 Methanol conversion to olefins	5
1.2 .4 Zeolite ZSM-5	6
1.2.5 SAPO-34	7
1.2.5.1 The structural features of SAPO-34	7
1.2.5.2 Impregnation of SAPO-34	10
1.2.5.3 The synthesis of SAPO-34	12

1.2.5.4 The effect of templates in the synthesis of SAPO-34 12

1.2.6 Characterization techniques for SAPO 34 based materials 13

1.2.6.1 X-ray diffraction (XRD) 13

1.2.6.2 Scanning electrons microscopy (SEM) 14

1.2.6.3 Ammonia temperature programmed desorption (NH_3-TPD) 15

1.2.6.4 SS NMR Spectroscopy. 15

1.2.7 The properties of SAPO-34 16

1.2.7.1 The acidity of SAPO-34 16

1.2.7.2 Activity of SAPO-34 17

1.2.7.3 Selectivity of SAPO-34 18

CHAPTER TWO - METHODS AND MATERIALS 19

2 SYNTHESIS OF SAPO. 19

2.1 Experimental 19

2.1.1 Chemicals and materials 19

2.1.2 General method 22

2.1.2.1 Method 1 22

2.2.1.2 Method 2 25

2.2 Characterization 26

2.2 1 X-ray diffraction 27

2.2.2 Solid State Nuclear Magnetic Resonance spectroscopy 27

2.2.3. Ammonia temperature programmed desorption 27

2.2.4 Scanning electron microscopy 27

2.3 Catalytic test 28

CHAPTER THREE - Catalyst characterization 30

3.1 X-ray Diffraction Patterns 30

3.1.1Introduction 30

3.1.2 Results and discussion 31

3.1.2.1. Influence of crystallization temperature on the formation of molecular sieve SAPO. 31

3.1.2.2. Influence of crystallization time on the synthesis of molecular sieve. 33

3.1.2.3 Influence of the P content in the synthesis gel on the synthesis of molecular sieve SAPO. 34

3.1.2.4 The effects of Na^+ as a promoter of SAPO molecular sieve. 35

3.1.2.5 Influence of the Si content in the synthesis gel on the formation of molecular sieve SAPO. 36

3.1.2.6 The effects of modified SAPO 39

3.1.2.7. The influence of templates 40

3. 2 SEM spectroscopy 42

3.2.1 Introduction 42

3.2.2 Results and discussion 42

3.3 NH_3-TPD 51

3.3.1 Introduction 51

3.3.2 Results and discussion 51

3.3.2.1 Phosphorus content 51

3.3.2.2 Silicon content 53

3.3.2.3 Templates 53

3.4. Solid state NMR spectroscopy (^{29}Si, ^{27}Al and ^{31}P) 54

3.4.1 Introduction 54

3.4.2 Results and discussions 55

3.4.2.1 Solid states ^{29}Si NMR spectroscopy 55

3.4.2.2 Solid states ^{27}Al NMR spectroscopy 56

3.4.2.3 Solid states NMR ^{31}P spectroscopy 57

3.5 Summary and Conclusions 59

CHAPTER FOUR – Catalytic Test 60

4.1 Introduction 60

4.2 Results and Discussion 62

4.2.1 The effects of crystallization temperature on the MTO reactions 62

4.2.1.1 The effects of crystallization temperature on % methanol Conversion 63

4.2.1.2 The effects of crystallization temperature on light olefins 64

4.2.1.3 The effects of crystallization temperature on product distribution of hydrocarbons 65

4.2.1.4 The relationship between the characterization of SAPO molecular sieve and the MTO reaction 67

4.2.1.5 Conclusions 68

4.2.2 The effects of crystallization time 68

4.2.2.1 The effects of crystallization time on % methanol conversion 70

4.2.2.2 The effects of crystallization time on light olefins 71

4.2.2.3 The effects of crystallization time on product distribution of hydrocarbons 74

4.2.2.4 The relationship between the characterization of SAPO molecular sieve and the MTO reaction 82

4.2.2.5 Conclusions 83

4.2.3 The influence of phosphate content on methanol conversion 83

4.2.3.1 The effects of phosphorus on % methanol conversion 84

4.2.3.2 The effects of phosphorous contents on light olefins 85

4.2.3.3 The effects of phosphorus contents on product distribution of hydrocarbons 86

4.2.3 4 The relationship between the characterization of SAPO molecular sieve and the MTO reaction 88

4.2.3.5 Conclusions 88

4.2.4. The effects of the promoter (Na^+) in SAPO 89

4.2.4.1 The effects of the promoter on % methanol conversion 90

4.2.4.2 The effects of promoter (Na^+) on light olefins 91

4.2.4.3 The effects of promoter (Na^+) on product distribution of Hydrocarbons 93

4.2.4.4 The relationship between the characterizations of SAPO molecular sieve on the MTO reaction 98

4.2.4.5 Conclusions 98

4.2.5 The effect of silicon content 99

4.2.5.1 The effects of silicon content on % methanol conversion 100

4.2.5.2 The effects of silicon contents on light olefins 101

4.2.5.3 The effects of silicon contents on product distribution of Hydrocarbons 104

4.2.5.4 The relationship between the characterization of SAPO molecular sieve and the MTO reaction 106

4.2.5.5 Conclusions 106

4.2.6. The effect of modified and unmodified molecular sieve 107

4.2.6.1 The effects of modified and non-modified on % methanol Conversion 108

4.2.6.2 The effects of modified and non-modified on light olefins 109

4.2.6.3 The effects of modified and no modified on product distribution of hydrocarbons 113

4.2.6.4 The relationship between the characterizations of SAPO molecular sieve and the MTO reaction 119

4.2.6.5 Conclusions 119

4.2.7. The use of structure directing agent 119

4.2.7.1 The effects of SDA on % methanol conversion 120

4.2.7.2 The effects of SDA on light olefins 121

4.2.7.3 The effects of SDA on product distribution of Hydrocarbons 123

4.2.7.4 The relationship between the characterizations of SAPO molecular sieve and the MTO reaction 124

4.2.7.5 Conclusions 125

4.3. Summary and conclusions 125

CHAPTER FIVE - General Conclusions 127

5.1. Conclusions 127

5.2. Recommendations for the future work 129

REFERENCES 130

APPENDIX A XRD PATTERNS FOR SAPO 138

APPENDIX B SEM FOR SAPO 140

APPENDIX C STANDARD FOR HYDROCARBONS 142

APPENDIX D FORMULAS FOR CALCULATIONS 151

LIST OF FIGURES

Figure 1.1 Ethylene demand distribution 2008 3

Figure 1.2 Propylene demand distribution 2008 4

Figure 1.3 Butylene demand distribution 2008 4

Figure 1.4 The pore structure of ZSM-5 7

Figure 1.5 The pore structure of SAPO-34 8

Figure 1.6 (a) AlPO4 and (b) SAPO-34 9

Figure 1.7 Pore structures of different SAPOs 10

Figure 1.8 Substitution of one Si with Al in pure silicate and substitution of P with Si in aluminophosphate 17

Figure 2.1 Gel preparation 23

Figure 2.2 An autoclave for synthesis of SAPO 24

Figure 2.3 A flow diagram for MTO reactor system 29

Figure 3.1 X-ray diffractions for SAPO-34 (References) 30

Figure 3.2 XRD patterns of SAPO-34 for the synthesis temperature ranges (170–210) ºC within 5 days and calcined at 550 ^{0}C for 3hours. 32

Figure 3.3 X-ray powder diffraction patterns for SAPO molecular sieves, synthesized at 200 ^{0}C within different days (1 - 6) days, calcined at 550 ^{0}C. 33

Figure 3.4 XRD patterns of SAPO molecular sieves synthesized at the mole ratio range from 0.3 to 0.6 P_2O_5/Al_2O_3 for 5 days at 200 ºC, calcined at 550 ^{0}C for 3 hours). 34

Figure 3.5 XRD patterns for SAPO molecular sieves with sodium added as a promoter. 35

Figure 3.6 The XRD patterns for SAPO molecular sieves synthesized at the SiO_2/Al_2O_3 mole ratio range 0.6 to 2.4 for 5 days at 200 ºC, calcined at 550 ^{0}C for 3 hours. 38

Figure 3.7 The XRD patterns for unmodified and modified SAPO catalyst 39

Figure 3.8 XRD patterns for SAPO catalysts prepared using piperidine and TEAOH templates. 41

Figure 3.9 (a)-(c) SEM images for SAPO synthesized within 3 days at different magnifications. (a) magnification of 1000, (b) magnification of 2000 and (c) magnification of 5000. 43

Figure 3.10 (a)-(d) SEM images for SAPO synthesized within 5 days at different magnifications. (a) magnification 500, (b) magnification 1000, (c) magnification 1500. And (d) magnification 10000 44

Figure .3.11 (a)-(d) SEM image for SAPO synthesized at 200 ºC for 5 days with the mole ratio of P_2O_5/Al_2O_3 = 0.3 at different magnifications. (a) magnification 2000, (b) magnification 4000, (c) magnification 5000 and (d) magnification 7500. 45

Figure 3.12 (a)-(d) SEM image for SAPO synthesized at 200 ºC for 5 days with the mole ratio of SiO_2/Al_2O_3 = 2.4. (a) magnification 30, (b) magnification 100, (c) magnification 5000 and (d) magnification 7500. 46

Figure 3.13 (a)-(d) SEM image for SAPO synthesized using TEAOH as a template. at 200 ºC for 5 days. (a) magnification 2000, (b) magnification 3000, (c) magnification 4000 and (d) magnification 10000. 47

Figure 3.14 (a)-(d) SEM image for Fe-SAPO synthesized using piperdine as a template. at 200 ºC for 5 days at different magnification. (a) magnification 2000, (b) magnification 7500, (c) magnification 10000 and (d) magnification 15000. 48

Figure .3.15 (a)-(d) SEM image for Co-SAPO synthesized using piperidine as a template at 200 ºC for 5 days at different magnification. (a) magnification 250, (b) magnification 4000. (c) magnification 5000 and (d) magnification 7500. 49

Figure 3.16 a)-(d) SEM image for Ni-SAPO synthesized using piperidine as a template at 200 ºC for 5 days at different magnification. (a) Magnification 2000, (b) magnification 3000. (c) magnification 3000 and (d) magnification 4000. 50

Figure 3.17 The NH_3-TPD profile for lower and higher phosphorus content SAPO catalysts. 52

Figure 3.18 The NH3-TPD spectra for lower and higher silicon content SAPO 53

Figure 3.19 The NH_3-TPD profiles for SAPO made with Piperidine and TEAOH 54

Figure 3.20 ^{29}Si SS NMR spectra of SAPO low and high silicon content 55

Figure 3.21 ^{27}Al SS NMR spectra of SAPO catalyst low and high silicon contents. 56

Figure 3.22 ^{31}P SS NMR spectrum of SAPO low and high silicon content 57

Figure 4.1 The effect of crystallization temperature of SAPO molecular sieve (PS-01-PS-04) on % methanol conversion at 400 ºC for 1 hour. 64

Figure 4.2 The effect of crystallization temperature of SAPO molecular sieve on light olefins selectivity at 400 ºC for 1 hour. 64

Figure 4.3 The effect of crystallization temperature of SAPO molecular sieve PS-01 – PS-04 on product distribution of hydrocarbons from 0 - 100 % at 400 ºC reactor temperature for 1 hour. 65

Figure 4.4 The effect of crystallization temperature of SAPO molecular sieve on product distribution of hydrocarbons from 0 -100 % at 400 ºC for 1 hour. 67

Figure 4.5 The effect of crystallization time of SAPO molecular sieve on % methanol conversion at 400 ºC for 5 hour. 71

Figure 4.6 The effect of crystallization time of SAPO molecular sieve on ethylene selectivity at 400 ºC for 5 hour. 72

Figure 4.7 The effects of crystallization time of SAPO-34 molecular sieve on propylene selectivity at 400 ºC for 5 hour. 73

Figure 4.8 The effect of crystallization time of SAPO molecular sieve on butylenes selectivity at 400 ºC for 5 hour. 74

Figure 4.9 The effect of crystallization time of SAPO molecular sieve of sample PS-07 synthesized for 3 days on product distribution of hydrocarbons from 0 - 100 % at 400 ºC reactor temperature for 5 hour. 75

Figure 4.10 The effect of crystallization time of SAPO molecular sieve of sample PS-07 synthesized for 3 days on product distribution of hydrocarbons from 0 - 5 % at 400 ºC reactor temperature for 5 hour. 76

Figure 4.11 The effect of crystallization time of SAPO-34 molecular sieve synthesized for 4 days on product distribution of hydrocarbons from 0 - 100 % at 400 ºC reactor temperature for 5 hour. 77

Figure 4.12 The effect of crystallization temperature of SAPO molecular sieve of sample PS-08 synthesized for 4 days on product distribution of hydrocarbons

from 0 - 10 % at 400 ºC reactor temperature for 1 hour. 77

Figure 4.13 The effect of crystallization time of SAPO molecular sieve of sample PS-03 synthesized for 5 days on product distribution of hydrocarbons from 0 - 100 % at 400 ºC reactor temperature for 5 hour. 78

Figure 4.14 The effect of crystallization time of SAPO molecular sieve of sample PS-03 synthesized for 5 days on product distribution of hydrocarbons from 0 - 10 % at 400 ºC reactor temperature for 5 hour. 79

Figure 4.15 The effect of crystallization time of SAPO molecular sieve of sample PS-09 synthesized for 6 days on product distribution of hydrocarbons from 0 - 100 % at 400 ºC reactor temperature for 5 hour. 80

Figure 4.16 The effect of crystallization time of SAPO molecular sieve of sample PS-09 synthesized for 6 days on product distribution of hydrocarbons from 0 - 100 % at 400 ºC reactor temperature for 5 hour. 81

Figure 4.17 The % methanol conversions vs. P_2O_5/Al_2O_3 ratio of the SAPO molecular sieve for samples PS-10 – PS-11, PS-03, and PS-07. 85

Figure 4.18 The effects of phosphorus content of SAPO molecular sieve on light olefins selectivity within 1 hour at reaction temperature of 400 ºC. 86

Figure 4.19 The effects of phosphorus content of SAPOs molecular sieve on the product distribution of hydrocarbons ranges from 0 % to 100 %. 87

Figure 4.20 The effects of phosphorus content on the product distribution of hydrocarbons range from 0 % to 10 %. 87

Figure 4.21 The % methanol conversions vs. time on stream of the molecular sieve with P_2O_5/Al_2O_3 ratio of 0.3 plus sodium oxide. 91

Figure 4.22 The effects of addition of sodium content to molecular sieve on ethylene

selectivity. 92

Figure 4.23 The effects of addition of sodium content to molecular sieve on propylene selectivity. 93

Figure 4.24 The effect of the addition of sodium oxide (0.013 mol) in the SAPO molecular sieve with the P_2O_5/Al_2O_3 molar ratio of 0.3 on product distribution of hydrocarbons from 0 - 100 % at 400 ºC reactor temperature for 1 hour. 94

Figure 4.25 The effect of the addition of sodium oxide (0.013 mol) in the SAPO molecular sieve with the P_2O_5/Al_2O_3 mole ratio of 0.3 on product distribution of hydrocarbons from 0 - 5 % at 400 ºC reactor temperature for 1 hour. 95

Figure 4.26 The effect of the addition of sodium oxide (0.200 mol) in the SAPO molecular sieve with the P_2O_5/Al_2O_3 molar ratio of 0.3 on product distribution of hydrocarbons from 0 - 100 % at 400 ºC reactor temperature for 1 hour. 96

Figure 4.27 The effect of the addition of sodium oxide (0.200 mol) in the SAPO molecular sieve with the P_2O_5/Al_2O_3 mole ratio of 0.3 on product distribution of hydrocarbons from 0 - 5 % at 400 ºC reactor temperature for 1 hour. 97

Figure 4.28 The % methanol conversion vs. Time on stream for molecular sieve with high and low silicon content. 101

Figure 4.29 The ethylene selectivity vs. time on steam on the molecular sieve with low and high silicon content 102

Figure 4.30 The propylene selectivity vs. time on steam on molecular sieve with low and high silicon contents. 103

Figure 4.31 The effects of high content of SAPO molecular sieve on the product distribution of hydrocarbons ranges from 0 % to 100 %. 104

Figure 4.32 The effects of high silicon content of SAPO molecular sieve on

the product distribution of hydrocarbons ranges from 0 - 5 %. 105

Figure 4.33 The methanol conversion vs. time on stream of modified and unmodified SAPO molecular sieve. 110

Figure 4.34 The ethylene selectivity vs. time on steam on modified and non-modified SAPO molecular sieve. 111

Figure 4.35 The propylene selectivity vs. time on steam on modified and unmodified SAPO molecular sieve. 112

Figure 4.36 The product distribution of hydrocarbons on non-modified molecular sieve ranges from 0 -100 % after 5 hours. 113

Figure 4.37 The product distribution of hydrocarbons on SAPO molecular sieve from the ranges 0 – 5 % 114

Figure 4.38 The product distribution of hydrocarbons on Fe-SAPO molecular sieve. 114

Figure 4.39 The product distribution of hydrocarbons on Fe-SAPO molecular sieve. 115

Figure 4.40 The product distribution of hydrocarbons on Co-SAPO molecular sieve. 116

Figure 4.41 The product distribution of hydrocarbons on Co-SAPO molecular sieve. 116

Figure 4.42 The product distribution of hydrocarbons on Ni-SAPO molecular sieve. 117

Figure 4.43 The product distribution of hydrocarbons on Ni--SAPO molecular sieve. 117

Figure 4.44 Methanol conversions vs. Time on stream over molecular sieves prepared

with different structure directing agents 121

Figure 4.45 The influence of propylene selectivity, on the catalysts synthesized with piperidine and TEAOH structure directing agent. 122

Figure 4.46. The product distribution of hydrocarbons on MTO reactions over SAPO with different structure directing agent s from 0 – 100 % for 5 hours 123

Figure 4.47. The product distribution of hydrocarbons on MTO reactions over SAPO with different structure directing agent s from 0 – 5 % for 5 hours 124

LIST OF TABLES

TABLE PAGE

Table 2.1 Chemicals and materials 19

Table 2.2 Equipments 20

Table 2.3 Synthesized samples for SAPOs prepared at different crystallization temperature. 20

Table 2.4. Synthesized samples for SAPOs prepared at different crystallization time. 21

Table 2.5. Synthesized samples for SAPOs prepared with different phosphorus contents. 21

Table2.6 Synthesized samples for SAPOs with high and low sodium contents. 22

Table 2.7. Synthesized samples for SAPOs with high and low silicon contents. 22

Table 2.8. Synthesized samples for SAPO containing metals. 25

Table 2.9 List of instruments 26

Table 4 1 Response factors (propane equivalent) determined by TÜV-Nord using two J.U.M. FID´s, Model VE 7, the FID 2 was tested 9 months after the FID 1. 61

Table 4.2 Retention time and response factor for hydrocarbons. 62

Table 4.3 Summary of % methanol conversion, particle size and products distribution of hydrocarbons of catalysts synthesized at temperature ranges from 170 ^{o}C-210 ^{o}C. 63

Table 4.4 Summary of % methanol conversion, particle size and products distribution of hydrocarbons of catalysts synthesized in different days (2-6). 69

Table 4.5 % Methanol conversion, the particle size and the product distribution of the molecular sieve with different P_2O_5/Al_2O_3 molar ratios, reaction temperature and the product distribution of hydrocarbons. 84

Table 4.6 The % Methanol conversion, the particle size and the product distribution of the molecular sieve with P_2O_5/Al_2O_3 mole ratios plus sodium oxide, reaction temperature and the product distribution of hydrocarbons. 90

Table 4.7 The % Methanol conversion, % XRD Crystallinity and the particle size of the molecular sieve with SiO_2/Al_2O_3 mole ratios, reaction temperature and the product distribution of hydrocarbons. 99

Table 4.8 The % Methanol conversion and the particle size of the molecular sieve with modified and non-modified, reaction temperature and the product distribution of hydrocarbons. 107

Table 4.9 The particle size of the catalysts, % methanol conversion and products distribution of hydrocarbons for five hours reaction time for structure directing agents. 119

ABBRIVIATIONS AND ACRYNOMY

$AgNO_3$ – Silver nitrate

$Al(OH)_3$ - Aluminium hydroxide

AlO_4 - Aluminium oxide

$AlPO_4$ – Aluminiumphosphate

$C_2^=$ - Ethylene

$C_3^=$ - propylene

$C_4^=$ - butylene

Co - cobalt

$Cocl_3.6H_2O$ - Cobalteous chloride hexahydrate

Co-SAPO-34 – Cobalt silicoaluminophosphate-34

DME - Dimethylether

EDC – Ethylene dichloride

$Fecl_3.6H_2O$ - Iron chloride hexahydrate

Fe-SAPO-34 – Iron silicoaluminophosphate-34

H_2O - Water

H_2SO_4 - Sulphuric acid

HCl - Hydrochloric acid

HDPE – High density polyethylene

HMDA – Hexamethylenediamine

LDPE – Low density polyethylene

LLDPE – Linear low density polyethylene

MeAPO – Metal aluminophosphate

Mg - Magnesium

MnAPSO-34 – Manganese silicoalumonophosphate-34

MTG - Methanol to gasoline

MTH - Methanol to hydrocarbons

MTO – Methanol to olefins

NaOH - Sodium hydroxide

NH_3-TPD - Ammonia temperature programmed desorption

NH_4C - Ammonium Chloride

NiCL3 - Nickel chloride hexahydrate

Ni-SAPO-34 – Nickel silicoaluminophosphate-34

PIP - Piperidine

SAPO-34 – Silicoaluminophosphate-34

SB Latex – Styrene butadiene latex

SB Rubber – Styrene butadiene rubber

SDA – Structure directing agent

SEM - Scanning electrons microscopes

SiO_2 - Silica

SS NMR Spectroscopy – Solid states nuclear magnetic resonance

TEA - Triethylamine

TEAOH - Tetraethylammonium hydroxide

TO_4 - Titanium oxide

VAM – Vinyl acetate monomer

XRD - X-ray diffraction

Zn - Zinc

ZSM-5 - Zeolite Socony Mobil-5

CHAPTER ONE-INTRODUCTION

1. 1 BACKGROUND

1.1.1 Rationale of the study

The high demand of light olefins is a serious problem faced worldwide. Methanol-mediated routes to liquid hydrocarbon fuels are again arousing interest [1]. Since methanol may be derived from renewable resources with promising potential in the production of light olefins from methanol as feedstock. Most of the researchers used ZSM-5 as a catalyst for MTO reaction, the problem was that the light olefins selectivity especially ethylene and propylene was low instead the selectivity of methane, bigger hydrocarbons such as C_5-C_8 and aromatics was high [2]. Other researchers synthesized SAPO-34 molecular sieve which is highly acidic and the molecular sieve performed similar to ZSM-5 [3]. This work focuses on the synthesis of SAPO-34 molecular sieve for use as active, highly selective and durable catalysts for the production of $C_2^=$, $C_3^=$ and $C_4^=$ olefins via the MTO process. Most of the crystals of SAPO-34 molecular sieves were synthesized under hydrothermal conditions by using different kinds of amines like, tetraethylammonium hydroxide (TEAOH), morpholine, N,N,N`N`-tetraethylethane-1,2-diamine (TEEDA) as templating agents, including the mixture of TEAOH and Morpholine [4]. The use of piperidine as a structure directing agent for the synthesis of SAPO-34 samples which is suitable for use in the methanol-to-olefins (MTO) conversion is not extensively investigated. Until now, SAPO-34 molecular sieve synthesized using piperidine as a structure-directing agent (SDA) has been reported by only one paper. This molecular sieve was used as a catalyst for aldol condensation of acetaldehyde with formaldehyde reaction [5].

1.1.2 Problem statement

The dependence on crude oil for the production of fuels and chemicals is receiving vehement opposition from an environmental point of view.

1.1.3 Aim

The use of unconventional (SDA) piperidine to synthesize SAPO-34 molecular sieve and test the resulting material as a catalyst for the conversion of methanol to olefins.

1.1.4 Objectives

The objectives of the study are to:

(i) Explore piperidine as a SDA for the synthesis of SAPO-34.

(ii) Investigate the influence of parameters such as crystallization temperature, crystallization time, and phosphorus and silicon contents.

(iii) Incorporate metals into te synthesis gel and study their influence on the catalytic performance of SAPO-34.

1.1.5 Research Approach

The synthesis, characterization and the performance of SAPO molecular sieves samples for the conversion of methanol under MTO conditions was done.

1.1.6 Dissertation outline

Chapters 1 include the rationale of the study and literature review. In these concepts the research problems were outlined and the solutions to the problems were discussed. Literature review has highlighted the background of the study.

Chapter 2 describes the methodology of the synthesis for SAPOs molecular sieves, characterization of SAPOs molecular sieves and how SAPOs catalysts were used on the MTO reactions.

Chapter 3 focuses on the analysis of the data obtained from the X-ray diffraction, scanning electron microscopy and ammonium temperature programmed desorption of the SAPOs molecular sieves.

Chapter 4 concentrates on the analysis of the data obtained from the GC chromatography during MTO reactions in the presence of SAPOs molecular sieve.

Chapter 5 is the general conclusions of this work and recommendation of the future work.

Finally are the references.

1.2 Literature Review

1.2.1 General Introduction

A rapid depletion of crude oil has resulted in the need for alternative feedstock for petrochemicals [6-8]. Conventional sources such as heavy crude oil are labour and resource intensive to produce, requiring extra energy for refinement to chemicals, resulting in higher production costs and up to three times more greenhouse gas emissions per barrel of oil [9]. Since gas reserves are far from major industrial population centres, the transportation of the gas between the supply and demand centres is a critical factor in the cost and use [10]. This provided another motivation for researchers to investigate alternative chemical sources such as methanol to make chemicals. Methanol-mediated routes to liquid hydrocarbon fuels are again attracting interest [1], since methanol may be derived from renewable resources. The production of light olefins from methanol as feedstock is a promising route for use in the chemical industry. The commercial light olefins such as ethylene ($C_2^=$), propylene ($C_3^=$), and butylene ($C_4^=$), are important intermediates for the petrochemical industry [11]. Recently, the annual growth rate of the global olefin market has been slow at 3-4 % [12]. The annual growth rate of ethylene demand is expected to remain around 3-4 % in the coming decades, but that of propylene is expected to be around 4-7 % [13]. Figures 1.1-1.3 shows the demand distribution of light olefins in 2008.

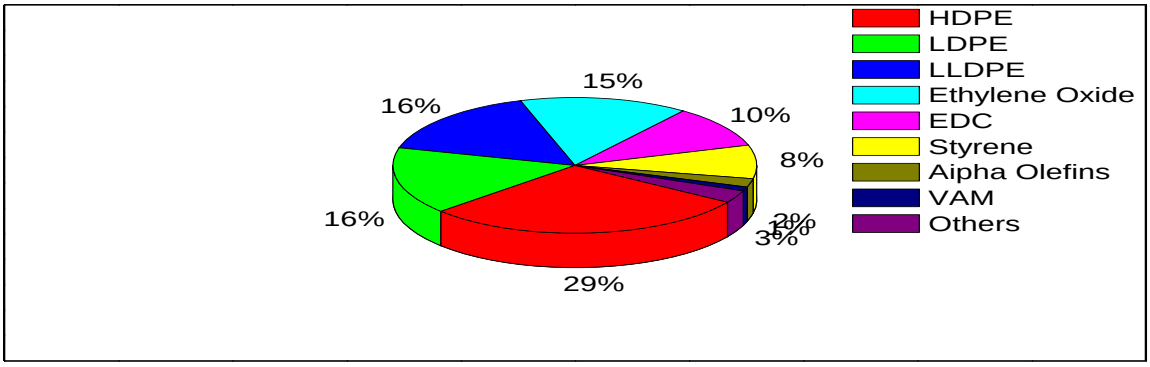


Figure 1.1 Ethylene demand distribution 2008 [14]

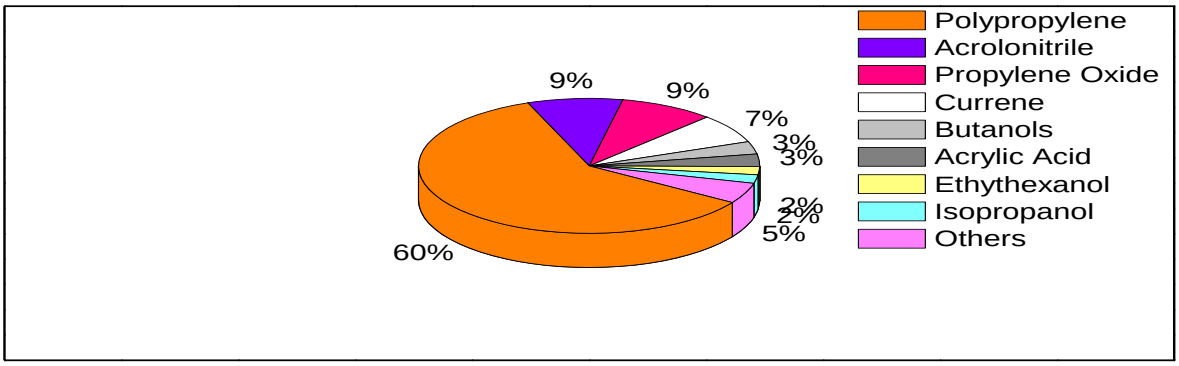


Figure 1.2 Propylene demand distribution 2008 [14]

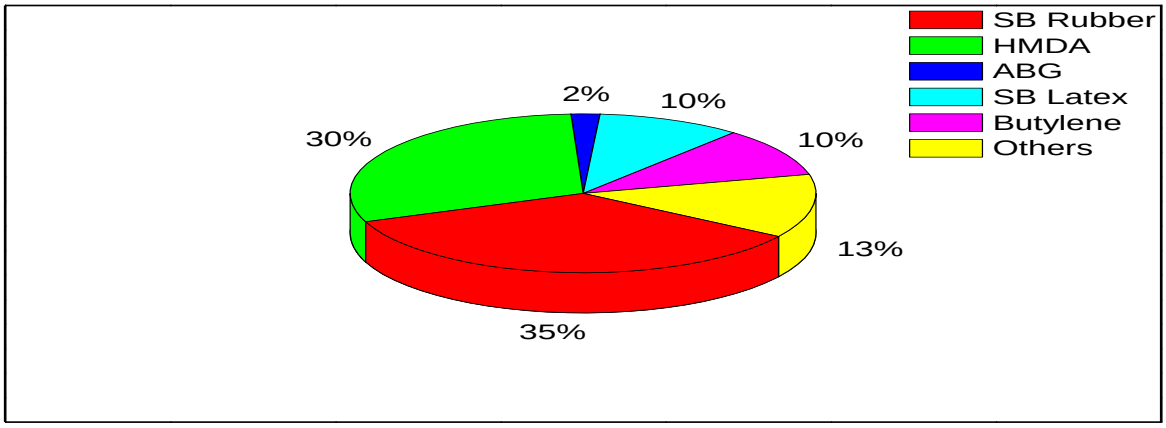


Figure 1.3 Butylene demand distribution 2008 [14]

This work focuses on refining the synthesis of SAPO-34 materials for use as active, highly selective and durable catalysts for the production of $C_2^=$, $C_3^=$ and $C_4^=$ olefins from methanol. The SAPO-34 molecular sieves are conventionally synthesized under hydrothermal conditions using different kinds of amines like tetraethylammonium hydroxide (TEAOH) [15], morpholine [16], and N, N-diisopropylethylamine [17] as templating agents, including mixtures of TEAOH and morpholine [4]. The use of piperidine as a structure directing agent for the synthesis of SAPO-34 samples that has also been reported [18].

Although much effort has been devoted to the use of SAPO-34 in the MTO process, the formation of large amounts of methane is still a major problem [19].

The selectivity to methane reduces the selectivity to $C_2^=$, $C_3^=$ and $C_4^=$ olefins. A method of avoiding the formation of methane during the MTO process by introducing

an alkali metal such as sodium and transition metals such as iron (Fe), cobalt (Co) and nickel (Ni) into SAPO-34 framework is described.

1.2.2. History of Zeolites

A zeolite molecular sieve was discovered by mineralogists and other researchers in nineteenth century. The first zeolites A and X were synthesized in 1950 [20]. The structure of zeolite A was published in 1956 [21, 22]. In the same year, the research laboratory of Linder Air Products, a division of Union Carbide and Carbon Corporations identified the structure of a zeolite A with a cubic structure with a_0 = 12.32 Å. It had a 3-dimensional network consisting of cavities of 11.4 Å. The diameter was separated by a circular opening of 4.2 Å [5]. Eighteen years later, zeolites were defined as the hydrated aluminosilicates that are built up from an extended three dimensional network of AlO_4 and SiO_4 tetrahedra [23]. The IUPAC nomenclature of zeolites was proposed in 1979 [24]. Nowadays, examples of molecular sieves include zeolites as well as carbons, glasses and oxides. Molecular sieves with high crystallinity and uniform pore size are the zeolites [25]. Zeolites are represented by the empirical formula:

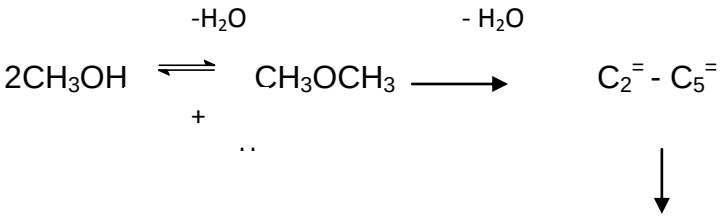
$$M_xD_y[Al_{x+y}\ Si_{n-(x+y)}\ O_{2n}]\ mH_2O$$

where M is a positively charged exchangeable ion of the valence n, x is the number of monovalent cations, y is the number of bivalent cations and m is the number of water molecules in the zeolite formula [26]. Among the different types of zeolites, ZSM-5 (Zeolite Socony Mobil-5) and SAPO-34 molecular sieves have shown the best results in the methanol to hydrocarbons (MTH) conversion. Since light olefins are the most important intermediates in the petrochemical industries, alternative technologies are needed to produce light olefins. Alternative technologies such as steam cracking processes, Fischer Tropsch processes, and MTO processes have been conducted over molecular sieves for this purpose [27-31].

1.2.3 Methanol conversion to olefins

Methanol is a liquid which can be obtained by gasification, partial oxidation or steam reforming of biomass coal and natural gas [7]. The production of light olefins from methanol was first realized around 1954 [33]. During the development of Mobil

catalyst, methanol was converted to gasoline (MTG). ZSM-5 catalyst was used as a catalyst for reaction. Methanol was firstly dehydrated to dimethylether (DME). Which was further dehydrated and converted to light olefins. A final reaction step led to the production of a mixture of high olefins, *n*-paraffin, aromatics and naphthalene. The reaction below shows the formation of olefins and other higher olefins ($C_5^=$-$C_8^=$ together with higher paraffins and aromatics from methanol.



n-parafins, aromatics, C_6+ olefins [34,35].

The conversion of methanol to light olefins using a molecular sieve catalyst such as ZSM-5 was investigated by many researchers [36-42].

SAPO-18 modified with metals like Mg and Zn and unmodified SAPO-18 catalysts were also regarded as better catalysts for the selectivity of light olefins in the MTO reaction [43]. It was discovered that when SAPO-34 catalyst converts methanol to olefins, the main product was methane [44-45]. The SAPO-34 catalyst was used in several chemical reactions such as hexane catalytic cracking [45], and conversion of chloromethane to light olefins [47]. The catalytic performance of methanol to light olefins on ZSM-5 and SAPO-34 catalysts is affected by their structures.

1.2.4 Zeolite ZSM-5

The crystalline microporous zeolite ZSM-5 is constructed from a network of corner-shared SiO_4 and AlO_4 tetrahedra [48]. The framework is composed of TO_4 (T = Si and Al) polyhydra, linked by their corners and may contain cation and water inside the channel/cages. ZSM-5 is a medium-pore zeolite formed by ten-membered ring with 0.45-0.60 nm diameter [49]. The pore opening determines the size of molecule that can enter the zeolite. That is the reason why big molecules such as aromatics, *n/iso* parafins and naphthalene are produced when ZSM-5 catalyst is used in methanol conversion to olefins and gasoline. Figure 1.4 shows the pore structure of

ZSM-5. The ZSM-5 framework has two intersecting channels system i.e. sinusoidal running parallel to the [001] plane and the other one running parallel to the [010] plane [50].

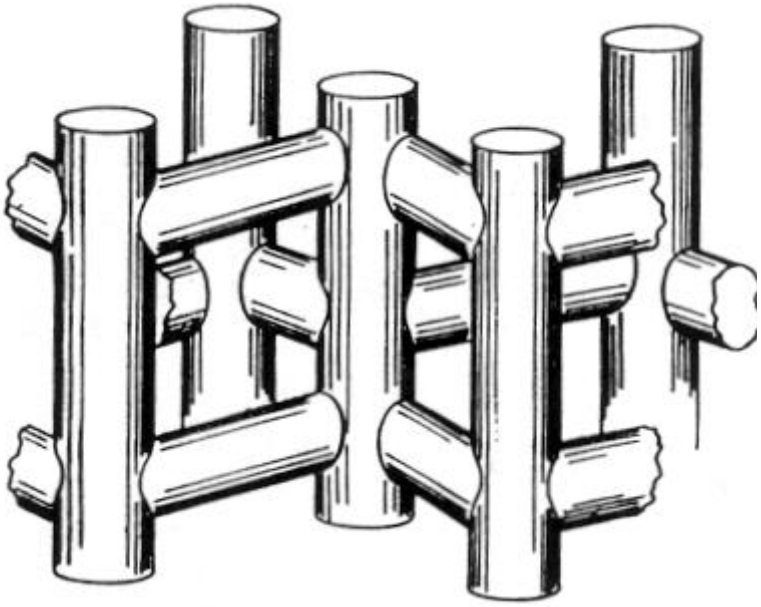


Figure 1.4 The pore structure of ZSM-5 [47].

1.2.5 SAPO-34

In 1982, Wilson *et al*. [51], discovered a microporous crystalline aluminophosphate at Union Carbide, and other aluminophosphate molecular sieves that belong to the SAPO family such as metal aluminophosphate (MeAPO). The metal silicoaluminophosphate (MeAPSO) were identified by Zhang *et a*l. [52]. Venna [53] prepared a SAPO-34 molecular sieve on an alumina disk, and observed good performance in the separation of CO_2/N_2 gas mixtures. The SAPO-34 molecular sieves are synthesized using microwaves, and this molecular sieve is also recognized as a good catalyst for MTO reactions [54].

1.2.5.1 The structural features of SAPO-34

SAPO is a molecular sieve catalyst with formula:

$$M\ [(SiO_2)_x\ (AlO_2)_y\ (PO_2)_z]\ w\ H_2O;\ x + y + z = 1$$

where M is a positively charged exchangeable ion of the valence 2, x is the number of monovalent cations, y is the number of bivalent cations, w is the number of water molecules in the zeolite formula. Molecular sieves are special because of its best selectivity to light olefins, but hit has a short lifetime, and have microporous particles with dimension < 20 Å dimension, and mesoporous > 20 Å uniform pore dimensions sieving based on particle size. The pore structure of SAPO-34 is shown in figure 1.5 [55].

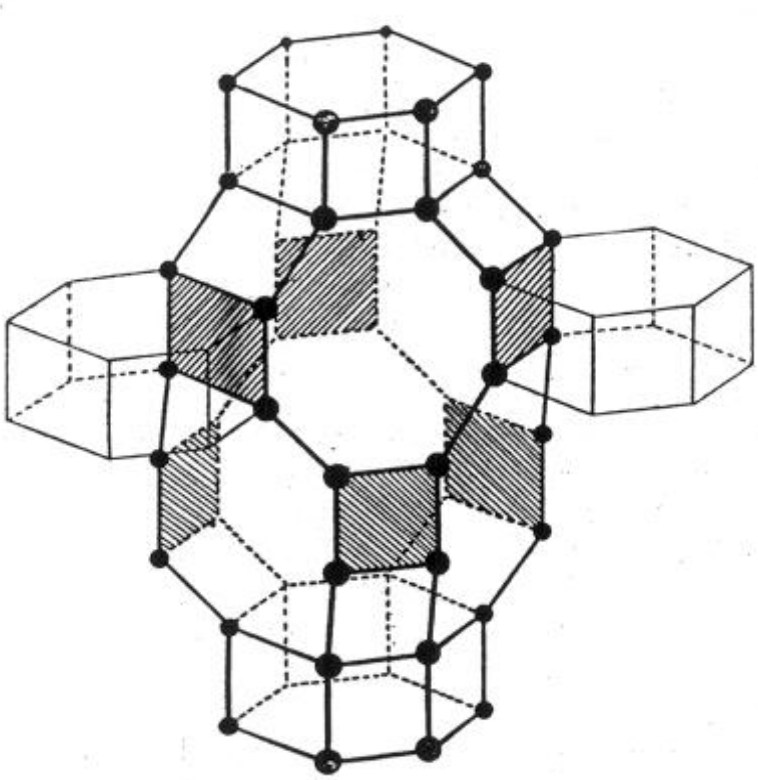
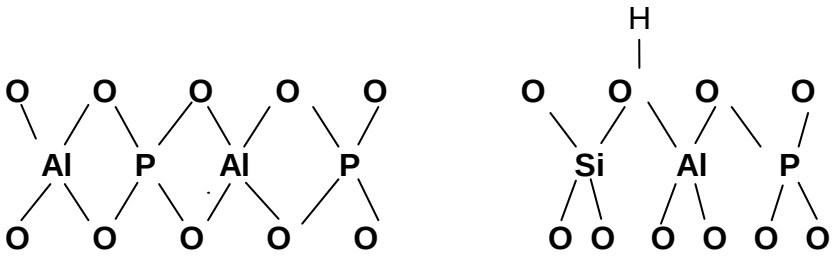


Figure 1.5 The pore structure of SAPO-34 [55].

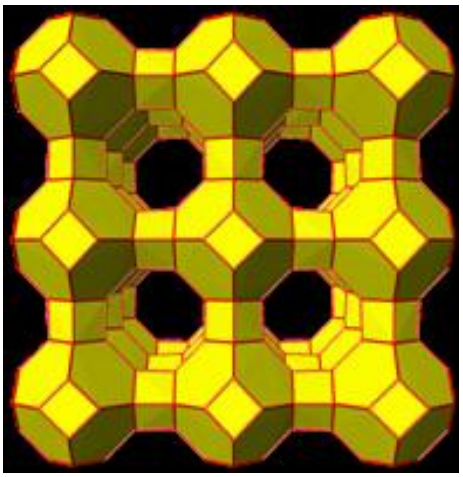
Figure 1.5 shows the Zeolite-like structure of the silocaluminophosphate molecular sieves that can have different types of the pore structure. The SAPO-34 framework is determined from the $AlPO_4$ frame work. Figure 1.6 (a), shows the arrangement of Al and P atoms in the $AlPO_4$ framework. Therefore $AlPO_4$ has electrically neutral framework because it is composed of the same number of AlO_4 and PO tetrahedral.



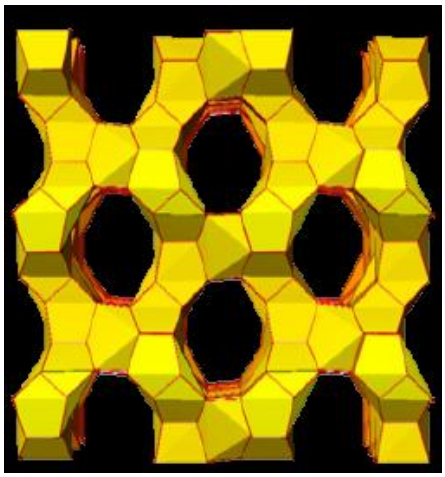
(a) (b)

Figure 1.6 (a) $AlPO_4$ [56] (b) SAPO-34 [57]

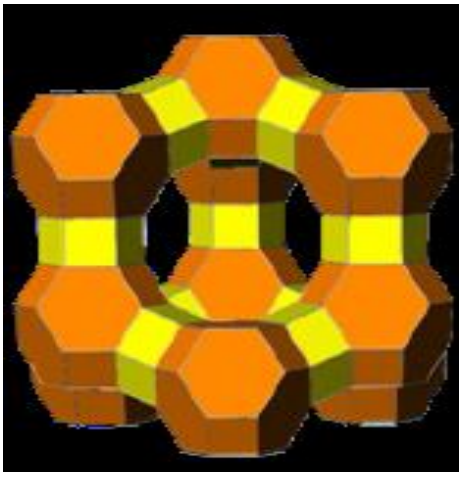
When Si atom is incorporated into $AlPO_4$ framework, Si atom replaces Al or P atoms and generate SAPO framework in figure 1.6 (b). SAPO molecular sieves are classified into large pores like SAPO-5 with the pore dimension of (7 - 8 Å), medium pores like SAPO-11 with the pore dimensions of (5 - 6 Å), and small pores like SAPO-34 and SAPO-44 with pore dimensions of (3 - 4 Å) [58]. Figure 1.7 illustrates the pore dimensions of different zeolites.



(a) Small 8-membered ring ~ 4 Å (SAPO-34 and SAPO-44)



(b) Medium 10-membered ring ~ 5-6 Å (SAPO-11)



(c) Large 12-membered ring ~ 6-8 Å
(SAPO-5)

Figure 1. 7 Pore structures of different SAPOs [59].

The SAPO size is determined by the oxygen packing mode. Thus SAPO-34 has a small pore structure with pore sizes of 0.35-0.45 nm and is formed by a 6-12-membered ring [59]. SAPO-34 has the chabazite-like structure, constructed with the double six-membered rings and forming one cavity per unit cell [60-62]. It uses its small pores to permit the selective formation of light olefins even at 100 % methanol conversion.

SAPO-5 with the large pores has the pore dimension of (7 - 8 Å). Its lattice is overall charge neutral; an aluminium phosphate does not possess strong acidity. The silicon and some other elements with the ability of tetrahedrally are bonded with oxygen and could be substituted into the framework structures (SAP0, MeAPO and E1APO) and create the acidic sites The MTO reaction results in light olefins together with aromatics, The selectivity of light olefins increases with decreasing partial pressure of methanol, while the selectivity of aromatics decreases with decreasing partial pressure [63]. SAPO-5 with AFI structure, comprises of cylindrical channels formed by 12-membered rings with a diameter of 0.74 nm [64], and ZSM-5 is a medium-pore zeolite formed by ten-membered ring with 0.45-0.60 nm diameter [49].

1.2.5.2 Impregnation of SAPO-34

Metal impregnation on the SAPO-34 molecular sieve framework plays an important role in the improvement of the catalytic performance particularly on the product distribution and selectivity towards $C_2^=$ and $C_3^=$ in the MTO process. The recommended metals that are good for molecular sieve incorporation are Ni, La, Y, [30, 65]. The SAPO-34 catalyst incorporated with Fe, Co, and Ni is designated as MeSAPO-34. The SAPO-34 incorporated with Ni produced higher ethylene selectivity in the MTO reaction [66-68].

In 2000, Kang [69] used the same MeSAPO-34 molecular sieves for the MTO reactions and realised that the NiSAPO-34 catalyst with low acidity enhanced the % methanol conversion as well as ethylene selectivity due to the catalyst acidity. The order of increasing % methanol conversion and ethylene selectivity was SAPO-34 < CoSAPO-34 < FeSAPO-3 < NiSAPO-34.

The comparison of MTO reactions on different zeolite molecular sieves such as β zeolite, ZRP and SAPO-34 was studied by Shanda *et al.* [70]. They suggested that the product distribution from the MTO reaction depends on the acidity of the catalyst. The activity of the catalyst increased with an increase in catalyst acidity and also the production of light olefins increased. DME was enhanced when a β-zeolite catalyst was used. The selectivity to light olefins also increased and the methane product decreased on SAPO-34 catalyst impregnated with metals such as K, Cs, Pt, Mo, Ag and Ce. The decrease in order of light olefin selectivity is as follows: CsSAPO-34 > KSAPO-34 > CeSAPO-34 I> CsSAPO-34 > AgSAPO-34 > CsSAPO-34 II > SAPO-34 > MoSAPO-34 [71].

Impregnation of zeolites by metals affects the activity, selectivity and deactivation of the high silica MFI zeolite in the MTO process [68]. Metals such as Ag, Ca, Cd, Cu, Ga, In, and Si incorporated on MFI zeolites improved the light olefins selectivity from 14 % to 18 % [72]. A SAPO-34 molecular sieve modified with Co, Mn, and Ni metals. A positive impact on the activity, selectivity and life-time in the MTO reaction was noted on SAPO-3 modified with Fe, Mn and Ni. MnAPSO-34 had higher activity and light olefins selectivity than CoAPSO-34 and NiAPSO-34.

1.2.5.3 The synthesis of SAPO-34

The synthesis of SAPO-34 molecular sieve catalyst has attracted attention from many researchers because of its good selectivity towards light olefins. The zeolites such as CAL-1 and ALPO-Kanemite prepared with optimum reaction depend on the concentration of silicon desired in the structure. For low silicon concentrations, SiO_2/Al_2O_3 = 0.4, no set of adequate conditions was found; the samples prepared were always contaminated with the starting lamellar materials. At SiO_2/Al_2O_3 molar ratios of 0.8 and 1.2, crystalline samples were obtained after 24 h. For silicon concentration still larger, an optimum set of reaction conditions could not be determined. The best sample with SiO_2/Al_2O_3) 1.6 in the gel was obtained with HMI/Al_2O_3) 1.5 only after 48 h of reaction time, and even then, the crystallinity of the sample thus prepared was poor. Those catalysts have XRD patterns that are similar to that of SAPO-34, but the SEM micrograph differs from SAPO-34 with rough cubic crystalline materials. Those catalysts were synthesized at a crystallization temperature of 190 ^{0}C [73]. When a gel is heated to 473 K within 60 min and kept at this temperature for 16 h under rotation, the formation of SAPO-34 crystalline materials can compete with the SAPO-5 crystalline [74]. In 2009, Zhu *et al.* [75] synthesized a hierarchical and conventional SAPO-34. The hierarchical zeolites were hydrothermally treated at 185 ºC for 72 h under autogeneous using pressure. the conventional SAPO-34 zeolites were prepared by the same procedure other than using pseudoboehmite (73 wt% Al_2O_3) as aluminum source and silica sol (40 wt% SiO_2) as silicon source. Molecular sieve SAPO-34 showed the stronger acid sites presenting by the adsorption of ammonia at higher temperature that range from 300 ^{0}C to 700 ^{0}C.

The researchers have employed a composite method using ZSM-5/MCM-41/SBA to synthesize zeolite molecular sieve that results in the formation of hierarchical pore structures and with Lewis acid and Brønsted acid sites similar to SAPO-34 [76].

1.2.5.3.1 The effect of structure directing agent s in the synthesis of SAPO-34

In 1997, Dumitriu *et al.* [5] synthesized a sample of pure SAPO-34 molecular sieve and using piperidine as a structure directing agent. The gel was heated at 200 ^{0}C for 4-8 days. It was realized that SAPO-34 and SAPO-20 compete in the same

synthesis gel. This molecular sieve was used as a catalyst for the aldol condensation of acetaldehyde with formaldehyde. The SAPO-34 molecular sieve can be prepared within a short period (1-5 days) when using common structure directing agent s such as morpholine and TEAOH at a temperature of 200 ^{0}C. In this study, SAPO-34 molecular sieve with gel composition of 1.0 Al_2O_3: 0.6 P_2O_5:1.1 PIP/TEAOH: 2.4 SiO_2: 100 H_2O, at 200 ^{0}C was synthesized within 5 days. Piperidine was used as a structure directing agent. The prepared acid catalyst was then tested for activity in the MTO process.

Cu-containing SAPO-34 was prepared with and without a structure-directing agent (SDA) [77]. A morpholine SDA was used to synthesize CuSAPO-34, and XRD patterns of the catalysts revealed the existence of SAPO-34, when the SDA was introduced in the gel. In the absence of SDA, SAPO-20 was observed. The synthesis of SAPO-34 and MnSAPO-34 in the presence of a morpholine organic structure directing agent produced a material with XRD patterns with the highest peak at the $2\theta = 9.9^0$ [78]. SAPO-34 microspheres prepared from the soft triethylamine (TEA) SDA also have a cubic crystalline structure [79]. Mixtures of structure directing agent s play an important role in the framework and the crystallinity of SAPO-34 molecular sieves. When a single structure directing agent such as morpholine or TEAOH was used as the SDA, cubic crystal materials were formed [61]. Cyclohexylamine structure directing agent forms rectangular and cubic SAPO-34 crystalline materials with particle sizes that range from 0.6-3 μm. In contrast, mixtures of structure directing agent s such as TEAOH and morpholine, TEAOH, dipropylamine and cyclohexylamine, result in the formation of spherical types of structure [80].

1.2.6 Characterization techniques for SAPO 34 based materials

1.2.6.1 X-ray diffraction (XRD)

XRD is one of the analytical techniques that reveals detailed information about the chemical composition and crystallographic structure of natural and manufactured materials. It is also known as the most important non-destructive tool to analyse all kinds of materials [81]. XRD is used to determine the arrangement of atoms in a crystalline solid. A diffraction patterns is obtained by measuring the intensity of the diffracted rays as a function of the angle of incidence. The crystallinity of a crystal

can be determined by the sharpness of the peak observed in the XRD profile. The broadening of a peak is related to the crystal size and can be determined by using the Scherrer equation [82, 83].

$$D = \frac{0.9 \times \lambda}{\beta \cos\theta} \times 0.1$$

where D is the particle size, β is the broadening of the diffraction line measured at half the maximum peak intensity, θ is the diffraction angle. λ is the wavelength of a Cu cathode vary Kα rays.

1.2.6.2 Scanning electrons microscopes (SEM)

SEM is an analytical technique that measures a largely magnified image of a crystal by using electrons instead of light [84]. Blenken *et al.* [85] investigated the morphology of SAPO-34 using a scanning electron microscope (SEM) micrograph and it showed cubic crystals ranging from 0.2 to 2 µm in size with some smaller particles surrounding the crystals. Tan *et al.* [86] studied the crystal morphology of SAPO-34. The SEM image also revealed the cubic SAPO-34 crystals with a size=3 µm. Van Herden *et al.* [87] discovered that the SEM images for SAPO-34 shows agglomerated particles with undefined morphology. Chae *et al.* [88] studied the physicochemical characteristics of a ZSM-5/SAPO-34 composite catalyst using triethylamine as a structure directing agent. ZSM-5/SAPO-34 composites have no interaction between the ZSM-5 and SAPO-34 particles, because most of the particles showed the large cubic shape crystals which are assigned to ZSM-5 and submicron crystals that are assigned to SAPO-34.

Wan *et al.* [89] investigated the crystal morphology for $AlPO_4$-5 using SEM images of the samples prepared with a gel containing 10 H_2O, 20 H_2O, 30 H_2O and 40 H_2O mole concentration of water. The SEM photographs revealed that when the concentration of water is 10 and 20 M hexagonal platelets were observed while 30 and 40 M concentration of water gave spherical crystalline materials of $AlPO_4$-5. The highest concentration of water limits the formation of $AlPO_4$-5 [90]. Jhung *et al.* [91] studied the morphology of SAPO-5 and SAPO-34 using SEM image and identified SAPO-5 materials as hexagonal crystals. Lee *et al.* [92] studied the synthesis of SAPO-34 using diethylamine (DEA) and tetraethylammonium hydroxide (TEAOH) as

the structure directing agent s. SEM images showed the cubic-like rhombohedra that indicate the presence of SAPO-34 when TEAOH was used as a structure directing agent while in the case of DEA, pure SAPO-11 was observed with sliced crystals aggregating into large particles ranging from 16-20 µm.

1.2.6.3 Ammonia temperature programmed desorption (NH_3-TPD)

Temperature programmed desorption is one of the most widely used and flexible techniques for characterization of acid sites on an oxide surfaces. It determines the quantity and the strength of the acids sites on alumina, amorphous and crystalline silica-alumina. The activity of a zeolite is tested by the acidity of the catalyst. The acidity of SAPO depends strongly on Si content position and ordering in a lattice [93]. Ammonia desorption peaks in a NH_3-TPD show how ammonia adsorbs in different ways on catalyst acidity solid. The ammonia can adsorb on the bridge hydroxyl groups of Brønsted acid sites with different acid strength [84, 94]. Popova *et al.* [90] investigated its temperature programmed desorption of ammonia on SAPO-34 and discovered that there are two main peaks which are observed in the lower temperature region (190 ^{0}C to 250 ^{0}C) and at a higher temperature region (320 ^{0}C to 590 ^{0}C) [45] which could be assigned to weak and strong Brønsted acid sites. The data are similar to [91-94] that described by sites. Zadbakhsh *et al.* [95], studied the temperature programmed desorption of ammonia on SAPO–34 and observed three peaks. The first peak at 214 ^{0}C was assigned to weak Brønsted acid sites arising from hydroxyl groups attached to the centres of P-OH. The second peak arises at 380 ^{0}C was assigned to a weak Brønsted acid sites arising from hydroxyl groups attached to the centres of Al-OH. The third peak arises from the bridge hydroxyl of –Si–(OHO)–Al group [86] and is considered as strong Brønsted acid sites similar to the [96].

1.2.6.4 SS NMR Spectroscopy.

SS NMR Spectroscopy is a type of spectroscopy that characterizes the presence of anisotropic interactions [97]. NMR spectroscopy gives information about the local structural environment of atoms and their nearest neighbour atoms. Crystalline silicates such as the isotopes silicon-29 and aluminium-27 can be used in NMR

experiment to distinguish the framework of alumina silicates in an interface, and determine the number of crystallographic silicon sites present in a crystalline material. NMR spectroscopy can also estimate the bond strength, Si-O-(Si, Al) bond angles and detect Al (4), Al (6), Al (4)/Si and Al (6)/Al (4) ratios [98].

1.2.7 The properties of SAPO-34

The most important properties of a catalyst are how well it does the job of converting the reactant into the product. This is measured by three parameters:

(i) Acidity

(ii) Activity

(iii) Selectivity

Poisoning and enhancement of a catalyst are needed so that this catalyst should be the generable, reproducible, mechanically and thermally stable. This catalyst is required for possesses suitable morphological characteristics and the economical use.

1.2.7.1 The acidity of SAPO

Internal acidity resulting from the replacement of framework elements, high thermal stability, large surface area, accessibility for modification (introduction of metal atom) and ion-exchange (exchange of charge compensating ions),are the important factors that affect the light olefins selectivity of zeolite [99]. SAPO-34 has weaker acidity compared to the ZSM-5, and thus low potential for the promotion of reactions which need strong acid sites for hydrogen transfer, oligomerization and coking. Because of SAPO-34's pore opening and its acidity it is regarded as the most suitable catalyst for the conversion of methanol to ethylene and propylene [80]. The acid density is low in SAPO because of the clustering of silicon atoms those results from the substitution of phosphorus by silicon on the $AlPO_4$ framework. A reaction for the substitution of phosphorus by silicon is shown in the figure 1.7 [100].

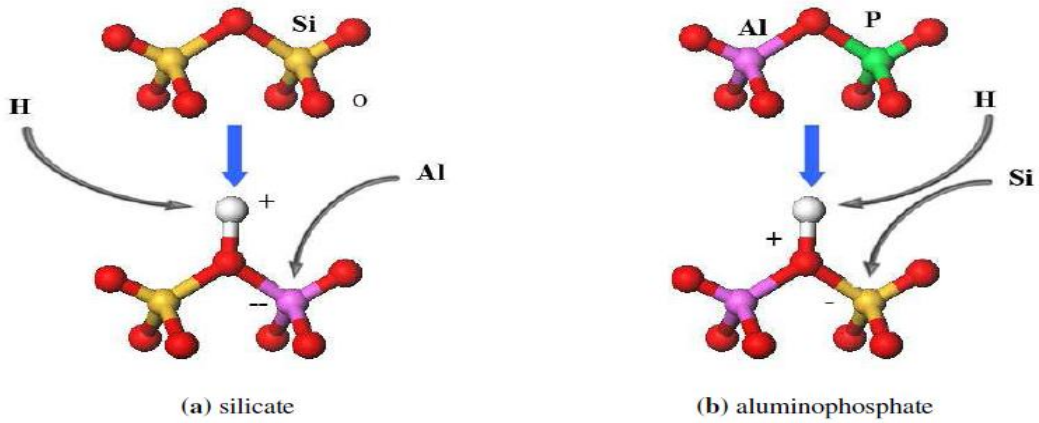


Figure 1.8 Substitution of one Si with Al in pure silicate and substitution of P with Si in aluminophosphate [85]

The substitution of one Si atom with an Al atom in pure silicate and substitution of P with Si in aluminophosphate creates BrØnsted acid site. Protons are attracted to the oxygen leaving a negative charge on Al or P. SAPO-5 has high silicon content in order to increase the number of the acid sites [101]. When ion-exchanging with 1 molar of $NH_4Cl/HCl/H_2SO_4$, a proton is introduced into silicoaluminophosphate forming a proton silicoaluminophosphate (H-SAPO).

Zeolite catalysts which are ion-exchanged with HCl at 80 ºC, or NH_4Cl and H_2SO_4 at room temperature show different selectivity [102]. The best zeolite proton exchanger for light olefins synthesis in the MTO is H_2SO_4 because it deposits sulphur compounds on the zeolite and reduces the pore opening. HCl proton exchange causes the enlargement of the pore opening due to excessive dealumination and hot HCl improves % crystallinity of the zeolite. Catalysts decationized to about 45 % or more yield principally ethylene. Lower degrees of decationization result in high propylene selectivity. SAPO-34 molecular sieve catalysts treated hydrothermally at 700 ºC has 80 % crystallinity. Catalyst life-time increases, selectivity to light olefins ($C2^{=}$-$C_3^{=}$) increases and paraffin productivity decreases [103].

1.2.7.2 Activity of SAPO-34

The activity of the catalyst is the rate of consumption of the reactants, and also the products can be specified [32]. A high activity and stable catalyst used in a reaction with small amount of reactants at a particular temperature, results in a high amount of product selectivity [34]. SAPO-34 has been found to be active on the first five

hours and thereafter it reaches its maximum, due to the increases in the acidity on the catalyst and the blockage of the pores because of coke formation [35].

1.2.7.3 Selectivity of SAPO-34

A high selectivity produces high yields of a desired product while suppressing undesirable competitive and consecutive reactions [104]. This can be affected by the texture of the catalyst in particular pore volume and pore size distribution. It is enhanced by reducing an internal diffusion limitation, which in the case of consecutive reaction rapidly reduces selectivity. The selectivity of SAPO-34 molecular sieve to light olefins depends on acidity of the molecular sieve. The formation of light olefins especially $C_2^=$ and $C_3^=$ are highly favored on the molecular sieve containing lower acidic sites [105]. The selectivity of light olefins on other zeolites such as ZSM-5 and other SAPO-34 prepared with different SDA was low. High methane production was also the main problem. Other products like paraffins and aromatics were the main products.

In this study, SAPO molecular sieves prepared with an unconventional piperidine SDA comprised low acid sites. Those molecular sieves supposed to be highly selective towards the light olefins and reduce the production of paraffins and aromatics in MTO reaction. Unfortunately the molecular sieves have low olefins selectivity and still paraffins and high hydrocarbons are observed. What is interesting is that when Na_2O is loaded in the molecular sieve, the activity of the molecular sieve is promoted the production of methane in MTO reaction is reduced.

CHAPTER TWO - METHODS AND MATERIALS

2 SYNTHESIS OF SAPO.

2.1 Experimental

2.1.1 Chemicals and materials

Table 2.1 Chemicals and materials

Name	Composition	Suppler (Company)
Ortho-phosphoric acid	85%	Saarchem
Aluminium hydroxide ($Al(OH)_3$)	47 %	Merck
Piperidine	99 %	Sigma Aldrich
Tetraethylammonium hydroxide (TEAOH)	35.00 %	Sigma Aldrich
Fumed silica (SiO_2)	98.00 %	Degussa
Distilled Water (H_2O)	100.0 %	UL
Ammonium chloride (NH_4Cl)	98.00 %	Rochelle Chemicals
Silver nitrate ($AgNO_3$)	99.80 %	Merck
Sodiun hydroxide (NaOH)	85.00 %	Rochelle Chemicals
Iron chloride ($Fecl_3.6H_2O$)	99.00 %	Rochelle Chemicals
Cobalteous chloride	99 .00 %	UnivAR
Nickle chloride	98.00 %	Rochelle Chemicals
pH meter universal indicator	0-14	Rochelle Chemicals
Filter paper		Rochelle Chemicals

Table 2.2 Equipments

Equipment	**Quantity**	**Name of the Company**
Beaker	**400 ml**	**Lasec**
Separating funnel	**100 ml**	**Lasec**
Hot plate	**0-200 ºC**	**Heidolph MrBoolk**
Thermometer	**-10-110 ºC**	**Sigma Aldrich**
Magnetic stirrer	**9 × 60 polyg**	**Imelmann (PTY) LTD**
Overhead stirrer	**10 m/m D/E**	**IKA RW 16**
Stainless steel Autoclave	**4848Reactor Controller**	**Parr**
Test tube	**10 ml**	**Lasec**
Pasture pippette	**5 ml**	**Lasec**
Filter paper	**11.00 cm**	**Sigma Aldrich**
Oven	**Ecotherme**	**Labotec**
Furnace	**Carbite**	**Banford Sheffield MicroSEP (PTY) LTD**

Table 2.3 Synthesized samples for SAPOs prepared at different crystallization temperature.

Samples	Crystallization Temperature (^{0}C)	Crystallization Time (Days)	P_2O_5/ Al_2O_3 Ratio	Piperidine/ Al_2O_3 Ratio	SiO_2/ A_2O_3 Ratio	H_2O/ Al_2O_3
SP-1	170	5	0.6	1.1	0.8	100
SP-2	190	5	0.6	1.1	0.8	100
SP-3	200	5	0.6	1.1	0.8	100
SP-4	210	5	0.6	1.1	0.8	100

Table 2.4. Synthesized samples for SAPOs prepared at different crystallization time.

Samples	Crystallization Temperature (^{0}C)	Crystallization Time (Days)	P_2O_5/ Al_2O_3 Ratio	Piperidine/ Al_2O_3 Ratio	SiO_2/ A_2O_3 Ratio	H_2O/ Al_2O_3
SP-5	200	1	0.6	1.1	0.8	100
SP-6	200	2	0.6	1.1	0.8	100
SP-7	200	3	0.6	1.1	0.8	100
SP-8	200	4	0.6	1.1	0.8	100
SP-3	200	5	0.6	1.1	0.8	100
SP-9	200	6	0.6	1.1	0.8	100

Table 2.5. Synthesized samples for SAPOs prepared with different phosphorus content.

Samples	Crystallization Temperature (^{0}C)	Crystallization Time (Days)	P_2O_5/ Al_2O_3 Ratio	Piperidine/ Al_2O_3 Ratio	SiO_2/ A_2O_3 Ratio	H_2O/ Al_2O_3
SP-10	200	5	0.3	1.1	0.8	100
SP-11	200	5	0.5	1.1	0.8	100
SP-3	200	5	0.6	1.1	0.8	100
SP-12	200	5	0.7	1.1	0.8	100

Table2.6 Synthesized samples for SAPOs with high and low sodium content.

Samples	Crystallization Temperature (^{0}C)	Crystallization Time (Days)	P_2O_5/Al_2O_3 Ratio	Piperidine/ Al_2O_3 Ratio	SiO_2/A_2O_3 Ratio	$H_2O/$ Al_2O_3	Na_2O
SP-13	200	5	0.3	1.1	0.8	100	0.015
SP-14	200	5	0.3	1.1	0.8	100	0.200

Table 2.7. Synthesized samples for SAPOs with high and low silicon contents.

Samples	Crystallization Temperature (^{0}C)	Crystallization Time (Days)	P_2O_5/Al_2O_3 Ratio	Piperidine/ Al_2O_3 Ratio	SiO_2/A_2O_3 Ratio	H_2O/Al_2O_3
SP-15	200	5	0.6	1.1	0.6	100
SP-16	200	5	0.6	1.1	0.7	100
SP-3	200	5	0.6	1.1	0.8	100
SP-17	200	5	0.6	1.1	2.4	100

2.1.2 General method

Two methods of preparation for SAPO-34 catalysts were used: method one and method two.The methods of synthesing SAPO has been adopted from [5].

2.1.2.1 Method 1 (Synthesis of SAPO materials)

SAPO molecular sieves were synthesized using a hydrothermal method. The chemical composition of the gel was as follows:

1.0 Al_2O_3: 0.6 P_2O_5: 1.1 Piperidine: 0.8 SiO_2: 100 H_2O

Two mixtures A and B were prepared. Mixture A was prepared in a beaker by adding a 1:1 molar ratio of ortho-phosphoric acid and water drop by drop to a slurry mixture of $Al(OH)_3$ in distilled water. The mixture was stirred vigorously for 18 hours at room temperature. Mixture B was prepared in a bottle by adding piperidine to a slurry mixture of fumed silica in water and stirred vigorously for 18 hours at a temperature of range 90 to 100 ^{0}C. A gel in figure 2.1 was prepared by adding mixture B occasionally to mixture A for five minutes and stirred vigorously for 24 hours at room temperature.



Figure 2.1 Gel preparation

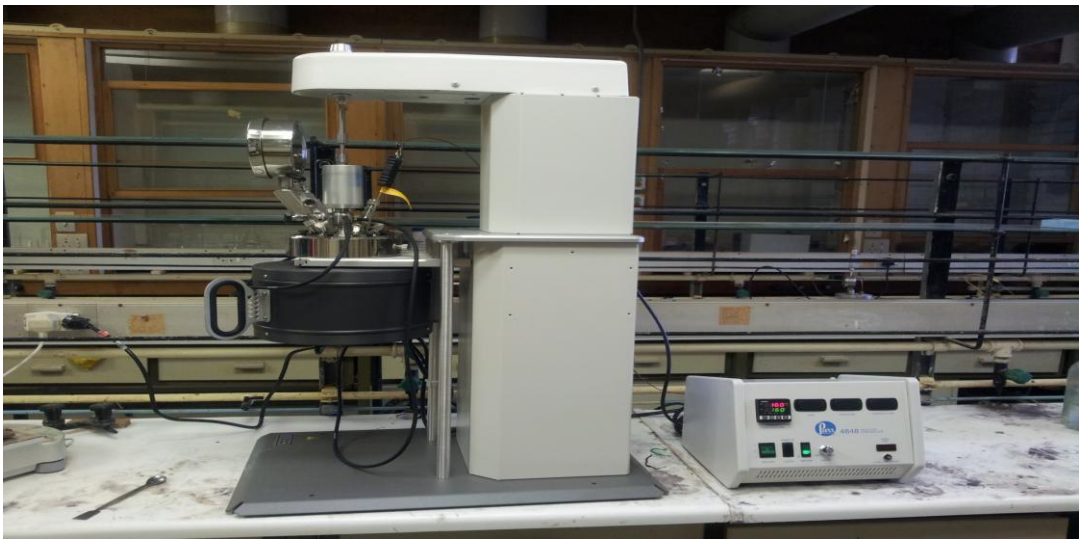


Figure 2.2 An autoclave for synthesis of SAPO-34

The resulting gel was crystallized in a stainless steel autoclave in figure 2.2 under autogenous pressure; the crystallization temperature and time were varied. Other mother liquors were prepared by varying phosphate, silicon and sodium contents. The autoclave was then quenched in cold water and the final pH of the mother liquor was 7. The mather liquors were filtered and washed with distilled water.

The samples were dried in an oven at 80 ^{0}C for 24 hours and calcined at 500 ^{0}C for 5 hours under static air to remove the structure directing agent . Ion-exchanged was achieved with 1.00 M NH_4Cl solution to introduce protons into SAPO's framework. The molecular sieve suspension was stirred with an overhead stirrer four times at room temperature with an interval of 1 hour. The samples were filtered and washed with distilled water to remove Cl^- ions (tested with $AgNO_3$). Clean SAPO-34 was air-dried at 80^{0}C for 24 hours and air calcined at 550 ^{0}C for 3 hours.

2.2.1.2 Method 2 (Synthesis of metal containing SAPO materials)

Table 2.8. Synthesized samples for SAPO containing metals

Samples	SP-18	SP-19	SP-20	SP-21
Crystallization Temperature (^{0}C)	200	200	200	200
Crystallization Time (Days)	5	5	5	5
P_2O_5/Al_2O_3 Ratio	0.6	0.6	0.6	0.6
Piperidine/ Al_2O_3 Ratio	1.1	1.1	1.1	1.1
SiO_2/A_2O_3 Ratio	0.8	0.8	0.8	0.8
H_2O/Al_2O_3	100	100	100	100
FeO mol	0	0.03	0	0
CoO mol	0	0	0.03	0
NiO mol	0	0	0	0.03

SAPO were synthesized hydrothermally from two mixtures. The chemical composition of SAPOs gel was as follows:

Al_2O_3: 0.6 P_2O_5: 1.1 Pip: 0.08 MeO: 0.8 SiO_2: 100 H_2O, Me = Fe, Ni or Co

The first mixture A was prepared by adding 100 ml H_2O to 37.84 g $Al(OH)_3$ and stirred at 32 ^{0}C for 120 minutes. Metal chloride was added to the mixture and stirred for 60 minutes at the same temperature. A 1:1mole ratio of ortho-phosphoric acid 85% and water was poured into the mixture of and stirred vigorously for 18 hours at room temperature to obtain uniform slurry.

The second mixture B was prepared by adding 12.50 g piperidine to slurry of 5.59 g fumed silica and stirred vigorously for 18 hours at 100 ^{0}C. Mixture B was added to mixture A continuously stirred vigorously for 6 hours at a temperature of 32 ^{0}C. The resulting gel with pH = 8 was aged for 24 hours at room temperature. This was crystallized in a stainless steel autoclave under autogenously pressure at the temperature of 200 ^{0}C for 5 days.

The autoclave was cooled in cold water and the pH of the contents was 8. The resulting products were filtered and washed with water to remove same impurities. The samples were dried in an oven at 80 ^{0}C for 24 hours and calcined at 500 ^{0}C for 5 hours under air to remove the structure directing agent . Ion-exchange was achieved by using 1 mole NH_4Cl solution. That was stirred with an overhead stirrer for 4 hours.

The samples were filtered and washed with distilled water to remove Cl^- ions and tested with $AgNO_3$ to check if the samples were still containing the Cl^- ions. Clean SAPO-34 was air dried at 80 ^{0}C for 24 hours and air calcined at 550 ^{0}C for three hours. Ion-exchanged samples were characterized with using SS NMR, SEM, and NH_3-TPD.

2.2 Characterization

Table 2.9 List instruments

Name	**Suppler (Company)**
X-ray powder diffraction	**Bruker SA**
Scanning electron microscope	**Jeol, Tokyo, Japan**
NH_3-TPD	**Labotech SA**
SS NMR (^{29}Si, ^{27}Al and ^{31}P)	**Varian**

2.2. 1 X-ray diffraction

X-Ray powder diffraction patterns of the samples were obtained on a Bruker AXS D8 equipped with a primary beam Göbel mirror, a radial Soller slit, a vanatec-1detector and using Cu- Kα radiation (40 kV, 40 Ma).[106]

2.2.2 Solid State Nuclear Magnetic Resonance spectroscopy

The solid state NMR spectra were acquired on a Varian VNMRS 500 MHz two-channel spectrometer using 3.2 mm zirconia rotors and a 3.2 mm Chemagnetics^{TM} T3 HXY MAS probe. The ^{29}Si spectra were acquired on a 6 mm Chemagnetics^{TM} T3 HX probe. The single pulse MAS experiments were recorded at ambient temperature with proton decoupling the acquisition parameters per nucleus. Adamantane was used as an external chemical shift standard where the downfield peak was referenced to 38.3 ppm [107].

2.2.3. Ammonia temperature programmed desorption

Ammonia temperature programmed desorption (NH_3–TPD) was performed in an in–house constructed apparatus developed and home build with a thermal conductivity detector. Other NH_3–TPD data were obtained from a Labotech Mass Spectrometer, Pfeiffer Vacuum, Omnistar^{TM} connected to the TPD apparatus. Experiments were performed as follows: A 0.2 g of the sample was degassed with helium (He) gas at a flow rate of 60 ml/min and the sample was then heated to 500 ^{0}C, and then cooled to 100 ^{0}C for 10 minutes. He gas was left flowing, and a mixture of NH_3 in He gas (4 % NH_3 balance He) was adsorbed on the catalyst for 1 hour at 100 ^{0}C. The mixture of NH_3 and He gas was replaced by He gas to remove the weakly adsorbed HN_3 on the surface of the catalyst for 15 minutes. Desorption was carried out in helium at a flow rate of 60 ml/min by heating the sample from 100 ^{0}C to 700 ^{0}C at a heating rate of 10 ^{0}C/min.

2.2.4 Scanning electron microscopy

The sample holders, a double sided tape was mounted on a transparency glass and cut into 12 mm x 5 mm pieces. During the sample preparation the cover of the tape is removed, the piece is held with a fine point tweezers and dipped into sample. The

excess material is gently removed from the tape by tapping the tweezers on the side of the sample bottle.

The other double sided tape is mounted on the stub and its covering is taken off. The double sided tape caving the material is now mounted on the one that is mounted on the stab. One stub material of 12 mm x 5 mm pieces of tape carrying the different samples. The stub containing the samples is now put in the Emitted K550X sputter coater (Ashford, England) and coated for 2 minutes with gold.

Samples were viewed in a JSM-840 Scanning Electron Microscope (JEOL, Tokyo, Japan) and operated at an accelerating voltage of 5 kV and a beam which would achieve the optimum resolution for a specific magnification. Low beam intensity was used as a precaution to avoid sample damage. The images were captured using Orion 6.60.4 (Orion, Brussels, Belgium) frame grabber.

At least three different spots of each sample were viewed to analyze each sample. Most samples were analyzed at the following magnifications: 10 000 X, 750 000 X, 5 000 X, 4 000 X, 3 000 X, 2 000 X, 1 000 X, 500 X and 100 X. Each sample was therefore analyzed for at least three hours [49].

2.3 Catalytic test

The catalytic activity tests for methanol conversion to light olefins were carried out in a glass quartz reactor with quartz wool inside in the temperature of 400 ^{0}C. For analysis 0.23 g SAPO-34 catalyst was loaded in the reactor. The reactor was surrounded by a heating jacket and the temperature was controlled by means of a thermocouple placed in the middle of the reactor. Methanol (99, 99 %) was bubbled from a glass bubbler by N_2 gas with the pressure of 50 kPa and a flow rate of 25 ml/min. Figure 2.3 is the reactor system used.

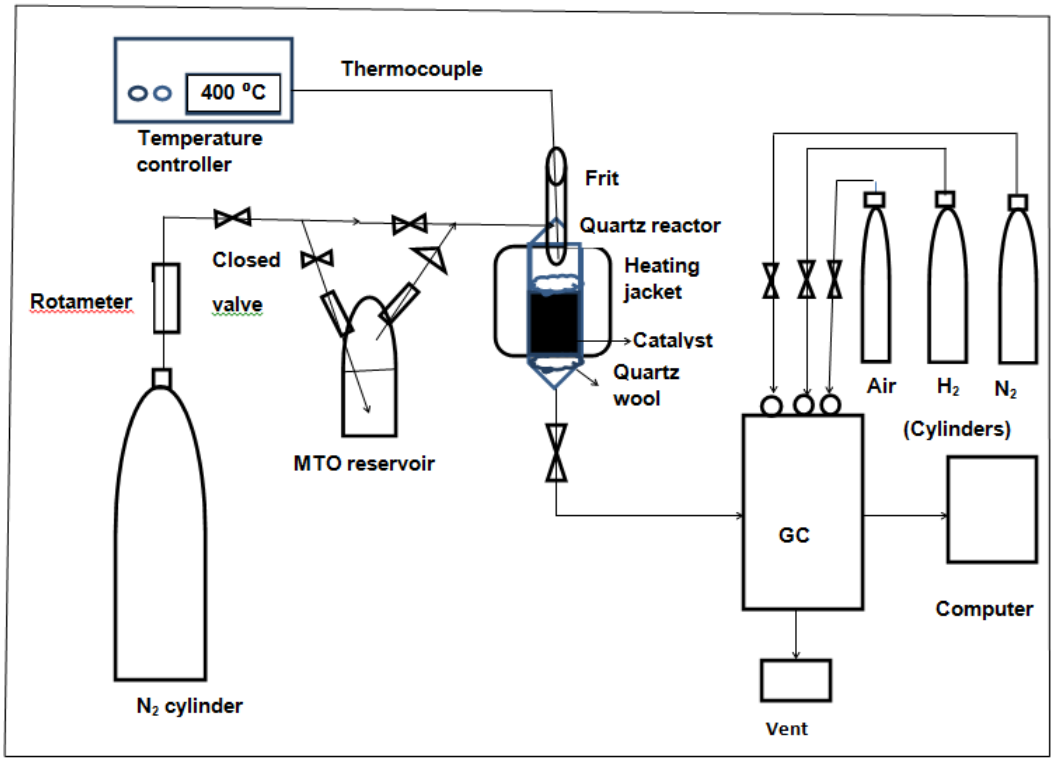


Figure 2.3 A flow diagram for MTO reactor system

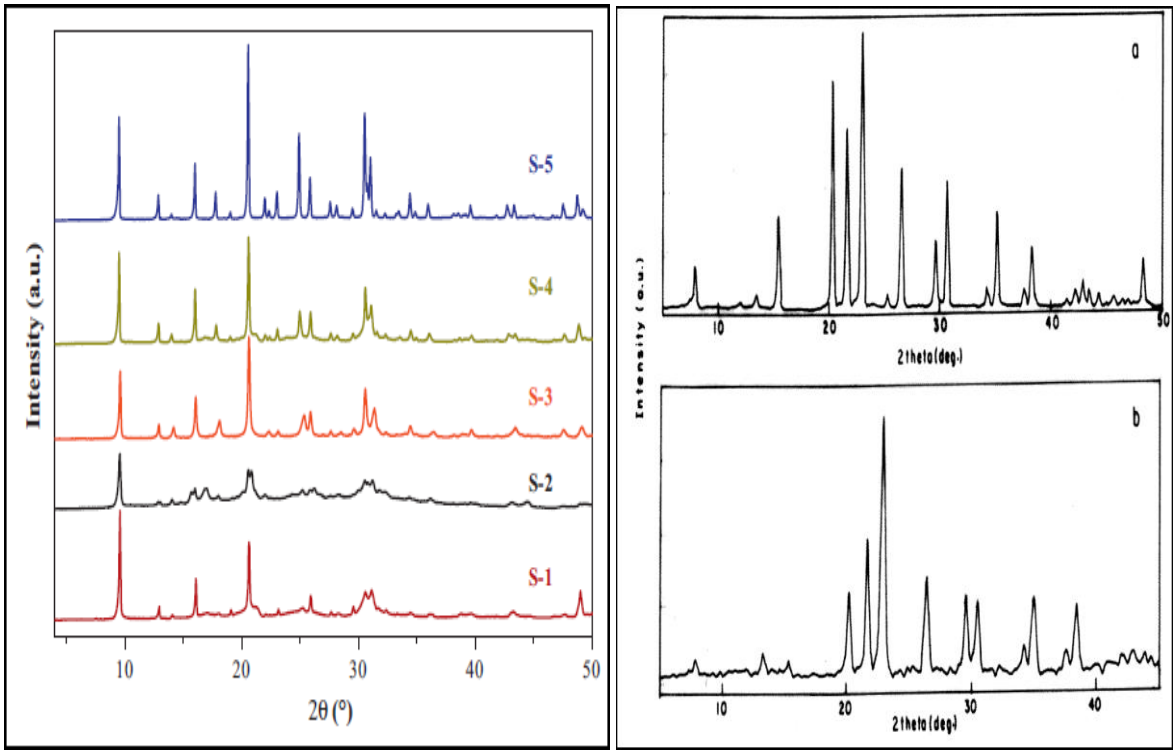
The exit gases from the reactor was monitored by a HP 5840A Gas Chromatogram (Hewlett Packard) with a Flame Ionization Detector and 2 m long packed columns The detector temperature was set at 220 ^{0}C, and the injector temperature used was 100 ^{0}C. The oven temperature was allowed to increase from 20 ^{0}C to 279 ^{0}C. N_2 was used as a carrier gas in GC with a pressure of 20 psi. GC was analysed using clarity software.

CHAPTER THREE - Catalyst characterization

3.1 X-ray Diffraction Patterns

3.1.1 Introduction

Figure 3.1 shows the XRD patterns for SAPO-5 and SAPO-34 molecular sieves with their significant peaks from the literature.



(a) (b)

Figure 3.1. XRD spectra for SAPO-34 (a) and SAPO-5 (b) [57] and [101]

The XRD patterns for pure SAPO-34 and SAPO-5 molecular sieves are shown in figure 3.1 (a) and (b). The XRD patterns of SAPO-34 molecular sieve has the peak at $2\theta = 21^0$ [92]**.** The existence of SAPO-34 crystalline materials is shown from the peaks that appears at $2\theta = 9.9^0, 13.0^0, 15.0^0, 18.0^0, 21^0, 26^0, 32^0$ [58, 91, 113, 114]. The particle size is readily shown by peaks on the XRD patterns was calculated using the Scherrer equation: [77]

$$D = (0.9 \times \lambda)/\beta \cos\theta \times 0.1$$

Example of the size measured of a sample prepared at 170 ^{0}C crystallization temperature for 5 days is given below.

The highest peak at 2θ = 23^0 was used for the analysis. Therefore θ = 11.5^0, and cos (11.5 ^{0}) = 0.4603

Thus, β = 11.5/180^0× π = 0.201

Finally

D = (0.9 ×λ× 0.1) /βcos θ

= 0.9 × 1.542 nm × 0.1/0.201× 0.4603

= 1.49 nm

3.1.2 Results and discussion

3.1.2.1. Influence of crystallization temperature on the formation of molecular sieve SAPO.

The X-ray diffraction patterns of SAPO molecular sieves synthesized at the temperature ranges from 170 ºC to 210 ºC in 5 days are shown in figure 3.2 and table 2.3 shows the synthesis regime and conditions, respectively. The XRD patterns for SAPO is corresponding to the CHA-structure of SAPO-34 reported in the literature [16-20].

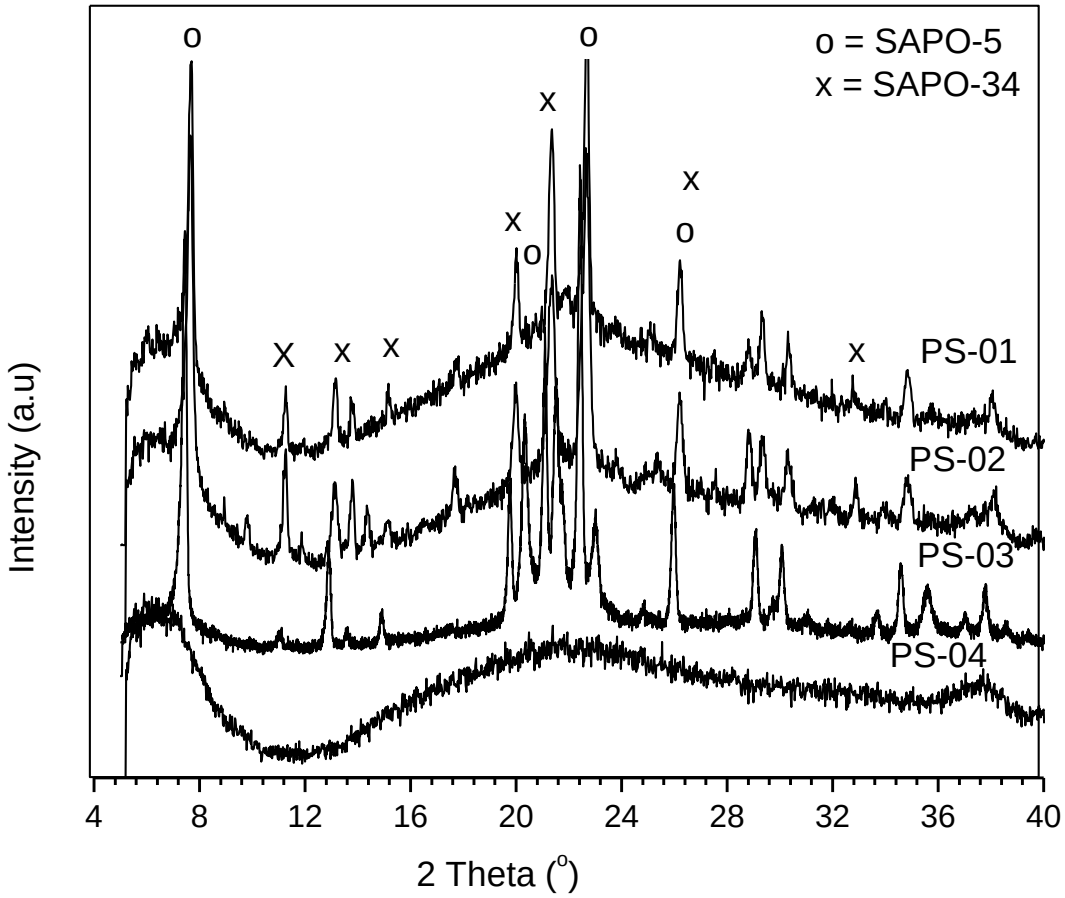


Figure 3.2 XRD patterns of SAPO for the samples (PS-01-PS-04) with the synthesis temperature ranges (170–210) ºC in 5 days and calcined at 550 ^{0}C for 3 hours.

The XRD patterns in figure 3.2 also revealed the presence of SAPO-5. The four peaks in the XRD patterns at 2θ = 7.9 ^{0}, 20 ^{0}, 23 ^{0}and 26 ^{0}, reveal the existence of SAPO-5, while the peaks at the two theta scale of 14.9 ^{0}, 21 ^{0}, 26 ^{0} and 31^0 account for crystalline materials for SAPO-34*.* The XRD patterns for the samples prepared at lower temperature 170-190 ^{0}C (PS-01 and PS-02) shows the presence of SAPO-5 while the one prepared at high temperature 200 ^{0}C (PS-03) shows the presence of both SAPO-5 and SAPO-34. When the crystallization temperature is low, more SAPO-5 crystalline material is synthesized. A sample synthesized at 200 ^{0}C within 5 days shows the promising structure for SAPO-34. The particle sizes are different to one another i.e. 1.49 and 4.30 nm. The SAPO synthesized at 210 ^{0}C (PS-04) does not show any peak. Thus temperature influences the synthesis of SAPO molecular

sieves. All samples consist of the combination of the XRD patterns shown in figure 3.1 (a) and (b).

3.1.2.2. Influence of crystallization time on the synthesis of molecular sieve.

Figure 3.3 shows the XRD patterns for SAPO molecular sieves of samples in table 2.4 prepared as a function of crystallization time.

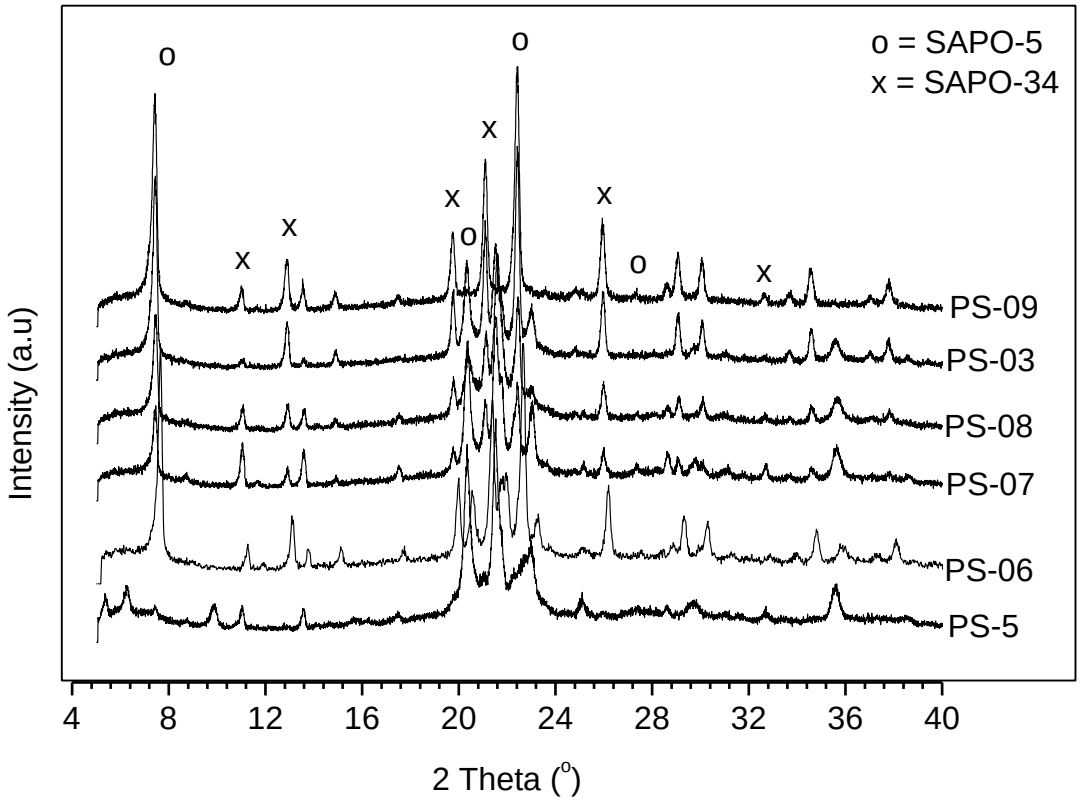


Figure 3.3. X-ray powder diffraction patterns for SAPO molecular sieves samples (PS-03, PS-05 – PS-09) synthesized at 200 ^{0}C within different days (1 - 6) days, calcined at 550 ^{0}C.

The XRD patterns of the 1 day synthesized material in figure 3.3, revealed the other type of SAPO, SAPO-5 and SAPO-34 materials and table 2.4 shows the synthesis regime and conditions of the molecular sieves. SAPO could be synthesized after 2 days. The XRD patterns for samples (PS-03, PS-06 – PS-08) prepared within 2-5 days shows the presence of both SAPO-5 and SAPO-34. They all have the peaks at 2θ = 7.9 ^{0}, 20 ^{0}, 23 ^{0} and 26 ^{0} assigned to SAPO-5 with multi peaks at 2θ = 20 ^{0}-23 ^{0} that shows the presence of impurities. The SAPO-34 material are shown from the

XRD patterns with the small peaks at 2θ = 9.9, 14.9 ^{0}, 21 ^{0}, 26 ^{0} and 32 ^{0}. The XRD patterns for the sample prepared within 6 days (PS-09) shows the presence of pure SAPO-5. This is revealed by the most intense peaks at 2θ = 7.9 ^{0} and 23 ^{0}. For SAPO-34 materials, XRD patterns supposed to have the most intense peaks at the 2θ = 9.9 ^{0} and 21 ^{0}. The average particle size of SAPO-34 samples is 1.49 nm.

3.1.2.3 Influence of the P content in the synthesis gel on the synthesis of molecular sieve SAPO.

SAPO material were synthesized at the different P_2O_5/Al_2O_3 mole ratios from 0.3 – 0.7. The XRD patterns of the samples are shown in figure 3.4. Table 2.5 shows the synthesis regime and conditions for the molecular sieves.

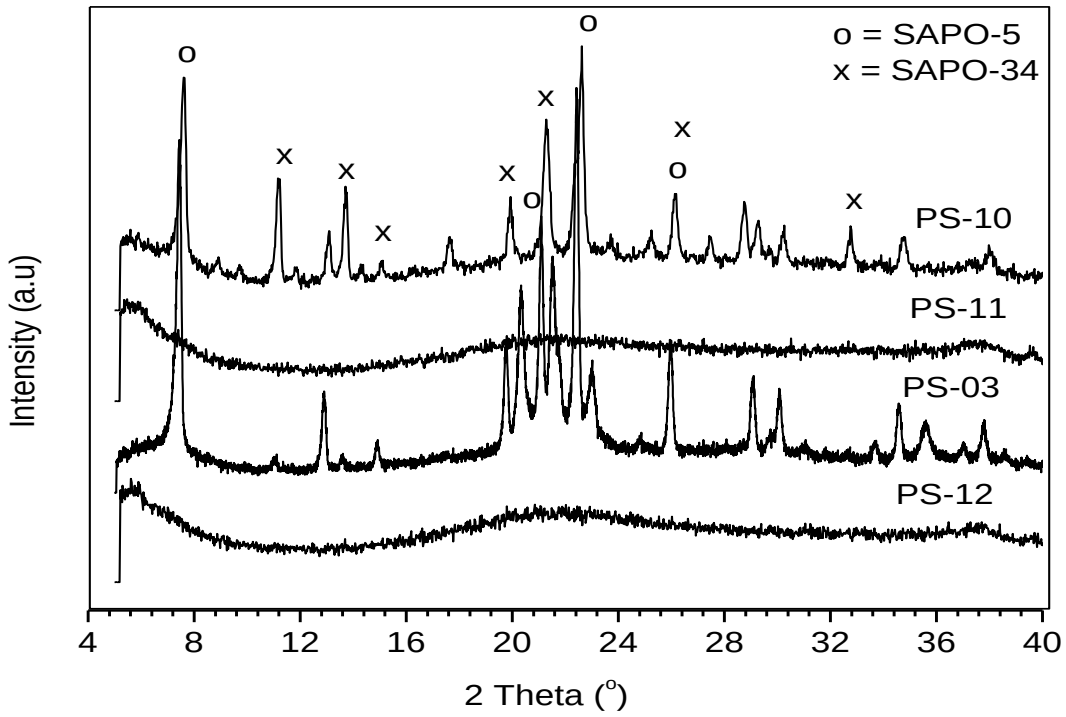


Figure 3.4 XRD patterns of SAPO molecular sieves samples (PS-03, PS10 –PS-12) of synthesized at the molar ratio range from 0.3 to 0.6 P_2O_5/Al_2O_3 for 5 days at 200 ºC, calcined at 550 ^{0}C for 3 hours).

The P_2O_5/Al_2O_3 molar ratio was found to influence the synthesis of SAPO significantly. The XRD patterns indicated the formation of both SAPO-34 and SAPO-

5 in the same gel at low phosphorus molar ratio, i.e. P_2O_5/Al_2O_3 = 0.3 (PS-10). The increase with P_2O_5/Al_2O_3 molar ratio for 0.3 and 0.6 (PS-03 and PS-10) but they decreased at a ratio of 0.7 (PS-12).

3.1.2.4 The effects of Na^+ as a promoter of SAPO molecular sieve.

Figure 3.5 shows the X-ray powder diffraction patterns for SAPOs molecular sieves prepared using the phosphorus molar ratio of P_2O_5/Al_2O_3 = 0.3 (PS-10) with varying sodium content 0.013 Na_2 (PS-13) and 0.2 Na_2O (PS-14)

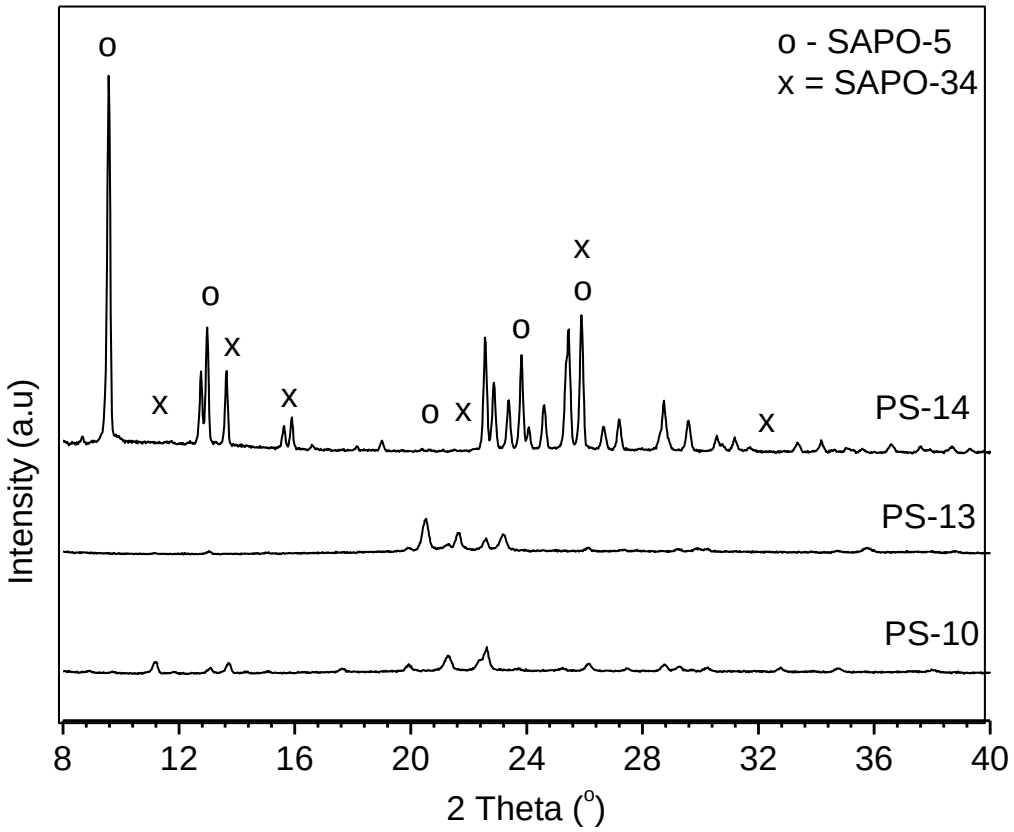


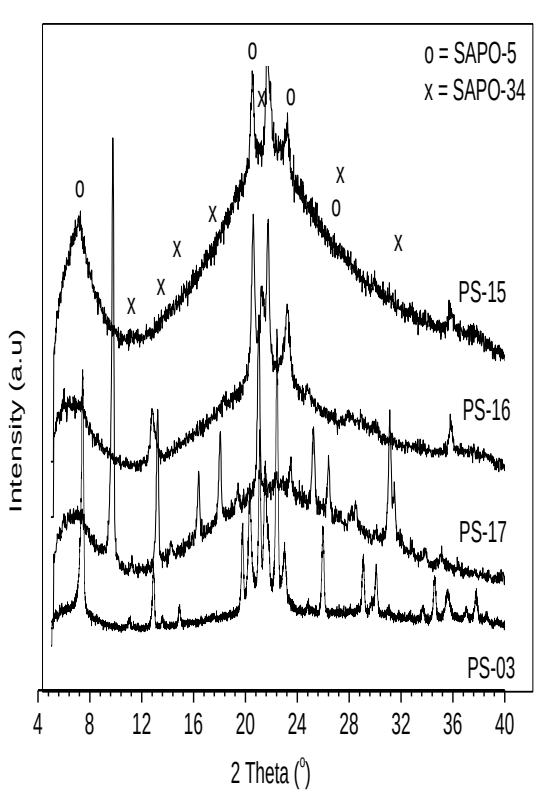
Figure 3.5 XRD patterns for SAPO molecular sieves samples (PS-10, PS-13-PS-14) with sodium added as a promoter.

Molecular sieves with higher sodium contents of sample PS-14 in figure 3.5 gave a more crystalline material with the particle size 3.8 nm. All the peaks that are attributed to SAPO-34 are present except a peak that appears on the 2θ = 21 ^{o}. The XRD patterns have the unusual peaks at 2θ = 13 ^{o} and multi peaks from 2θ = 22 ^{o} to

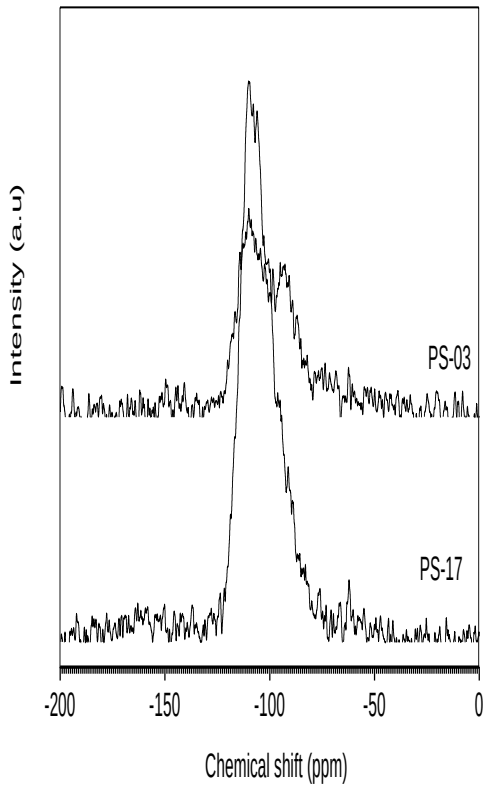
2θ = 27 ^{o}. These suggest that the material that was synthesized could not be either SAPO-5 or SAPO-34. Due to the present of Na_2O in the gel Na atoms substitute P atoms on the AlPO4 framework and form Ferrierite zeolite [108]. While the XRD patterns for the catalyst synthesized using the lower sodium content of sample PS-13 have the particle size of 4.32 nm and also have the deformed peaks at the 2θ = 9.9 ^{o}, 13 ^{o}, and 18 ^{o}. SAPO-5 can also be detected on the 2θ = 7.9 ^{o}. Molecular sieves prepared with low and without sodium content have SAPO-34 crystalline materials. The addition of sodium atoms in SAPO framework damages the structure of SAPO and result in other material.

3.1.2.5 Influence of the Si content in the synthesis gel on the formation of molecular sieve SAPO.

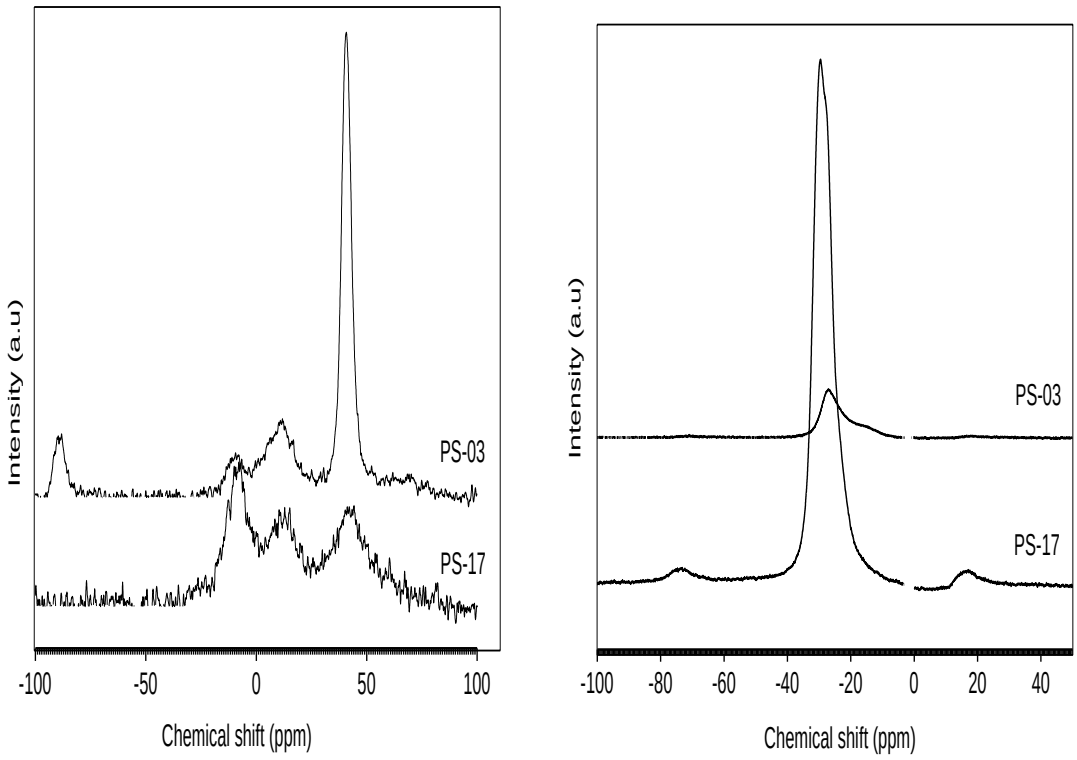
Figure 3.6 (a) shows the X-ray diffraction patterns of synthesized SAPO samples, in which the molar ratio of SiO_2/Al_2O_3 varied from 0.6 to 2.4, figure 3.6 (b) -(d) the SSNMR (^{29}Si, ^{27}Al and ^{31}P) for high and low silicon contents. Table 2.7 shows the synthesis regime and conditions of the molecular sieve.


o = SAPO-5
x = SAPO-34
PS-15
PS-16
PS-17
PS-03
Intensity (a.u)
2 Theta (°)
4
8
12
16
20
24
28
32
36
40

(a)


PS-03
PS-17
Intensity (a.u)
Chemical shift (ppm)
-200
-150
-100
-50
0

(b)



(c) (d)

Figure 3.6 (a)-(d) The XRD patterns, ^{29}Si, ^{37}Al and ^{31}P spectra for H- SAPO molecular sieves samples (PS-03, PS-15 – PS-17) synthesized at the SiO_2/Al_2O_3 molar ratio range 0.6 to 2.4 for 5 days at 200 ºC, calcined at 550 ^0C for 3 hours.

Figure 3.6 (a) shows the XRD patterns for SAPOs molecular sieves synthesized at the SiO_2/Al_2O_3 molar ratio range 0.6 to 2.4 (PS-03, PS-15 – PS-17) for 5 days at 200 ºC. The XRD patterns for the molecular sieves synthesized at the SiO_2/Al_2O_3 molar ratio 0.6 and 0.7 (PS-15 and PS-16) have few peaks. This shows that the samples were still at the intermediate stage. Therefore there was no formation of either SAPO-34 or SAPO-5. Molecular sieve containing a SiO_2/Al_2O_3 molar ratio of 0.8

(PS-03) results in the formation of both SAPO-5 and SAPO-34. The one containing a SiO_2/Al_2O_3 molar ratio of 2.4 (PS-17) gave rise to SAPO-34 phase and amorphous phase. This is supported by a broad single peak of ^{29}Si SSNMR spectrum for the sample with SiO_2/Al_2O_3 of 2.4 in figure 3.6 (b). ^{27}Al NMR spectrum for the molecular sieve [in figure 3.6 (c)] with low silicon content revealed one sharp with high peak

intensity of the Al resonance at the chemical shift of 40.31 ppm that corresponds to a tetrahedral Al site. This implies that more of Al atoms were not replaces by Si atoms in hydrolysis of AlPO4. The molecular sieve prepared with high silicon contents shows three well formed peaks that indicates good replacement of Al atoms by Si atoms. The XRD patterns for molecular sieve prepared with SiO_2/Al_2O_3 molar ratio of 2.4 have the peaks that are similar to the one that was discussed on 3.3.2. The XRD patterns correspond to the CHA-structure of SAPO-34 in the literature [42, 81, 109-111]. The SAPO particles increase with an increase in the molar ratio of SiO_2/Al_2O_3 from 0.8 to 2.4. These are because of the low and high silicon content in the catalyst. However a broad feature at $2\Theta = 13^0$-26^0 correspond to amorphous materials.

3.1.2.6 The effects of modified SAPOs

Figure 3.7 shows the X-ray diffraction patterns for SAPO molecular sieve prepared by adding metals like Fe, Co and Ni to the catalyst gel. One sample was prepared without adding any metal.

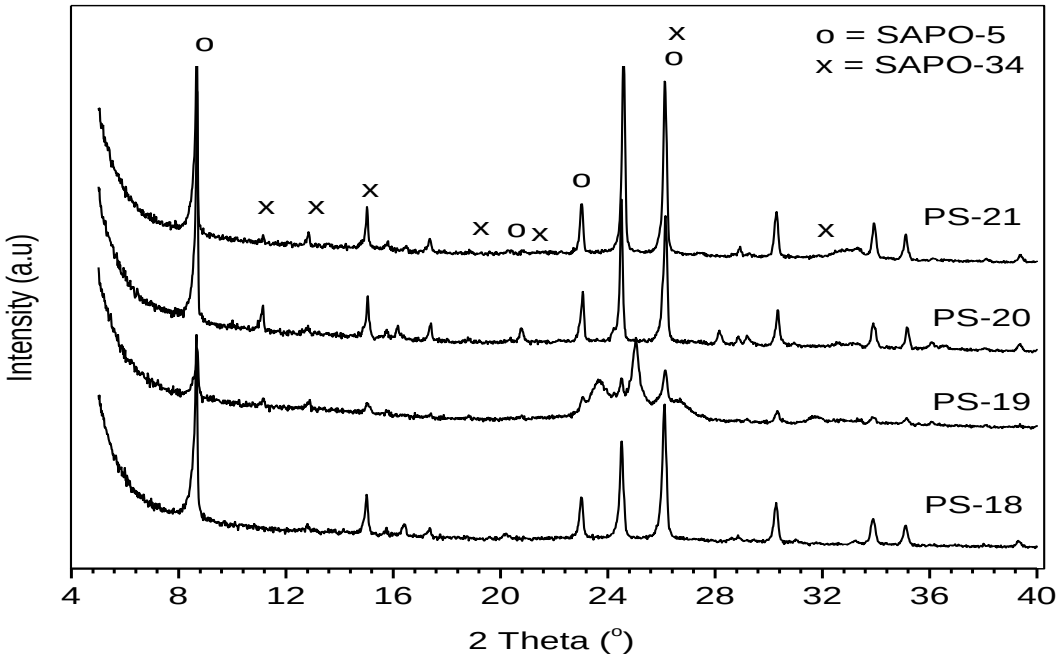


Figure 3.7 The XRD patterns for unmodified and modified SAPO catalyst

The method for the synthesis of SAPO molecular sieve using stirring method for 24 hours was not successful. Therefore the method for the synthesis of SAPO was

changed. The first mixture A was prepared by adding 100 ml H_2O to 37.84 g Al $(OH)_3$ and stirred at 32 ^{0}C for 120 minutes. Metal chloride was added to the mixture and stirred for 60 minutes at the same temperature. A 1:1mole ratio of ortho-phosphoric acid 85% and water was poured into the mixture of and stirred vigorously for 18 hours at room temperature to obtain uniform slurry.

The prepared gel was aged (not stirred) for 24 hours instate of stirring for 24 hours before it was crystallized in an autoclave. XRD patterns of the unmodified and modified catalyst in figure 3.7 revealed the most intense peak at 2θ = 9.4^0 with the particle size of 3.8 nm, and other peaks at 2θ = 11^0, 13^0,15^0, 26^0, 30^0 and 33^0. All those peaks are assigned to SAPO-34 molecular sieve. The peaks at the 2θ = 13^0, 23^0, 24^0, 30^0, are assigned to SAPO-5 molecular sieve. The sample Co-SAPO contained both SAPO-34 and SAPO-5, because it contains all peaks for SAPO-34 and some peak for SAPO-5 at 2θ = 9.9 ^{0}, 11^0, 15^0, 18^0, 19^0, 21 ^{0} and 23 ^{0}. Fe-SAPOs showed a peak at 9.4º, very small peaks at 2θ = 11^0, 13^0, 15^0, and medium peaks at 2θ = 26^0 and small peaks at 2θ = 30^0, 34^0, 35^0. Peaks at 2θ = 18^0, and 20^0/21^0, are absent. Fe-SAPO peaks in the range 22.4 ^{0} to 27 ^{0} are distorted while the rest of materials show well-defined peaks at that range. This is because Fe is less reactive when reacting with silicoaluminophosphate. Some of Fe particles are left unreacted and form an amorphous material. Therefore the catalyst should be synthesized for more than 5 days. Ni-SAPO XRD patterns did not show any difference compared to unmodified SAPOs because Ni is more reactive when reacting with silicoaluminophsphate and it react completely in the reaction.

3.1.2.7. The influence of structure directing agents

The XRD patterns of SAPO molecular sieves samples prepared using piperidine and tetraethylammonium hydroxide as structure directing agents are presented in figure 3.8.

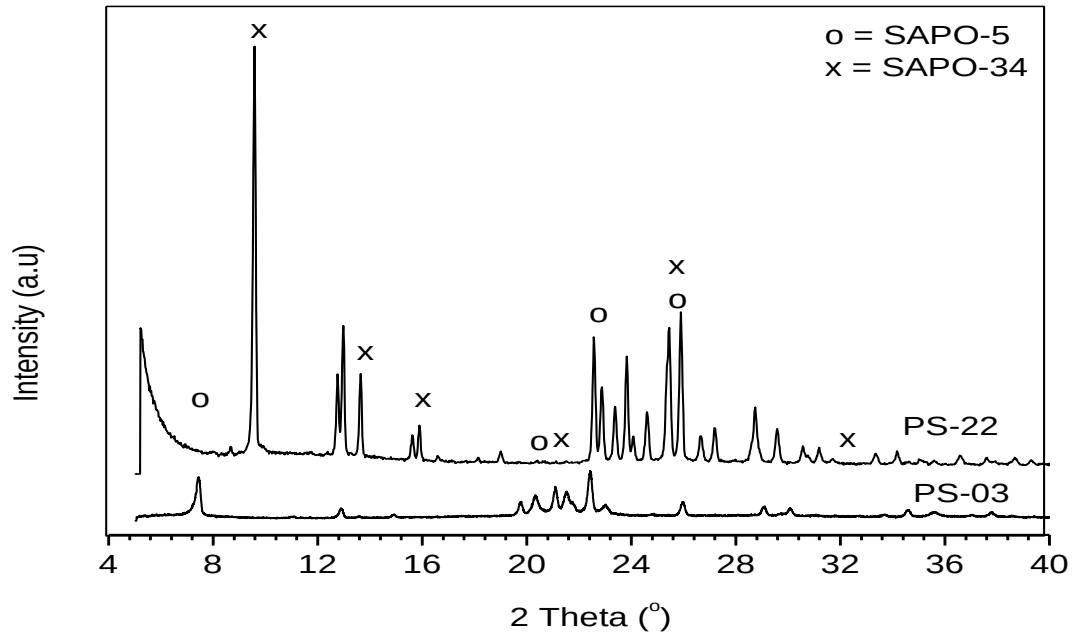


Figure 3.8 XRD patterns for SAPO molecular sieves prepared using piperidine (PS-03) and TEAOH (PS-22) structure directing agent s.

XRD patterns of both molecular sieves in figure 3.8 were different. SAPO molecular sieve prepared using TEAOH structure directing agent (PS-22) have peaks at 2θ = 9. 9 ^{0}, 13 ^{0}, 15 ^{0} and 26 ^{0} with the particle size of 1.49 nm. All peaks are assigned to SAPO-34. A peak at 2θ = 18 ^{0} is assigned to AlO_4 framework, so there was no replacement of Al atom by Si atom incorporated in the reaction. A peak at 2θ = 18 ^{0} should disappear and result with a peak at 2θ = 20 ^{0} or 2θ = 21 ^{0} so the peak at 2θ = 20 ^{0} or 2θ = 21 ^{0} is absent. The multi peaks in the range 2θ = 23 ^{0} to 2θ = 26 ^{0} do not suggest the presence of SAPO-5 or SAPO-34. The XRD patterns of this sample looks similar to Ferririete zeolite [109] When piperidine (PS-03) was used as a structure directing agent , only four peaks appear at 2θ = 13 ^{0}, 15 ^{0}, 21 ^{0}, and 26 ^{0} with the particle size of 3.8 nm and were assigned to SAPO-34 materials. The absent of a peak at 2θ = 18 ^{0} indicate that there was a replacement of Al atom by Si atom in the reaction. Peaks at 2θ = 7.4 ^{0}, 13 ^{0}, 22 ^{0}, 23 ^{0} and 30 ^{0}, are assigned for SAPO-5 materials.

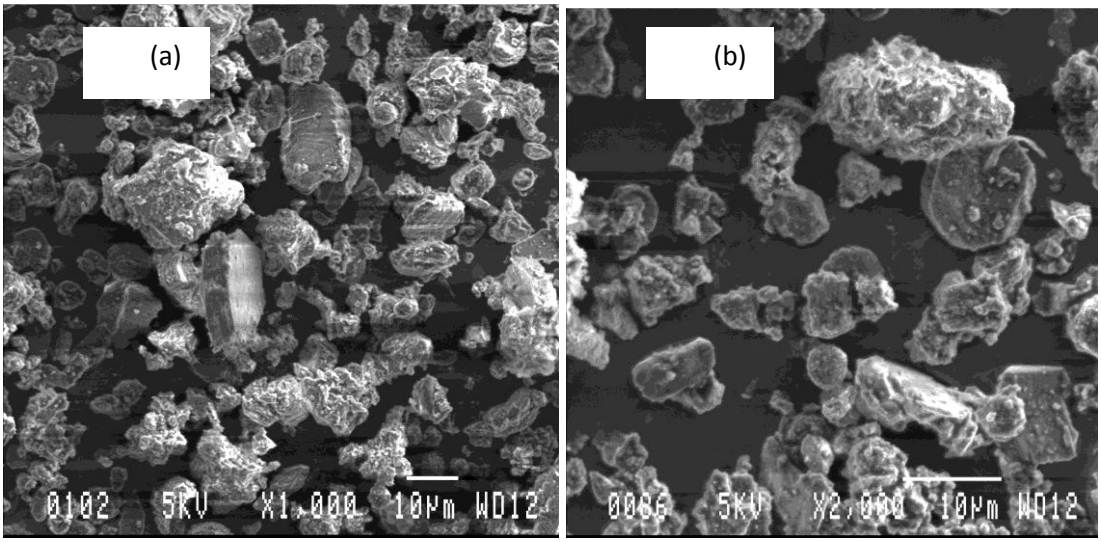
3.2 SEM spectroscopy

3.2.1 Introduction

The SAPO molecular sieves were synthesized using piperidine as a structure directing agent at 200 ºC within different days. The selected samples of SAPO prepared within 3 and 5 days, with P_2O_5/Al_2O_3 = 0.3 and 0.6 molar ratios, SiO_2/Al_2O_3 = 2.4 molar ratio, the samples containing metals like Fe, Co and Ni and a sample without a metal were characterized using SEM spectroscopy. One sample was synthesized using TEAOH as a structure directing agent. This sample was also characterized using SEM spectroscopy technique.

3.2.2 Results and discussion

Figure 3.9 (a)-(c) shows the typical SEM images of SAPO synthesized at 200 ºC within 3 days (PS-07) at different magnifications like 1000, 2000 and 5000.



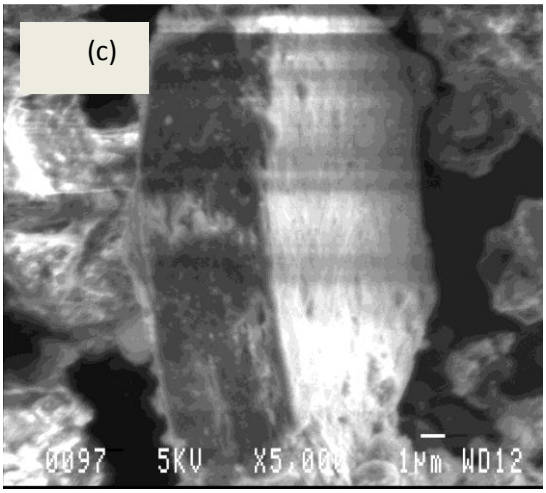
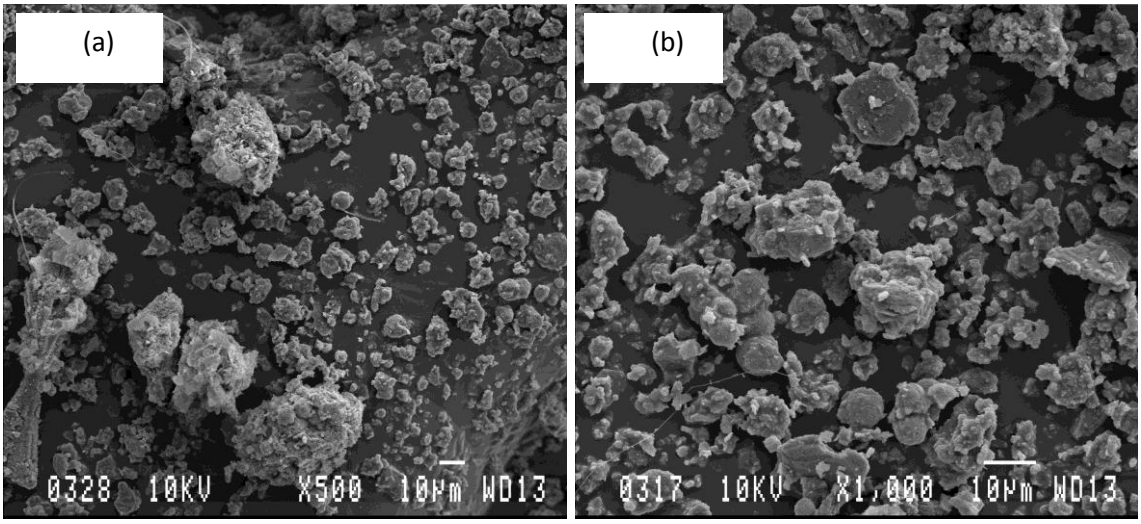


Figure 3.9 (a)-(c) SEM images for SAPO sample PS-07 synthesized within 3 days at different magnifications. (a) magnification of 1000, (b) magnification of 2000 and (c) magnification of 5000.

The SEM images show the particles with rough shape at the magnification of 1000 and 2000 [figure 3.9 (a) and (b)]. At magnification of 5000 [figure 3.9 (c)], pentagonal crystals are observed that indicate the presence of SAPO-5.This results are similar to the one shown from the literature [58]

Figure 3.10 (a)-(d) shows the typical SEM images of SAPO synthesized at 200 ºC for 5 days at different magnifications.



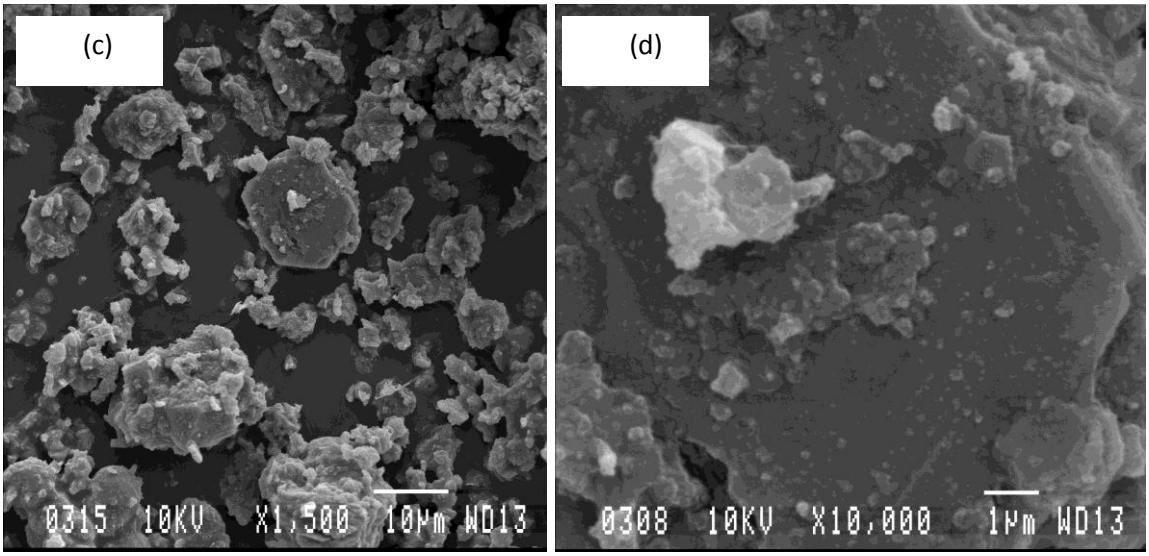


Figure 3.10 (a)-(d) SEM images for SAPO synthesized within 5 days at different magnifications. (a) magnification 500, (b) magnification 1000, (c) magnification 1500. And (d) magnification 10000

At lower magnifications 500 figure 3.10 (a), SEM images reveal irregular particles. At higher magnification of 1000, 1500 and 10000 [figures 3.10 (b-d)] the pentagon crystals were observed that indicating $AlPO_4$ at intermediate stage of growth and some of the Al and P atoms were not replaced by Si atom. The pentagon crystals can also indicate the presence of SAPO-5. The SAPO-5 changes to SAPO-34 when the crystallization time increases.

Figure 3.11 (a)-(c) shows the SEM images of SAPO synthesized at 200 ºC for 5 days with a $P_2\ O_{5/}Al_2O_5$ = 0.3 mole ratio at different magnifications like 2000, 4000, 5000 and 7500

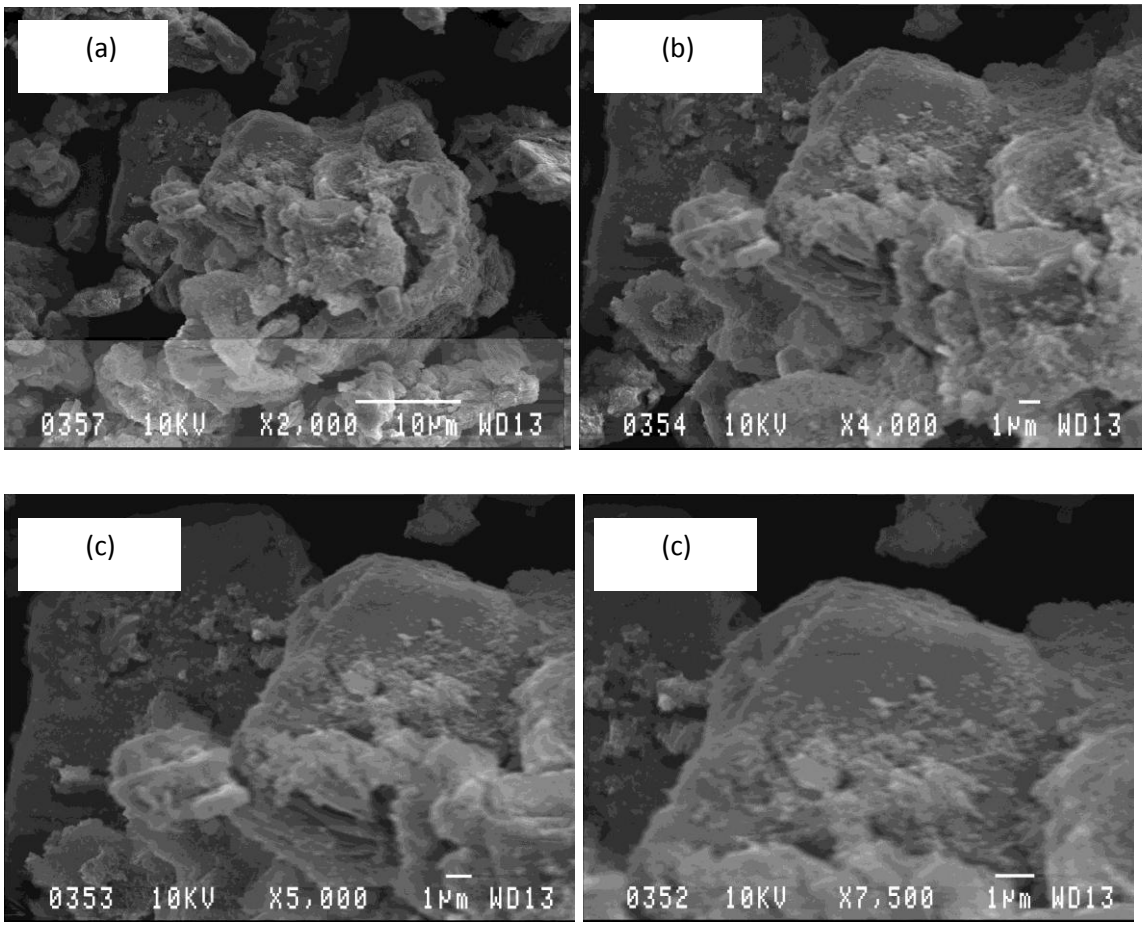


Figure .3.11 (a)-(d) SEM image for SAPO synthesized at 200 ºC for 5 days with the mole ratio of P_2O_5/Al_2O_3 = 0.3 at different magnifications. (a) magnification 2000, (b) magnification 4000, (c) magnification 5000 and (d) magnification 7500.

The morphology of the molecular sieve synthesized with P_2O_5/Al_2O_5 = 0.3 molar ratio at 200 ºC for 5 days is shown in Figure 3.11 (a-d). SEM image for SAPO-34 with the molar ratio of P_2O_5/Al_2O_3 = 0.3 shows rectangular crystals with amorphous particles at the magnification 2000, 4000, 5000 and 7500.This indicate the presence of SAPO-34 which is not well formed.

Figure 3.12 (a)-(d) show the micrographs of SAPO synthesized at 200 ºC for 5 days with a SiO_2/Al_2O_3 molar ratio of 2.4. at different magnifications like 30, 100, 5000 and 7500.

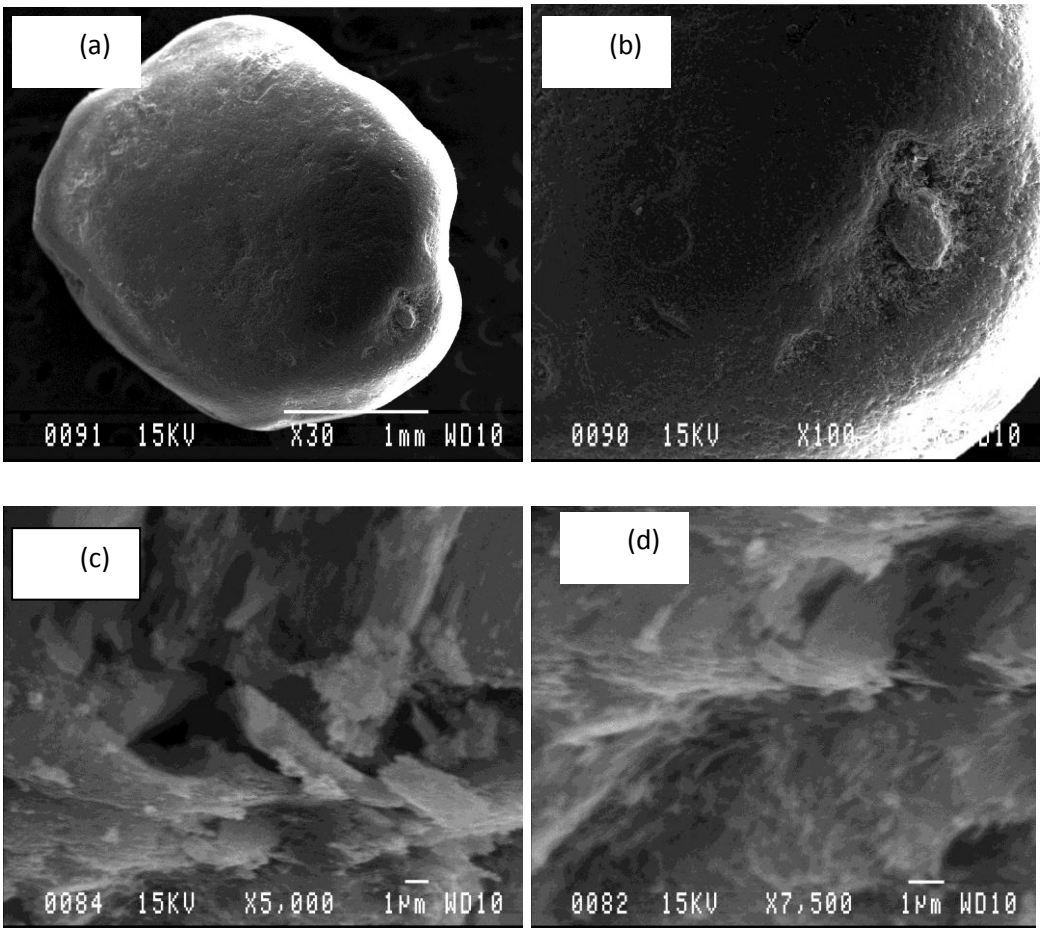


Figure 3.12 (a)-(d) SEM image for SAPO synthesized at 200 ºC for 5 days with the mole ratio of SiO_2/Al_2O_3 = 2.4. (a) magnification 30, (b) magnification 100, (c) magnification 5000 and (d) magnification 7500.

The morphology of the SAPO molecular sieve prepared at 200 ºC for 5 days with SiO_2/Al_2O_3 = 2.4 molar ratio using SEM technique is shown in [figure 3.12 (a)-(d)]. The irregular cubic crystal with amorphous particles is shown at the magnifications of 30 and 100 in [Figure 3.12 (a)-(b)]. The molecular sieve with SiO_2/Al_2O_3 = 0.80 molar ratio discussed in figure 3.10 (b)-(c) has the shape different to the shape of molecular sieve prepared with SiO_2/Al_2O_3 = 2.4. The shape of particle for this molecular sieve gave a pentagonal crystal with amorphous particle. These indicate the presence of SAPO-5 which can develop into SAPO-34 if a molecular sieve could be synthesized for more than 5 days. Figure 3.12 (c)-(d) shows SEM image of molecular sieve at magnification 5000 and 7500. Only amorphous materials were observed.

One sample was synthesized using TEAOH structure directing agent at 200 ºC for 5 days. Figure 3.13 (a)-(d) illustrate the SEM micrographs for this sample at different magnification like 2000, 3000, 4000 and 10000.

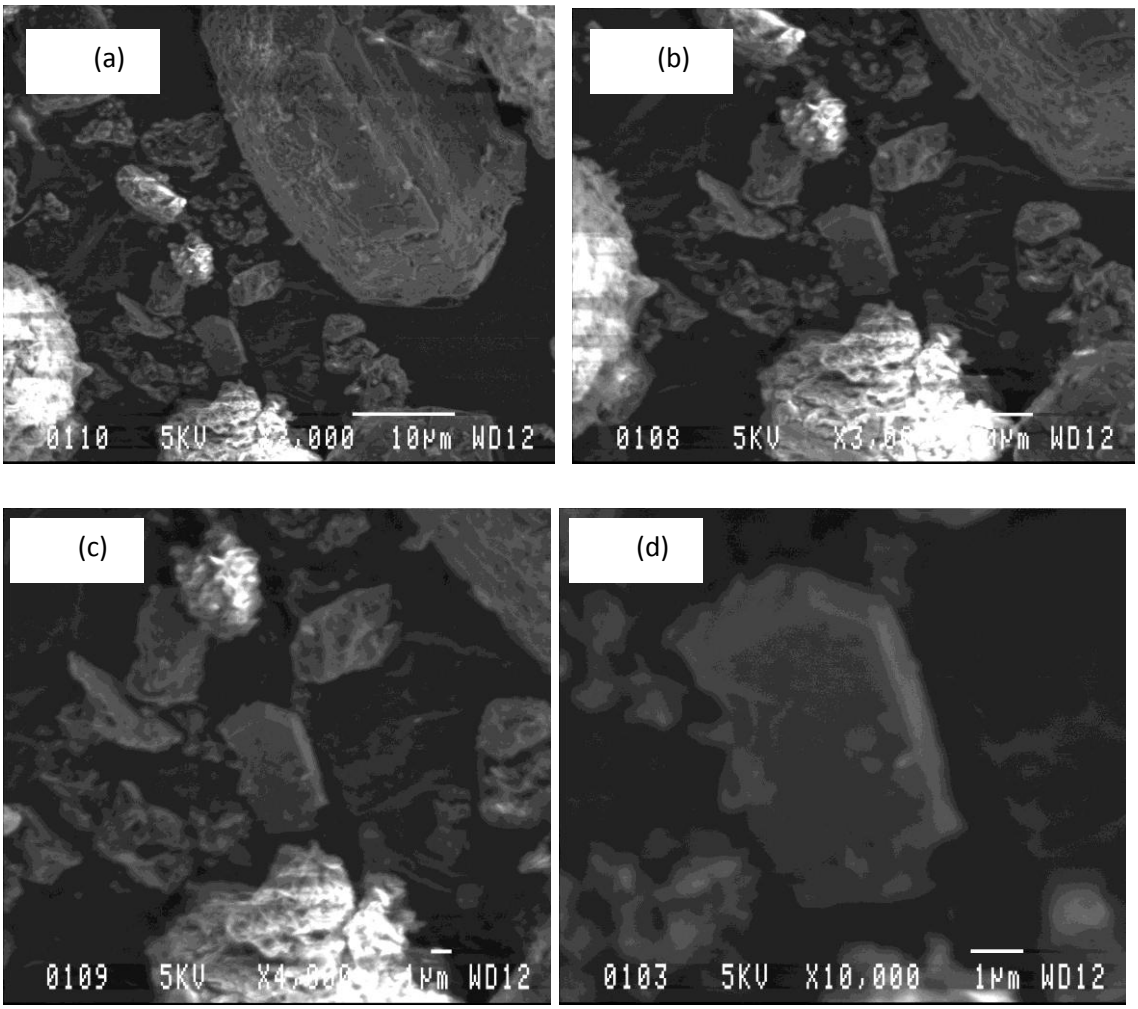


Figure 3.13 (a)-(d) SEM image for SAPO synthesized using TEAOH as a structure directing agent . at 200 ºC for 5 days. (a) magnification 2000, (b) magnification 3000, (c) magnification 4000 and (d) magnification 10000.

SEM micrographs revealed an irregular rectangular crystals in [(figure 3.13 (a-d)] at all magnifications also with amorphous materials. SAPO molecular sieves synthesized using piperidine and TEAOH structure directing agent s contain different morphology with pentagon and rectangular crystals. But when piperidine was used as structure directing agent in figure 3.10 (b)-(c), small pentagonal crystal of SAPO

molecular sieve was observed while for the SAPO catalyst prepared using TEAOH structure directing agent , crystals with bigger rectangular shape was observed..

Figure 3.14 shows the micrographs for Fe-SAPO-34 molecular sieve synthesized at 200 ºC for 5 days at different magnification like 2000, 7500, 10000 and 15000

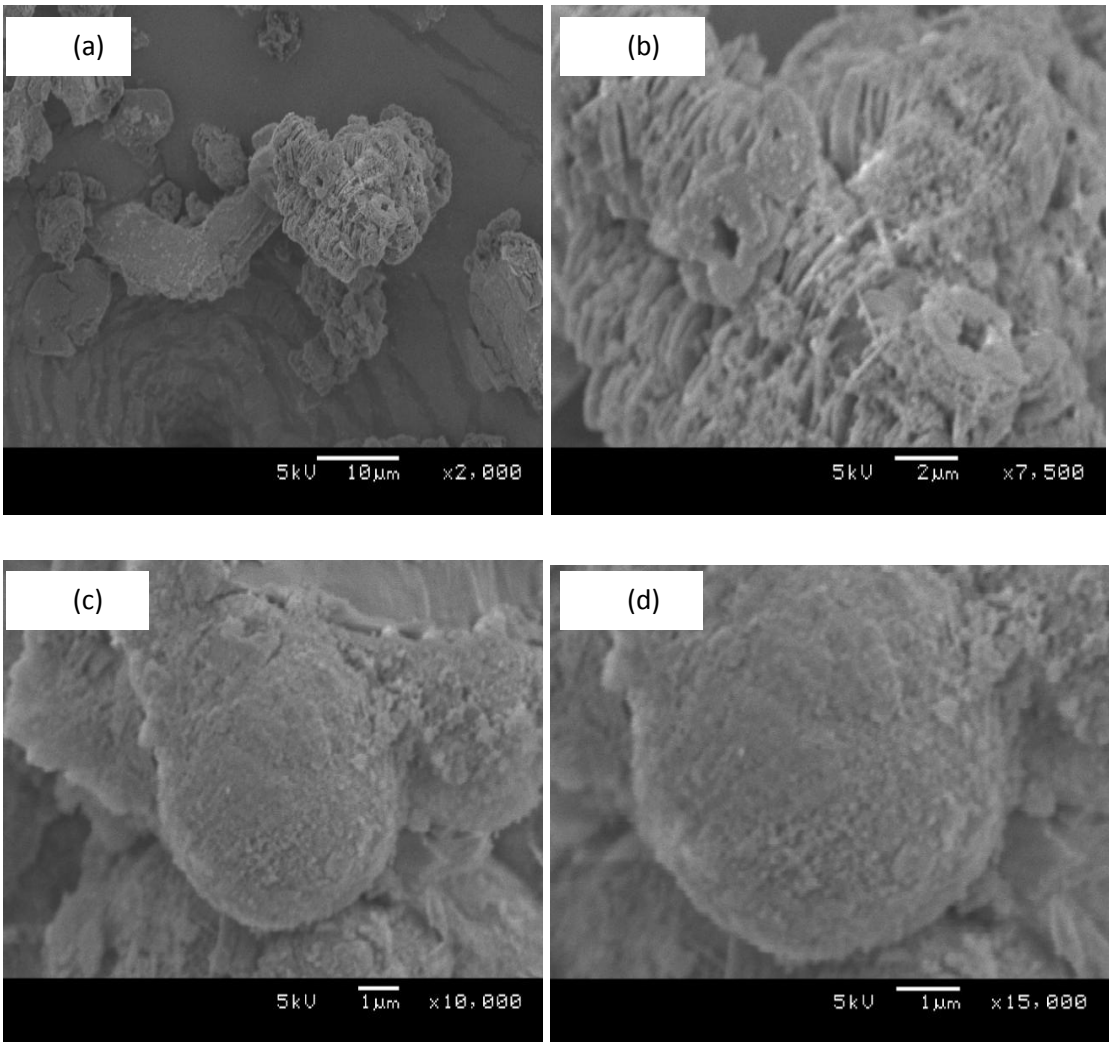


Figure 3.14 (a)-(d) SEM image for Fe-SAPO synthesized using piperdine as a structure directing agent at 200 ºC for 5 days at different magnification. (a) magnification 2000, (b) magnification 7500, (c) magnification 10000 and (d) magnification 15000.

SEM for Fe-SAPO catalyst in figure 3.14 revealed a mixture of two different materials. The first materials in [figure 3.14 (a)-(b)] with magnification of 2000 and 3000 show the groups of sliced crystals that indicate the presence of SAPO-11. The second material in [figure 3.14 (c)-(d)] with magnification of 10000 and15000 has small particles that form a spherical shape that indicate the presence of $AlPO_4$-5.

This finding is similar to the finding in literature [23] All crystals do not show the existence of SAPO-34. Fewer amounts of Si atoms were incorporated into AlPO framework and form SAPO-11. Fe atoms did not take part in the reaction.

Figure 3.15 shows the morphology of Co-SAPO molecular sieve at different magnification like 250, 4000, 5000 and 75000.

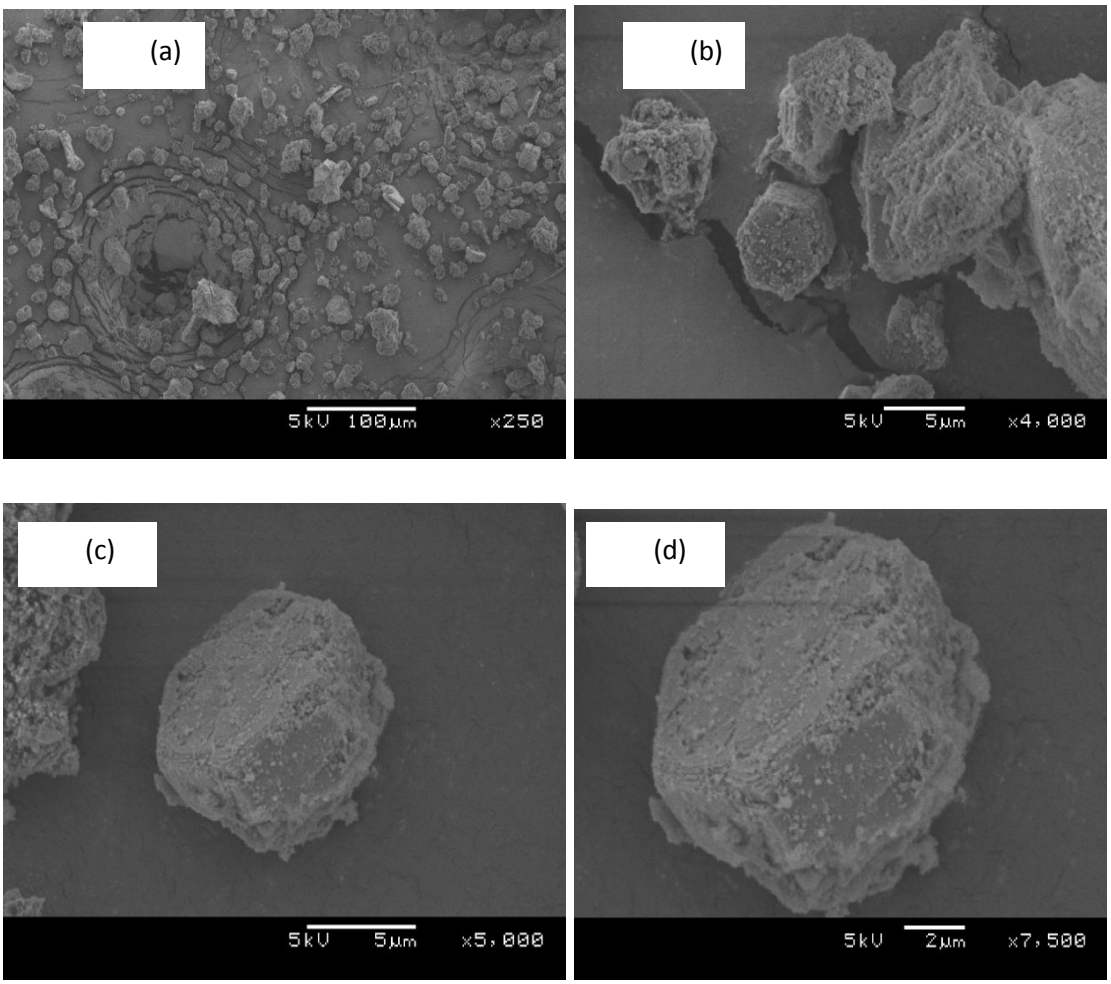


Figure .3.15 (a)-(d) SEM image for Co-SAPO synthesized using piperidine as a structure directing agent at 200 ºC for 5 days at different magnification. (a) magnification 250, (b) magnification 4000. (c) magnification 5000 and (d) magnification 7500.

SEM images for Co-SAPO molecular sieve show smallest particles in [figure 3.15 (a)] at magnification of 250. SEM images in [figure 3.15 (b)-(d)] at magnification 4000, 5000 and 7500 show similar particles with hexagonal crystals that has amorphous materials. When Co atoms are incorporated into SAPO framework, it

changes the structure of the molecular sieve and result in the formation of hexagonal crystals. These will need more than 5 days for Co-SAPO to develop into cubic crystals.

Figure 3.16 shows the micrographs for Ni-SAPO molecular sieve synthesized using piperidine structure directing agent at 200 ºC for 5 days at different magnification like 2000, 3000, 3000 and 4000

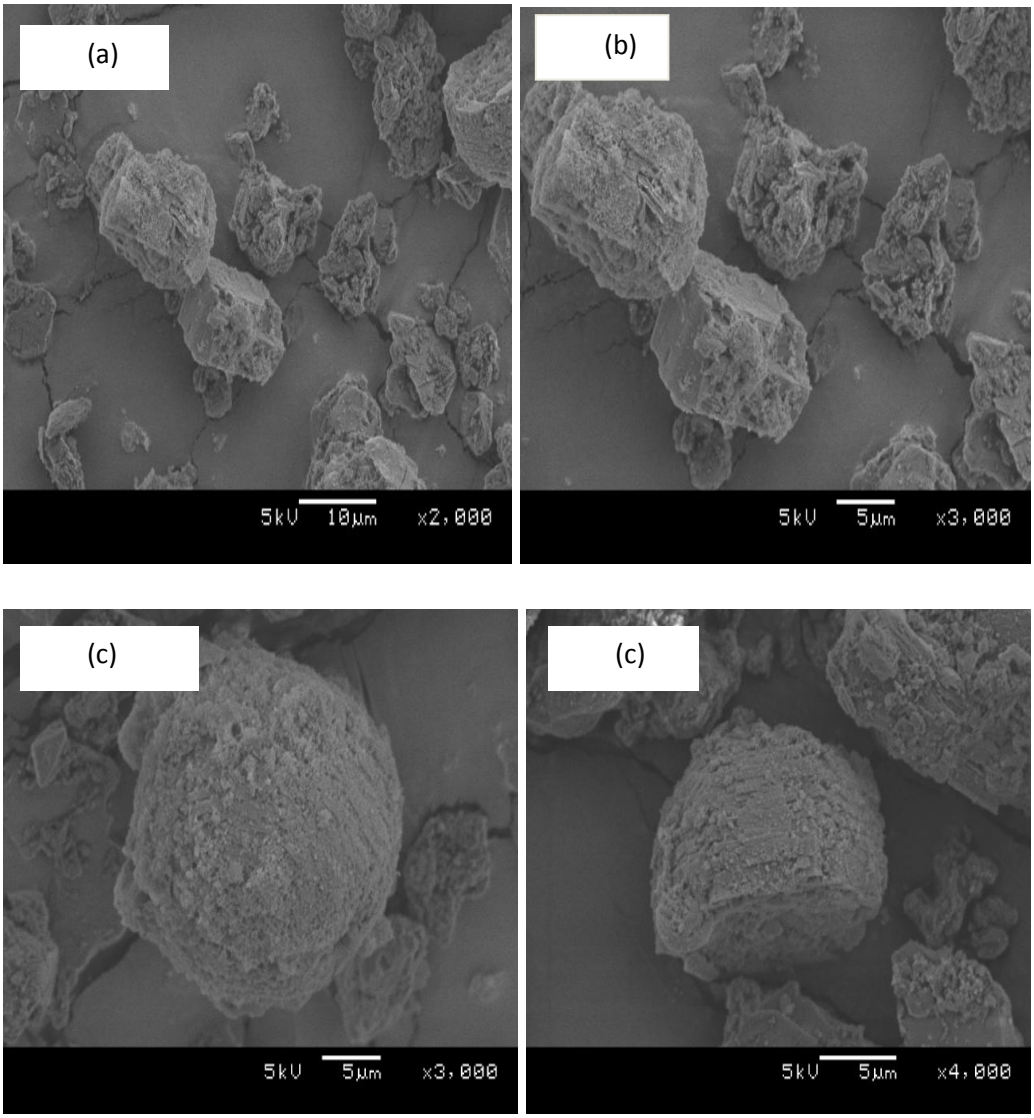


Figure 3.16 a)-(d) SEM image for Ni-SAPO synthesized using piperidine as a structure directing agent at 200 ºC for 5 days at different magnification. (a) Magnification 2000, (b) magnification 3000. (c) magnification 3000 and (d) magnification 4000.

SEM images of Ni-SAPO at different magnifications of 2000-4000 show two different materials in [figure 3.16 (a)-(d)]. Figure 3.16 (a)-(b) at magnifications 2000-3000

show the similar damaged cubic crystals with amorphous materials. These indicate the presence of Ni-SAPO when Ni atom is incorporated in to SAPO-34 framework, Ni react completely with silicoaluminophosphate and form cubic crystals Molecular sieve containing Ni atoms may be synthesized at low crystallization temperature in order to obtain the clear cubic crystals. Figure 3.16 (c)-(d) at magnifications 3000-4000 show the similar rough spherical materials that is different to the material in figure 3.16 (a)-(b)

3.3 NH_3-TPD

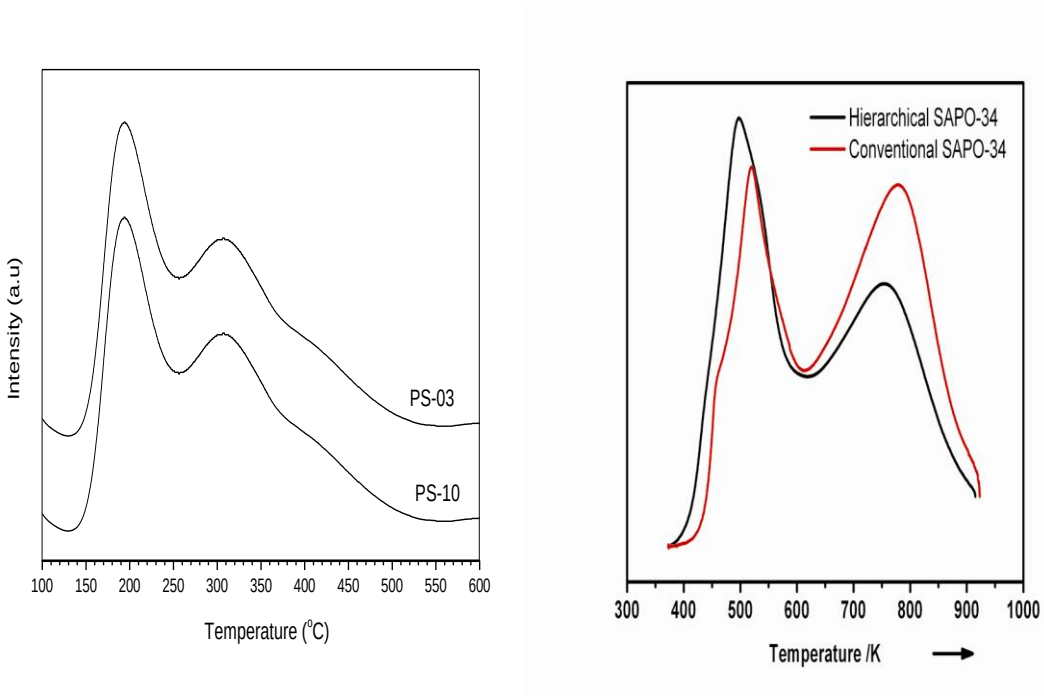
3.3.1 Introduction

The selected samples for SAPO molecular sieve were synthesized. The characterization of those molecular sieves using NH_3-TPD techniques were compared to the molecular sieve synthesized using piperidine as a structure directing agent, at 200 C for 5 days. The gel composition for this molecular sieve was 1.0 Al_2O_3: 0.6 P_2O_5:1.1 TEAOH: 0.8 SiO_2: 100 H_2O.

3.3.2 Results and discussion

3.3.2.1 Phosphorus content

NH_3-TPD profiles for the SAPO molecular sieve synthesized using piperidine as structure directing agent at 200 ºC for 5 days with P_2O_5/Al_2O_3 = 0.3 mole ratio (low phosphorus content). This molecular sieve was compared with the SAPO-34 molecular sieve with similar method of synthesis but has P_2O_5/Al_2O_3 = 0.6 mole ratio high phosphorus content). Figure 3.17 (a) and (b) shows the NH3-TPD profiles for the SAPO molecular sieves prepared in this study and the molecular sieve synthesizes elsewhere.



(a) **(b)**

Figure 3.17 (a) – (b). (a). The NH_3-TPD profile for lower (PS-10) and higher (PS-03) phosphorus content SAPO catalysts. (b) NH3--TPD spectra of various SAPO-34 [110]

Figure 3.17 (a) shows NH_3-TPD profile for SAPO molecular sieve prepared with lower and higher phosphorus contents (P_2O_5/Al_2O_3 = 0.3 and 0.6 molar ratios). NH_3-TPD profiles for the molecular sieves prepared in this study and a molecular sieve prepared by other researchers in figure 3.17 (a) and (b) looks similar and they both desorbed on the same regions. The first peak for desorption of ammonia appeared on the lower temperature region at 200 ^{0}C for all catalysts prepared with lower and higher phosphorus content. The peak is assigned to a weak Brønsted acid site for the (0.3 and 0.6) mole ratio samples. The second peak for desorption of ammonia appeared in the medium temperature regions between (250–350) ^{0}C for all catalysts. The peak is also assigned to weak Brønsted acid site. The peaks for the desorption of ammonia appears on the same region on the molecular sieves prepared in this study and on the molecular sieves prepared elsewhere [110].

3.3.2.2 Silicon content

Figure 3.18 shows NH_3-TPD profile for both low and silicon content samples.

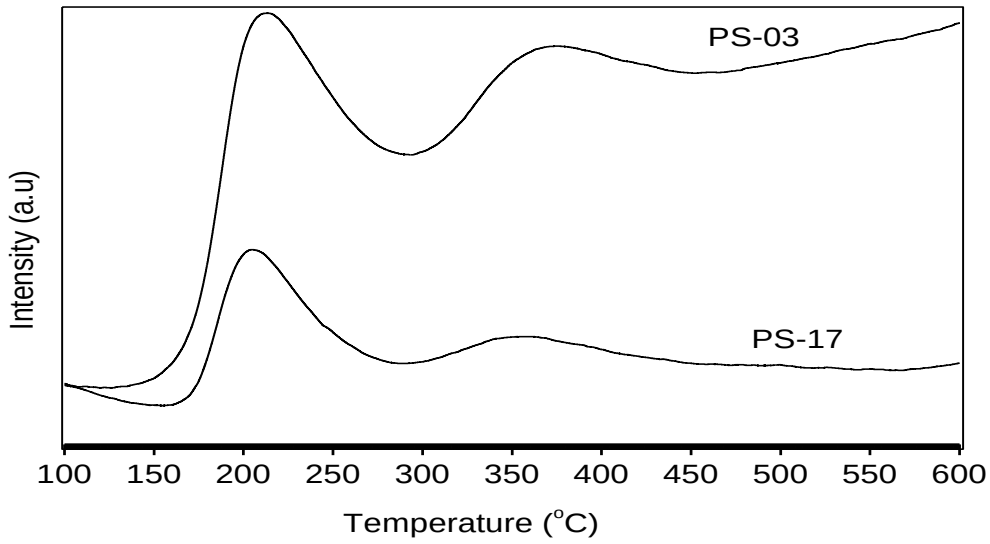


Figure 3.18 The NH3-TPD spectra for lower and higher silicon content SAPO.

The desorption peaks of the molecular sieves prepared with low and high silicon contents appeared in the same temperature region (temperature regions of (190 – 250) ^{0}C and the other one ranges from (340 - 380)^{0}C) but with different intensities. SAPOs molecular sieve prepared with lower silicon content has larger amount of Al acidity than the one for SAPO molecular sieve with high silicon contents. All the peaks are assigned to weak Brønsted acid site.

3.3.2.3 Structure directing agent s

Figure 3.19 illustrate the ammonia temperature programmed desorption of SAPO synthesized with piperidine and TEAOH structure directing agents.

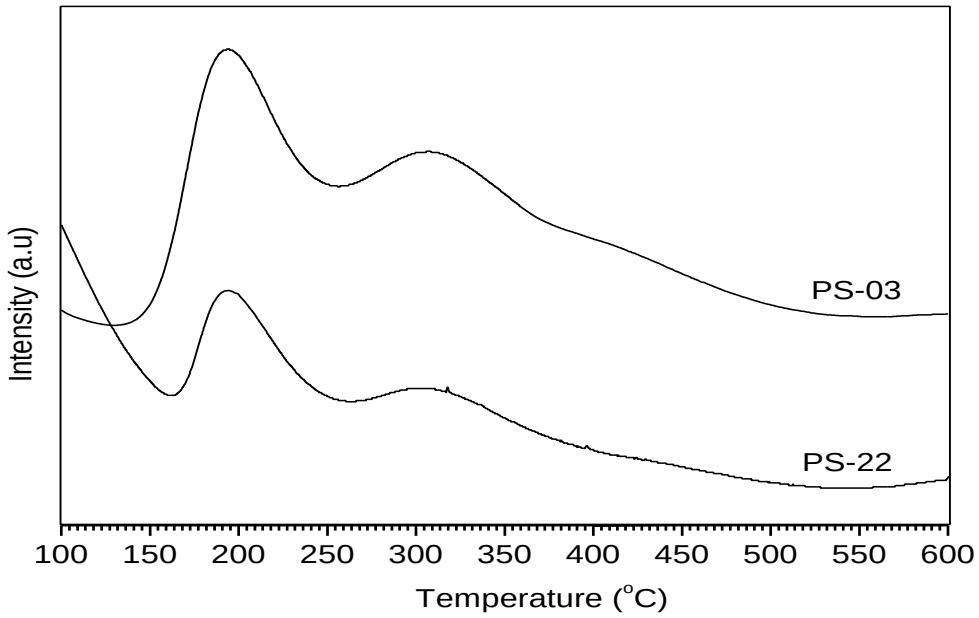


Figure 3.19 The NH_3-TPD profiles for SAPO made with Piperidine and TEAOH

In both catalysts, NH_3-TPD profile revealed desorption peak at lower temperatures and one at higher temperatures. These peaks are assigned to weak and medium Brønsted acid sites corresponding to those in the literature [2, 9, 87, 116, 120]. The first peak at temperature regions of (190 -250) ^{0}C arises from weak Brønsted acid sites and is attributed to hydroxyl groups attached to the centres of P-OH-Al and the second peak that ranges from (340 -380) ^{0}C arises from the bridge hydroxyl of –Si–(OHO)–Al group [121].

3.4. Solid state NMR spectroscopy (^{29}Si, ^{27}Al and ^{31}P)

3.4.1 Introduction

Two samples synthesized using piperidine as a structure directing agent, at 200 ºC for 5 days with the mole ratio SiO_2/Al_2O_3 = 0.80 and 2.4 were characterized using SS NMR spectroscopy (.^{29}Si, ^{27}Al and ^{31}P). The data was collected and analyzed.

3.4.2 Results and discussions

3.4.2.2 Solid states ^{29}Si NMR spectroscopy

Figure 3.20 Shows the ^{29}Si SSNMR spectra of SAPO molecular sieve with SiO_2/Al_2O_3 = 0.80 and 2.4.

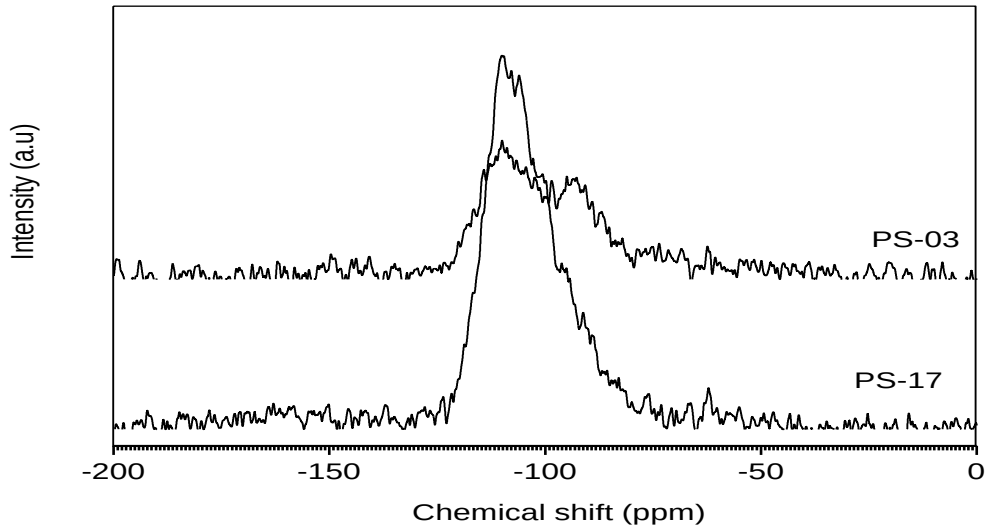


Figure 3.20 ^{29}Si SS NMR spectra of SAPO low and high silicon content

Two broad bands were seen with high intensities centred at the chemical shift of -95.19 and -110.44 ppm which are clearly distinguished. Those bands are assigned to the Si coordination states of Si (3Al) and Si (4Si) [1]. The chemical shift of -90 ppm, which accounts for Si substitution of only one P(SM2) to form a Si(4Al) coordination state [7], was not clearly distinguished because of the broadening of the peak (-120 to -80 ppm). This revealed the amorphous silicon and the other resonances that cannot be clearly seen. The Si atom was incorporated into the $AlPO_4$ framework by one substitution mechanism (SM3) where Si substituted for both Al and P atoms and gave rise to a negative charge framework of relatively strong acid sites [1, 24]. In the case of high silicon content, one broad peak at a chemical shift of -110 was observed. This peak is assigned to Si (4Si). Three integrated signals could be deconvolulet from the broad peak. Those bands are assigned to more Si coordination state of Si (3Al1Si), Si (2Al2Si) Si (1Al3Si) [92].

3.4.2.2 Solid states ^{27}Al NMR spectroscopy

Figure 3.21, Shows the solid state ^{27}Al NMR spectra for the low and high silicon content samples in the gel.

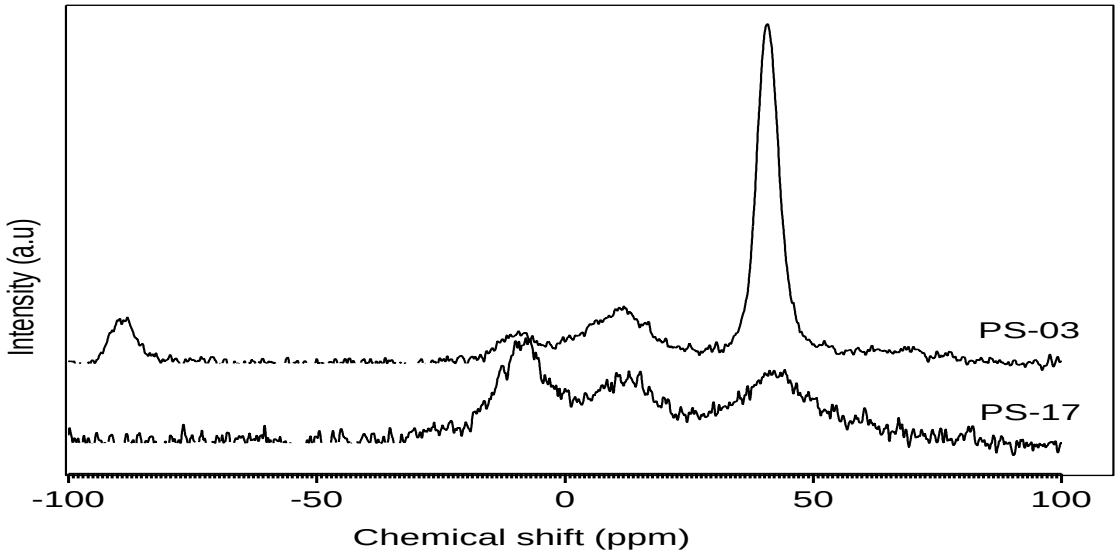


Figure 3.21. ^{27}Al SS NMR spectra of SAPO catalyst low and high silicon content.

^{27}Al NMR spectrum for the molecular sieve with low silicon content revealed one sharp with high peak intensity of the Al resonance at the chemical shift of 40.31 ppm that corresponds to a tetrahedral Al site. The two broad peaks with low intensities at the chemical shifts of 18.78 ppm and -13.81 ppm observed. These peaks are assigned to pentahedral and hexahedral coordination sites. The peaks are arising from the interaction of Al with extra-framework OH groups in the sieve cavities. A one small broad peak with low intensities at the chemical shift - 91.85 ppm arises from the amorphous Al species. ^{27}Al NMR spectrum for the high silicon contained in the gel showed three peaks at the chemical shifts of 41.05, 10.21 and -10.21 ppm that corresponds to tetrahedral, pentahedral and hexahedral Al sites. This finding is in agreement with the work reported by Wei *et al.* [44] and Vomscheid *et al*. [122]. Park *et al.* [123], suggested that the Al resonance at the chemical shift of 10 ppm is due to octahedral species.

3.4.2.3 Solid states NMR ^{31}P spectroscopy

Figure 3.22 presents the solid state ^{31}P NMR spectra for both low and high silicon containing samples in the gel.

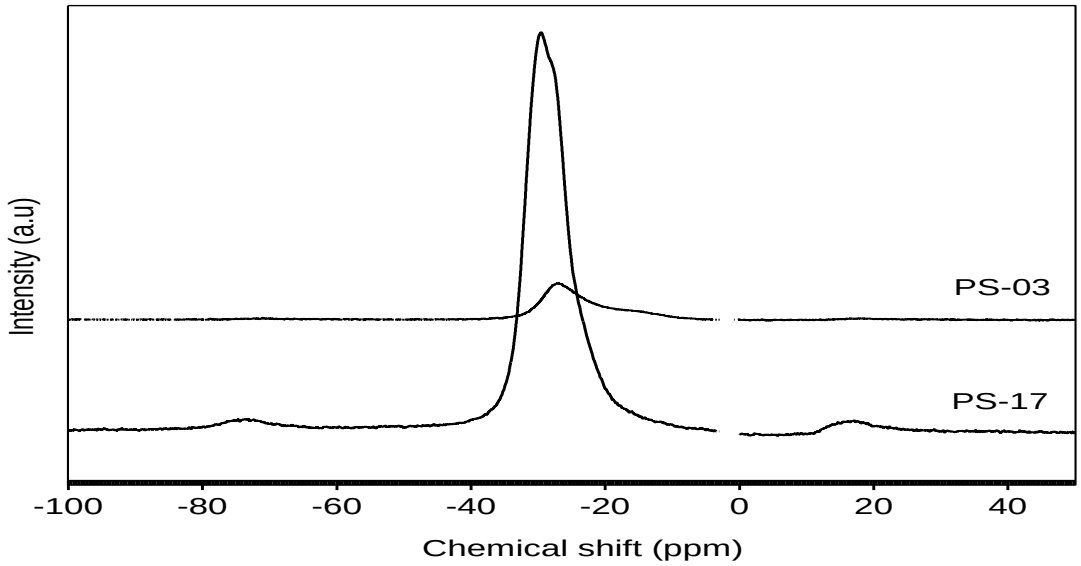


Figure 3.22. ^{31}P SS NMR spectrum of SAPO low and high silicon content

For the low silicon content, a broad high intensity peak appeared at the chemical shift of -30.03 ppm the P(4Al) environment and is attributed to tetrahedral phosphorous in the framework. It was discovered that the phosphorus amount in the low silicon content is very low which suggest that less P atoms were replaced by silicon atoms. The observations are related to the work in the literature [60, 99]. The other two small peaks that are shown with chemical shifts of -76.10 ppm and 15.37 ppm, arise from P (3Al, 1OH) [11].

3.3 Summary and Conclusions

The SAPO molecular sieve was synthesized using piperidine as structure directing agent at 200 ºC for 5 days. Among all molecular sieves synthesized at different temperatures ranges 170-210 ºC (PS-1 – PS-04), and time ranges 1-6 days (PS-03, PS-05 – PS-09. The XRD patterns for the molecular sieve that was synthesized at 200 ºC (PS-03) gave an evidence that the required crystallization temperature for SAPO-34 molecular sieve is 200 ºC. These molecular sieves were synthesized

within a short period of 5 days and have the small particle size of 1.49 nm. Molecular sieves were also synthesized at different P_2O_5/Al_2O_3 molar ratios range 0.3-0.7 (PS-10 – PS-12 and PS-03) XRD patterns suggested the structures of combined SAPO-5 and SAPO-34 at the P_2O_5/Al_2O_3 mole ratio of 0.3 and 0.6 (PS-10 and PS-03)

The XRD patterns confirmed the existence of both SAPO-5 and SAPO-34 phases in the same molecular sieves. Since the aim of this study is to synthesize SAPO-34 molecular sieve using piperidine as a SDA, pure SAPO-34 molecular sieve was not achieved due to the nature of a SDA. Therefore SAPO-34 should be synthesized for long period to increase the crystalline particle of this material

Two catalysts with high and low phosphorus contents (P_2O_5/Al_2O_3 mole ratio of 0.3 and 0.6 were made. Their particle sizes were similar. NH_3-TPD profiles for low and high phosphate content showed two peaks that appeared in the 190 ^{0}C to 250 ^{0}C and 340 ^{0}C-380 ^{0}C for the catalyst prepared with high amount of phosphate these peaks are assigned to weak Brønsted acid site

Solid state NMR spectra (^{29}Si, ^{27}Al and ^{31}P) and XRD revealed additional high coordination Al framework atoms when a high silicon content was used in the gel. Thus suggested that there was breakage of Al-O-P bonds by the structure directing agent and a new Si–O-Al bond was formed. The proposal is also revealed by the shift of XRD patterns from the $2\theta = 7.44^0$ in the low silicon to $2\theta = 9.99^0$ in the high silicon contained sample. This shows that there is no Si replacement by phosphorus. XRD profile showed the different patterns for all catalysts. It the patterns showed existence of SAPO-5 and SAPO-34 at the same time.

Solid state NMR spectroscopy (^{29}Si, ^{27}Al and ^{31}P) and XRD patterns both showed the additional high coordination of Al framework atoms for high silicon content in the gel. These suggest that there is breakage of Al-O-P bonds by the structure directing agent and a new of Si-O- Al bond is formed. The evidence is also revealed by the shift of XRD patterns from the 2 theta = 7.44^0 in the low silicon to 2 theta = 9.99^0 in the high silicon sample. This shows that there is no Si replacement by phosphorus. XRD patterns suggested SAPO-34 molecular sieve phase with the molar gel composition of Al_2O_3: 0.6 P_2O_5: 1.1 Pip: 2.4 SiO_2: 100 H_2O. and the existence of amorphous phase at the 2 theta scale ranges 13-32 º.

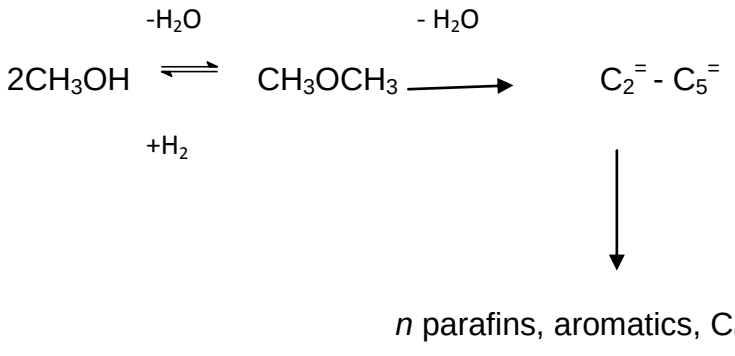
This work has demonstrated that the synthesis of SAPO-34 using piperidine as a structure directing agent results in the formation of Si-O-P and Si-O-Al, due to the substitution of Si atom by one P atom when low silicon content material was added to the gel. In the case of a high silicon sample, the formation of Si-O-P is avoided.

NH_3-TPD also showed evidence for two Brønsted acid sites in the catalyst framework. Weak acid sites that appeared on the lower temperature are assigned to P-OH hydroxyl groups, while the stronger acid site that appears at higher temperature is attributed to the bridging hydroxyl group – SiOHAl. More ethylene was produced from the weak acid sites and higher propylene is obtained from the stronger acid sites. The purpose of this study was to synthesize SAPO-34 molecular sieve using piperidine as SDA. The pure SAPO-34 phase was not successful, instead three phases of SAPO-5, SAPO-34 and amorphous were formed in the samples. This is due to the nature of the SDA used.

CHAPTER FOUR – Catalytic Test

4.1 Introduction

Methanol can be obtained by gasification, partial oxidation or steam reforming from raw materials such as biomass, coal and natural gas. SAPO-34 molecular sieves with micropores have evoked keen interest on the researchers. They are one of the best catalysts for the conversion of methanol to light olefins [92]. Methanol can be converted to dimethyl ether and water which can be processed at equilibrium catalytically to produce olefins. The chemical reaction steps of the methanol conversion to hydrocarbons can be summarized as follows:



n parafins, aromatics, C_6+ Olefins [2]

The production of light olefins from methanol on a SAPO-34 catalyst was investigated in this study. The factors that influence the methanol conversion to light olefins are catalyst crystallization time, the use of different structure directing agent s and the silicon content.

The formula used to calculate the concentration of each analyte from the GC data is as follows

$$C_{Anal\ i} = \frac{A_{Anali}}{FR_{Anali}}$$

Where $f_{RAnal\ i}$: carbon response factor of the analyte i, propane equivalent

$A_{Anal\ i}$: measured (displayed) value of the component i in mg C/m^3, FID calibrated with propane, with 1 ppm C_3H_8 = 1,61 mg C/m^3 under standard conditions (273 K, 1013 KPa), the area and the retention time data are contained in appendix C

$C_{Analy\ i}$: carbon concentration in mgC/m^3 of the measured analyte i. Table 4.1 was used to calculate concentration of the analyte. The concentrations of the analytes

were calculated using response factors form the literature [124]. Since FID was used in this work.

Table 4 1 Response factors (propane equivalent) determined by TÜV-Nord using two J.U.M. FID´s, Model VE 7, the FID 2 was tested 9 months after the FID 1.

Analytes	Molecular formula	Response factor for FID 2	Response factor FID 1
1,1,1-Trichlorethane	$C_2H_3Cl_3$	1.06	1.02
Trichlorethene	C_2HCl_3	1.03	1.01
Toluene	C_7H_8	1.02	1.03
Tetrachlorethylene	C_2Cl_4	1.22	1.20
iso-Propanol	C_3H_8O	0.82	0.81
Propane	C_3H_8	1.00	1.00
iso-Octane	0,99	0.98	0.97
Methanol	CH_4O	0.69	0.68
Methane	CH_4	1.26	1.25
n-Hexane	C_6H_14	0.85	0.86
n-Heptane	C_7H_{16}	0.91	0.95
4-Ethyl	Toluene	0.88	0.89
Ethanol	C_2H_6O	0.65	0.67
Isobutyl	Acetate	0.88	0.89
Acetate	$C_4H_8O_2$	0.70	0.72
Acid	$C_2H_4O_2$	0.58	0.55
Ether	$C_4H_{10}O$	0.75	0.77
Chloride	CH_2Cl_2	1.09	1.06
Chloroform	$HCCl_3$	0.82	0.78
Chlorbenzene	$C_6H_5_Cl$	1.01	1.04
n-Butane	C_4H_{10}	0.98	0.98
Benzene	C_6H_6	1.05	1.05
Acetylene	C_2H_2	0.92	0.94
Acetone	C_3H_6	0.72	0.73
Pentane	C_3H_{12}	0.98	0.97

Table 4.2 Retention time and response factor for hydrocarbons.

Hydrocarbons	Symbol	Retention Time (min)	Response Factor
Methane	C_1^-	0.68	1.26
Ethylene	$C_2^=$	2.44	1.01
Ethane	C_2^-	3.39	1.01
Propylene	$C_3^=$	8	1
Propane	C_3^-	9.3	1
DME	DME	9.9-10.8	0.69
MEOH	MeOH	11.2	0.69
Butylene	$C_4^=$	12	0.98
Butane	C_4^-	13	0.98
Pentylene	$C_5^=$	15.37	0.98
Pentane	C_5^-	16.34	0.98
Hexylene	$C_6^=$	18.34	0.85
Hexane	C_6^-	19.06	0.85
Heptylene	$C_7^=$	20.67	0.91
Heptane	C_7^-	21.44	0.91
Octylene	$C_8^=$	22.28	0.36
Octane	C_8^-	23.38	0.36

The Mol (M) is the concentration of that analyte in mol per minute multiplied by flow rate of the analyte in ml per minute. The calculations for % methanol and the selectivity of the analytes are shown in appendix D.

4.2 Results and Discussion

4.2.1 The effects of crystallization temperature on the MTO reactions

A series of experiments were conducted at 400 ^{o}C for one hour. Methanol was bubbled over and carried by nitrogen gas into a reactor. The reactions were performed on SAPO acid catalyst crystallized at temperatures from 170 ^{o}C to 210 ^{o}C. The table 4.3 indicates a summary of methanol conversion, particle size and product distribution of hydrocarbons from the catalysts synthesized in the temperature range from 170 -210 ^{o}C.

Table 4.3 Summary of % methanol conversion, particle size and products distribution of hydrocarbons of catalysts synthesized at temperature ranges from 170 ^{o}C-210 ^{o}C.

Sample	PS-01	PS-02	PS-03	PS-04
Crystallization temperature (^{o}C)	170	190	200	210
Particle size (nm)	1.49	4.3	1.49	1.49
Methanol conversion (mol %)	94	93	93	90
Reaction temperature (^{o}C)	400	400	400	400
TOS (h)	1	1	1	1
Hydrocarbons	Products distribution (mol %)			
C_2=	0.04	0.016	2.24	0.016
C_3=	0.05	0.001	1.68	0.019
C_4=	0	5.806	1.32	0
C_5=	0	0	1.65	0
C_6=	0	0	0.65	0
C_7=	0	0.040	0	0
C_8=	0	0	0	0
DME	46.21	60.987	5.36	52.250
MeOH	21.17	30.760	48.93	20.320
C1	0.40	0	0.70	0.141
C_2	0	0.003	0	0
C_3	0	0	0	0
C_4	0	1.955	0.56	0
C_5	0.03	0	0.79	0
C_6	0	0	1.30	0
C_7	6.19	0.423	0	0
C_8	0	0	0	0
Others	25.90	0	34.81	26.66

4.2.1.1 The effects of crystallization temperature on % methanol conversion

Figure 4.1 shows the effect of crystallization temperature for the molecular sieves (PS-01 – PS-04) on the % methanol conversion.

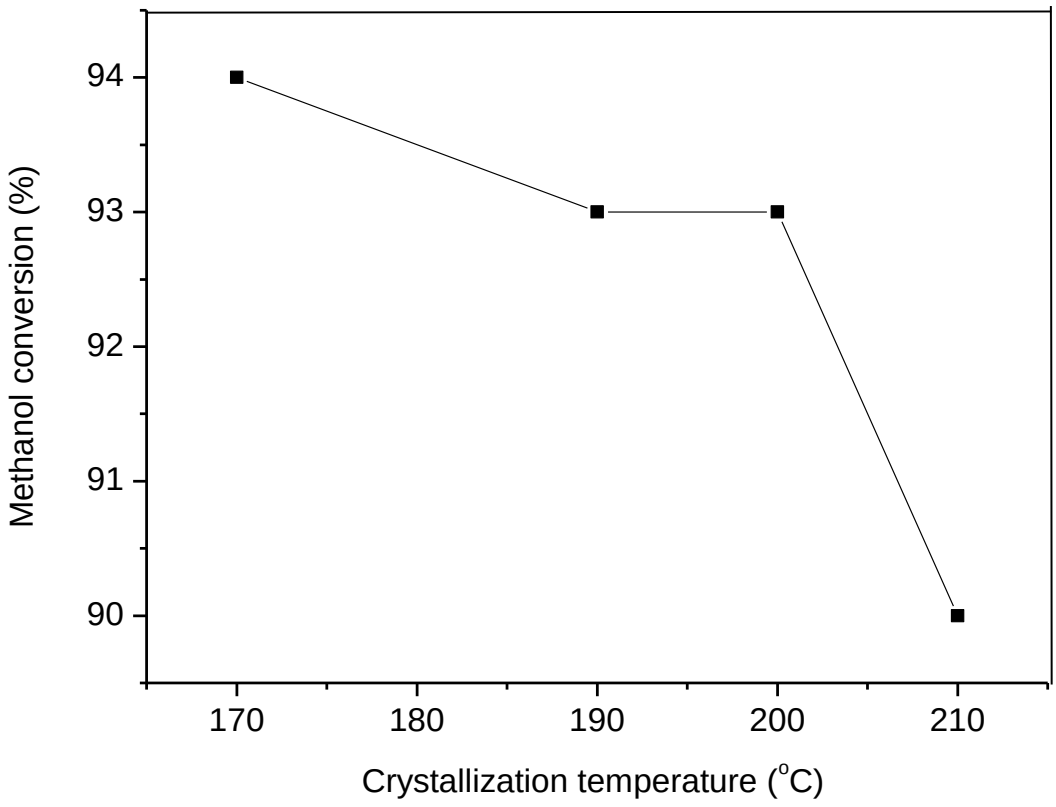


Figure 4.1 The effect of crystallization temperature of SAPO molecular sieve (PS-01-PS-04) on % methanol conversion at 400 ºC for 1 hour.

The results from figure 4.1 indicated high % methanol conversions between (90 % and 94 %). The % methanol conversion of a sample PS-01 made at 170 ºC is high, and then became constant from 190 - 200 ºC for samples PS-02 – PS-03. The % methanol conversion was low at 210 ºC for sample PS-04. The % methanol conversion decreased with increasing crystallization temperature. Thus, suitable crystallization temperature for methanol conversion is from 170 – 200 ºC.

4.2.1.2 The effects of crystallization temperature on light olefins.

Figure 4.2 shows the effect of crystallization temperature for the molecular sieves (PS-01 – PS-04) on the ethylene, propylene and butylene selectivity.

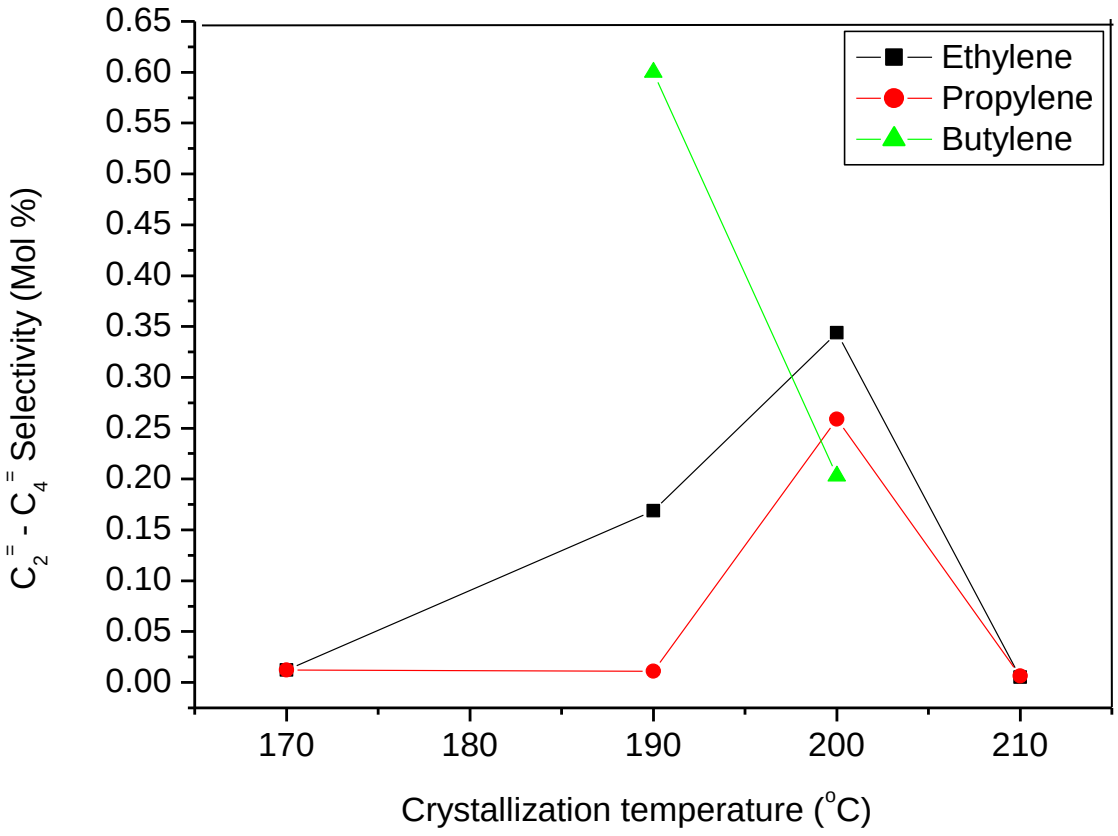


Figure 4.2 The effect of crystallization temperature of SAPO molecular sieve on light olefins selectivity at 400 ºC for 1 hour.

Ethylene and propylene selectivity increased from 0.03 – 0.35 mol % with an increase in crystallization temperature from 170 - 200 ºC (PS-01 – PS-03) and decreased at 210 °C (PS-04) in figure 4.2. However, high amount of butylenes 0.60 mol % was observed at the crystallization temperature of 190 °C and then decreased to 0.17 mol % at 200 ºC. No trace of light olefins was observed at crystallization temperatures of 170 °C and 210 °C.

4.2.1.3 The effects of crystallization temperature on product distribution of hydrocarbons.

The effects of crystallization temperature on product distribution of hydrocarbons are shown in figure 4.3. The product distribution in figure 4.3 ranges from 0 % to 100 %.

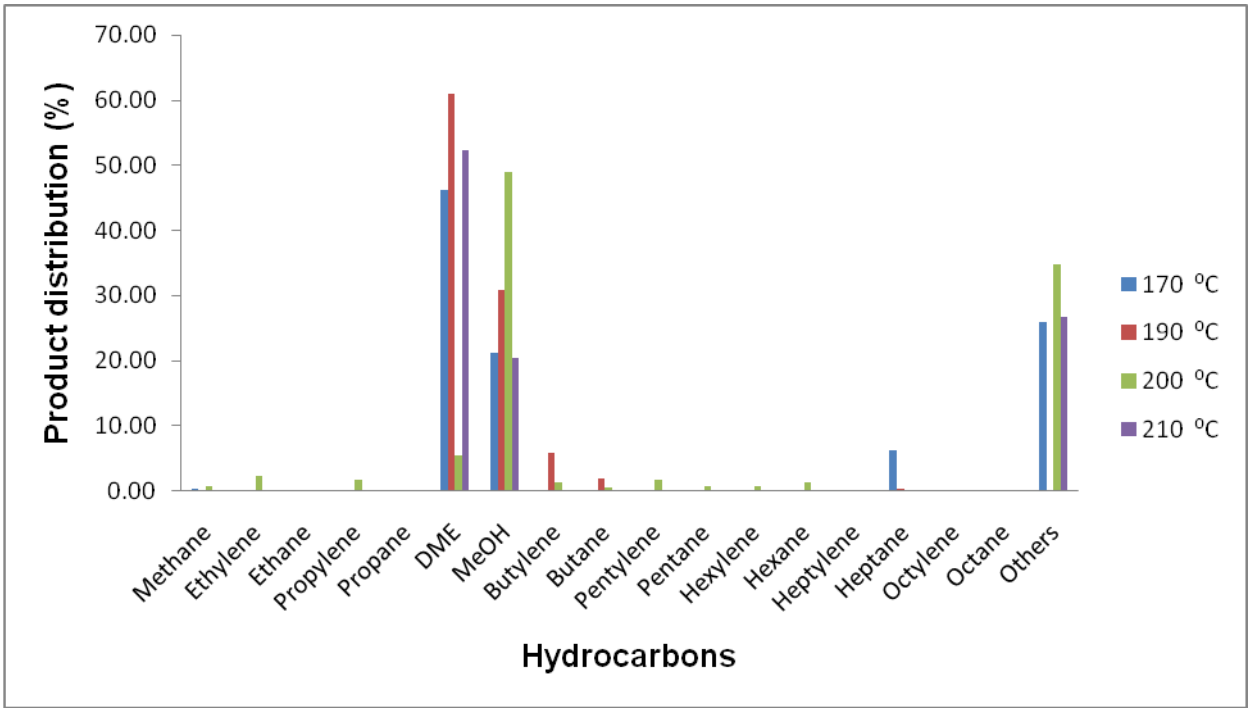


Figure 4.3 The effect of crystallization temperature of SAPO molecular sieve PS-01 – PS-04 on product distribution of hydrocarbons from 0 - 100 % at 400 °C reactor temperature for 1 hour.

The graph shown in figure 4.3 indicates that the major products obtained at different crystallization temperatures 170 - 210 ^{0}C are DME, MeOH and other hydrocarbons. Since DME and MeOH are regarded as reactants for the first and second step reactions [75]. Lower hydrocarbons were obtained in fewer amounts.

The effects of crystallization temperature on product distribution of hydrocarbons are shown in figure 4.4. The product distribution in figure 4.3 ranges from 0 % to 10 %.

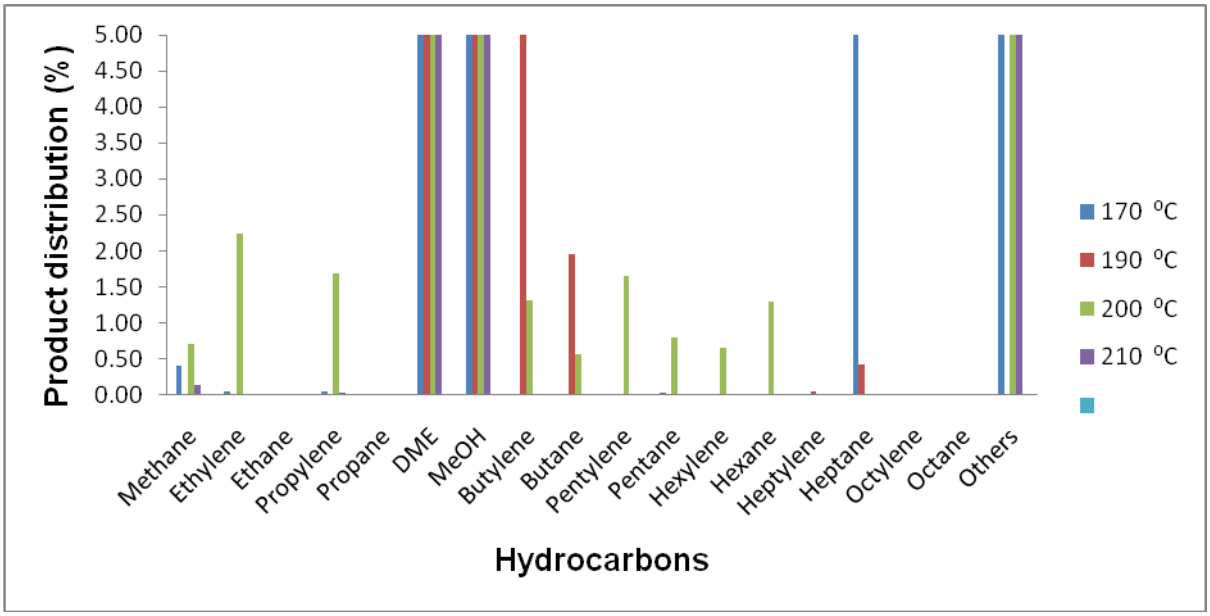


Figure 4.4 The effect of crystallization temperature of SAPO molecular sieve on product distribution of hydrocarbons from 0 -100 % at 400 ºC for 1 hour.

Figure 4.4 shows the effect of crystallization temperature of SAPO molecular sieve on product distribution of hydrocarbons from 0 -100 % at 400 ºC for 1 hour. The products such as ethylene and propylene are produced in larger quantities than butylene on the catalyst synthesized at 200 ^{0}C. The product distribution of pentylene is higher than that of hexylene and the others.

4.2.1.4 The relationship between the characterization of SAPO molecular sieve and the MTO reaction.

XRD patterns for the catalyst prepared at different crystallization temperatures were discussed in 3.2.

The particle sizes of the catalysts are similar 1.49 nm for the molecular synthesized at 170 and 200 ^{o}C, and different particle size 4.3 nm for the molecular sieve synthesized at 190 ^{o}C. Molecular sieve prepared at 210 ^{o}C did not show any peak. This is also confirmed by the XRD patterns. The product distribution for hydrocarbons on all catalysts differs from one another of the one hour time on stream. A large amount of butylene products selectivity was observed from the catalyst prepared at the crystallization temperature of 190 ^{o}C. An important reaction

is the incomplete dehydration of dimethyl ether to light olefins. Only small amount of light olefins were obtained from all the catalysts. The best product distribution of hydrocarbons was shown for the catalyst prepared at a crystallization temperature of 200 ^{o}C.

4.2.1.5 Conclusions

All samples of molecular sieves were tested in MTO for only 1 hour; the purpose was to check the suitable crystallization temperature for the light olefins selectivity. It was found that the selectivity of ethylene and propylene was high on the molecular sieve prepared at the crystallization temperature of 200 ^{0}C and only butylenes selectivity was high at the crystallization temperature of 190 ^{0}C. Thus molecular sieve prepared at the crystallization temperature of 200 ^{0}C is suitable for light olefins. Teresa [57], investigated the effects on the acidic molecular sieve activity in the MTO reactions. Molecular sieve was synthesized using different organic templates at the temperature ranging 150-200 ^{0}C. DME was the major product in MTO reaction with high methanol conversion. Light olefins selectivity was very much high ranging 70-90 %. This molecular sieve has shown only one phase of SAPO-34 without amorphous phase. Similar problem from our study is that in all molecular sieves, DME is a major product. Ethylene and propylene selectivity is very low. This is because of the amorphous phase which is present in all molecular sieves that prevent the formation of light olefins.

4.2.2 The effects of crystallization time.

The SAPO molecular sieve catalysts prepared at different crystallization times (short to long period) were tested in MTO at the reactor temperature of 400 ^{o}C for 5 hours. The effects of crystallization time on particle size, % methanol conversion and product distribution of hydrocarbons are shown in table 4.4

Table 4.4 Summary of % methanol conversion, particle size and products distribution of hydrocarbons of catalysts synthesized in different days (2-6).

Sample					PS-06					PS-07					PS-08
Crystallization time (Days)					2					3					4
Particle size (nm)					1.49					4.3					1.49
Methanol conversion (Mol %)	100	96	96	75	69	84	80	60	66	54	78	98	96	97	86
Reaction temperature (^{0}C)	400	400	400	400	400	400	400	400	400	400	400	400	400	400	400
TOS (h)	1	2	3	4	5	1	2	3	4	5	1	2	3	4	5
Hydrocarbons															
C_2=	1.61	0.34	0.19	0.05		0.10	0.01	0.03	0.03	0.07	0.08	0.62	0.005	0	0
C_3=	0.86	0.28	0.15	0.07	0.05	0.02	0.02	0.02	0.03	0.09	0.13	1.87	0.009	0	0
C_4=	2.7	0.7	0	0	0	0.30	0	0	0.04	0	0.26	0.57	0	0	0
C_5=	0.42	0.15	0	0	0	0	0	0	0	0	0.05	0.08	0	0	0
C_6=	40.5	0	0	0	0	0	0	0	0	0	0.29	0.19	0	0	0
C_7=	0	0	0	0	0	0	0	0	0	0	0.80	0	0	0	0
C_8=	0	0	0	0	0	0	0	0	0	0	0	0	0	0	0
DME	36.4	2.88	2.8	0.89	4.75	26.12	87.21	29.56	18.06	64.43	90.59	95.31	99.550	99.56	91.69
MEOH	8.22	88.09	86.62	95.86	88.46	60.26	10.24	65.74	74.83	34.74	6.21	0.39	0.437	0.44	8.31
C1	0.61	0.74	0.79	0.21	0	0.43	0.06	0.19	0.26	0.67	0.05	0.21	0	0	0
C_2	0.22	0.089	0.006	0	0	0.01	0	0	0	0	0	0.71	0	0	0
C_3	5.6	0.52	0.21	0	0	0	0	0	0	0	0.07	0.06	0	0	0
C_4	1.01	0.22	0	0	0	0.39	0	0	0	0	0.13	0	0	0	0
C_5	1.89	5.91	0.158	0	0	5.82	0	0	0	0	0.05	0	0	0	0
C_6	0	0	9.07	2.91	6.68	0	0	0	0	0	0.37	0	0	0	0
C_7	0	0	0	0	0	0	0.41	0.64	6.75	0	0.93	0	0	0	0
C_8	0	0	0	0	0	0	0	0	0	0	0	0	0	0	0
Others	0	0	0	0	0	0	0	0	0	0	0	0	0	0	0

Table 4.4 continue

Sample					PS-06					PS-07					PS-08
Crystallization time (Days)					2					3					4
Particle size (nm)					1.49					4.3					1.49
Methanol conversion (Mol %)	100	96	96	75	69	84	80	60	66	54	78	98	96	97	86
Reaction temperature (^{o}C)	400	400	400	400	400	400	400	400	400	400	400	400	400	400	400
TOS (h)	1	2	3	4	5	1	2	3	4	5	1	2	3	4	5
Hydrocarbons															
C_2=	1.61	0.34	0.19	0.05		0.10	0.01	0.03	0.03	0.07	0.08	0.62	0.005	0	0
C_3=	0.86	0.28	0.15	0.07	0.05	0.02	0.02	0.02	0.03	0.09	0.13	1.87	0.009	0	0
C_4=	2.7	0.7	0	0	0	0.30	0	0	0.04	0	0.26	0.57	0	0	0
C_5=	0.42	0.15	0	0	0	0	0	0	0	0	0.05	0.08	0	0	0
C_6=	40.5	0	0	0	0	0	0	0	0	0	0.29	0.19	0	0	0
C_7=	0	0	0	0	0	0	0	0	0	0	0.80	0	0	0	0
C_8=	0	0	0	0	0	0	0	0	0	0	0	0	0	0	0
DME	36.4	2.88	2.8	0.89	4.75	26.12	87.21	29.56	18.06	64.43	90.59	95.31	99.550	99.56	91.69
MEOH	8.22	88.09	86.62	95.86	88.46	60.26	10.24	65.74	74.83	34.74	6.21	0.39	0.437	0.44	8.31
C1	0.61	0.74	0.79	0.21	0	0.43	0.06	0.19	0.26	0.67	0.05	0.21	0	0	0
C_2	0.22	0.089	0.006	0	0	0.01	0	0	0	0	0	0.71	0	0	0
C_3	5.6	0.52	0.21	0	0	0	0	0	0	0	0.07	0.06	0	0	0
C_4	1.01	0.22	0	0	0	0.39	0	0	0	0	0.13	0	0	0	0
C_5	1.89	5.91	0.158	0	0	5.82	0	0	0	0	0.05	0	0	0	0
C_6	0	0	9.07	2.91	6.68	0	0	0	0	0	0.37	0	0	0	0
C_7	0	0	0	0	0	0	0.41	0.64	6.75	0	0.93	0	0	0	0
C_8	0	0	0	0	0	0	0	0	0	0	0	0	0	0	0
Others	0	0	0	0	0	0	0	0	0	0	0	0	0	0	0

4.2.2.1 The effects of crystallization time on % methanol conversion.

Figure 4.5, shows the % methanol conversion vs. time on stream on the molecular sieve synthesized at 200 ^{o}C in different days.

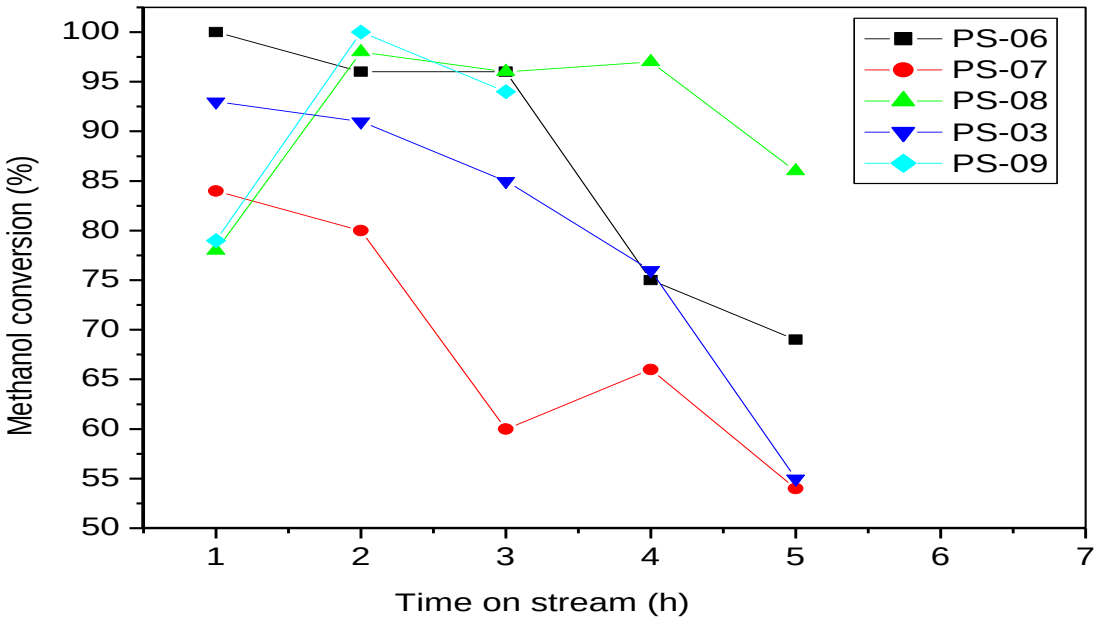


Figure 4.5 The effect of crystallization time of SAPO molecular sieve on % methanol conversion at 400 ºC for 5 hour.

According to results in figure 4.5, % methanol conversion fluctuated in odd (2-6 days) and even (3-5) no of days. The % methanol conversion increased from short period (2 days) to long period (6 days) but then decreased on the third hour with the time on stream in an odd pattern. The % methanol conversion increased from 3 days to 5 days and % methanol conversion decreased with an increase in time on stream.

4.2.2.2 The effects of crystallization time on light olefins.

Figure 4.6 shows the effect of crystallization time of molecular sieve synthesized at 200 ºC in different days on the ethylene.

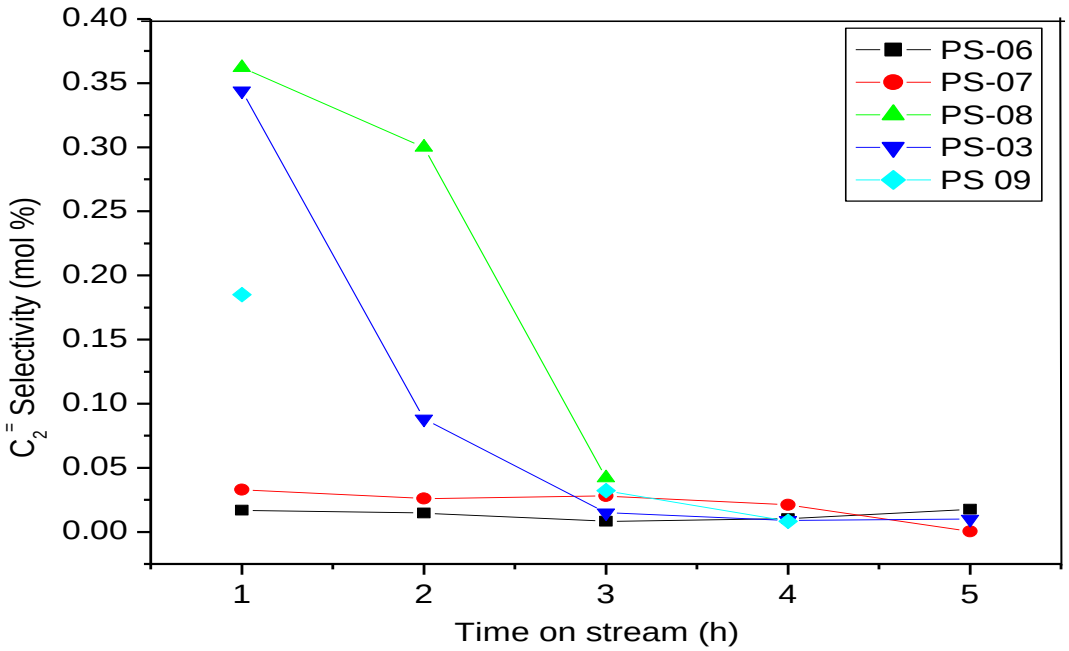


Figure 4.6 The effect of crystallization time of SAPO molecular sieve on ethylene selectivity at 400 ºC for 5 hour.

Figure 4.6 shows the effect of crystallization time of SAPO molecular sieve on ethylene selectivity at 400 ºC for 5 hour.The ethylene selectivity on the molecular sieve synthesized within 4 and 5 days is high 0.35 and 0.36 mol % on the 1st hour of reaction time, and then decreased gradually on the 2nd and 3rd hour. The amounts of ethylene remain constant from the 3rd to the 5th hour. The amount gradually decreased as the time on stream increased. The ethylene selectivity is low on the molecular sieve synthesized at 200 ºC for short period 2 - 3 days. The amount of ethylene remains constant from the 1st to 5th hour. SAPO molecular sieve synthesized for 6 days is highly active on the 1st hour, in active on the 2nd hour and became less active from the 3rd to the 4th hour. Thus ethylene selectivity decreases as the % methanol conversion decreased in time on stream. The SAPO molecular sieves synthesized for 4 and 5 days are suitable for the good ethylene selectivity. The MTO reaction should be done for only 1 hour at 400 ºC.

Figure 4.7 shows the effect of crystallization time of molecular sieve synthesized at 200 ºC in different days on the propylene selectivity, at the reaction temperature 400 ºC for 5 hour.

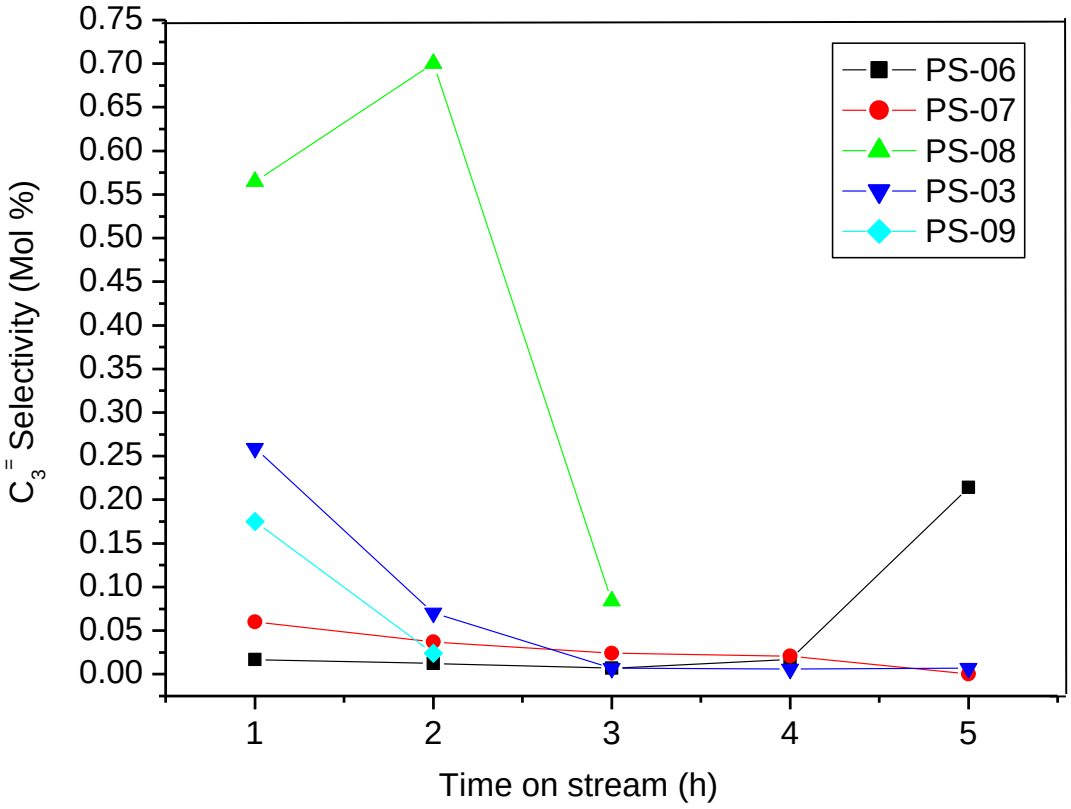


Figure 4.7 The effects of crystallization time of SAPO-34 molecular sieve on propylene selectivity at 400 ºC for 5 hour.

The results in figure 4.7 show the effects of crystallization temperature of SAPO-34 molecular sieve on propylene selectivity. The propylene selectivity was high on the molecular sieve synthesized for 4 days on the 1st and 2nd hours 0.55 and 0.73 mol %, and then decreased suddenly on the 3rd hour to 0.08 mol %. The amount of propylene on the molecular sieve synthesized within 5 and 6 days was lower than the amount of propylene on the molecular sieve synthesized for 4 days. Propylene selectivity remains low on the molecular sieve synthesized within short period from 2 – 3 days. Thus propylene selectivity decreases as the % methanol conversion decreased in time on stream. The suitable SAPO-34 molecular sieve for good propylene selectivity is the one that was synthesized within 4 days. This molecular sieve is more active on the 1st and 2nd hour and became less active on the 3rd hour. Molecular sieve synthesized for 6 days is active on the 1st and 2nd hour. The amount of propylene decreased gradually in time on stream.

Figure 4.8 shows the effect of crystallization time of molecular sieve synthesized at 200 ºC in different days on the butylene selectivity, at the reaction temperature 400 ºC for 5 hour.

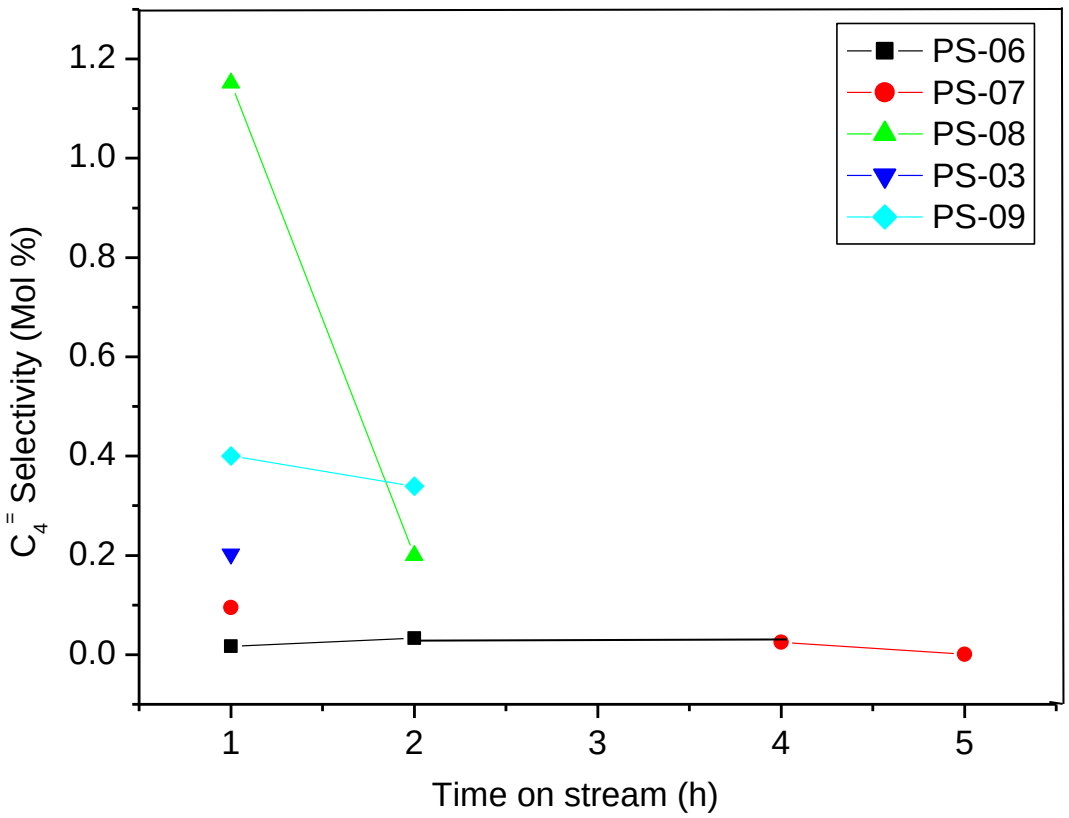


Figure 4.8 The effect of crystallization time of SAPO molecular sieve on butylenes selectivity at 400 ºC for 5 hour.

From figure 4.8 FID detected large amounts of butylenes at the crystallization time of 4 days for the 1st hour. The amount suddenly decreased as the time on stream increased to 2 hours. Butylene can only be detected in the first two hours and decreased with an increase in time on stream.

4.2.2.3 The effects of crystallization time on product distribution of hydrocarbons.

The effects of crystallization time on product distribution of hydrocarbons are shown in figure 4.9. The product distribution in figure 4.3 ranges from 0 % to 100 %.

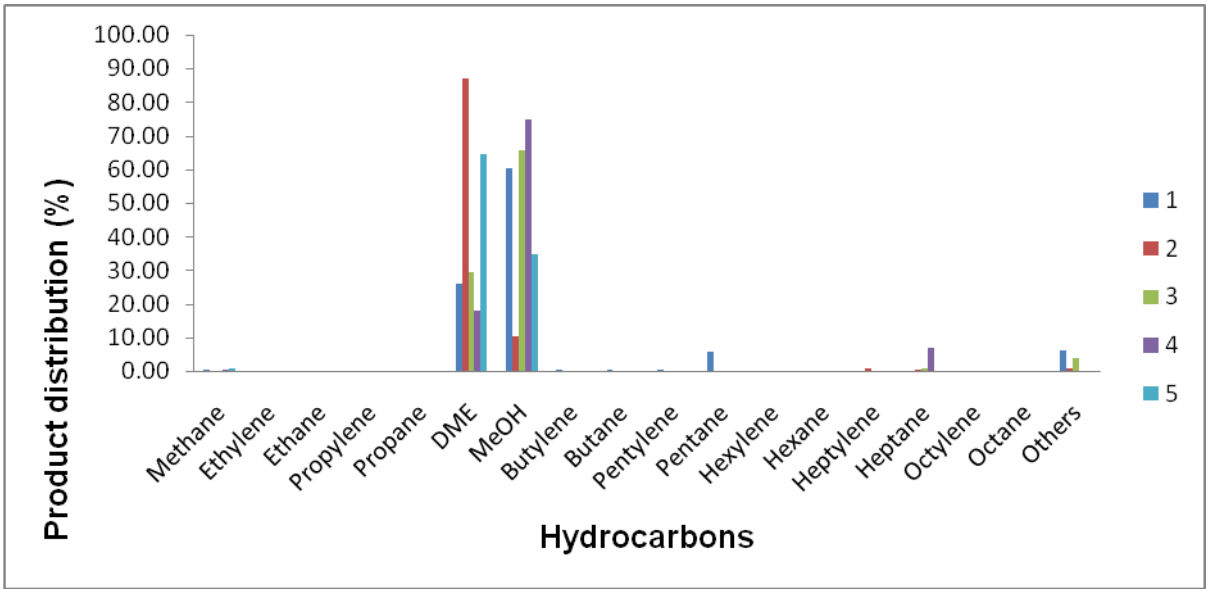


Figure 4.9 The effect of crystallization time of SAPO molecular sieve of sample PS-07 synthesized for 3 days on product distribution of hydrocarbons from 0 - 100 % at 400 ºC reactor temperature for 5 hour.

Figure 4.9 shows the large quantity of DME appeared on the 2nd hour and the 5th hour and less quantity of DME on the 1st, 3rd and the 4th hour. A large amount of MeOH was obseved on the 1st, 3rd and the 4th hour, while a less amount of MeOH appeared on the 2nd hour and the 5thhour. A less amount of pentane was observed on the 2nd hour and also heptane was observed on the 4th hour. Thus the product distribution of DME increased in a decreased MeOH product distribution.

The effects of crystallization time on product distribution of hydrocarbons are shown in figure 4.10. The product distribution in figure 4.3 ranges from 0 % to 10 %.

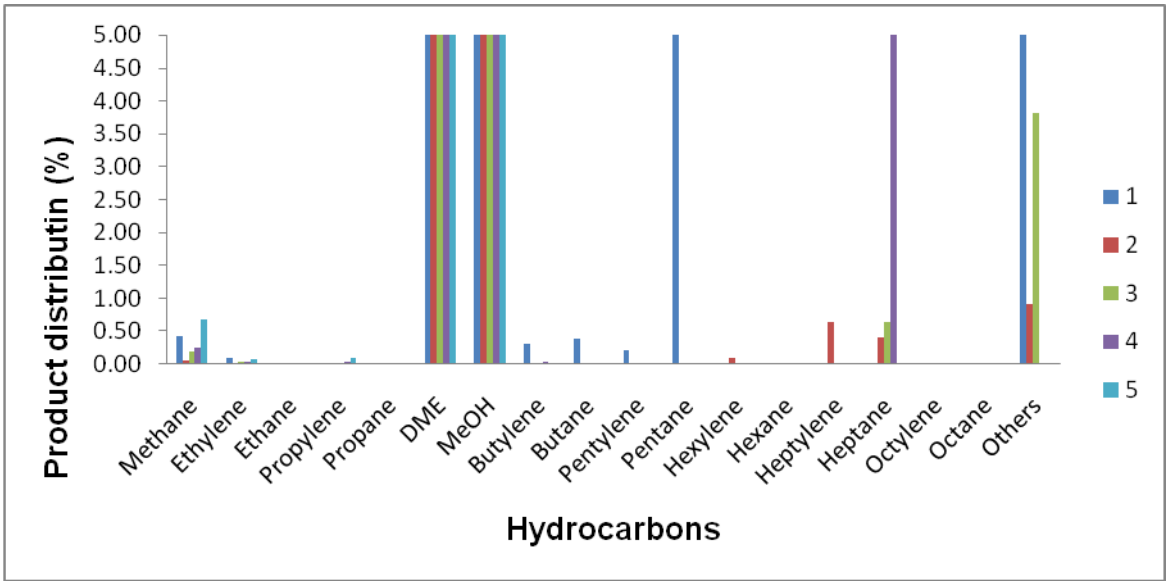


Figure 4.10 The effect of crystallization time of SAPO molecular sieve of sample PS-07 synthesized for 3 days on product distribution of hydrocarbons from 0 - 5 % at 400 ºC reactor temperature for 5 hour.

The product distribution shown in figure 4.10 indicated that only less amount of methane, butylenes, butane, and pentylene was obtained on the 1st hour. Heptylene distribution was observed on the 2nd hour.

The effects of crystallization time on product distribution of hydrocarbons are shown in figure 4.11. The product distribution in figure 4.12 ranges from 0 % to 100 %.

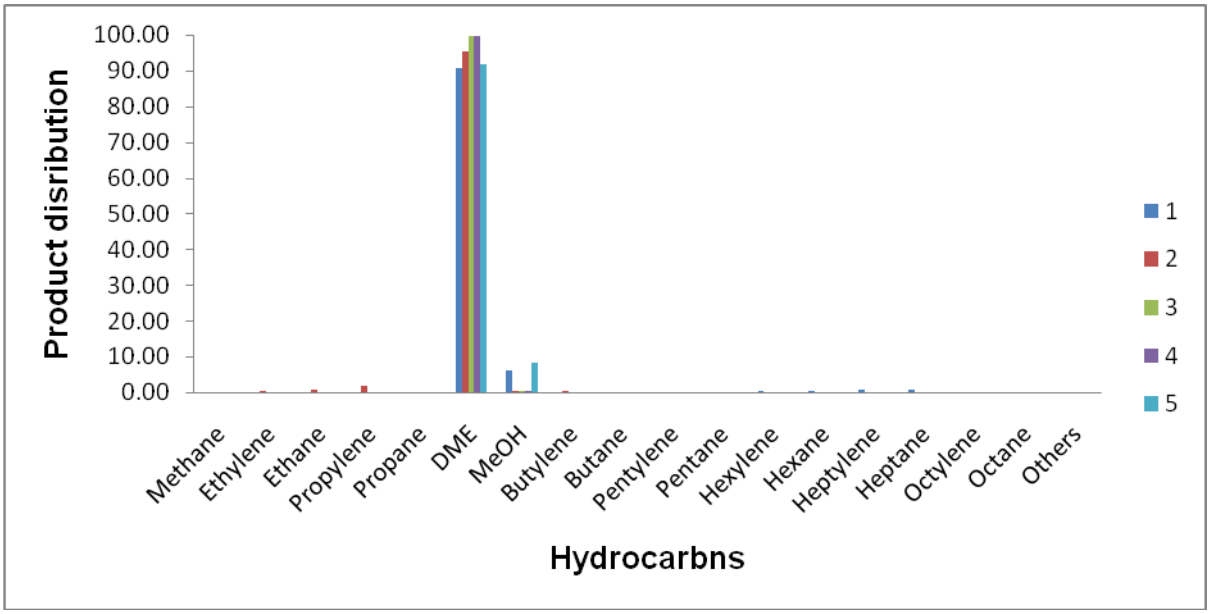


Figure 4.11 The effect of crystallization time of SAPO-34 molecular sieve synthesized for 4 days on product distribution of hydrocarbons from 0 - 100 % at 400 ºC reactor temperature for 5 hour.

DME product distribution appeared in large amount and MeOH appeared in less amount from the 1st to the 5th hour in figure 4.11. Thus % methanol conversion was high and large amount of MeOH was converted to large amount of DME and less amount of other hydrocarbons.

The effects of crystallization time on product distribution of hydrocarbons are shown in figure 4.12. The product distribution in figure 4.12 ranges from 0 % to 10 %.

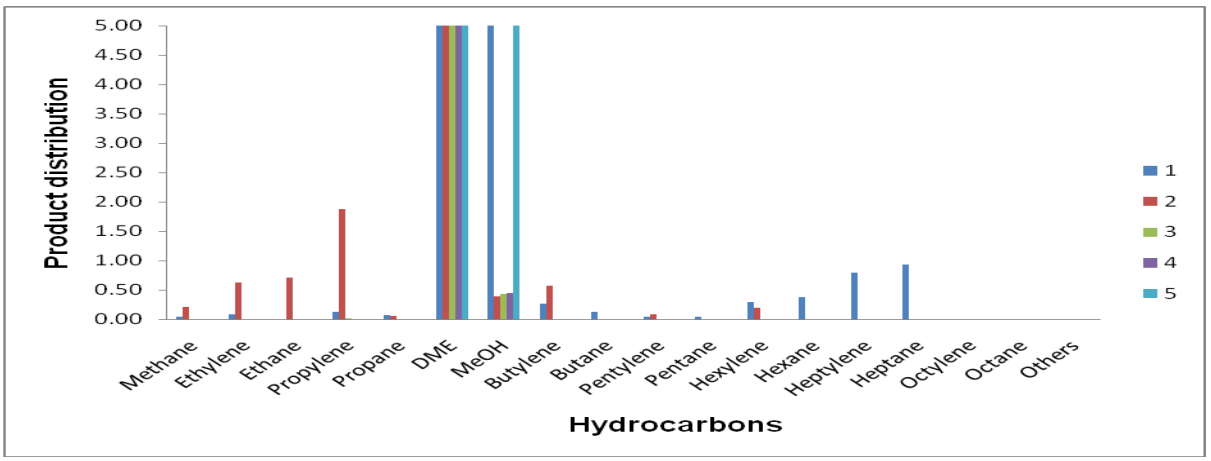


Figure 4.12 The effect of crystallization temperature of SAPO molecular sieve of sample PS-08 synthesized for 4 days on product distribution of hydrocarbons from 0 - 10 % at 400 ºC reactor temperature for 1 hour.

Figure 4.12 shows that the major product on the molecular sieve synthesized within 4 days is propylene. Less quantity of other hydrocarbons like ethylene, ethane, hexylene, hexane, heptylene and heptane are obtained on the 1st and 2nd hour.

The effects of crystallization time on product distribution of hydrocarbons are shown in figure 4.13. The product distribution in figure 4.13 ranges from 0 % to 100 %.

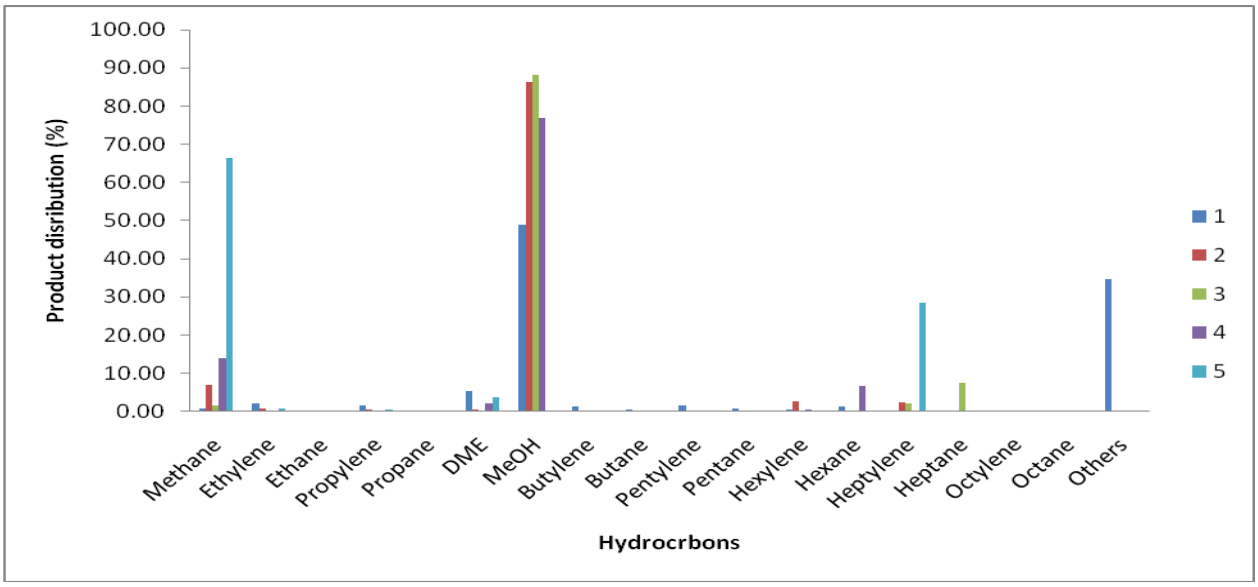


Figure 4.13 The effect of crystallization time of SAPO molecular sieve of sample PS-03 synthesized for 5 days on product distribution of hydrocarbons from 0 - 100 % at 400 ºC reactor temperature for 5 hour.

The product ditribution of MeOH appeared in large amount from the 1st to the 4th hour in figure 4.13. Other hydrocarbons like methane and heptylene were also obtained in large amount.

The effects of crystallization time on product distribution of hydrocarbons are shown in figure 4.14. The product distribution in figure 4.14 ranges from 0 % to 100%.

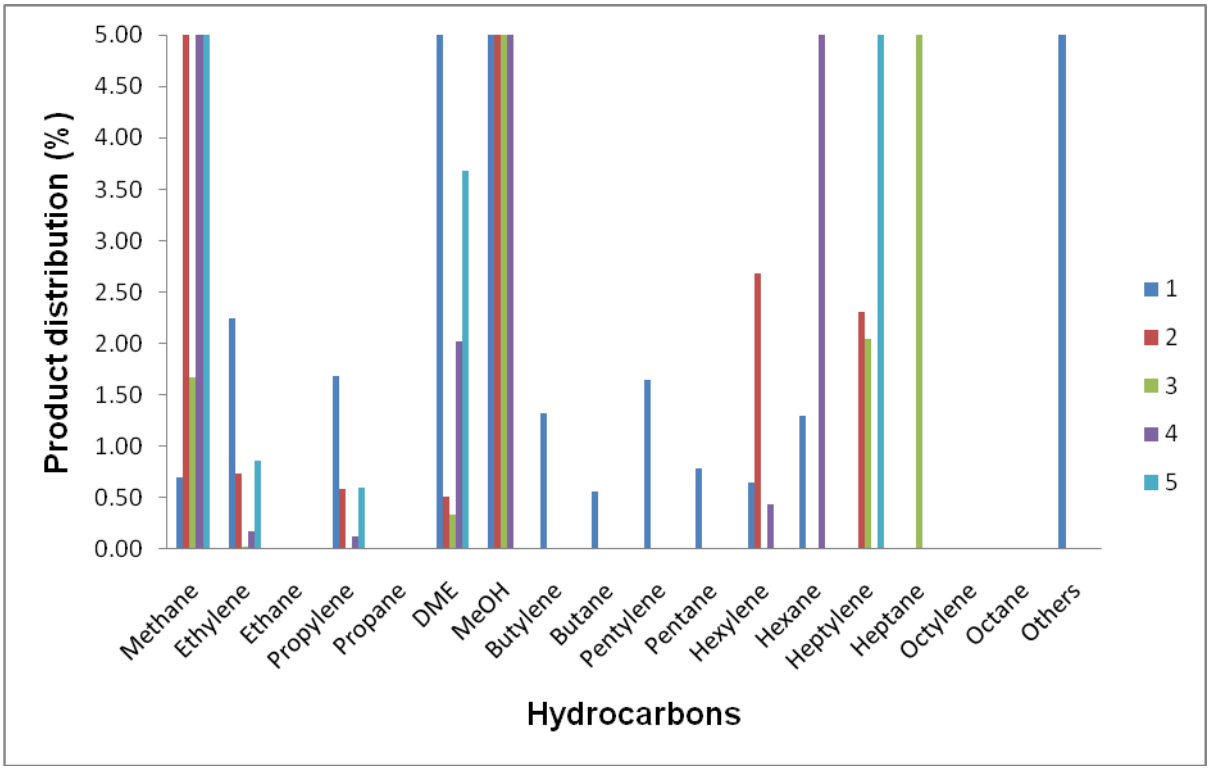


Figure 4.14 The effect of crystallization time of SAPO molecular sieve of sample PS-03 synthesized for 5 days on product distribution of hydrocarbons from 0 - 10 % at 400 ºC reactor temperature for 5 hour.

The figure 4.14 shows the effects of crystallization time of SAPO-34 molecular sieve synthesized for 5 days on product distribution of hydrocarbons from 0 - 10 % at 400 ºC reactor temperature for 5 hour. A large quantity of methane, DME, MeOH, hexylene hexane, heptylene, heptanes and other hydrocarbons were obtained from the 1st to the 5th hour. Light olefins were obtained in fewer amounts in the 1st hour.

The effects of crystallization time on product distribution of hydrocarbons are shown in figure 4.15. The product distribution in figure 4.15 ranges from 0 % to 100 %.

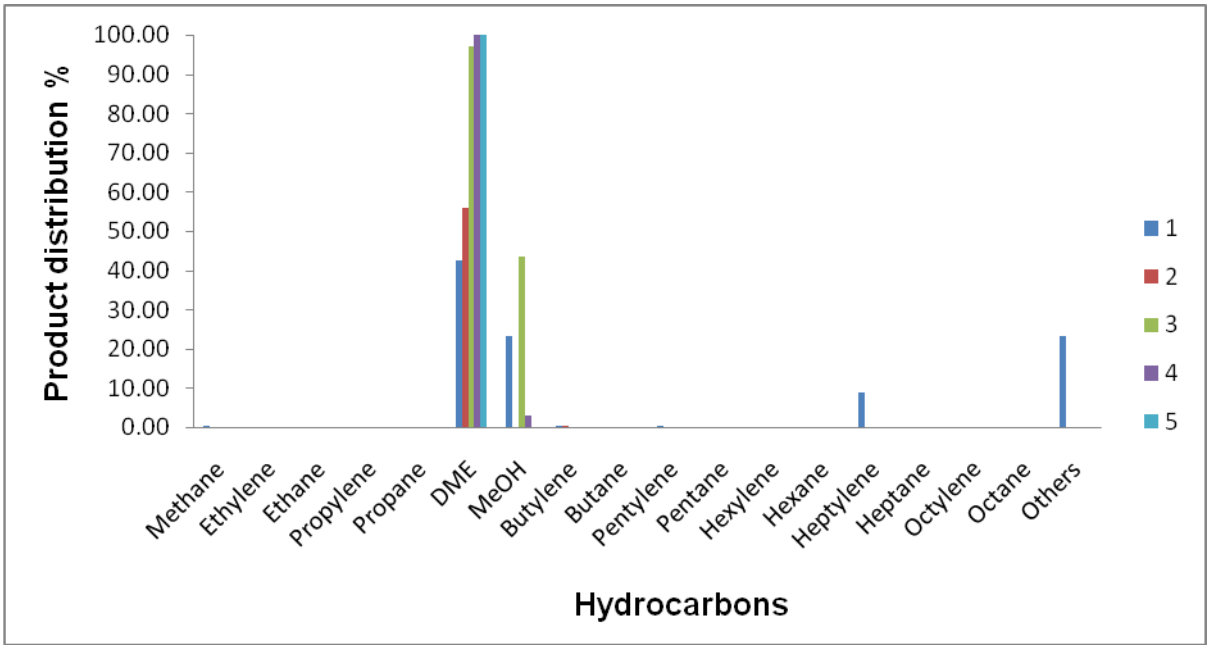


Figure 4.15 The effect of crystallization time of SAPO molecular sieve of sample PS-09 synthesized for 6 days on product distribution of hydrocarbons from 0 - 100 % at 400 ºC reactor temperature for 5 hour.

From the figure 4.15 it is clearly shown that DME ie the major product. Heptylene, MeOH and other hydrocarbons are less in the 1st hour time on stream. Some other hydrocarbons are very much small.

The effects of crystallization time on product distribution of hydrocarbons are shown in figure 4.16. The product distribution in figure 4.16 ranges from 0 % to

100 %.

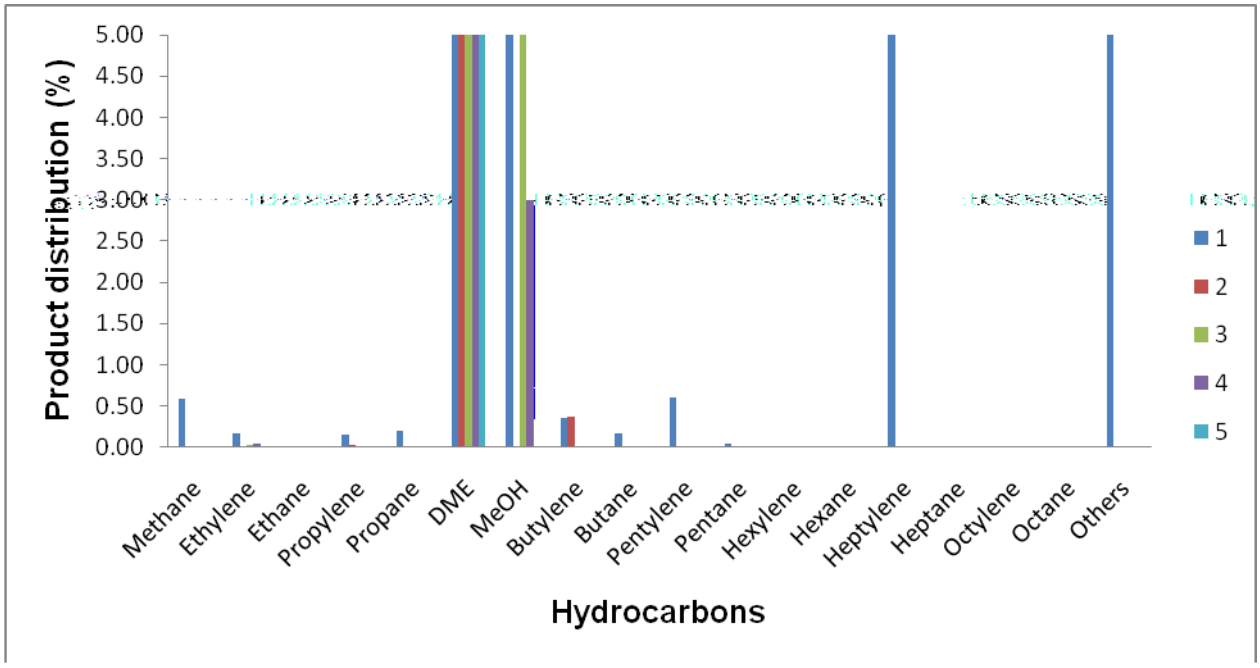


Figure 4.16 The effect of crystallization time of SAPO molecular sieve of sample PS-09 synthesized for 6 days on product distribution of hydrocarbons from 0 - 100 % at 400 ºC reactor temperature for 5 hour.

The Figure 4.16 The effect of crystallization time of SAPO molecular sieve synthesized for 6 days on product distribution of hydrocarbons from 0 - 100 % at 400 ºC reactor temperature for 5 hour. The product distribution of DME, MeOH, heptylene and other hydrocarbons appeared in larger quantity. Methane and pentylene appeared in fewer amount and light olefins were obtained in a very small number in the 1st hour.

The product distribution for light olefins improved within two hours on the molecular sieve synthesized for four days. However the hydration of DME to MeOH in a reverse reaction was encountered. The results are shown in figure 4.11 – 4.16. As such, more of the DME did not undergo the forward reaction to form light olefins and other products, only a small amount of DME took part in the chemical reaction. A large amount of light olefins were observed in the first hour of the reaction, but decreased from the second hour to the fifth hour (catalyst prepared within five days). Among higher olefins, pentylene was produced in larger quantity in the first hour, while a higher paraffin product distribution was noted from the third to the fifth day TOS. The product distribution of heptylene was very high when compared with the other products (the catalyst synthesized within six days).

Table 4.4 indicated % methanol conversion decreased with reaction time. The selectivity to light olefins on the catalyst prepared within 2 - 3 days crystallization time was much smaller than the selectivity to light olefins on the catalyst that synthesized within the crystallisation time of 5 – 6 days. The selectivity of light olefins from the catalyst prepared with a crystallisation time of 4 days is the highest.

4.2.2.4 The relationship between the characterization of SAPO molecular sieve and the MTO reaction.

The XRD patterns for the SAPO molecular sieves prepared at 200 C ranges from 2 - 4 days in figure 3.3 were very close to one another, also the catalytic performance on SAPO supposed to be the same. Surprisingly, the % methanol conversion, ethylene and propylene selectivity on molecular sieves were different. Molecular sieve prepared in 4 days was highly active to % methanol conversion, ethylene and propylene than molecular sieves prepared within a short period of 2 - 3 days. A molecular sieve prepared in a long period of 6 days has different the shape of the peaks from 2θ scale of 20º - 23º. This molecular sieve is active from the 1st to 2rd hour then becomes deactivated from the 4th to the 5th hour.

SEM spectroscopy for the molecular sieves prepared in 3 and 5 days are different. A rough hexagonal shape of the SAPO molecular sieve prepared in 3 days in figure 3.9 indicate that a molecular sieve was still in intermediate stage, even the catalytic performance on MTO was low. SEM spectroscopy for the molecular sieve prepared in 5 days in showed pentagonal crystal that was active to % methanol conversion, ethylene and propylene.

The product distribution of on all molecular sieves prepared within short periods (2 – 5) days and long period 6 days were low with high DME product distribution. Since the main aim of the study was to synthesize the molecular sieves containing piperidine SDA that are highly selective towards ethylene and propylene, the molecular sieves performance was not good due to the nature of molecular sieve. Ethylene and propylene selectivity was very much low; only DME was main product.

4.2.2.5 Conclusions

Liu, G. *et al.* [121] prepared SAPO-34 molecular sieve using DEA template at 200^0 C crystallization temperature for 2 days. This catalyst was tested in MTO reaction at the reactor temperature of 450^0C. This molecular sieve has shown a good ethylene and propylene selectivity ranging 74 -81 %. Compared to the molecular sieve prepared at 200 ^{0}C for 2 days using piperidine template, prepared in this study, the molecular sieve was not well formed and even the ethylene and propylene selectivity was very much low. A good molecular sieve was the one prepared within for days. However the XRD patterns for the molecular sieve have shown three phases of SAPO-5, SAPO-34 and amorphous phase. The methanol conversion to DME was successful, but the hydration of DME to light olefins was unsuccessful due to the amorphous phase that blocks the surface of the molecular sieve. Thus all molecular sieves are good for methanol conversion to DME not light olefins.

4.2.3 The influence of phosphate content on methanol conversion.

The SAPO molecular sieves were synthesized with various phosphorus contents (P_2O_5/Al_2O_3 molar ratios varying from 0.3 - 0.7) at a crystallization temperature of 200 $^{\circ}$C for 5 days. The resulting molecular sieves were tested for the MTO reaction at a reactor temperature of 400 $^{\circ}$C for 1 hour. Table 4.5 shows the % Methanol conversion, the particle size and the product distribution of the molecular sieve with different P_2O_5/Al_2O_3 molar ratios, reaction temperature and the product distribution of hydrocarbons.

Table 4.5 % Methanol conversion, the particle size and the product distribution of the molecular sieve with different P_2O_5/Al_2O_3 molar ratios, reaction temperature and the product distribution of hydrocarbons.

Sample	PS-10	PS-11	PS-03	PS-12
P_2O_5/Al_2O_3 ratio	0.3	0.5	0.6	0.7
Particle size (nm)	1.49	0	1.49	0
Methanol conversion (mol %)	99	100	93	22
Reaction temperature (^oC)	400	400	400	400
TOS (h)	1	1	1	1
Hydrocarbons	Products distribution (mol %)			
C_2=	0.011	0.000	2.24	0.053
C_3=	0.467	0.000	1.68	0.079
C_4=	0	0.000	1.32	0.119
C_5=	0	0	1.65	0.005
C_6=	0	0	0.65	0.023
C_7=	0	0.000	0	8.215
C_8=	0	0	0	0
DME	90.119	3.18	5.36	66.490
MeOH	0.00	36.17	48.93	24.505
C1	0.00	0.02	0.70	0.348
C_2	0.010	0.000	0	0
C_3	0	0	0	0
C_4	0	0.000	0.56	0.089
C_5	9.393	57.68	0.79	0.024
C_6	0	0	1.30	0.050
C_7	0.00	0.000	0	0
C_8	0	0	0	0
Others	0.223	2.94	34.81	0

4.2.3.1 The effects of phosphorus on % methanol conversion

Figure 4.17 indicates the effects of phosphorus content for SAPO molecular sieve on the % methanol conversion.

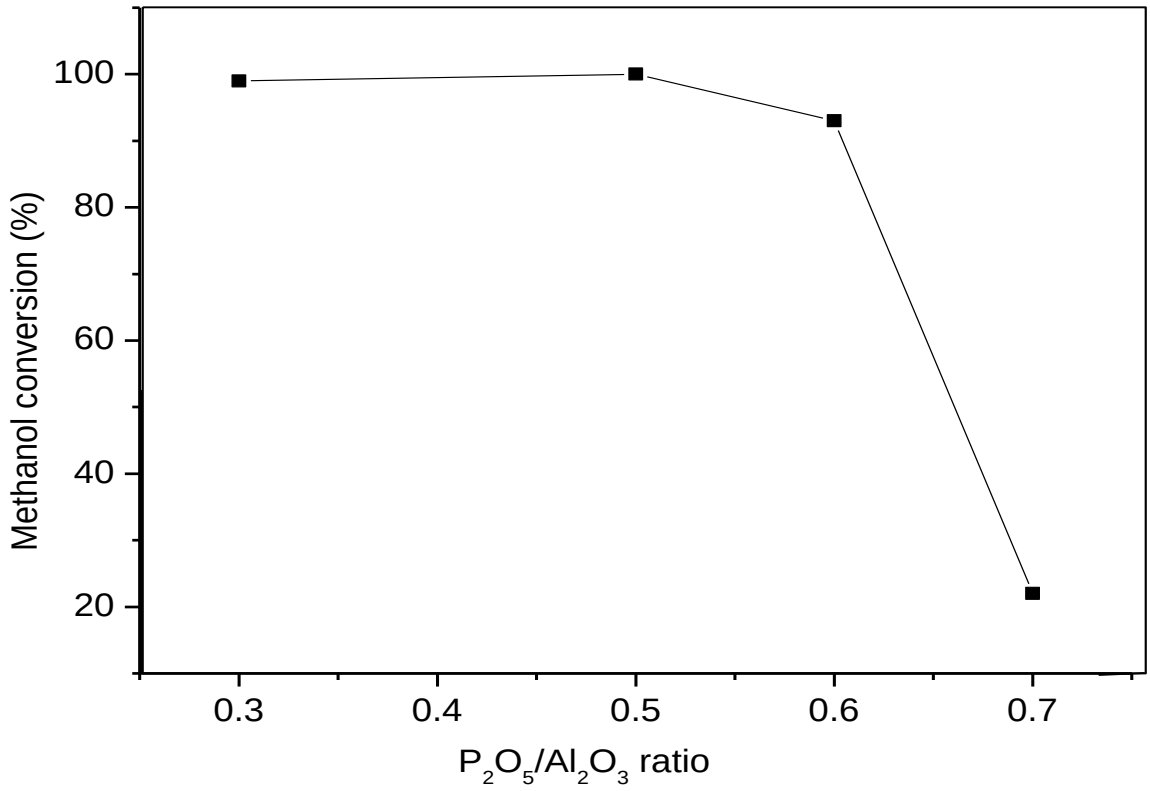


Figure 4.17 The % methanol conversions vs. P_2O_5/Al_2O_3 ratio of the SAPO molecular sieve for samples PS-10 – PS-11, PS-03, and PS-07.

Figure 4.17 shows that % methanol conversion is very high at low P_2O_5/Al_2O_3 molar ratios (0.3-0.6). A sudden decline of % methanol conversion appeared at the P_2O_5/Al_2O_3 molar ratio of 0.7. The results indicate that the SAPO-34 catalyst is good for methanol conversion if it has low phosphorus content (0.3 -0.6 P_2O_5/Al_2O_3 molar ratio) and poor methanol conversion at a high phosphorus content (0.7 P_2O_5/Al_2O_3 molar ratio).

4.2.3.2 The effects of phosphorous contents on light olefins

Figure 4.18 shows the effects of phosphorus content of SAPO molecular sieve on light olefins selectivity at the reaction temperature of 400 $^{\circ}$C for 1 hour.

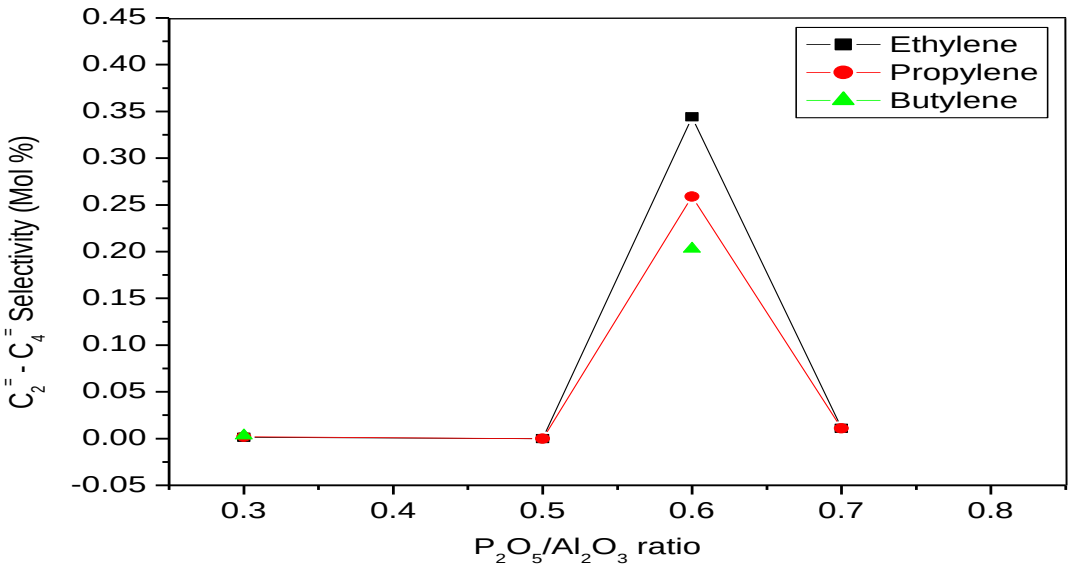


Figure 4.18 The effects of phosphorus content of SAPO molecular sieve on light olefins selectivity within 1 hour at reaction temperature of 400 ºC.

High light olefins selectivity with high ethylene and low butylene selectivity was observed at the P_2O_5/Al_2O_3 molar ratio of 0.6 in figure 4.18. Low light olefins selectivity with similar ethylene, propylene and butylenes selectivity was also observed at the P_2O_5/Al_2O_3 molar ratios of 0.3, 0.5 and 0.7. This shows that SAPO molecular sieve with P_2O_5/Al_2O_3 molar ratio: 0.6 is suitable for good light olefins selectivity.

4.2.4.3 The effects of phosphorus contents on product distribution of hydrocarbons.

Figure 4.19 shows the effect of phosphorus content in (P_2O_5/Al_2O_3 molar ratio from 0.3-0.7) on the pruduct distribution in the MTO reactions after 1 hour. The effects of phosphorus content on the product distribution of hydrocarbons ranges from 0 % to 100 %.

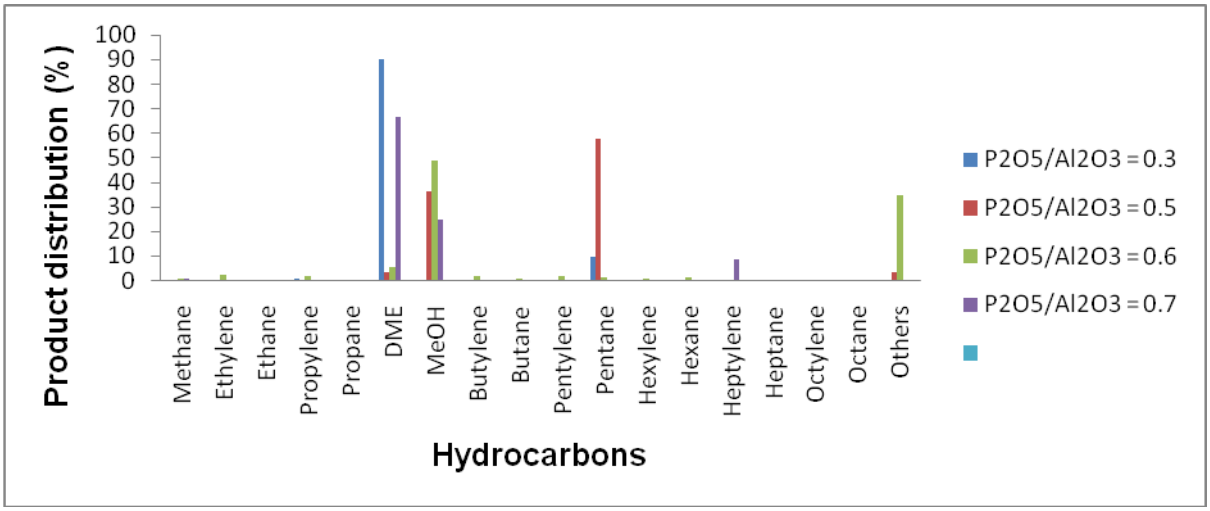


Figure 4.19 The effects of phosphorus content of SAPOs molecular sieve on the product distribution of hydrocarbons ranges from 0 % to 100 %.

A large amount of MeOH and DME remained unreacted while small amounts of hydrocarbons were obtained in figure 19. The pruduct distribution of light olefins and pentylene were also noted.

The effects of phosphorus content on the product distribution of hydrocarbons ranges from 0 % to 10 %.are shown in figure 4.20

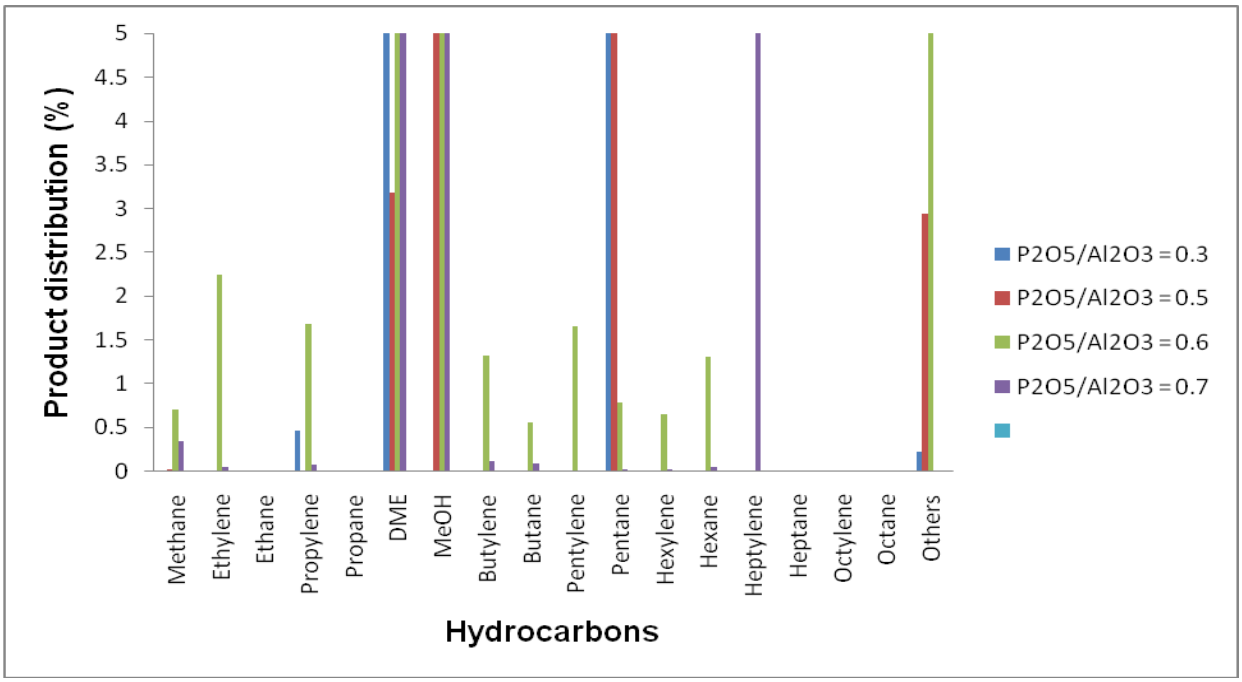


Figure 4.20 The effects of phosphorus content on the product distribution of hydrocarbons range from 0 % to 10 %.

A large amount of heptylene was observed for the molecular sieve synthesized with a P_2O_5/Al_2O_3 molar ratio of 0.7 in figure 4.20. Therefore the best molecular sieve for the production of light olefins in MTO reactions is the molecular sieve synthesized with P_2O_5/Al_2O_3 molar ratio of 0.6.

4.2.4.4 The relationship between the characterization of SAPO-34 molecular sieve and the MTO reaction.

XRD patterns for the molecular sieves prepared with different P_2O_5/Al_2O_3 mole ratios were discussed in 3.2.3.The results indicated that the molecular sieve comprises both SAPO-5 and SAPO-34.

XRD spectra for the catalysts prepared with different phosphate contents were different. The XRD patterns for the catalysts synthesized with P_2O_5/Al_2O_3 molar ratio 0.3 and 0.6 had similar particle sizes. NH_3-TPD desorption appeared at temperature region of 190 - 250 ^oC and 340 - 380 ^oC for the catalyst prepared with a P_2O_5/Al_2O_3 molar ratio of 0.6. The % methanol conversion on different phosphorus containing samples increased with a decrease in TOS and decreased suddenly for the catalyst synthesized with a high P_2O_5/Al_2O_3 molar ratio in table 4.5. Therefore the phosphorus content plays a major role in the preparation of SAPO, light olefins selectivity and product distribution of hydrocarbons.

4.2.4.5 Conclusions

The % methanol conversion on different phosphorus containing samples increases with an increased in TOS and decreased for the molecular sieves with a high P_2O_5/Al_2O_3 molar ratio. Molecular sieve with P_2O_5/Al_2O_3 molar ratio of 0.6 produced high light olefins selectivity and product distribution. Molecular sieve with P_2O_5/Al_2O_3 molar ratio of 0.3, 0.5, and 0.7 produced lower light olefins selectivity and product distribution. The overall light olefins selectivity and products distribution on the molecular sieves were very much low with high DME and MeOH product distribution. Therefore the molecular sieves prepared using piperidine as SDA with different phosphorus containing samples did not perform well in MTO reaction.

4.2.4. The effects of the promoter (Na^+) in SAPO.

Samples of SAPO molecular sieve with P_2O_5/Al_2O_3 mole ratios of 0.3 plus addition of different sodium content (Na_2O mol of 0.013 and 0.200) were compared. Those molecular sieves were tested for the MTO reaction at a reactor temperature of 400 ^{o}C for 5 hours time on stream. Figure 4.6 shows the % Methanol conversion, the particle size and the product distribution of the molecular sieve with P_2O_5/Al_2O_3 mole ratios plus sodium oxide, reaction temperature and the product distribution of hydrocarbons.

Table 4.6 The % Methanol conversion, the particle size and the product distribution of the molecular sieve with P_2O_5/Al_2O_3 mole ratios plus sodium oxide, reaction temperature and the product distribution of hydrocarbons.

Sample	PS-10					PS-13					PS-14
P_2O_5/Al_2O_3 = 0.3 + y Na_2O	y = 0.00					y = 0.013					y = 0.200
Particle size (nm)	3.8					1.99					1.49
Methanol conversion (Mol %)	25	35	100	100	100	100	47	96	100	100	100
Reaction temperature (^{0}C)	400	400	400	400	400	400	400	400	400	400	400
TOS (h)	1	1	2	3	4	5	1	2	3	4	5
Hydrocarbons			Product distribution								
C_2=	0.011	0.014	0.0410	0.028	0.027	0.025	0.003	0.030	0.026	0.126	0.014
C_3=	0.467	0.010	0.0820	0.036	0.031	0.021	0.005	0.046	0.026	0.013	0.014
C_4=	0	15.291	0	0	0.00	0	15.691	0	0	0	0
C_5=	0	0.490	0.1640	0.032	0.138	0	6.786	5.407	0	0	0
C_6=	0	0.188	3.3540	9.590	14.636	0	0	0	0	0	0
C_7=	0	0.893	0	15.069	0	0	0	0	0	0	0
C_8=	0	0	0	0	0	0	0	0	0	0	0
DME	90.119	13.103	96.1770	75.045	84.958	99.785	9.568	64.509	95.461	99.862	99.973
MeOH	0.00	65.527	0.00	0.00	0.00	0.00	65.703	22.620	0	0	0
C1	0.00	0.019	0.00	0.192	0.205	0.165	0.012	0	0	0	0
C_2	0.010	0.000	0.0100	0.008	0.004	0.004	0	0	0	0	0
C_3	0	0	0	0	0	0	0	0	0	0	0
C_4	0	0	0	0	0	0	0	0	0	0	0
C_5	9.393	1.475	0	0	0	0	0	0	0	0	0
C_6	0	0.256	0	0	0	0	0.284	0	0	0	0
C_7	0.00	2.074	0.00	0.00	0.00	0	1.160	7.388	4.488	0	0
C_8	0	0	0	0	0	0	0	0	0	0	0
Others	0.223	0.659	0	0	0	0	0.093	6.285	7.189	0	0

4.2.4.1 The effects of the promoter on % methanol conversion

Figure 4.21 shows the effects for the addition of sodium oxide in the SAPO molecular sieve with the P_2O_5/Al_2O_3 molar ratio of 0.3 on methanol conversion.

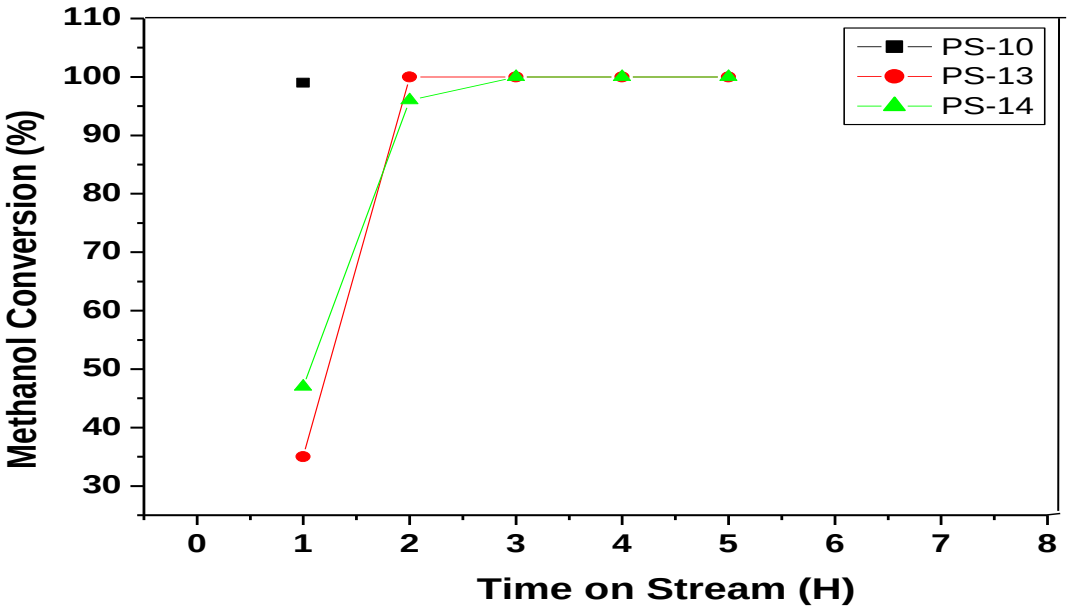


Figure 4.21 The % methanol conversions vs. time on stream of the molecular sieve with P_2O_5/Al_2O_3 ratio of 0.3 plus sodium oxide.

According to the results on figure 4.21, the addition of sodium oxide to the catalyst leads to lower % methanol conversion in the 1st hour, but % methanol conversion increased from the 2nd hour to the 5th hour. Thus addition of low and high sodium content to the molecular sieve improved the % methanol conversion

4.2.4 2 The effects of promoter (Na^+) on light olefins.

Figure 4.22 shows the effects for the addition of sodium oxide in the SAPO-34 molecular sieve with the P_2O_5/Al_2O_3 molar ratio of 0.3 on ethylene selectivity.

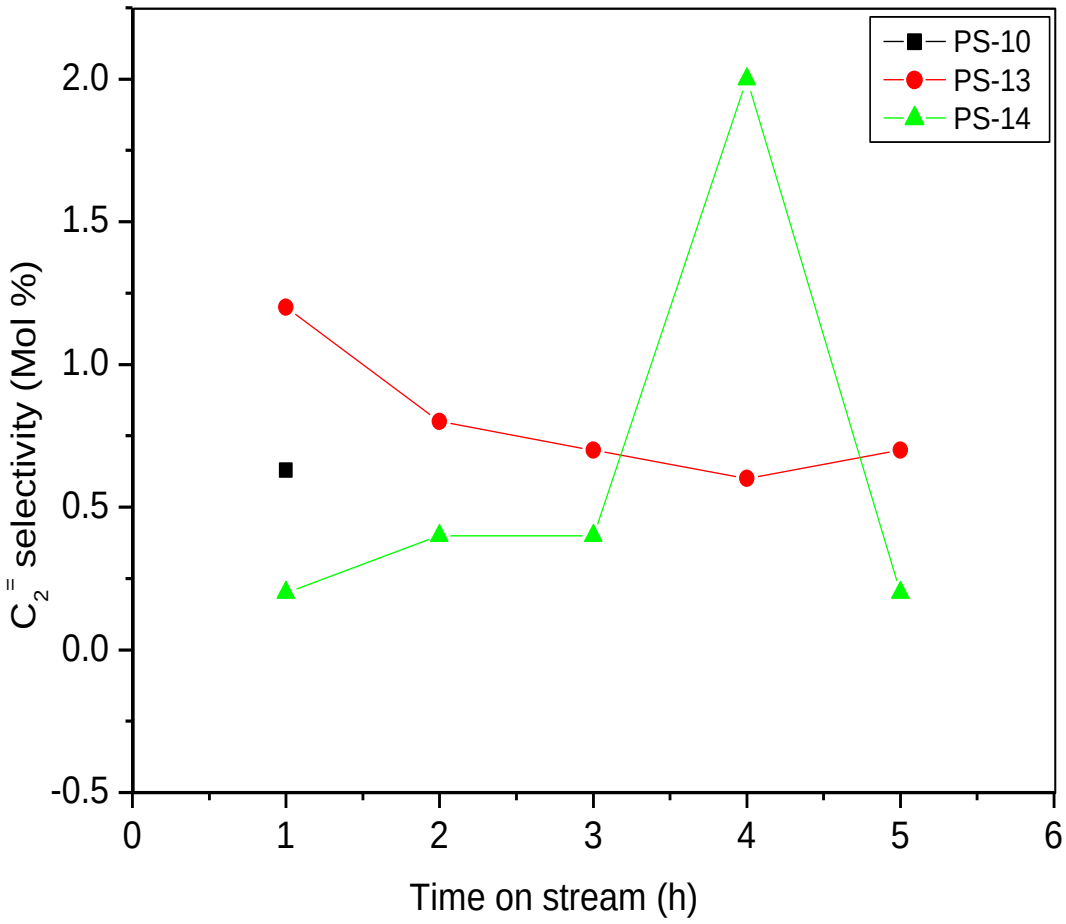


Figure 4.22 The effects of addition of sodium content to molecular sieve on ethylene selectivity.

Addition of 0.013 mol sodium oxide to the gel composition of SAPO improved ethylene selectivity from the 1st to the 5th hour in figure 4.22. Ethylene selectivity decreased with increase in time from the 1st to the 5th hour for the low sodium content catalyst and increased with increase in time but a sudden decline was observed from the 4th hour to the 5th hour. Ethylene selectivity decreased with an increased % methanol conversion in time on stream.

Figure 4.23 shows the effects for the addition of sodium oxide in the SAPO molecular sieve with the P_2O_5/Al_2O_3 molar ratio of 0.3 on propylene selectivity.

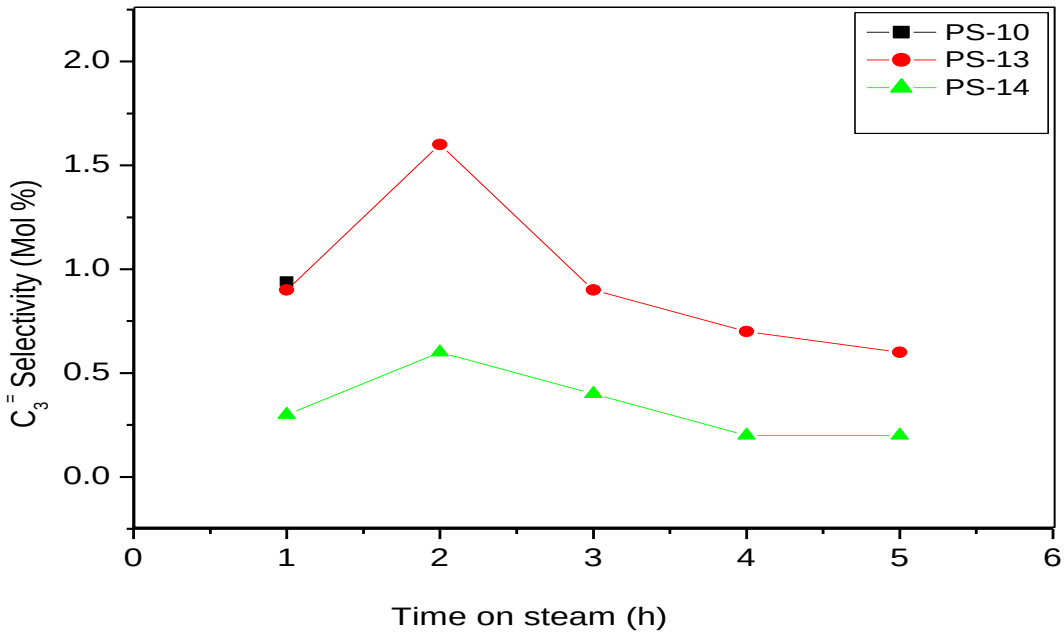


Figure 4.23 The effects of addition of sodium content to molecular sieve on propylene selectivity.

Addition of 0.013 mol sodium oxide to the gel composition of SAPO improved propylene selectivity, compared to the catalyst with higher sodium oxide content (0.2) in figure 4.23. Propylene selectivity from both low and high sodium oxide catalyst increased from the 1st to the 2nd hour and declined from the 3rd to the 5th hour. Addition of low and high Na_2O content into gel composition of 1 Al_2O_3: 0.3 P_2O_5: 1.1 Pip: 0.8SiO_2: 100 H_2O of the catalyst plays a major rule in the product distribution of hydrocarbons.

4.2.4.3 The effects of promoter (Na^+) on product distribution of hydrocarbons

Figure 4.24 shows the effects for the addition of sodium oxide (0.013 mol) in the SAPO-34 molecular sieve with the P_2O_5/Al_2O_3 molar ratio of 0.3 on product distribution. The product distribution of hydrocarbons ranges from 0 % to 100 %.

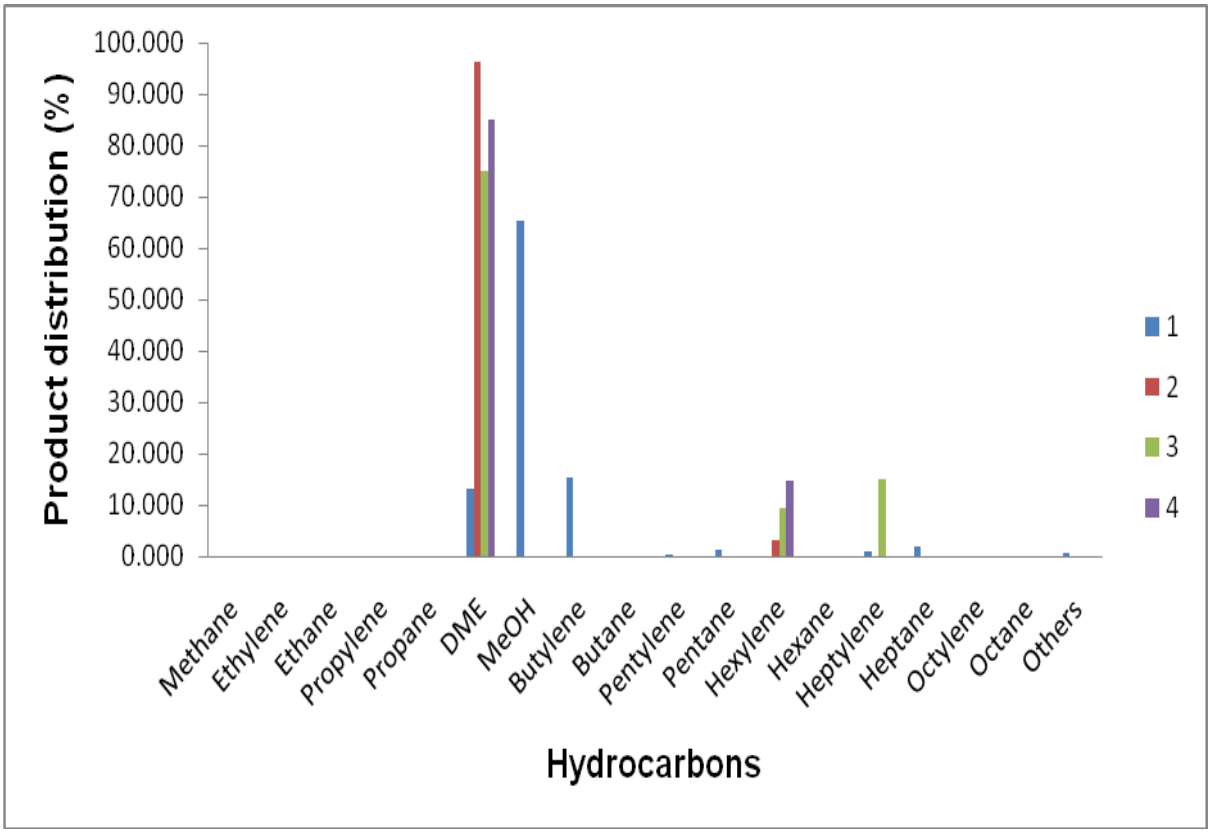


Figure 4.24 The effect of the addition of sodium oxide (0.013 mol) in the SAPO molecular sieve with the P_2O_5/Al_2O_3 molar ratio of 0.3 on product distribution of hydrocarbons from 0 - 100 % at 400 ºC reactor temperature for 1 hour.

A large amount of DME product distribution on the molecular sieve with less sodium oxide is obseved from the 1st to the 5th hour. MeOH appeared on the 1st hour in figure 4.24. Butylene product distribution is obtained in fewer amount in the 1st hour. Hexylene and heptylene product distribution appeared in fewer amount in the 3rd and 4th hour. No product distribution appeared in the 5th hour.

Figure 4.25 shows the effects for the addition of sodium oxide (0.013 mol) in the SAPO-34 molecular sieve with the P_2O_5/Al_2O_3 molar ratio of 0.3 on product distribution. The product distribution of hydrocarbons ranges from 0 - 5 %.

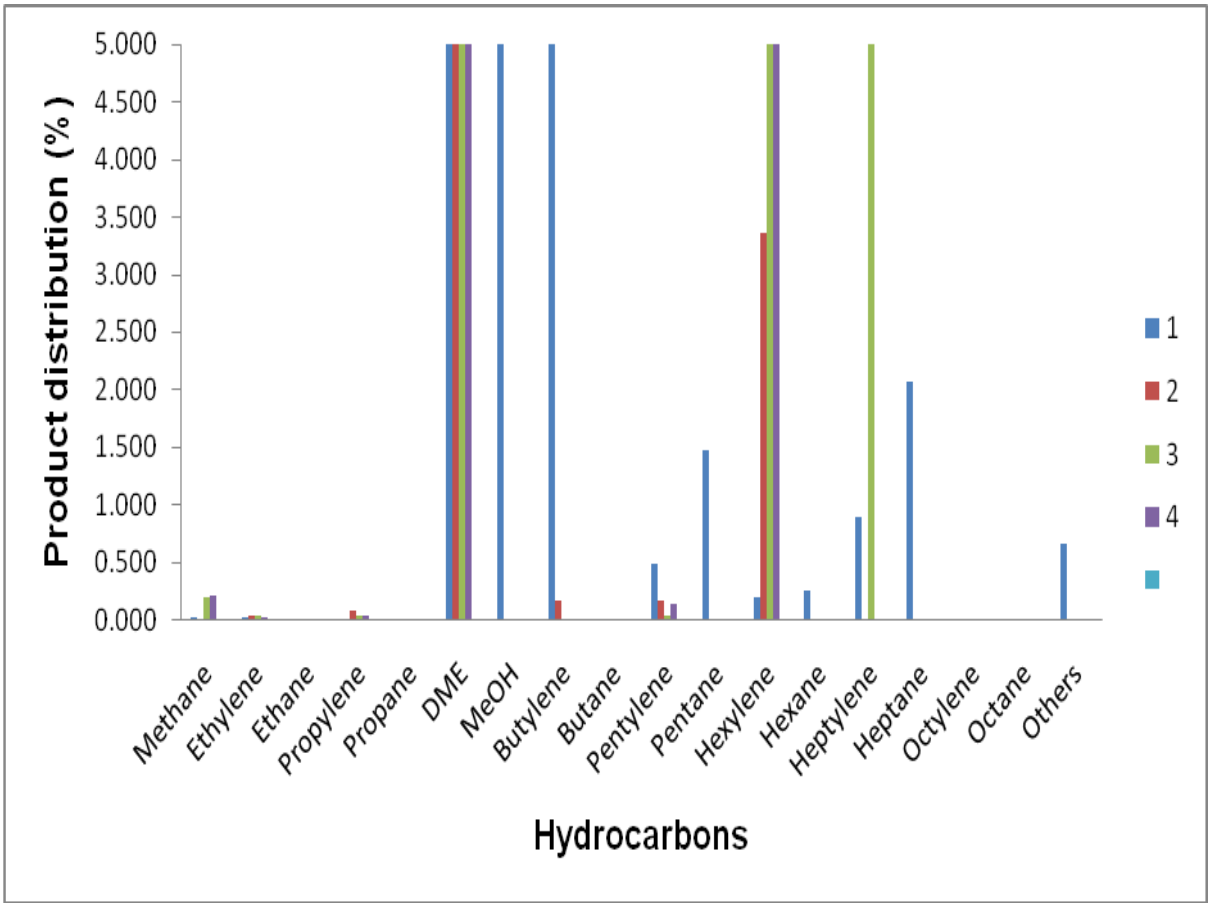


Figure 4.25 The effect of the addition of sodium oxide (0.013 mol) in the SAPO molecular sieve with the P_2O_5/Al_2O_3 mole ratio of 0.3 on product distribution of hydrocarbons from 0 - 5 % at 400 ºC reactor temperature for 1 hour.

The effect of the addition of sodium oxide (0.013 mol) in the SAPO molecular sieve with the P_2O_5/Al_2O_3 molar ratio of 0.3 on product distribution of hydrocarbons is shown in figure 4.25. A large quantity of DME, MeOH, hexylene and heptylene product distribution was observed at different time. Few quantities of methane, pentylene, hexane and other hydrocarbons product distribution appeared in the 1st hour. Decreasing the sodium oxide results in increasing the products distribution of butylenes and heptylene in the 1st and 3rd hour.

Figure 4.26 shows the effects for the addition of sodium oxide (0.200 mol) in the SAPO-34 molecular sieve with the P_2O_5/Al_2O_3 molar ratio of 0.3 on product distribution. The product distribution of hydrocarbons ranges from 0 to 100 %.

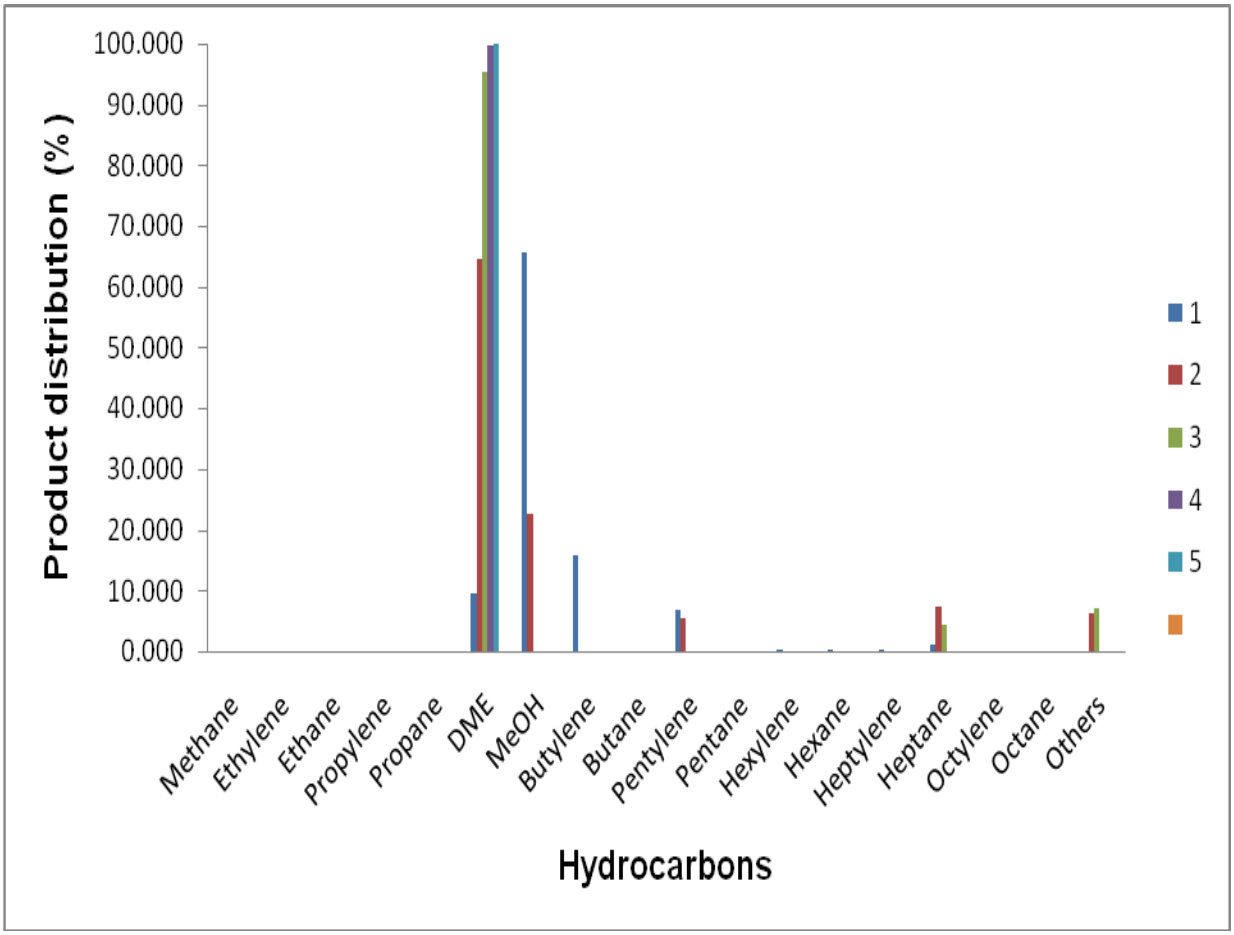


Figure 4.26 The effect of the addition of sodium oxide (0.200 mol) in the SAPO molecular sieve with the P_2O_5/Al_2O_3 molar ratio of 0.3 on product distribution of hydrocarbons from 0 - 100 % at 400 ºC reactor temperature for 1 hour.

Figure 4.26 shows the effect of the addition of sodium oxide (0.200 mol) in the SAPO molecular sieve with the P_2O_5/Al_2O_3 molar ratio of 0.3 on product distribution of hydrocarbons. The product distribution of DME and MeOH were observed in large amount. Butylene, heptanes and other hydrocarbons were obtained in small amount from the 1st to the 5th hour.

Figure 4.27 shows the effects for the addition of sodium oxide (0.200 mol) in the SAPO molecular sieve with the P_2O_5/Al_2O_3 molar ratio of 0.3 on product distribution. The product distribution of hydrocarbons ranges from 0 - 5 %.

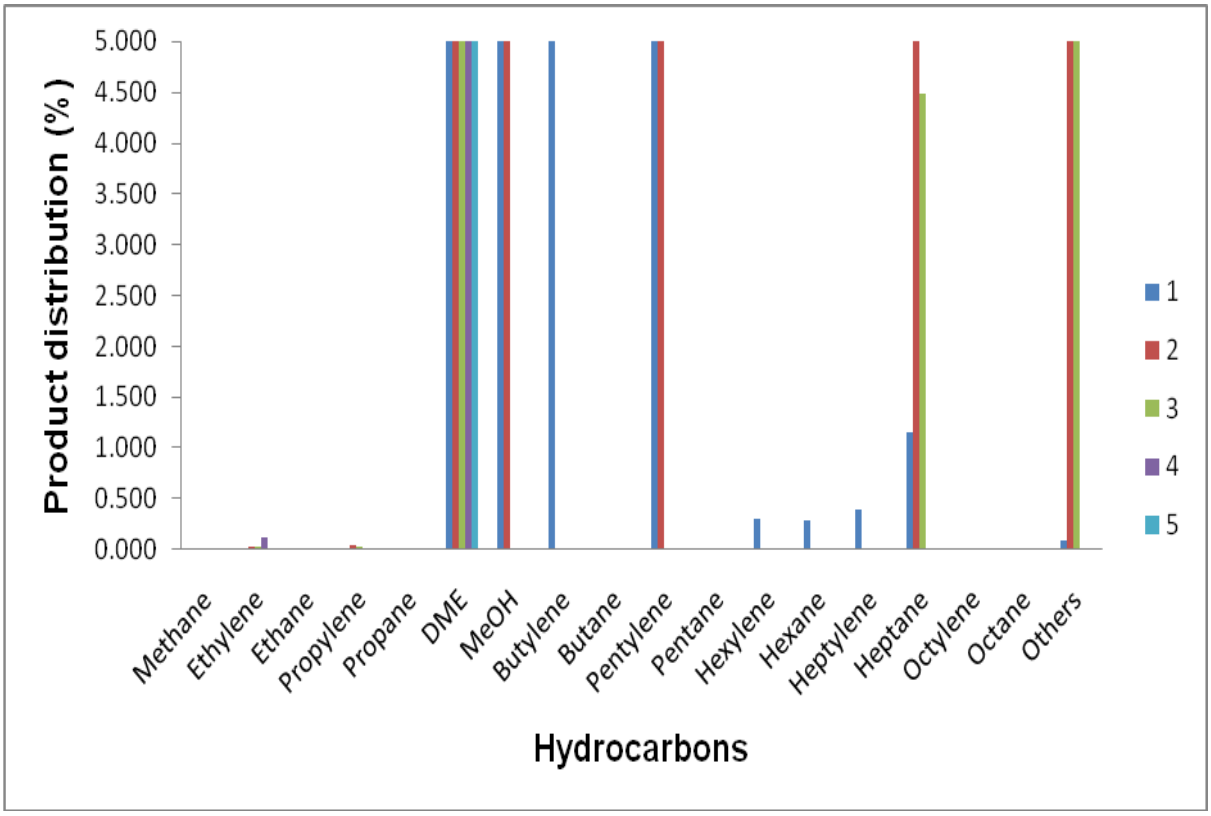


Figure 4.27 The effect of the addition of sodium oxide (0.200 mol) in the SAPO molecular sieve with the P_2O_5/Al_2O_3 mole ratio of 0.3 on product distribution of hydrocarbons from 0 - 5 % at 400 ºC reactor temperature for 1 hour.

From the figure 4.27 it shows that addition of high sodium oxide results in large amount of DME, butylene, pentylene, heptanes and other hydrocarbons from the 1st to the 5th hour. Fewer amounts of ethylene, propylene, hexylene, hexane, and heptylene were observed in the 1st hour. Product distribution of methane was observed.

Addition of low Na_2O content into gel composition of a catalyst resulted in a less ethylene and propylene in the 5th hour, and more of butylene was produced in the 1st hour. From figure 45, large amounts of hexylene and heptylene were obtained from the 2nd to the 4th hour in the reaction. Pentane and heptane were only produced during the 1st hour. Addition of high Na_2O content into gel composition of the molecular sieve reduced the methane and improved the product distribution of light olefins and other alkenes in the MTO reaction.

4.2.4.4 The relationship between the characterization of SAPO molecular sieve and the MTO reaction.

Table 4.6 shows the effects of the addition of sodium into the gel containing the SAPOs molecular sieves. Addition of low (0.013 Na_2O) and high (0.200 Na_2O) sodium contents plays a major role in the synthesis of SAPO molecular sieves and the MTO process. Methanol conversion (%) increased for both molecular sieves prepared with high and low sodium contents. Introducing sodium atom into SAPO framework reduces the acidity of the catalyst and catalyst become less acidic and more alkaline. Particle size of the catalyst prepared with low sodium content was smaller than the particle size of a catalyst prepared with high sodium content. A catalyst containing low sodium content produces both methane and light olefins with large amount methane, while a catalyst prepared with a high sodium content did not contain methane.

Obrzut *et al.* [71] studied the reduction of methane formation in MTO reaction by modifying SAPO-34 with metal ions such as K, Cs, Pt, AG and Ce. Non-modified SAPO-34 produced high methane, molecular sieve with K ion decreased methane formation. The purpose of this study is to reduce the methane conversion in MTO reaction. However, in this study a low and high N_2O was used to promote the molecular sieve activity and light olefins selectivity. What was achieved is the absent of methane in MTO reactions when high amount of N_2O was added to the molecular sieve, but light olefins selectivity was less than the one from less amount of N_2O. Adding more N_2O changes the molecular acid strength to more alkalinity therefore reduces light olefins selectivity because high light olefins selectivity is obtained on the weak acidic molecular sieve not on the alkaline molecular sieve. The main problem in this study is that MeOH is converted to DME than light olefins.

4.2.4.5 Conclusions

% Methanol conversion increased with an increase in TOS on the molecular sieves prepared using piperidine as a SDA with higher and lower sodium contents. Molecular sieve with high sodium contents reduces the formation of methane in MTO reaction, molecular sieve with low sodium contents improves the light olefins selectivity and product distribution.

4.2.5 The effect of silicon content.

Two SAPO molecular sieves with low (SiO_2/Al_2O_3 molar ratios of 0.80) and high silicon contents (SiO_2/Al_2O_3 molar ratios of 2.4) were prepared at crystallization temperature of 200 $^{\circ}C$ for 5 days. The synthesized molecular sieves with SiO_2/Al_2O_3 molar ratios of 0.8 and 0.24 were tested in the MTO reactions at the reactor temperature of 400 $^{\circ}C$ for 5 hours. Table 4.7 shows the effects of low and high silicon content on % Methanol conversion, the particle size and the product distribution of hydrocarbons for the molecular sieve, reaction temperature.

Table 4.7 The % Methanol conversion, % XRD Crystallinity and the particle size of the molecular sieve with SiO_2/Al_2O_3 mole ratios, reaction temperature and the product distribution of hydrocarbons.

Sample					PS-03					PS-17
SiO_3/Al_2O_3 = x					x = 0.800					x = 2.40
Particle size (nm)					1.49					3.8
Methanol conversion (Mol %)	93	91	85	76	55					0
Reaction temperature (^{0}C)	400	400	400	400	400	400	400	400	400	400
TOS (h)	1	2	3	4	5	1	2	3	4	5
Hydrocarbons			Product distribution							
C_2=	2.24	0.73	0.02	0.18	0.86	0.009	0.001	0.009	0.005	0.00
C_3=	1.68	0.58	0.01	0.12	0.60	0.004	0.001	0.004	0.00	0.00
C_4=	1.32	0	0	0	0	0	0	0	0.00	0
C_5=	1.65	0	0	0	0	0	0	0	0	0
C_6=	0.65	2.68	0	0.44	0	0	4.478	0	0	0
C_7=	0	2.31	2.04	28.43	0	0	0	0	0	0
C_8=	0	0	0	0	0	0	0	0	0	0
DME	5.36	0.51	0.33	2.02	3.68	96.980	66.050	98.150	67.190	0.00
MeOH	48.93	86.30	88.29	76.86	0	0.00	25.750	0.00	23.738	100.00
C1	0.70	6.90	1.67	13.81	66.43	1.481	0.144	1.499	0.205	0.00
C_2	0	0	0	0	0	0	0	0	0.002	0
C_3	0	0	0	0	0	0	0	0	0	0
C_4	0.56	0	0	0	0	0	0	0	0	0
C_5	0.79	0	0	0	0	0.000	0	0	0	0
C_6	1.30	0	0	6.57	0	0	0	0	0	0
C_7	0	0	0	7.65	0	0.215	0.00	0.218	7.820	0
C_8	0	0	0	0	0	0	0	0	0	0
Others	34.81	0	0	0		0.118	0.076	0.120	1.040	0

4.2.5 1 The effects of silicon content on % methanol conversion.

Figure 4.28 shows the effects for silicon content in the SAPO molecular sieve on methanol conversion.

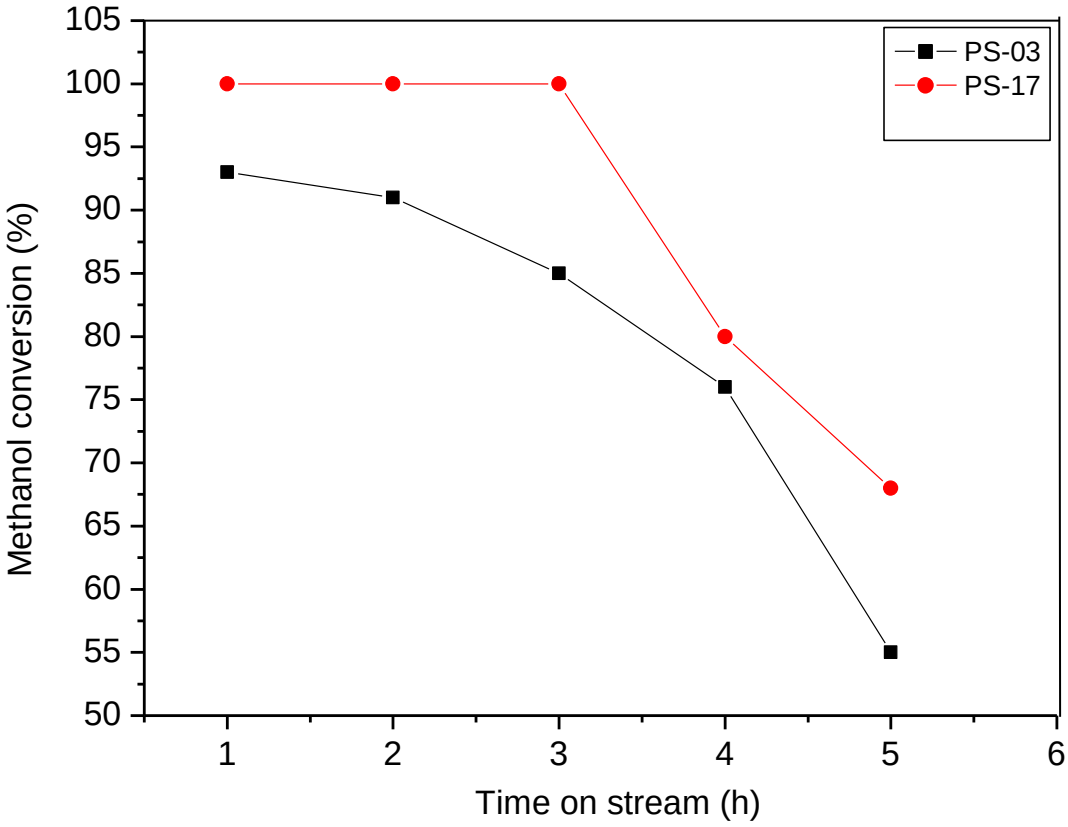


Figure 4.28 The % methanol conversion vs. Time on stream for molecular sieve with high and low silicon content.

The % methanol conversion is seems to depend mainly on a silicon content of SAPO. Figure 4.28 illustrates how the silicon content of SAPO affects the % methanol conversion. High % methanol conversion was observed from the 1st to the 3rd hour and then declined in the 4th hour for high silicon content (SiO_2/Al_2O_3 = 2.4). In contrast the % methanol conversion for the low silicon content (SiO_2/Al_2O_3 = 0.800), % methanol conversion was only high in the 1st hour decreased with an increase in time. The trends for % methanol conversion for low and high silicon content were similar i.e. the % methanol conversion decreased as time on stream increased.

4.2.5 2 The effects of silicon contents on light olefins.

Figure 4.29 shows the effects for silicon content in the SAPO molecular sieve on ethylene selectivity

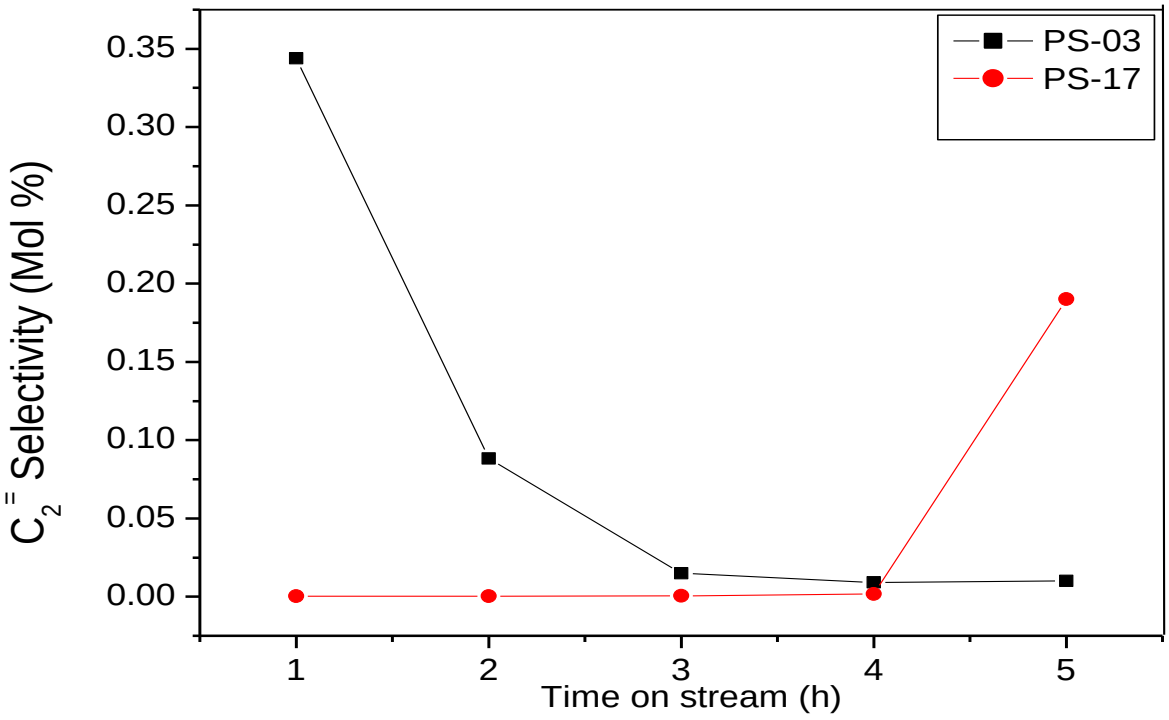


Figure 4.29 The ethylene selectivity vs. time on steam on the molecular sieve with low and high silicon content

Figure 4.29 shows that the selectivity of ethylene on the molecular sieve having low silicon content was higher than the selectivity of ethylene on the molecular sieve having high silicon content from the 1st hour to the 3rd hour. Ethylene selectivity became constant on the molecular sieves having both low and high silicon contents from the 3rd to the 4th hour. A sudden increase of ethylene selectivity was observed on the molecular sieve contains high silicon content, while ethylene selectivity on the molecular sieve containing low silicon content remain constant from the 4th to the 5th hour. Thus ethylene selectivity on low silicon content decreased with a decreased time on stream. Ethylene selectivity on the high silicon content remained constant for 4 hours then increased in the 5th hour.

Figure 4.30 shows the effects for silicon content in the SAPO molecular sieve on propylene selectivity.

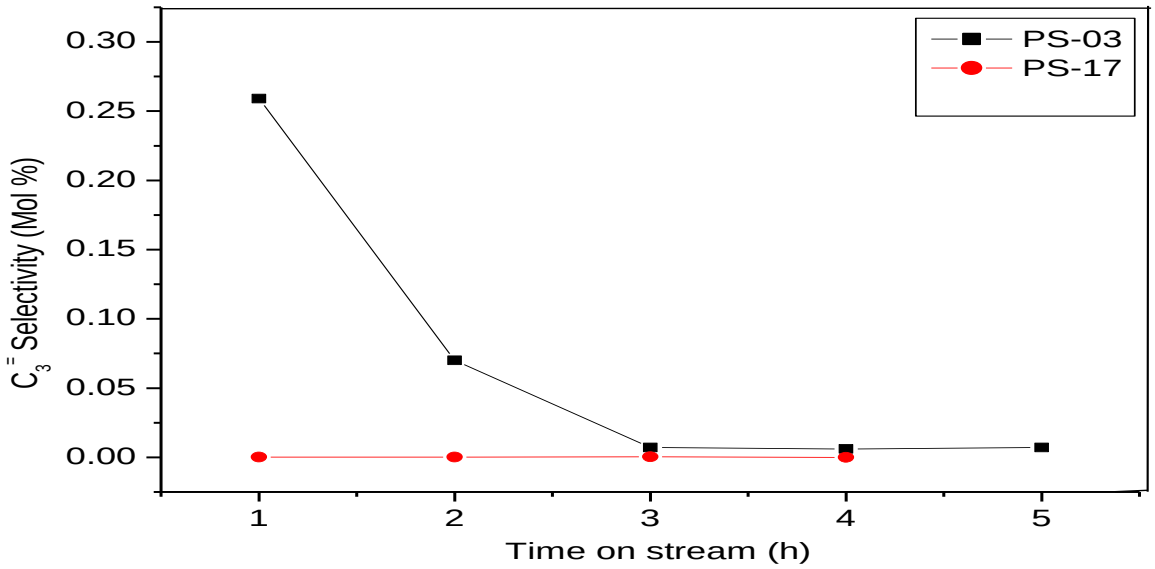


Figure 4.30 The propylene selectivity vs. time on steam on molecular sieve with low and high silicon contents.

Figure 4.30 shows that the selectivity of propylene on the molecular sieve having low silicon content was higher than the selectivity of propylene on the molecular sieve having high silicon content from the 1st hour to the 3rd hour. Propylene selectivity became constant on the molecular sieves having both low and high silicon contents from the 3rd to the 4th hour. The propylene selectivity on the molecular sieve containing low silicon content remains constant from the 4th to the 5th hour. Thus propylene selectivity on low silicon content decreased with a decreased time on stream. Propylene selectivity on the high silicon content remained constant from the 1st hour to the 4th hour. No propylene selectivity was detected in the 5th hour.

Light olefins selectivity and % methanol conversion are seemed to depend mainly on a silicon content of SAPO. Figure 4.29 - 4.30 showed that ethylene and propylene selectivity are low and remain constant on a high silicon content of SAPO molecular sieve. However the ethylene and propylene selectivity was higher on the low silicon content molecular sieve than on the high silicon content. Ethylene and propylene selectivity decreased with increases in time on stream on the lower silicon content.

Thus molecular sieve having low silicon content is more active and stable than the molecular sieve with high molecular sieve.

The product distribution of hydrocarbons was determined on those two molecular sieves with low and high silicon contents. The molecular sieve with molar ratio of SiO_2/Al_2O_3 = 2.4 gives SAPO-34 phase and amorphous phase. The products distribution on the molecular sieve with low silicon content was discussed in figure 4.14 and 4.15.

4.2.5.3 The effects of silicon contents on product distribution of hydrocarbons.

Figure 4.31 shows the effect high (SiO_2/Al_2O_3 = 2.4) silicon content in on the product distribution in the MTO reactions after 5 hours. The effects of silicon content on the product distribution of hydrocarbons ranges from 0 % to 100 %.

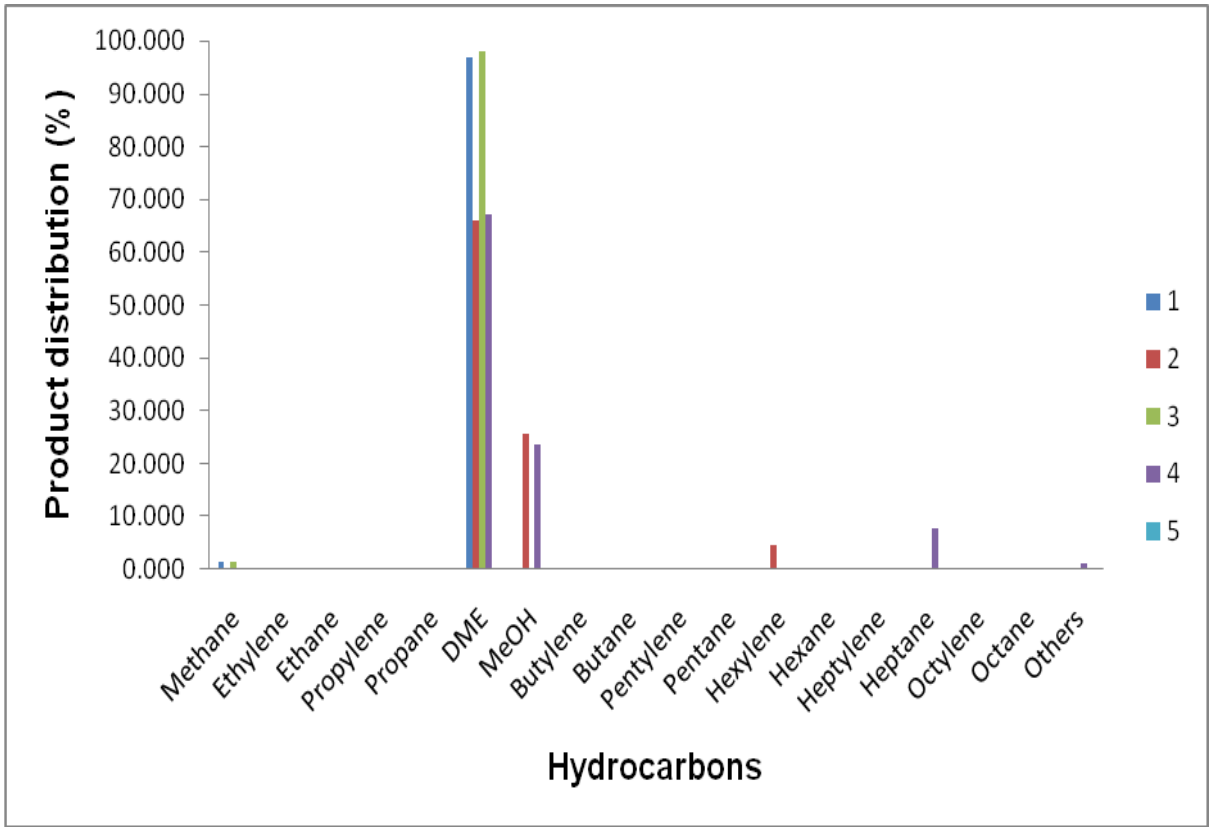


Figure 4.31 The effects of high content of SAPO molecular sieve on the product distribution of hydrocarbons ranges from 0 % to 100 %.

The effects of high content of SAPO molecular sieve on the product distribution of hydrocarbons ranges from 0 % to 100 % are shown in figure 4.31. Large amounts of

DME product distribution were observed from the 1st to the 5th hour. Fewer amounts of methane, hexylene and haptane were obtained in the 2nd and 4th hour. Thus SAPO-34 molecular sieve having high silicon content did not produce many hydrocarbons. It was stated from the figure 4.31 that the production of alkane could be reduced by addition of high sodium oxide to the molecular sieve.

Figure 4.32 shows the effect of high silicon content of molecular sieve on the pruduct distribution in the MTO reactions after 5 hour. The effects of high silicon content on the product distribution of hydrocarbons ranges from 0 - 5 %.

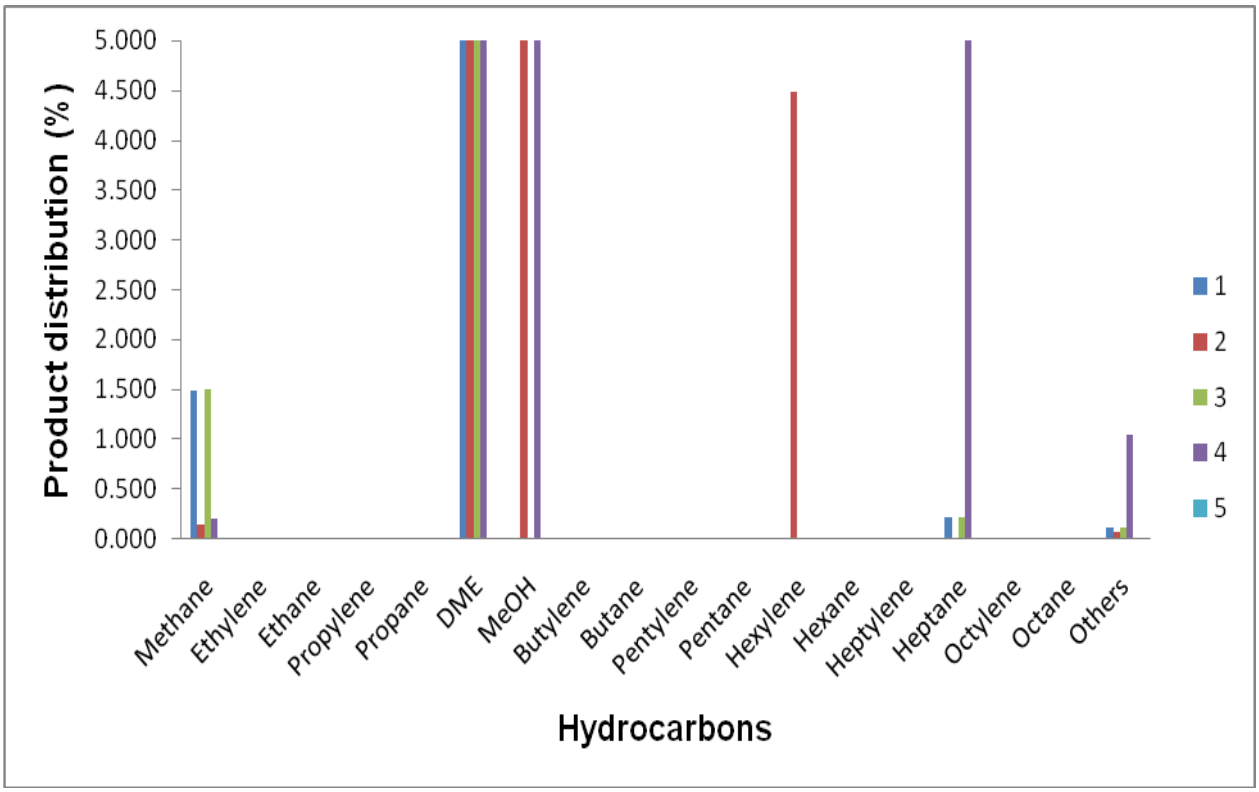


Figure 4.32 The effects of high silicon content of SAPO molecular sieve on the product distribution of hydrocarbons ranges from 0 - 5 %.

Figure 4.32 show the effects of high silicon content of SAPO molecular sieve on the product distribution of hydrocarbons ranges from 0 - 5 %. The major products that were produced on this catalyst were methane, hexylene, heptane, DME and MEOH. The light olefins were produced in very small quantities. However, the catalyst that contains the combination of SAPO-5 and SAPO-34 discussed in figure 4.15 and 4.16 has a higher product distribution of light olefins.

4.2.5 4 The relationship between the characterization of SAPO molecular sieve and the MTO reaction.

XRD patterns for molecular sieves prepared with low and high silicon contents differ from one another. The patterns for catalyst synthesized with high silicon content revealed the existence of SAPO-34 with some amorphous particles.

The methanol conversion (%) for a catalyst with high silicon content is higher than methanol conversion over a catalyst prepared with lower silicon content. NH_3-TPD experiments showed desorption in same temperature region. High intensity indicates that more ammonia was adsorbed for lower silicon catalyst and less ammonia was adsorbed for catalyst with high silicon content. They both contained weak Brønsted acid sites but different in the amount of acid strength. SEM micrographs showed pentagon crystals that indicated the presence of SAPO-5 without SAPO-34. SEM micrograph of the catalyst with high silicon content did not show the present of SAPO-34. Solid state NMR spectra suggested the breakage of Al-O-P bonds and formation of a new Si-O-Al bond for both catalysts.

Selectivity of light olefins for the catalyst with high silicon content was lower because of lower acid strength. The selectivity of light olefins over the catalyst with low silicon content was higher due to the enhanced acid strength. What was interesting was that only methane, ethylene and propylene and some impurities were produced from the catalyst with high silicon content. From the discussion above, the methane content could be reduced by adding sodium atoms to the catalyst. The low production of light olefins from both catalysts is associated with MTO process taking place at room temperature instead of taking place at the boiling temperature of methanol. This resulted in a high amount of DME produced from the dehydration of methanol. Dehydration of DME to light olefins was noted.

4.2.5.5 Conclusions

The molecular sieve containing low silicon contents has three phases, SAPO-5, SAPO-34 and amorphous phase. Its particle size is smaller, but many hydrocarbons were produced with low light olefins selectivity on this molecular sieve. Molecular sieve with high silicon contents contains two phases, SAPO-34 and amorphous phase. Its particle size is high. This evident was obtained from the XRD patters in

figure 3.6 only methane, ethylene, propylene and DME were produced on this molecular sieve. Since the main objective of this study is to synthesize a molecular sieve which is good in MTO, we can say that molecular with high silicon content is the promising molecular sieve for MTO. However, there was low light olefins selectivity on this molecular sieve than the selectivity on the molecular sieve synthesized with low silicon contents. This is because of the high amount of amorphous materials that blocks the surface of the molecular sieve. MeOH to DME is still a major problem and only less MTO reaction occur.

4.2.6. The effect of modified and non-modified molecular sieve.

Since the SAPO molecular sieve prepared earlier with the use of piperidine was less active to % methanol conversion, ethylene and propylene selectivity, a new method for the preparation of SAPO also with piperidine structure directing agent was introduced in 2.1.2.2. Modified SAPO catalysts with Fe, Co and Ni chloride were also prepared using the similar method. All molecular sieves were tested for the MTO reaction at a reactor temperature of 400 ^{o}C. Table 4.8 shows The % Methanol conversion and the particle size of the molecular sieve with modified and non-modified, reaction temperature and the product distribution of hydrocarbons.

Table 4.8 The % Methanol conversion and the particle size of the molecular sieve with modified and non-modified, reaction temperature and the product distribution of hydrocarbons.

					PS-18					PS-19
SAPO-34 + Metal					SAPO-34					FeSAPO-34
Particle size (nm)					3.8					3.8
Methanol conversion (Mol %)	90	94	100	100	95	23	97	97	96	96
Reaction temperature (^{0}C)	400	400	400	400	400	400	400	400	400	400
TOS (h)	1	2	3	4	5	1	2	3	4	5
Hydrocarbons			Product distribution							
C_2=	0.040	0.032	0.021	0.209	0.026	0.006	0.035	0.022	0.016	0.018
C_3=	1.947	0.032	0.015	0.105	0.013	0.010	0.035	0.024	0.016	0.018
C_4=	0	0	0	0	0	0	0	0	0	0
C_5=	0.046	0.013	0.137	0	0	0.003	0	0	0	0
C_6=	0	0	0	0	0	2.492	5.784	7.508	8.152	0
C_7=	3.691	6.686	5.398	6.697	48.102	0	0	0	0	0
C_8=	0	0	0	0	0	0	0	0	0	0
DME	51.021	70.336	94.393	30.2	71.430	15.496	74.557	74.864	64.827	72.767
MeOH	31.452	21.602	0	0	18.317	81.880	18.833	17.568	23.524	26.196
C1	0.647	1.286	0	0.313	0.345	0.038	0.741	0	0.466	1.001
C_2	0.010	0.130	0.100	0	0	0.001	0.014	0.015.	0.008	0
C_3	9.153	0	0	0	0	0	0	0	0	0
C_4	0.000	0	0	0	0	0	0	0	0	0
C_5	0	0	0	0	0	0	0	0	0	0
C_6	0	0	0	0	0	0	0	0	0	0
C_7	1.972	0	0	0	0	0.000	0	0	0	0
C_8	0	0	0	0	0	0	0	0	0	0
Others	0	0	0.026	68.311	3.704	0.073	0	0.000	2.993	0.000

Table 4.8 continues

Sample					PS-20					PS-21
SAPO-34 + Metal					CoSAPO-34					NiSAPO-34
Particle size (nm)					3.8					3.8
Methanol conversion (Mol %)	4	84	78	91	92	82	100	96	97	98
Reaction temperature (^{0}C)	400	400	400	400	400	400	400	400	400	400
TOS (h)	1	2	3	4	5	1	2	3	4	5
Hydrocarbons			Product distribution							
C_2=	0.094	0.093	0.097	0.064	0.040	0.000	2.468	0.019	0.014	0.008
C_3=	0.006	0.074	0.028	0	0	0.01	0.494	0.00	0.00	0.00
C_4=	0	0	0	0	0	0	0	0	0	0
C_5=	2.059	0	0	0	0	0.000	0	0	0	0
C_6=	0	0.000	0	0	0	0.000	0.00	0	0.00	0
C_7=	0.125	0.000	0	0	0	0.000	0.00	0.00	0.00	0
C_8=	0	0.000	0	0	0	0	0	0	0	0
DME	0.125	0.000	0.000	0.00	0	87.94	0	88.161	91.085	96.440
MeOH	96.879	94.231	97.497	97.094	99.960	0.00	0	0.00	0.00	0
C1	0.103	2.411	1.808	2.874	0	0.12	74.038	0.00	0.00	0.00
C_2	0	0.037	0.014	0	0	0.03	23.001	0	0	0
C_3	0	0	0	0	0	0	0	0	0	0
C_4	0	0.000	0	0	0	0	0	0	0	0
C_5	0	0.000	0	0	0	0	0	0	0	0
C_6	0	0.000	0	0	0	0	0	0	0.00	0
C_7	0.000	3.153	0.556	0	0	0	0	0	0.00	0
C_8	0	0	0	0	0	0	0	0	0	0
Others	0.048	0	0	0	0	0	0	0	0	0

4.2.6.1 The effects of modified and non-modified on % methanol conversion

Figure 4.33 shows the effects of modified and non-modified SAPO molecular sieve on % methanol conversion.

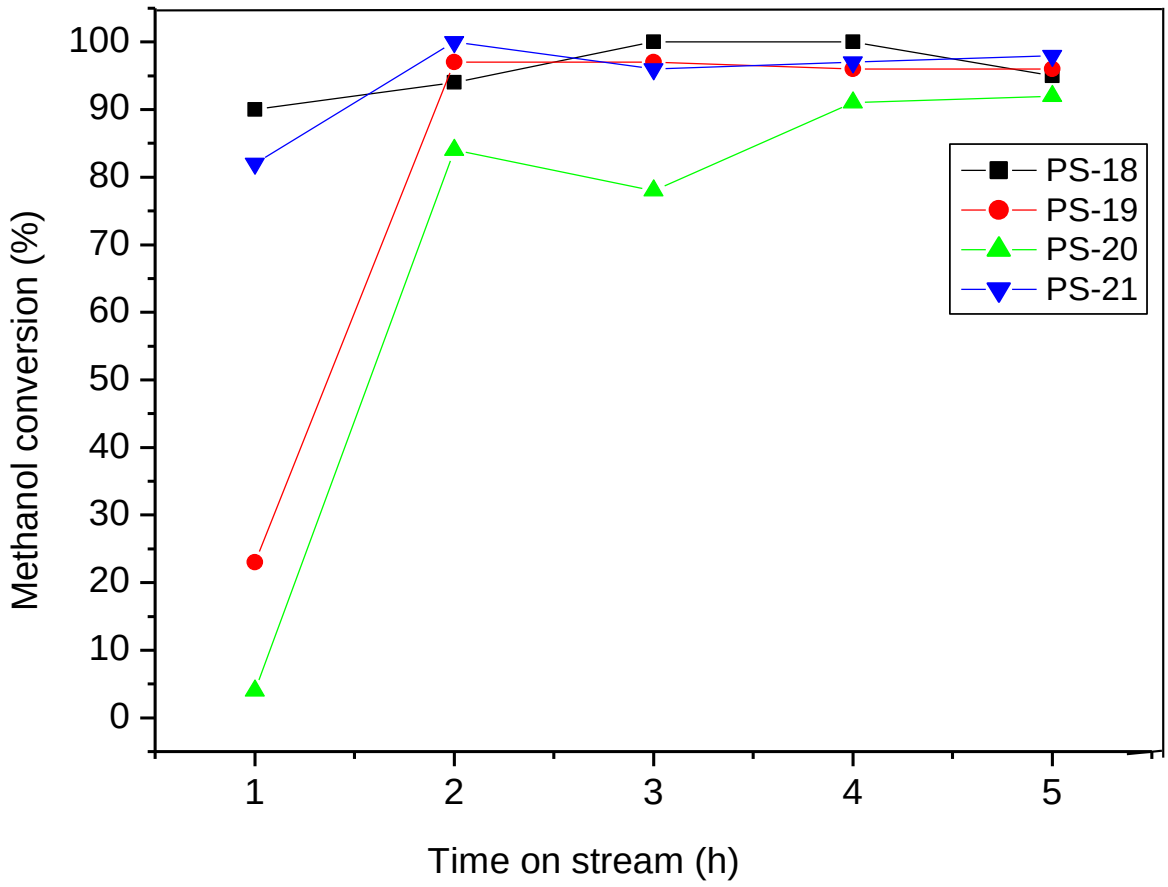


Figure 4.33 The methanol conversion vs. time on stream of modified and unmodified SAPO molecular sieve.

The results in figure 4.33 show the effects of modified and non-modified SAPO molecular sieve on % methanol conversion. The % methanol conversions on the unmodified and Ni-SAPO molecular sieve were high from the 1st to the 5th hour (90-100%). The methanol conversions on the Fe-SAPO and Co-SAPO were low from the 1st hour and then increased from the 2nd hour to the 5th hour in time on stream. But % methanol conversion was on Co-SAPO lower than the % methanol conversion on Fe-SAPO. Thus good molecular sieves for % methanol conversion are unmodified SAPO-34 and Ni-SAPO. The % methanol conversion on modified and non-modified molecular sieves increased as the time on stream increased.

4.2.6.2 The effects of modified and non-modified on light olefins

Figure 4.34 shows the effects of non-modified SAPO molecular sieve on ethylene selectivity.

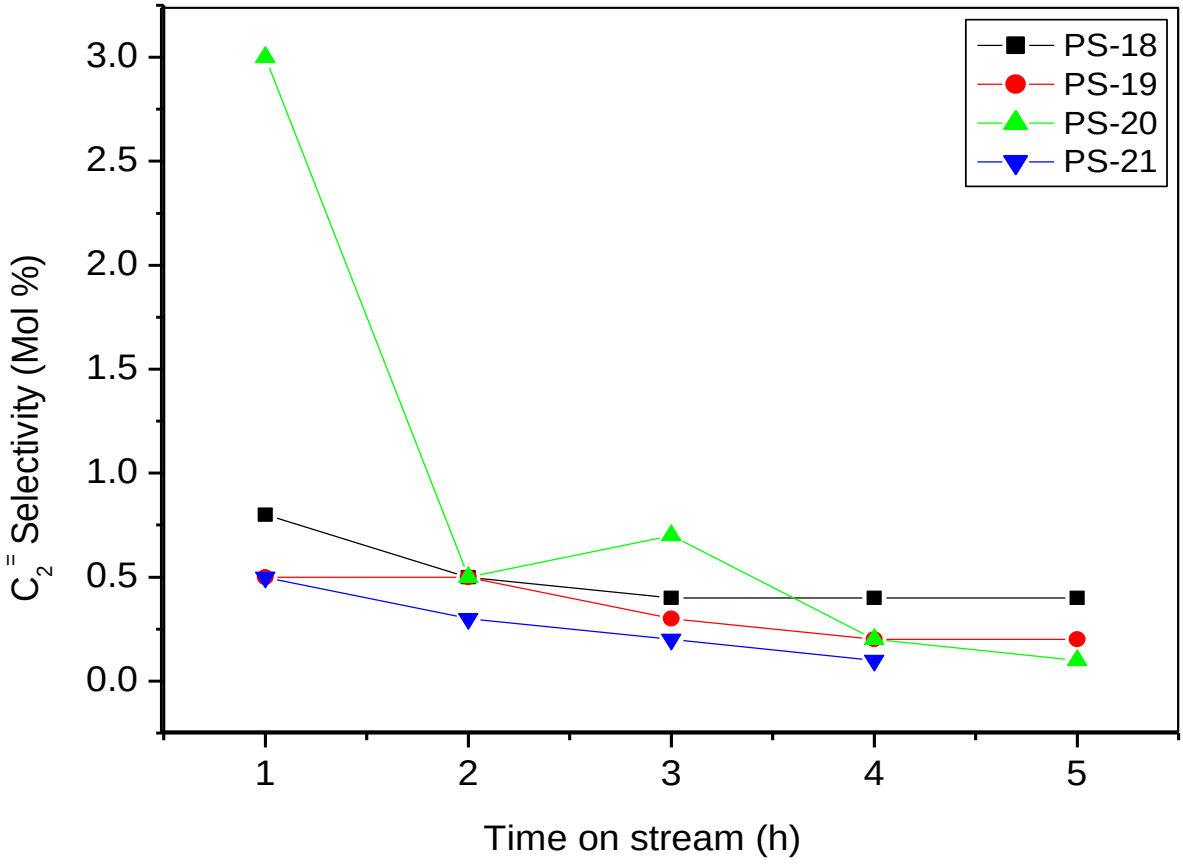


Figure 4.34 The ethylene selectivity vs. time on steam on modified and non-modified SAPO molecular sieve.

High selectivity of ethylene (3.0 mol %) as observed on the Co-SAPO molecular sieve on the1st hour, and then decreased suddenly (3.0-0.5 mol %) from the 1st to the 2nd hour. The ethylene selectivity on this molecular sieve decreased as the time on stream decreased. The ethylene selectivity on SAPO, Ni-SAPO and Fe-SAPO was low and decreased as the time on stream decreased. Thus the good molecular sieve for ethylene selectivity is Co-SAPO.

Figure 4.35 shows the effects of modified and unmodified SAPO molecular sieve on propylene selectivity.

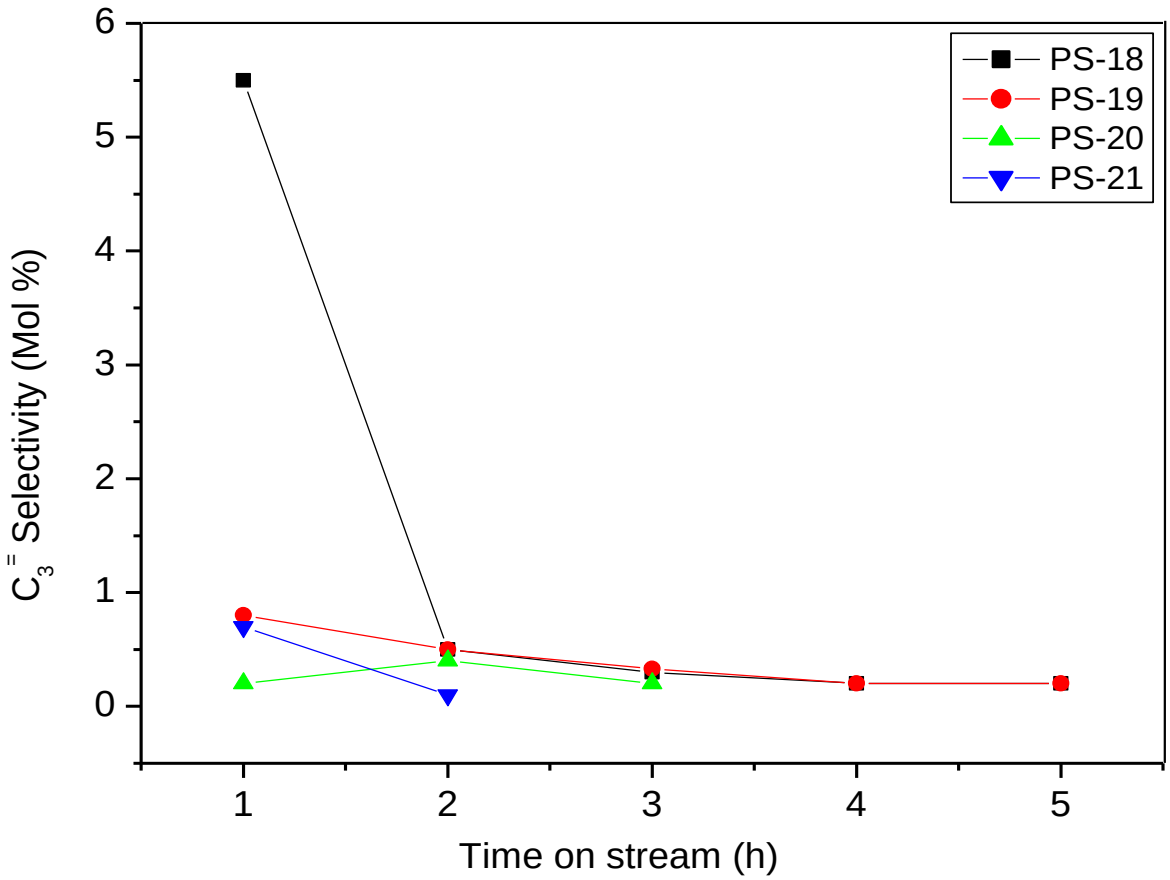


Figure 4.35 The propylene selectivity vs. time on steam on modified and unmodified SAPO molecular sieve.

Figure 4.35 show the effects of modified and unmodified SAPO molecular sieve on propylene selectivity. High (5.5 mol %) propylene selectivity was observed on the SAPO molecular sieve in the 1st hour. This propylene selectivity decreased from the 1st to the 2nd (5.5-0.5 mol %) on the same molecular sieve. All modified molecular sieves have low propylene selectivity. Ni-SAPO was less active from the 1st to the 2nd hour, and then became inactive from the 2nd to the 5th hour. The Co-SAPO molecular sieve was active from the 1st to the 3rd hour. SAPO and Fe-SAPOs are active and stable throughout the reaction Thus good molecular sieve for the propylene selectivity is non-modified SAPO compared to the other molecular sieves incorporated with Fe, Co and Ni.

The % methanol conversion on Co-SAPO molecular sieve was lower than % methanol conversion on Fe-SAPO and Ni-SAPO. But the Co-SAPO molecular sieve

improved ethylene selectivity, while Fe-SAPO and Ni-SAPO reduced the selectivity of ethylene. The non-modified SAPO molecular sieve produced higher propylene in the 1st hour than the modified SAPO molecular sieve.

4.2.6 3 The effects of modified and non modified on product distribution of hydrocarbons

Figure 4.36 show the effect of non-modified SAPO molecular sieve on product distribution. The product distribution of hydrocarbons ranges from 0 - 100 % for 5 hours.

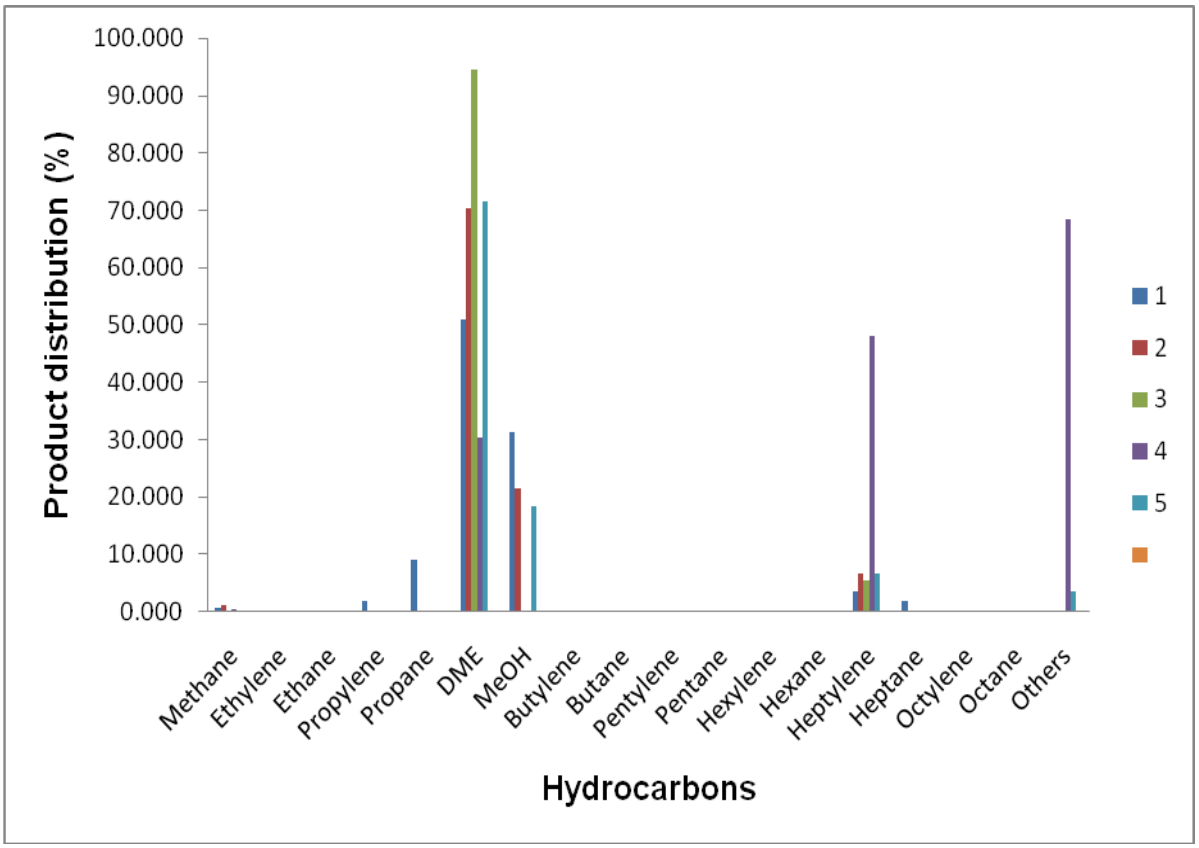


Figure 4.36 The product distribution of hydrocarbons on non-modified molecular sieve ranges from 0 -100 % after 5 hours.

Figure 4.37 show the effect of non-modified SAPO molecular sieve on product distribution. The product distribution of hydrocarbons ranges from 0 - 5 % after 5 hours.

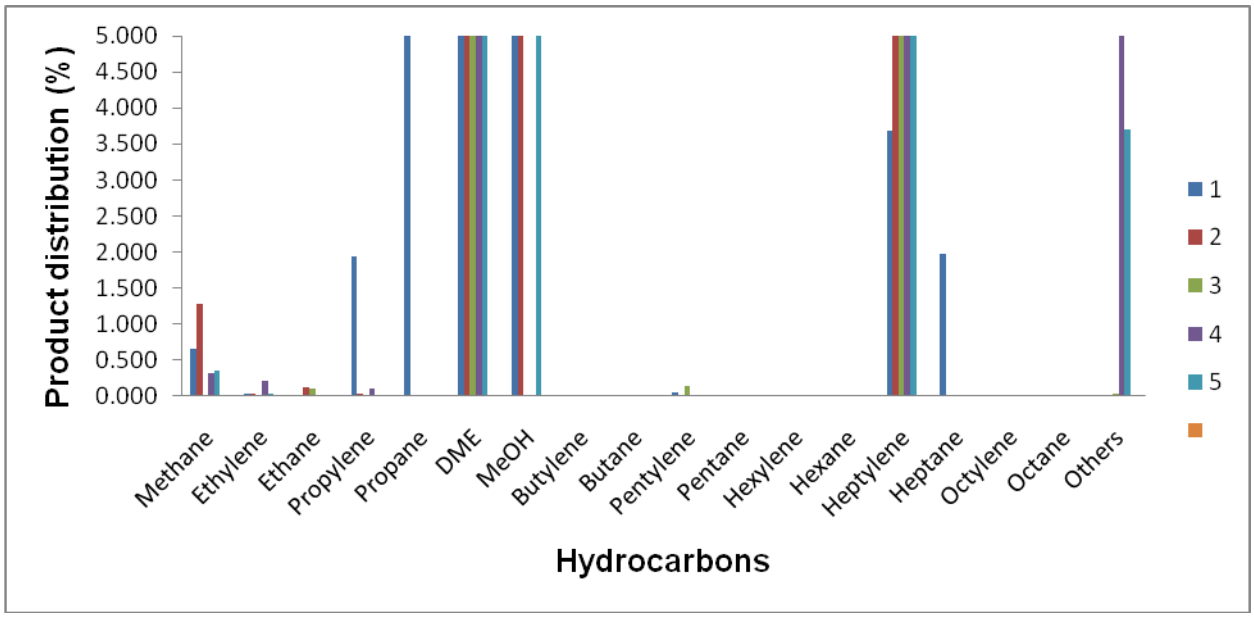


Figure 4.37 The product distribution of hydrocarbons on SAPO molecular sieve from the ranges 0 – 5 %

Figure 4.38 show the effect of Fe-SAPO molecular sieve on product distribution. The product distribution of hydrocarbons ranges from 0 - 100 % for 5 hours.

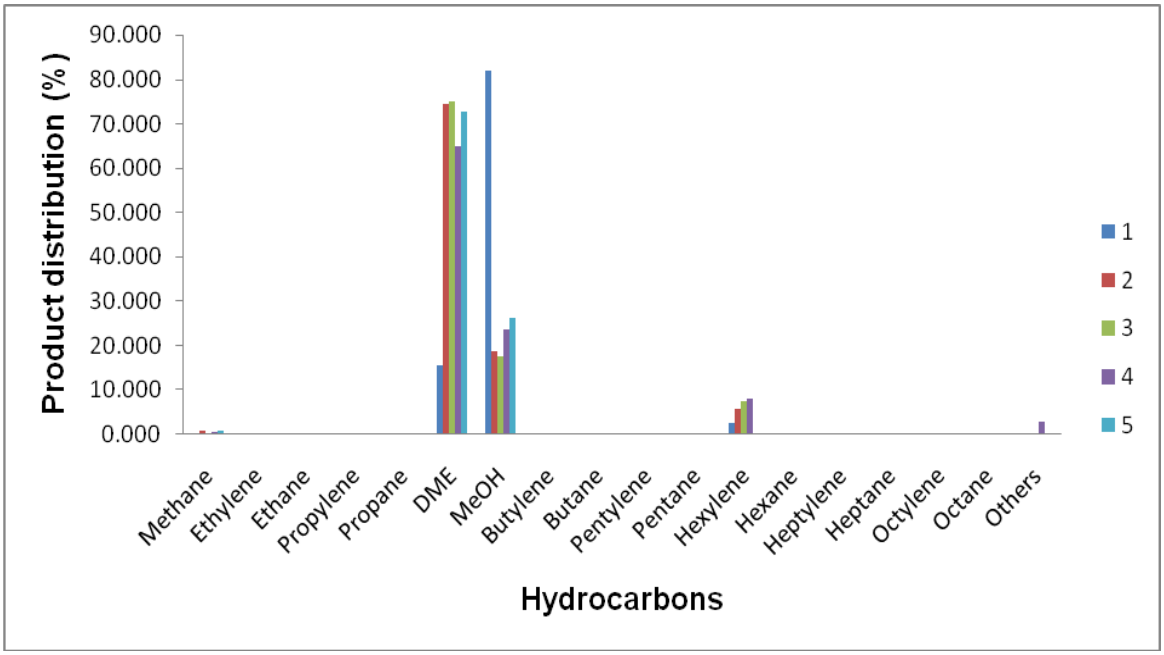


Figure 4.38 The product distribution of hydrocarbons on Fe-SAPO molecular sieve.

Figure 4.38 show the effect of Fe-SAPO molecular sieve on product distribution. The product distribution of hydrocarbons ranges from 0 - 5 % for 5 hours.

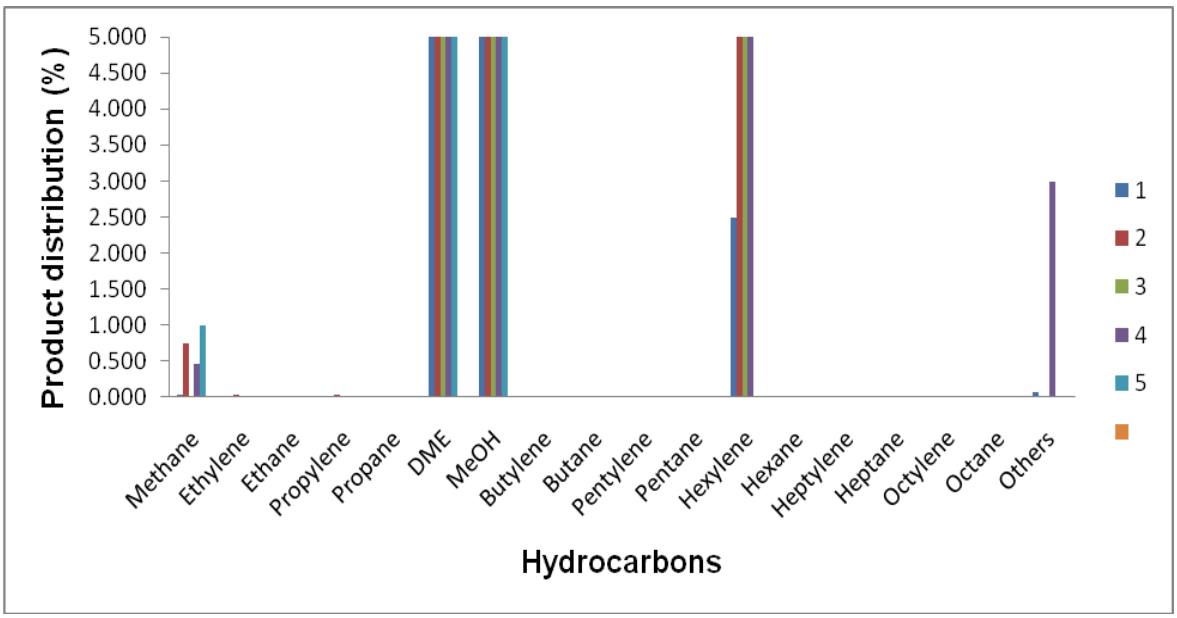


Figure 4.39 The product distribution of hydrocarbons on Fe-SAPO molecular sieve.

Figure 4.39 show the effect of Co-SAPO molecular sieve on product distribution. The product distribution of hydrocarbons ranges from 0 - 100 % for 5 hours.

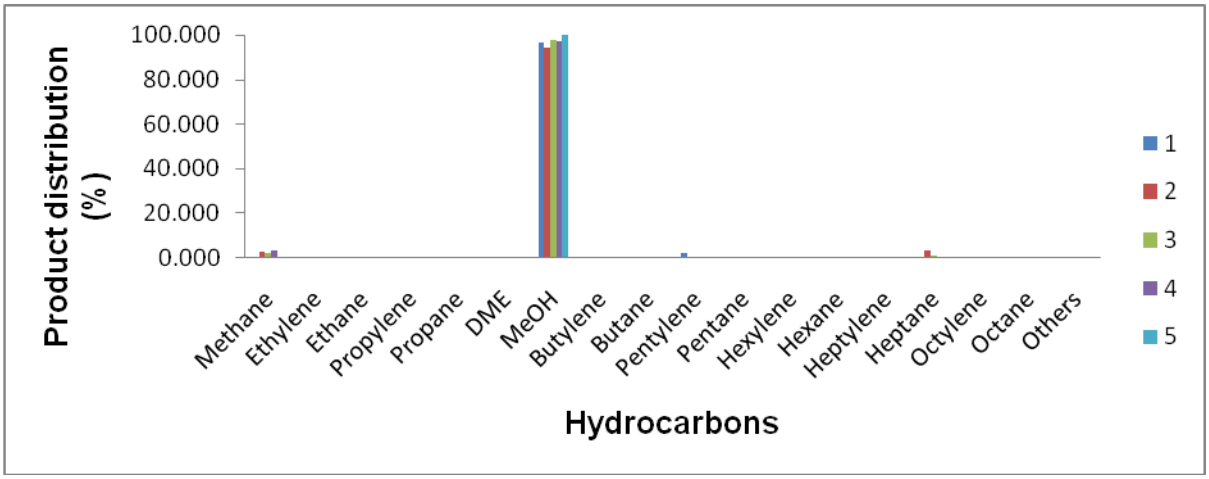


Figure 4.40 The product distribution of hydrocarbons on Co-SAPO molecular sieve.

Figure 4.41 show the effect of Co-SAPO molecular sieve on product distribution. The product distribution of hydrocarbons ranges from 0 - 5 % for 5 hours.

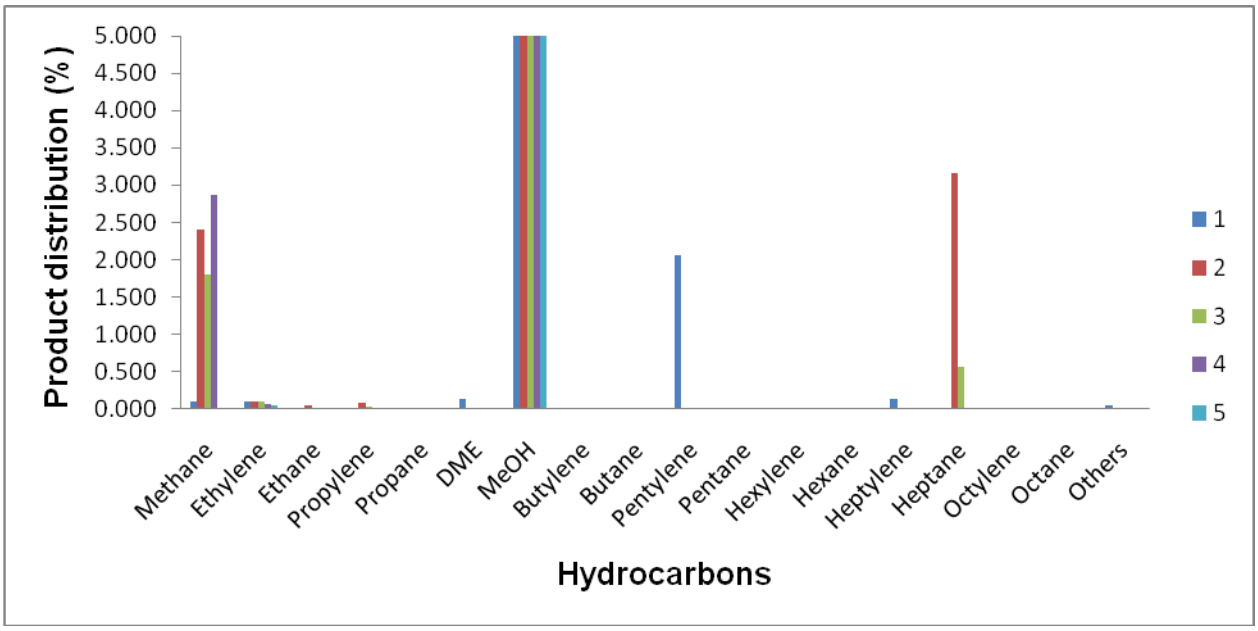


Figure 4.41 The product distribution of hydrocarbons on Co-SAPO molecular sieve.

Figure 4.41 show the effect of Ni-SAPO molecular sieve on product distribution. The product distribution of hydrocarbons ranges from 0 - 100 % for 5 hours.

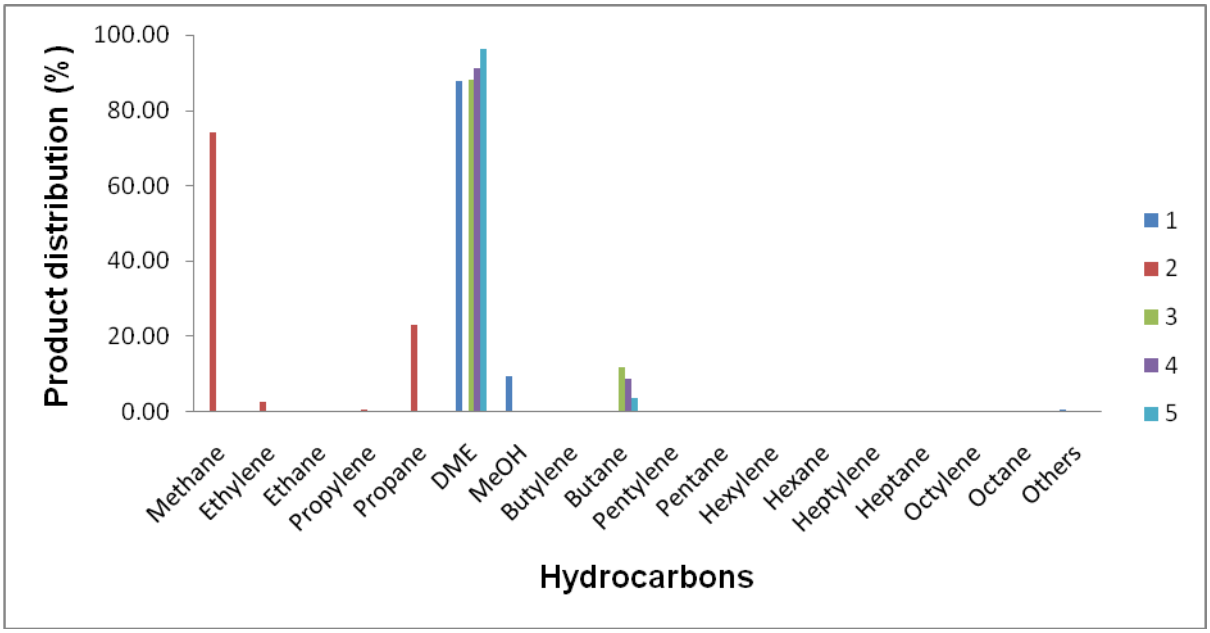


Figure 4.42 The product distribution of hydrocarbons on Ni-SAPO molecular sieve.

Figure 4.42 show the effect of Ni-SAPO molecular sieve on product distribution. The product distribution of hydrocarbons ranges from 0 - 5 % for 5 hours.

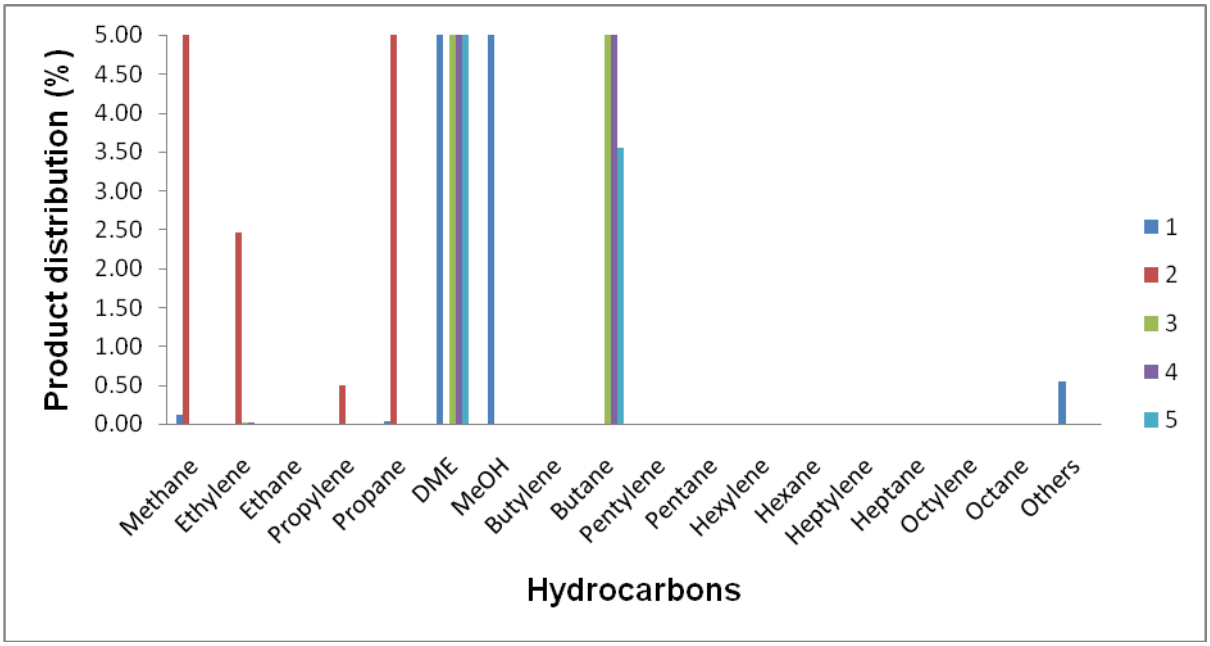


Figure 4.43 The product distribution of hydrocarbons on Ni--SAPO molecular sieve.

Figure 4.36 - 4.43 showed high product distribution of propylene and propane on non-modified SAPO molecular sieve wthin 1 hour reaction. This decreased from the second hour until the 5th hour. Ethylene was hardly formed and butylene was not

seen from the 1st hour to the second hour. Large amount DME and MeOH were formed. Only small amount of pentylene were observed within 3 hours. An excess of heptylene was produced from the 1st hour, while heptanes appeared within one hour.

Fe-SAPO promoted the production of hexylene over light olefins within the first to the 4th hour. Ethylene and propylene amount were reletively small. Their products like methane and unidentified hydrocarbons existed in small amounts but product distribution of DME and MeOH was very high. Major preduced products on SAPO catalyst containing Co metal were methane, MEOH, and heptane with a very small amount of ethylene and propylene. A large amount of pentylene was only obsrved within 1 hour. Hydrocarbons produced from Ni-SAPO were ethylene, propane, DME and butane. The amount of DME was very high compared to that of ethylene, propane and butane.

Figure 4.41 showed that high product distribution of propylene and propane observed on non-modified SAPO molecular sieve within 1 hour reaction. This decreased from the second hour until the 4th hour. Ethylene was hardly formed and butylene was not seen from the 1st hour to the 2nd hour. Large amount DME and MeOH were formed. Only small amount of pentylene were observed within 3 hours. An excess of heptylene was produced from the 1st hour, while heptanes appeared within one hour.

Fe-SAPO promoted the production of hexylene over light olefins within the 1st to the fouth hour. Ethylene and propylene amount were reletively small. Ther products like methane and unidentified hydrocarbons existed in small amounts but product distribution of DME and MeOH was very high. The major products produced on SAPO catalyst containing Co metal were methane, MeOH, and heptane with avery small amount of ethylene and propylene. A large amount of pentylene was only obsrved within 1 hour. Hydrocarbons produced from Ni-SAPO wre ethylene, propane, DME and butane. The amount of DME was very high compared to that of ethylene, propane and butane.

4.2.6.4 The relationship between the characterization of SAPO molecular sieve and the MTO reaction.

Modified and non-modified molecular sieve were prepared with Fe, Co and Ni chloride. Table 4.8 shows that all molecular sieves has similar particle size of 3.8 nm because of the highest peak that appeared at 2Ɵ scale 9.9. Molecular sieves prepared with Co metal and the molecular sieve prepared without metal has shown the different from others. Molecular sieve with Co metal has high ethylene selectivity and molecular sieve without metal has high propylene selectivity. The XRD patterns for two molecular sieves in figure 3.7 have similar peak at 2Ɵ scale of 21^0 which is responsible for light olefins selectivity. This peak is very small that it can be negligible in the molecular sieves prepared with Fe and Ni metals. These contribute to the light olefins selectivity. SEM does not show exactly SAPO-34 structure. From the literature, molecular sieve incorporated with Ni metal has high ethylene selectivity in MTO compared with selectivity on the molecular sieve prepared with Fe and Co metals [59-61]. The findings are different from our study in the sense that Co containing molecular sieve has high ethylene selectivity and molecular sieve without metal has high propylene selectivity. When other zeolites molecular sieves such as MFI and SAPO used for MTO reactions, they were active, the life time is long and the selectivity in MTO increased with the less amount of methane [72]. Methane could be eliminated by introducing Na_2O to the molecular sieve's framework. The evidence is shown in 4.2.4.2.

4.2.6.5 Conclusions

Molecular sieve containing Co metal improves ethylene selectivity and non-modified (without metal) molecular sieve improves propylene selectivity. Molecular sieves containing Fe and Ni metal improve light olefins slightly. All molecular sieves are active and more stable in MTO reactions. Thus all molecular sieves are good for MTO reactions. However there is still the present of high DME product than light olefins.

4.2.7. The use of structure directing agent

Two different structure directing agent s (piperidine and TEAOH) were used to prepare SAPO molecular sieve catalysts. Molecular sieve synthesized with TEAOH

structure directing agent was regarded as a control experiment to judge the piperidine – structure directing agent synthesis. The catalysts were tested for the MTO reaction at a reactor temperature of 400 °C for 5 hours. Table 4.9 shows the effect of the structure directing agent s on MTO reaction.

Table 4.9 The particle size of the catalysts, % methanol conversion and products distribution of hydrocarbons for five hours reaction time for structure directing agents.

Sample	PS-03					PS-22				
Template	Piperidine					TEAOH				
Particle size (nm)	1.49					4.00				
Methanol conversion (Mol %)	93	91	85	76	55	87	100	100	100	100
Reaction temperature (^{0}C)	400	400	400	400	400	400	400	400	400	400
TOS (h)	1	2	3	4	5	1	2	3	4	5
Hydrocarbons	Products distribu									
C_2=	2.24	0.73	0.02	0.18	0.86	0.055	0.023	0.028	0.013	0.011
C_3=	1.68	0.58	0.01	0.12	0.60	0.035	0.032	0.016	0.013	0.007
C_4=	1.32									
C_5=	1.65									
C_6=	0.65	2.68		0.44						
C_7=		2.31	2.04	28.43						
C_8=										
DME	5.36	0.51	0.33	2.02	3.68	66.438	87.298	77.446	79.912	92.079
MEOH	48.93	86.30	88.29	76.86		16.651				
C1	0.70	6.90	1.67	13.81	66.43	1.649	0.239	0.221		0.196
C_2						0.005	0.009			
C_3						0.480				
C_4	0.56									
C_5	0.79					0.066				
C_6	1.30			6.57						
C_7				7.65		14.618	12.392	22.288	20.063	7.707
C_8										
Others	34.81									

4.2.7 1 The effects of structure directing agent s on % methanol conversion

Figure 4.44 show the influence upon % methanol conversion, on the catalysts synthesized with piperidine and TEAOH structure directing agent.

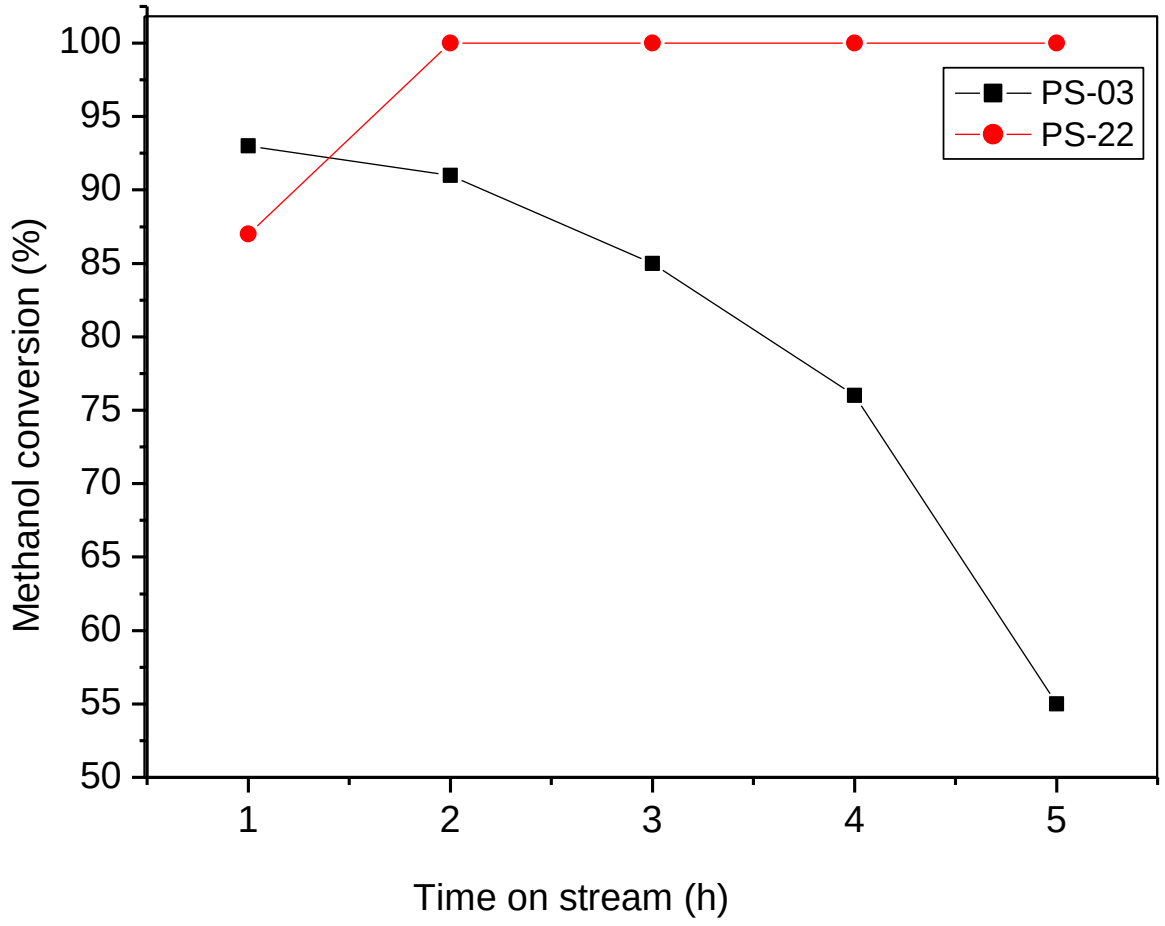
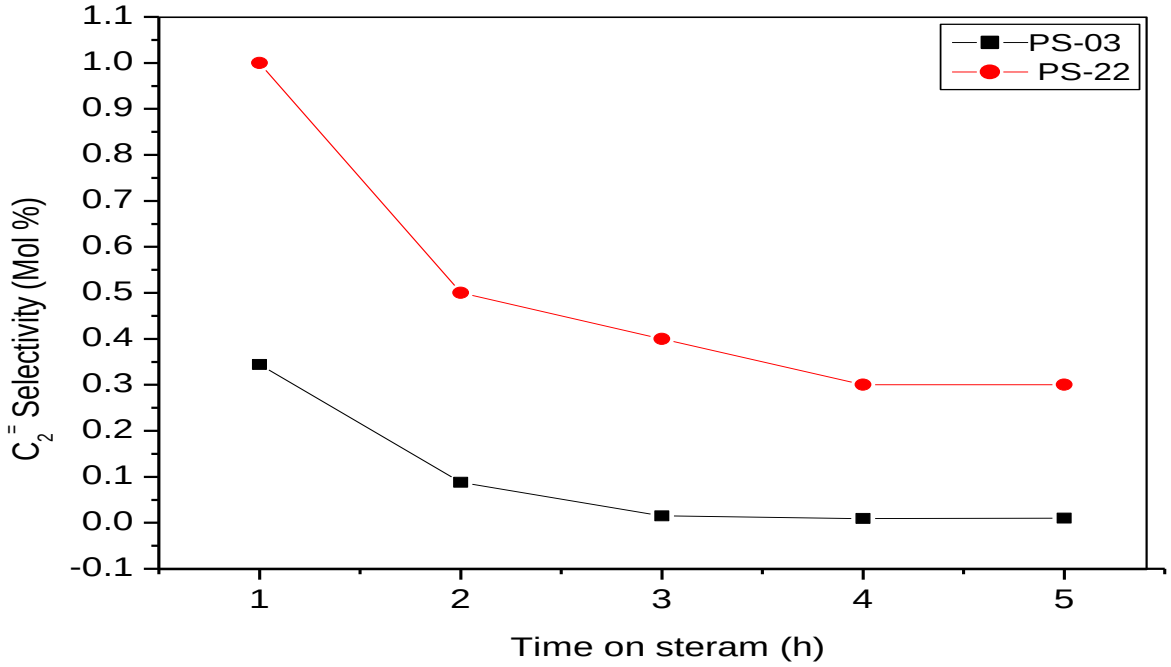


Figure 4.44 Methanol conversions vs. Time on stream over molecular sieves prepared with different structure directing agent s

4.2.7 2 The effects of structure directing agent s on light olefins

Figure 48 show the influence of ethylene selectivity, on the catalysts synthesized with piperidine and TEAOH structure directing agent.



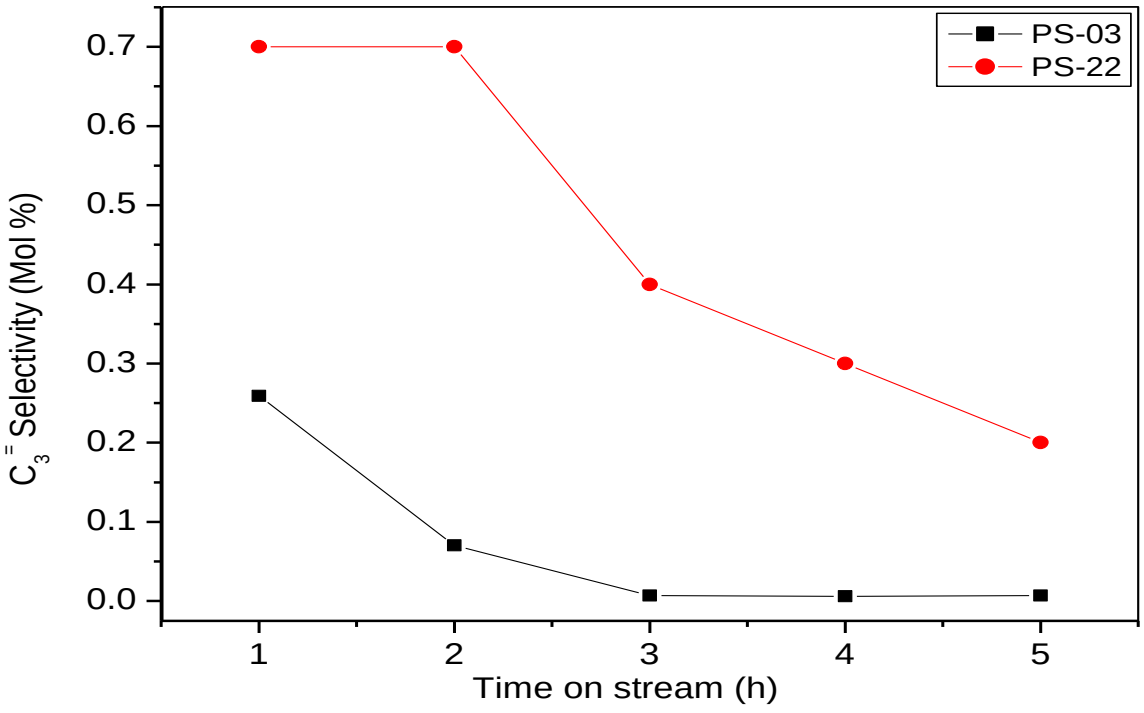


Figure 4.45 The influence of propylene selectivity, on the catalysts synthesized with piperidine and TEAOH structure directing agent.

From figure 4.44 - 4.45, it is clear that the structure directing agent s used to make the molecular sieves affected the % methanol and production of ethylene and propylene significantly. The % methanol on the molecular sieve prepared with TEAOH structure directing agent was low in the 1st hour, but increased to 100 % from the 2nd to the 5th hour. The % methanol conversion from the catalyst synthesized with piperidine was lower than % Methanol conversion for the catalyst prepared with TEAOH. This amount decreased with increase in time on stream. Ethylene and propylene selectivity produced from the catalyst prepared with TEAOH are higher than that from the catalyst prepared with piperidine. Ethylene and propylene selectivity for the catalyst prepared with TEAOH and piperidine shows a similar trend, i.e. they decreased with an increase in time. Thus TEAOH is a better structure directing agent to make catalyst for the production of ethylene and propylene.

4.2.7.3 The effects of structure directing agent s on product distribution of hydrocarbons.

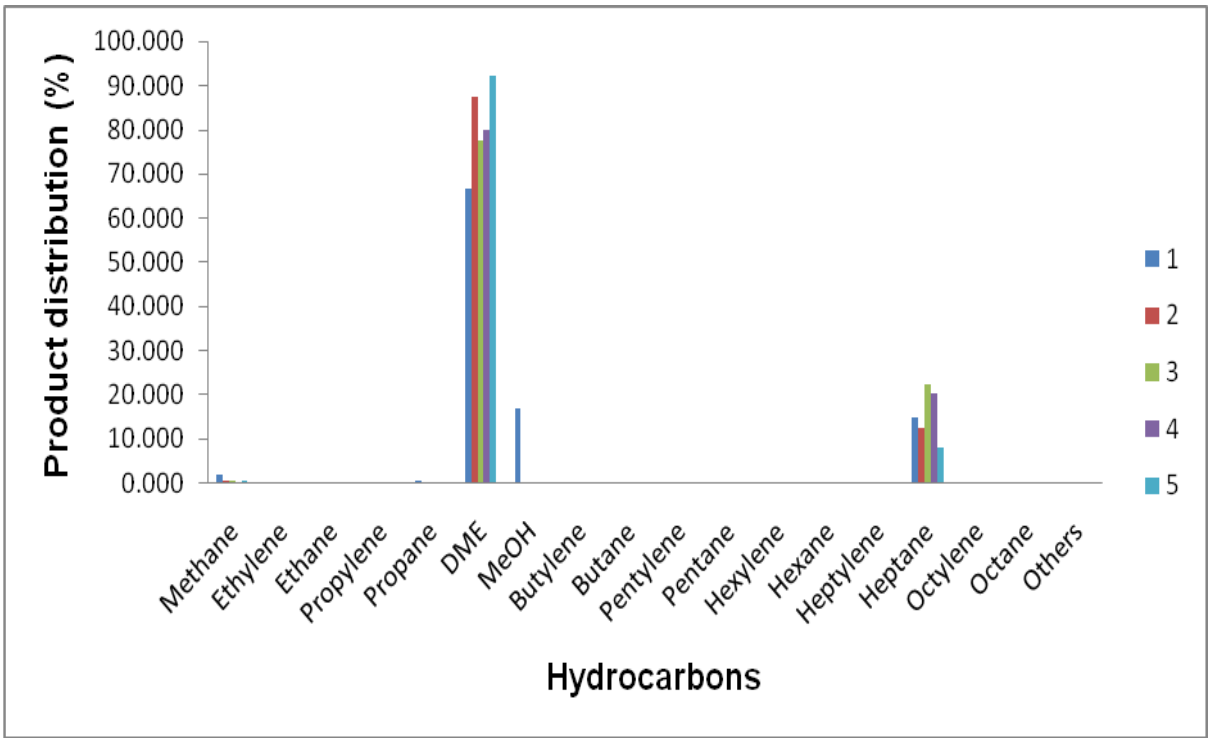


Figure 4.46. The product distribution of hydrocarbons on MTO reactions over SAPO with different structure directing agent s from 0 – 100 % for 5 hours.

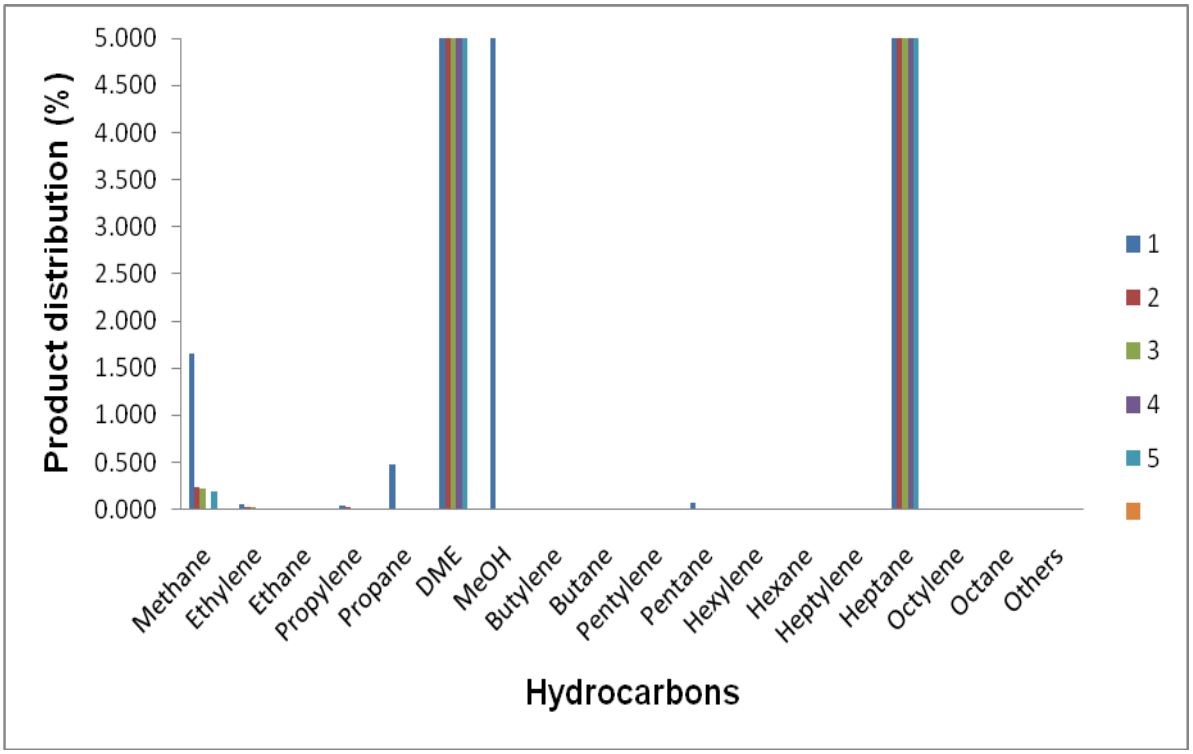


Figure 4.47. The product distribution of hydrocarbons on MTO reactions over SAPO with different structure directing agent s from 0 – 5 % for 5 hours

Figure 4.47 illustrate the hydrocarbon product distribution over a molecular sieve prepared with TEAOH structure directing agent. The product distributions of hydrocarbons on the molecular sieve synthesized with piperidine were discussed earlier on 4.2.2.2. Comparing the product of hydrocarbons on these two molecular sieves, it appears that the molecular sieve made from the TEAOH structure directing agent is more active towards methane, propane and heptane and less active towards ethylene and propylene. DME and MEOH are regarded as reactants and they appeared in large amount. A catalyst prepared with piperidine structure directing agent was more active towards ethylene, propylene and butylene and less active towards lower paraffins.

4.2.7.4 The relationship between the characterization of SAPO molecular sieve and the MTO reaction

The nature of structure directing agent s plays an important role in the rearrangement of catalytic framework.

SAPO molecular sieve synthesized using piperidine and TEAOH had XRD patterns that were different. They had different particle sizes of 1.49 nm and 3.8 nm diameter. Table 4.9 shows that both catalysts had similar % methanol conversions. The conversions increased with an increase in TOS. Selectivity to light olefins was observed from a catalyst synthesized with TEAOH structure directing agent . That is due to the low acidity in the very low temperature region of NH_3-TPD assigned for weak Brønsted acid site. Good light olefins selectivity can only happen if a catalyst is less acidic.

4.2.7.5 Conclusions

The same molecular sieve prepared using TEAOH SDA was synthesized by L. Ye *at al.* [117]. This molecular sieve was also tested in MTO conversions at higher reactor temperature of 425 C for 10 hours. The ethylene yield increased gradually with TOS. The maximum yield was 56 %. Propylene and butylenes yield was not mentioned. The weak acid site molecular sieve was not that active in the production of light olefins. Abramova A.V [ ] also synthesized a composite of SAPO-34 and *y*- Al_2O_3 molecular sieve using TEAOH template. This molecular sieve was tested in MTO reaction at a reactor temperature from 350-450 C. It was discovered that light olefins decreased in TOS. Similar to this study, light olefins selectivity was low and the main product was DME on both catalyst prepared with TEAOH and piperidine templates. Since our main objective is to synthesize molecular sieve which is supposed to be more active and 100 % selectivity, the objective is not achieved. Thus the problem is not solved.

4.3 Summary and Conclusions

The molecular sieve synthesized at the crystallization temperature of 190 ºC for 5 days has particle size of 4.3 nm. This molecular sieve was good in activity with the absence of methane selectivity and improved light olefins selectivity and product distribution. Molecular sieve synthesized at the crystallization temperature of 200 ºC has high % methanol conversion, less light olefins selectivity and product distribution and all hydrocarbons are produced on it. Therefore there is no 100 % selectivity to light olefins over SAPO molecular sieve.

Good light olefins selectivity was observed on the molecular sieve synthesized within four day, compared with the selectivity of light olefins on the SAPO molecular sieves prepared for 2 - 3 days, 5 - 6 days. This molecular sieve has a very small particle size of 1.49 nm. Thus 4 days could be a better crystallization time for the molecular sieve on MTO. The molecular sieve with low phosphate contents has high % methanol conversion, and better olefins selectivity as well as product distribution. It has a particle size of 1.49 nm. This molecular sieve was promoted by adding high sodium contents. The results have shown that methane selectivity was reduced. Thus methane selectivity as well as product distribution could be reduce by conducting the experiment for MTO on the molecular sieve that was synthesized at 190 ºC, for 4 days and this high sodium content could be added to the molecular sieve.

SAPO-34 phase with the particle size of 3.80 nm could be synthesized with high silicon content, but amorphous phase is also present in this molecular sieve. Only methane and small amount of light olefins are produced on that molecular sieve. Amorphous phase prevent the selectivity of light olefins, therefore light olefins result in lower selectivity. New method of synthesizing SAPOs in 2.1.2.2 is using piperidine as a structure directing agent is promising to improve light olefins selectivity. NH_3-TPD desorption have shown that molecular sieve with weak Brønted acid site are good for light olefins selectivity.

CHAPTER FIVE - General Conclusions

5.1. Conclusions

The SAPO molecular sieves were synthesized using an unconventional piperidine as a structure directing agent. Factors such as crystallization time, temperature, as well as silicon, phosphorus sodium contents, Na, Fe, Co and Ni impregnation were varied. One sample of SAPO molecular sieve was also synthesized by using TEAOH structure directing agent instead of piperidine structure directing agent.

The application of SAPO molecular sieve synthesized in four and five days at 200 ^{o}C showed the improvement of ethylene and propylene selectivity, but the challenge of the formation of methane with higher amount than the light olefins has still been noted. When the crystallization temperature was 190 ^{o}C there was no formation of methane. The products distribution of DME and MeOH were relatively high due to incomplete forward reaction of DME and MeOH. This is because of the nature of the SDA piperidine used to synthesize those SAPO molecular sieves. The catalyst synthesized using TEAOH as SDA was more stable and had a higher ethylene and propylene selectivity than the catalyst synthesized using piperidine structure directing agent. The selectivity to ethylene and propylene was high after changing the method for preparation of SAPO-34 using piperidine as a structure directing agent. Thus, piperidine is a good SDA for the synthesis of SAPO-34 and also improved the selectivity towards light olefins in MTO. The increase in reaction time causes a decrease in methanol conversion which agrees with the data found for ethylene and propylene selectivity with reaction time. A lower phosphorus content (P_2O_5/Al_2O_3 = 0.3) containing a higher sodium content (0.2 Na_2O) is more selective and stable towards the light olefins such as $C_2^{=}$- $C_3^{=}$ than the catalyst containing a lower phosphorus content.

Solid state NMR spectroscopy (^{29}Si, ^{27}Al and ^{31}P) and XRD patterns both showed the additional high coordination of Al framework atoms for high silicon content in the gel. These suggest that there is breakage of Al-O-P bonds by the structure directing agent and a new of Si-O- Al bond is formed. The evidence is also revealed by the shift of XRD patterns from the 2 theta = 7.44^{0} in the low silicon to 2 theta = 9.99^{0} in the high silicon sample. This shows that there is no Si replacement by phosphorus.

XRD patterns suggested pure SAPO-34 with the molar gel composition of Al_2O_3: 0.6 P_2O_5: 1.1 Pip: 2.4 SiO_2: 100 H_2O has been formed. XRD patterns and ^{29}Si SS NMR spectroscopy also confirmed the presence of amorphous phase that ranges 2θ scale of 13 º - 32 º and from -125 - 75 ppm. The amorphous material prevents the activity of the molecular sieves, and therefore results in the lower light olefins selectivity.

This work has demonstrated that the synthesis of SAPO using piperidine as a structure directing agent results in the formation of Si-O-P and Si-O-Al, due to the substitution of Si atom by one P atom when low silicon content material was added to the gel. In the case of a high silicon sample, the formation of Si-O-P is avoided.

NH_3-TPD also showed evidence for two Brønsted acid sites in the catalyst framework. Weak acid sites that appeared on the lower temperature are assigned to P-OH hydroxyl groups, while the stronger acid site that appears at higher temperature is attributed to the bridging hydroxyl group – Si-OH-Al. More ethylene was produced from the weak acid sites and higher propylene is obtained from the stronger acid sites.

Among the Fe-SAPO, Ni-SAPO and Co-SAPO catalysts, Co-SAPO has shown the best light olefin selectivity. However Co-SAPO-34 has a lower light olefins products distribution. Ni-SAPO-34 has high ethylene product distribution but also very high methane and ethane selectivity. All modified and unmodified catalysts contain the same particle size of 4.00 nm. From the SEM micrographs, the modified SAPO has a different morphology. The Fe-SAPO has a sliced plates shape, Ni-SAPO rough cubic structures and Co-SAPO has hexagonal crystals. No pure cubic crystals were observed. The aim of this study was to synthesize SAPO-34 molecular sieve using piperidine as SDA, characterize the molecular sieves and test the molecular sieves performance on MTO. More samples of SAPO molecular sieve were synthesized using piperidine with different crystallization time and temperature, as well as silicon, phosphorus and sodium contents. From the characterizations, three phases of SAPO-5, SAPO-34 and amorphous phase are present in the same material. Light olefins selectivity was low, and increased by introducing metal oxides into the SAPO molecular sieve gel. The presence of sodium oxide in the SAPO molecular sieve prevent the formation of methane also improves light olefins selectivity. Therefore

SAPO-34 molecular sieve was not successfully done. On the later stage a material was synthesized using the same piperidine as a SDA. The XRD patterns and SEM spectroscopy in appendix A and B confirmed a pure SAPO-34 phase without SAPO-5 and amorphous phase, this material was not tested.

5.2. Recommendations for the future work

SAPO molecular sieve prepared using piperidine as a SDA at 190 ºC for 5 days and molecular sieve prepared using similar SDA at 200 ºC for 4 days have shown good light olefins selectivity, although MTO reactions over those molecular sieves were not 100 % light olefins selectivity. A new method of synthesizing SAPO-34 is already introduced. The XRD patterns and SEM micrograph shown in appendix A and B show the existence of SAPO-34 phase only. It is recommended that more molecular sieves should be synthesized using piperidine as a SDA at 190 ºC for 4 days by introducing a new method. It is also recommended that a microwave system should be used to synthesize SAPO-34 molecular sieves. All molecular sieves will be tested and compared in MTO reactions.

REFERENCES

[1] Mokrani**,** T**.** Scurrell**,** M. *Catal. Rev. Sci. Eng***.** 50**,** 2008, 1-18.

[2] Stöcker, M. *Micro. Mes. Mats*, 29, 1999, 3-48.

[3] Travalloni, L. Gomes, A. C. Gaspar, A. B. and Da Silver, M. A. P. *Catalysis Today,* 2008, 133-135, 406-412.

[4] Nishamaya, N. Kawaguchi, M. Van Vu, Y. Hirota, D. Egashira, Y. and Ueyama, K. *Applied Catalysis A: General*, 362, 2009, 193-199.

[5] Dumitriu, A. Azzouz, V. Hulea, D. Lutic and K. Hessler, *Micro. Mats*, 10, 1997, 1-12.

[6] Marches, L. Frache, A. Martra, G. Causa, M. and Coluccia, S. *Micro. Mes. Mats*, 30, 1999, 145-153.

[7] Rao, M.R. Soni, D. and Sieli, G.M. Bhattacharyya, D Lummus Technology. Bloomfield new Jersey. Indian Oil Corp. Ltd. R$D center, Feb, 2011,45-49.

[8] Rane N.J. *Ph.D Thesis* Eindhoven University of Technology Library, 2007.

[9] Ren, T. *Ph.D Thesis* Utrecht University, China 2009.

[10] Vora, B. Chen, J.Q. Bozzano, A. Glover, B. and Barger, P. *Catal. Today*,

141, 2009, 77-83.

[11] Wahabi, S.M.A. Ph.D *Thesis,* Conversion of methanol to light olefins on SAPO-34 kinetic model and reaction design.Texas A & M University. Saudi Arabia, 2003.

[12] Nakamura, D. Global ethylene capacity grows 4% in 2005. Oil & Gas *J,* March 27, 2006.

[13] CMAI. *World Petrochemical Feedstocks Analysis. Houston, Texas: Chemical Market Associates Inc. and Purvin & Gertz,* 2005.

[14] World Propylene market // icis.com, *everyday internet pup*, 21 Jul, 2007.

[15] Wilson, S. Barger P. *Micro and Mes. Mats*, 29, 1999, 117.

[16] Vistad, Ø. B. AAkporiaye, D.E Taulelle, F. and Lillerud, K.P *Chem. Mats* 15, 2003, 1639.

[17] Maple, M.J. Williams, C.D. *Micro and Mes. Mats* 111, 2008, 627-631.

[18] Kim, H. G. Lee, K. Y. Jang, H. G. Song, Y. S. Seo, G. Korean J. Chem. Eng, 27 (6), 2010, 1773-1779.

[19] Tosheva, L. *Licentiate Thesis. Lulea University of Technology Lulia Sweden*

1999.

[20] Currao, A. *Zeolites atlas low quality. Department of Chemistry and Biochemistry. University of Bern.*

[21] Breck, D.W. Eversole, W.G. Milton, R.M. Reed, T.B. and Thomas, T.L. *J. Amer. Chem. Soc. 78* 1956, 5963–5971.

[22] Reed, T.B. and Breck, D.W. *J. Amer. Chem. Soc, 78,* 1956, 5972–5977.

[23] Breck D. W. *Zeolites Molecular Sieve. John. Wiley, New York*, 4 1974.

[24] Barrer, R.M. *Pure Appl. Chem,* 51 (5), 1979, 1091–1100.

[25] Flanigen, E.M. Van Bekkum, H. Jacobs, P.A. Jensen, J.C. *Stud. Surf. Sci. Catal*, 137, 2001, 11-35.

[26] Mravec, D. Hudec, J. Janotka, I. *Chem. Pap*, 59 (1), 2005, 62-69.

[27] Qi, G. Xie, Z. Yang, W. Liu, H. Zhang, C. and Chen, Q. *Fuel Proc Tech*: 88, 2007, 437-441.

[28] Bulatov, R.M.and Jirnov, B.S, *Oil and Gas Business*, Ufa. State. Petroleum. Technological University.2009.

[29] Wang, X. Xie, C. Li, Z. and Zhu. G. *Res. Inst Petr. Processing, SINOPEC. Beijing China* 149-168.

[30] Bulatov, R.M. and Jirnov, B.S. *Oil and Gas*, Ufa State Petroleum Technological University. Business. 2009.

[31] Taylor, C. E. Baltrus, J. P. and Driscoll. D. Fischer Tropsch fuel: http://www.netl.doe.gov/publications/factsheets/rd/R&D089.November 2011.

[32] Sakoh, H, Nitta, M, and Aomura, K. *Appl. Catal*, 8, 1883, 187.]

[33] Barger, P.T.A. and Hieghts, I.L. *US Patent* no 5095163 1991.

[34] Wei, Y He, Y. Zhang, D. Xu, L. Meng, and S. Su; Z. B.L *Micro and Mes Mats:* 90, 2006, 188-197.

[35] Zhang, S. Zhang, B. Gao, Z. and Han, Y. *Ind. Eng. Chem. Res,* 49, 2010, 2103-2106.

[36] Marchi, A. J. and Froment G. F. *Appl. Catal* 1991, 71, 139.

[37] Gronvold, A. G. Dypuik, M K .T. *Stud Surf. Sci. Catal*. 81, 1994, 399.

[38] Chen, N. M. and Reagan, W. *J. Catal*. 59, 1979, 133.

[39]. Mhlaba, R. *MSc Thesis* University of Limpopo SA, 2008.

[40] Sendran, U. Mahay, A. and De Lasa, H. I. *Chem. Eng. J*. 45, 1990, 33-42

[41] Kaizer, S.W. *U.S Patent* no 4, 499, 327, February 12 1985.

[42] March M K .T Ese, L. Causa, M. and Coluccia, S. *Micro. Mes Mats* 30, 1999, 145-153.

[43] Wendelbo, R. Akporiaye, D. Anderson, A. Dahl, I.M. and Mostad, H.B. *Appl. Catal. A. Gen,* 142, 1996, L197-L207.

[44] Dahl, I.M. and Kolboe, S. *J. Catal*. 149, 1994, 458-464.

[45] Nawaz, Z. and Wei, F. *Ind. Eng. Chem. Res*, 48, 2009, 7442-7447.

[46] Uzunova, E.L. Goltl, F. Kresse, G. and Hafrer, J. *J. Phys. Chem. C*, 113 (13), 2009, 5274 -5291.

[47] Wei, Y. Zang, D. Chang, F. Xia, Q. Su, B. C.and Lui. Z. *Chem. Comm*, 2009, 5999–6001.

[48] Lethbridge, A.D.Z. Keeble, D.S Walker, D. Thomas, P.A. and Waltona, R.I. *J. Appl. Cryst* ISSN 0021-8898, 2009, 169-175.

[49] Ramatsetse, P.B. *MSc Dissertation* University of the North 1999.

[50]. Kokotailo, G.T. Lawton, S.L. Olson, D.H. Meier, W. *Nature,* 272, 1978, 437-438.

[51] Wilson, S.T Lok, B.M. and Flanigen, E.M. *US Patent*, 4810440, 1982.

[52] Zhang, J. Dong, J. Zhang, W. Xu, Q. and Song, C. *Fuel. Chem. Div. Prep*, 47(1), 2002, 181-182.

[53] Venna, S.R. and Carreon, M.A. *Amer. Chem. Soc*, 27, 2011, 2888–2894.

[54] Maekawa, H. Kubota, Y. and Sugi, Y. *Chem. Lett*. 2004, 33, 1126.

[55] Dent, L.S. and Smith, J.V. Crystal Structure of Chabazite, A Molecular Sieve. *Nature,* 181, 1958, 1794-1796.

[56] Oh, S.H. and Lee, W.Y. *Korean. J. of Chem. Eng*, 9 (1), 1992, 37-44.

[57] Teresa Álvaro-Mu˜noz, Carlos Márquez-Álvarez, Enrique Sastre, Catalysis Today 179 (2012) 27– 34.

[58] Ashtekar, S. Satyanarayana, C.V.V. and Chakrabarty, D.K *Chem. Sci*. 106 (3), 1994, 621-628.

[59] Bare, S. R Process *Advanced Characterization*, *UOP LLC Modern* 2007.

[60] Prakash, M. and Unnikrishna S., *J. Chem. Soc Farady. Trans*, 90, 1994, 2291-2296.

[61] Aguayo, A. T. Gayubo, A. G. Vivanco, R. Olazar, M. Bibao, J. *App.Catal. A Gen.* 142, 1996, L197.

[62] De Quimica, E. Gomes, A. C. L. Gaspar, .A. B. Da Silva, M. A.P *Catal Today*, 135, 2008, 406-412.

[63] Yang, S. M. Wang, S. I. and Huang, C. S. *National Central University,Chung-Li, Taiwan,* 9, 1991, 429-435.

[64] Baerlocher, C.H. Meier, W.M. Olson, D.H., *Atlas of zeolite framework types*, **5**th *rev. ed., Elsevier, Amsterdam, New York,* 2001.

[65] Lu, J. Wang, X. and Li, H. *Catal. Lett*, 97, 2009, 255-261.

[66] Kang, M. Um, M. H. and Inui, T. *Environ. Eng. Res*, 3 (3), 1998, 175-182.

[67] Kang, M. and Inui, T. *Catal. Lette*. 53, 1998, 171.

[68] Janallan, A.M Nafaty, U.A. and Abdillahi, M.M. *App.Catal A: Gen.* 154, 1997, 117-127.

[69] Kang, M. *J. Molec. Catal. A. Chem*, 160, 2000, 437-444.

[70] Shanda, M. Dangchao, Y. and Huixin W. *Energy Source. Part A*, 30, 2008, 881-890.

[71] Obrzut, D.L. Adekkanatel, M.P Thundimadathil, J. Liu, J. Dubois, D.R Guin, J.A. React.Kinet. *Catal. Lett*, 80 (1), 2003, 113-121.

[72] Chen, J. QBozzano, A. Glover, D. Fuglerud, T. Kvisle, S. *Catal. Today,* 106, 2005 103.

[73] Pastore, O.H. De Oleveira, E.C. and Superti, G.B. *J. Phys. Chem. C* 2007, *111,* 3116-3129.

[74] Tian, P. Su, X. Wang, X. Chang, Q. X. Fan, D. Meng, S and. Liu, Z *Amer. Chem. Soc. Chem. Mats*, 23, 2011, 1406-1413.

[75] Zhu, J. Cui, Y. Wang, Y. and Wei, F. *Supp. Mats. Chem. Com.* 2009.

[76] Qian, X.F. Li, B. Hu, Y. Y. Niu, G.X Yahong, D. Zhang, H. Chae, R.C. Tang, Y. SuA., D.S. Asîrî, M. and Zhao, D.Y. *Chem. Eur. J*, 18, 2010, 931-939.

[77] Ivor, B. and Ulrich, M. *Euro. Pat. Appl. EP 2269733 Al,* 2010.

[78] Back, G. Kim, Y. Cho, Y.S. Lee, Y.I. Lee, C.W. Korn, J. *Mag*. *Res. Soc*, 6, 2002, 20-37.

[79] Lui, Y. Wang, L. Zhang, J. Che, F. and Anpo, M. *Res. Chem. Inter*. DIO 10.1007/s1164-011-0302-2, 2011.

[80] Lin, S. Li, J. and Sharma, R. P. *Top. Catal*, 53, 2010, 1304-1310.

[81] Benedikt, B. Gentz, M. Kumosa, L. Predecki, P.K. Armentrout, D. Kumosa, M. and Sutter, J.K. *International Centre for Diffraction Data, Advances in X-ray Analysis*, 46, 2003.

[82] Kenneth, W.W. Kenneth, D.G. Raymond, E.D. *General Chemistry with Qualitative Analysis,* 4th Edition, 1992, 480.

[83] Bhattacharjee, A. Mandal, H. Roy, M. and Chini, T.K. *Environ. Monit. Assess*, 176, 2011, 473-481.

[84] Lixiong, Z.; Mengdong, J. and Enze, M*. Stud. Surf. Sci. Catal*. 1997, 105, 2211.

[85] Blenken, F. *MSc Thesis. The effect of acid strength on the MTO reaction University of Oslo,* 2007.

[86] Tan, J. Liu, Z.M. Boa, X.H. Han, X.W.. He, C.Q. Zhai, R. S *Micro and Mes Mats*, 53, 2002, 97-108.

[87] Van Herden, H. Mintova, S. and Bein, T. *Chem. Mats,* 20, 2008, 2956-2963

[88] Chae, H.J Song, Y.H Jeong; K.E Kim, C.U. and Jeong, S.Y. *J. Phys. Chem. of Solids*, 7**,** 2010, 600-603.

[89] Wan, Y. Williams, C.D. Duke, C.V.A. and. Cox, J.J. *J. Mats. Chem*, 0, 2000, 2857-2862.

[90] Popova, M. Minchev, C. Kanazirev, V. *Appl. Catal. Gen* 169, 1998, 227-235.

[91] Jhung, S.H. Chang, J.S. Hwang, J.S. and Park, S.E. *Micro and Mes Mats,* 64, 2003, 33-39.

[92]. Lee Y.J. Back, S.C. and Jon, K.W. *App. Catal A: Gen* 329, 2007, 130-136.

[93] Wang, L. Guo, C. Yan, S. Huang, X. Li, Q. *Micro. Mes. Mats*, 64, 2003, 63-68

[94] Kumara, N. Nieminen, V. Demirkan, K. Salmi, T. Yu, D. and Murzin, E. L. *Appl. Catal. A: Gen*, 235, 2002, 113–123.

[95] Zadbakhsh, A. Farhadi, F. Khorasheh, F. and Yan, Z.F. *J. Porous Mater*, DOI 10.1007/s10 934-008-9237-4, 2008.

[96] Patil, G.E. Kajale, D.D. Chavan, D.N. Pawar, N.K. Ahire, P.T. Shinde, S.D. Gaikwad, V.B. and Jain, G.H. *Bull. Mater. Sci*, 34 (1), 2011, 1-9.

[97] Berendt, R.T. Sperger, D.M.P. Isberster,K. and Munson E. J. *Trends in Anal. Chem,* 25 (10), 2006, 977-984.

[98] Kirkpatric, R.J. Schramm, S. Turner, G. and Ann W.H.Y. *Rev. Earth. Planet. Sci*, 13, 1985, 29-47.

[99] Adekkanattu, P. Dubois, D. Obizut, D. Huany, X. Thundimadathil, J. Lui, J. and Guin, J. *Aubum University. Development of microporous shape selective Catalysts for Ethylene, Propylene and other valued-Added products via C-1 Chemistry.*

[100] Mogk, D. GSA *Abstract* 39 (6) 2007. 557.

[101] Venkatathri, N. J*. Sci. Ind. Res*, 64, 2005, 509-511.

[102] Fernandes, L.D, Corma, A. Martines, A. Aguiar, E.F.S and Montereiro, J.L.F. Braz. J. *Chem. Eng*: 15, 1998, 2.

[103] Gubish, D. and Bandermann, F. *Chem. Eng. Technol*, 2, 1989), 55.

[104] Arcuri, K.B Agee, K.L. and Agee, M. A. *US Patent* 09/455047 1999.

[105] Nawaz, Z. Tang, X. and Wei, F. *Braz. J. Chem. Eng*, 26, 2009, 705-712.

[106] Uzunova, E.L. Goltl, F. Kresse, G. Hafrer, J. *J. Phys. Chem. C*, 113 (13), 2009, 5274 -5291.

[107] Ferrini, C. Herein, D. Lanke, D. and Rodmerk, D. *Eur. Pat. Appl,* EP 20070013300, 2009.

[108] Chauhan, N. L. Murthy, Z. V. P. Das, J. And Parikh, P. Ind.J. Chem. Tech. 18, 2011, 335-342.

[109] Zainab Binti, Ramli Jaba Tan, Proceeding of Annual Fundamental Science Seminar, Sains, 2003, 147-152.

[110] Jie Zhu, Yu Cui, Yao Wang, and Fei Wei The Royal Society of Chemistry Beijing, 2009.

[111] Jacobs, W.A. Pelltier, S.W. *J. Amer. Chem. Soc.* 1954.

[112] Froment, G.F. Dehertog, W.J.H. and Marchi, A.J.M. *Catal*, 33-63.

[113] Chen, D. Gronvold, A. Mojord K. and Holman, A. *Res,* 46. 2007, 4116-4183.

[114] Schweitze, *J. Rem, Purdue* University. West Lafayette, IN47907, 765, 2010, 494-6371.

[115] Lok, B.M. Messina, C.A Petton, R.L. Gajek, R.T. Cannan, T.R. and Flanigen, E. M. *US Patent* no 4.440, 871,1984.

[116] Zhang, D. Wei, Y. Xu, L. Du, A. Chang, F. Su, B. Liu, Z. *Catal. Lett*, 109 nos. 1-2, 2006.

[117] Ye, L. Cao, F Ying, W. Fang, D. Sun, Q. *J. Porous. Mater*, DOI 10.1007/S 10934–010–9374–4, 2010.

[118] Pop, G. Bozga, G. Ganea, R. Natu, N. *Ind. Eng. Chem. Res*, 48. 2009, 7065–7071.

[119].Lisi, L Marchese, L. Pastore, H.O Frache, A. Ruoppolo, G. and Russo, G. *Topics. catal,* 22, nos. 1, 2003, 95–99.

[120] Blenken, F. Bjorgen, M. Palumbo, L. Bordiga, S. Svelle, S. Lillerud, K.P. Olsbye, U. *Top. Catal*, 52, 2009, 218-228.

[121] Liu, L.G. Tian, P. Li, J. Zhang, D. Zhou, F. Liu, Z. *Micro and Mes Mater,* 111, 2008, 143-149.

[122] Vomscheid, R. Briend, M. Peltre, M.J. and Bathomeuf, D. *J. Chem. Soc. Fara. Trans,* 91, (18), 1995, 3281-3284.

[123] Park, Y.K. Beak, S.W. and Ihm, S.K. *J. Ind. Eng. Chem,* 7 (3), 2001, 167-172.

[124] J.U.M. Engineering Ges.m.b.H. Gauss-Str. 5, 85757 Karlsfel.

APPENDIX A

XRD PATTERNS FOR SAPO

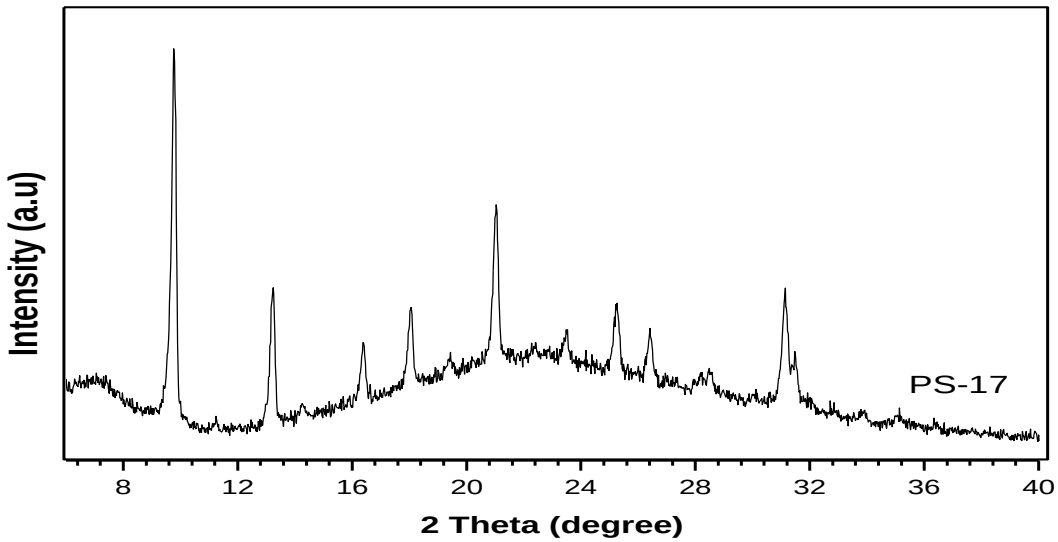


Figure SAPO

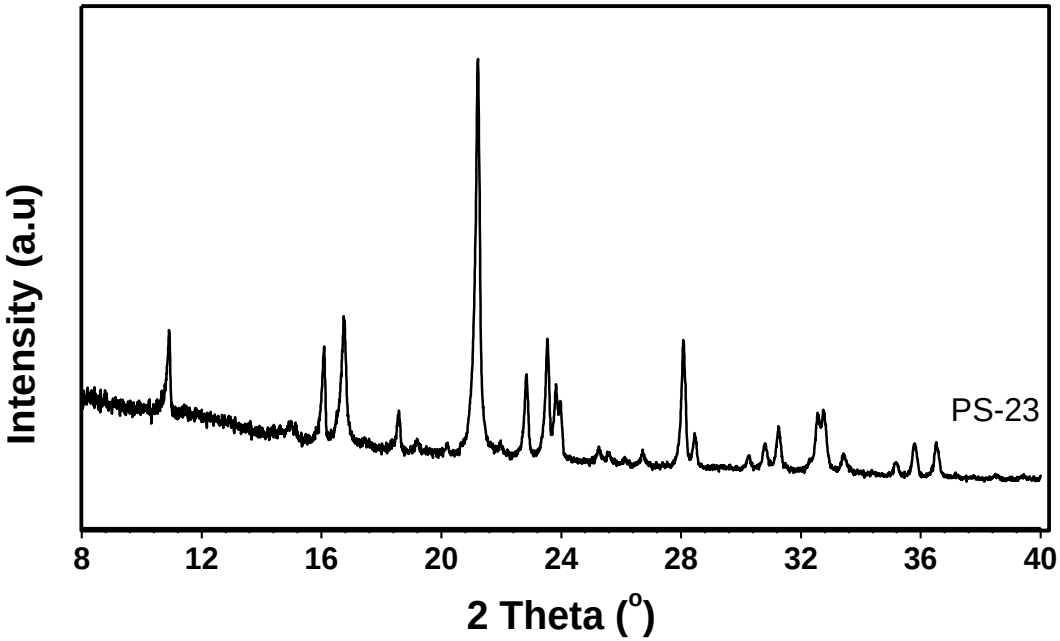


Figure SAPO-34

APPENDIX B

SEM FOR SAPO-34

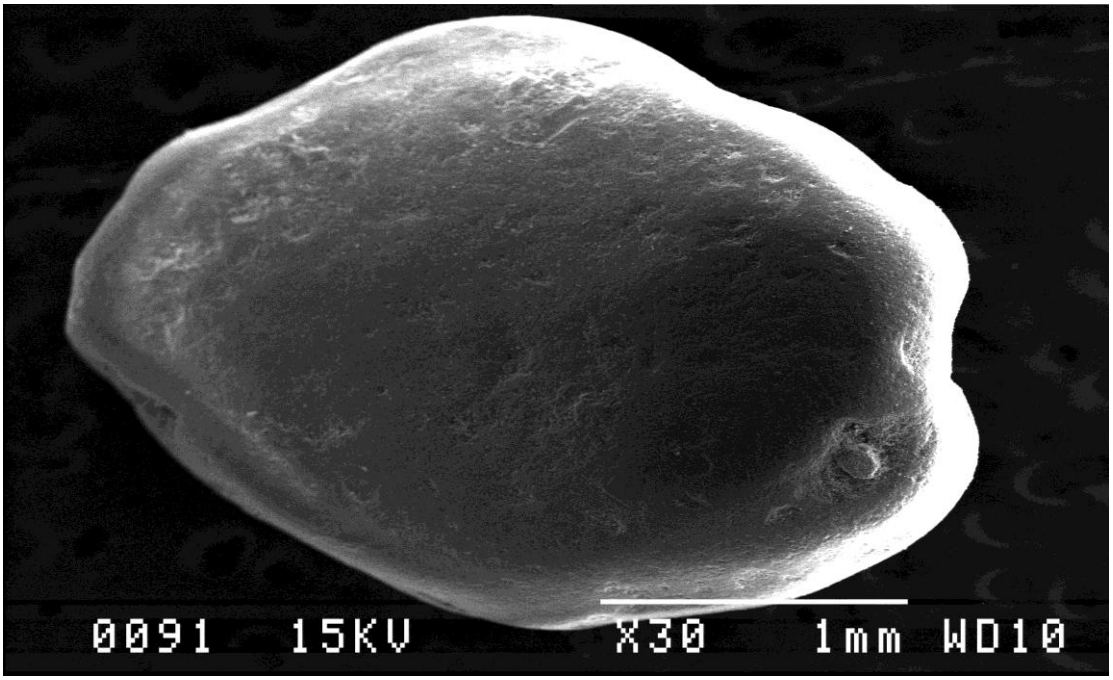


Figure SAPO PS-17

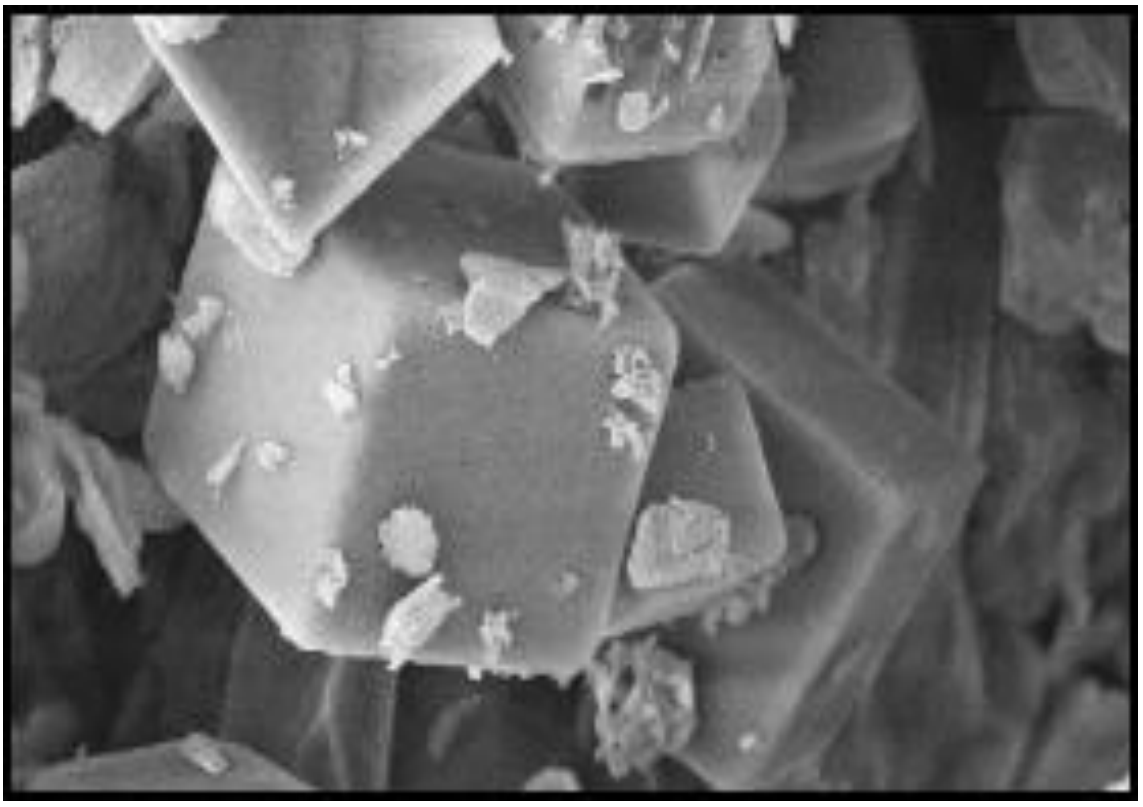
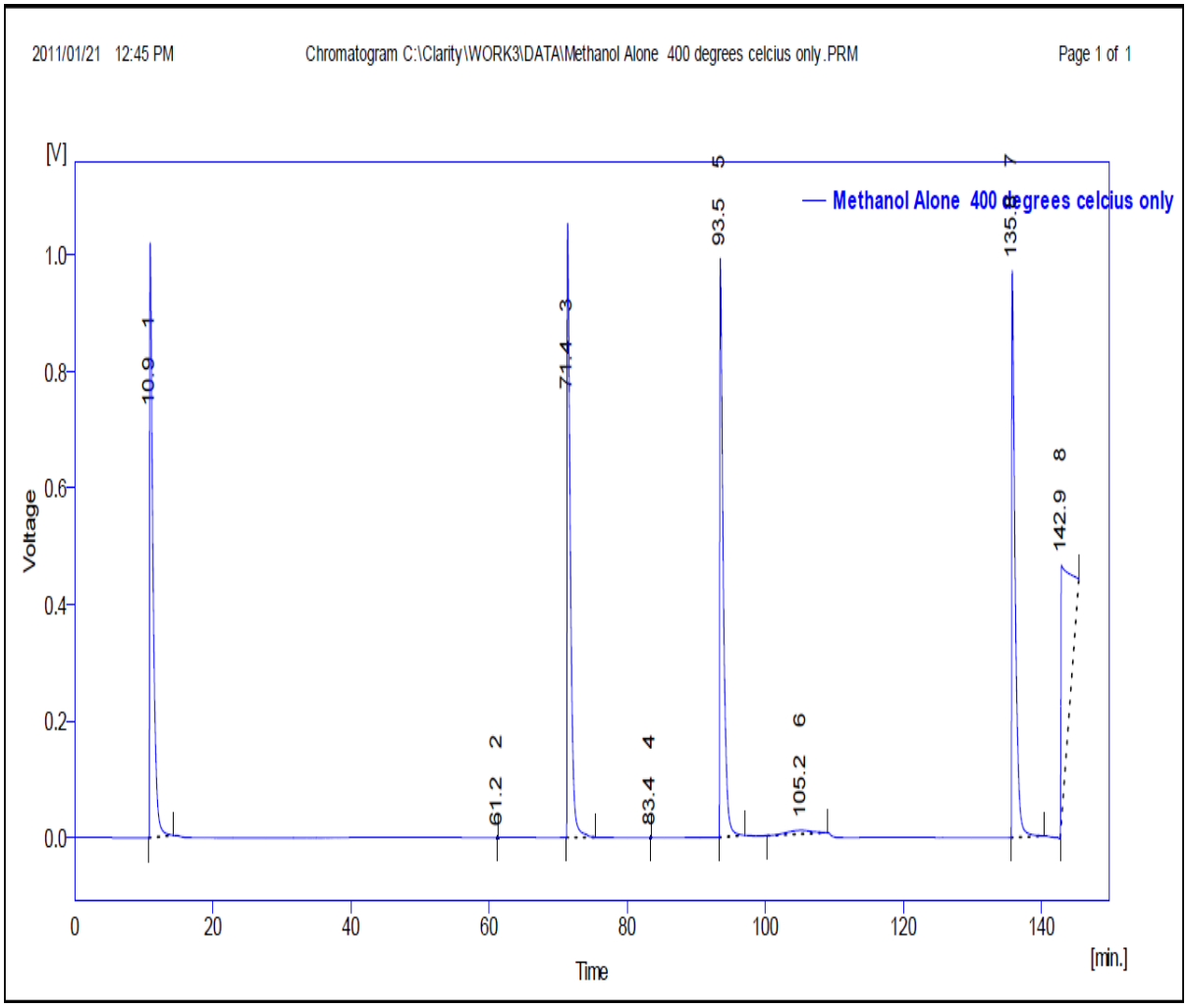


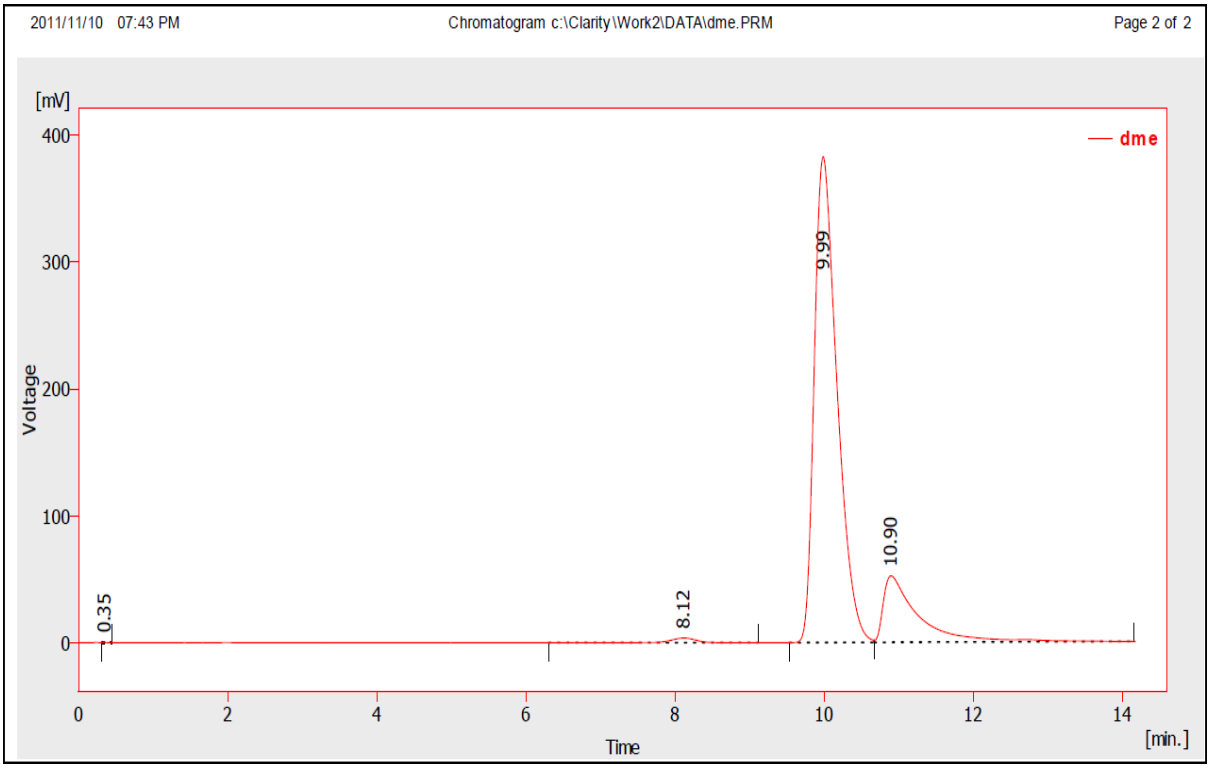
Figure PS-23

APPENDIX C

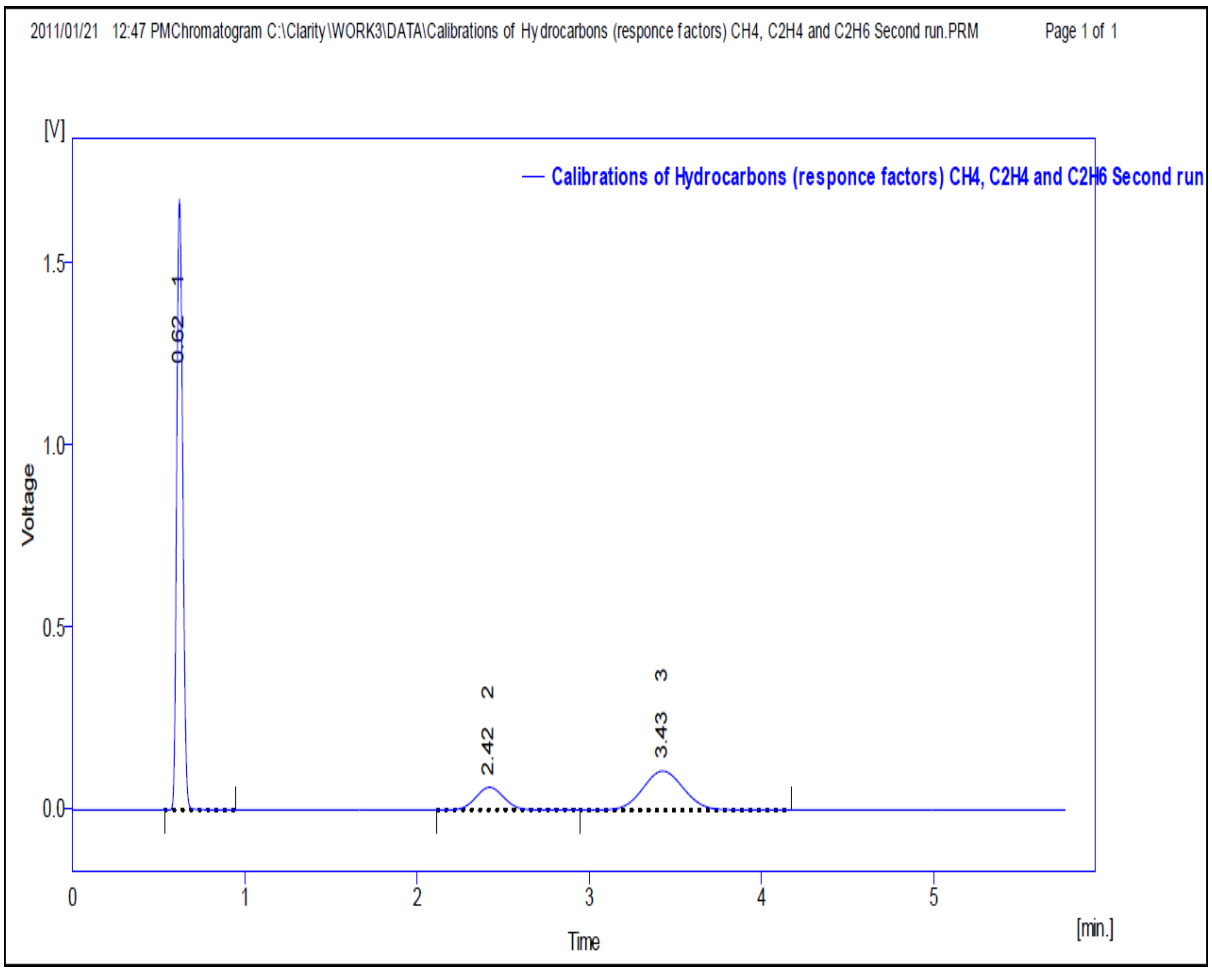
STANDARDS HYDROCARBON



	Reten. Time [min]	Area [mV.s]
1	10.930	34135.014
2	61.227	0.982
3	71.380	34040.552
4	83.393	0.831
5	93.503	33471.846
6	105.227	1588.439
7	135.777	33083.146
8	142.897	35155.829
	Total	171476.639

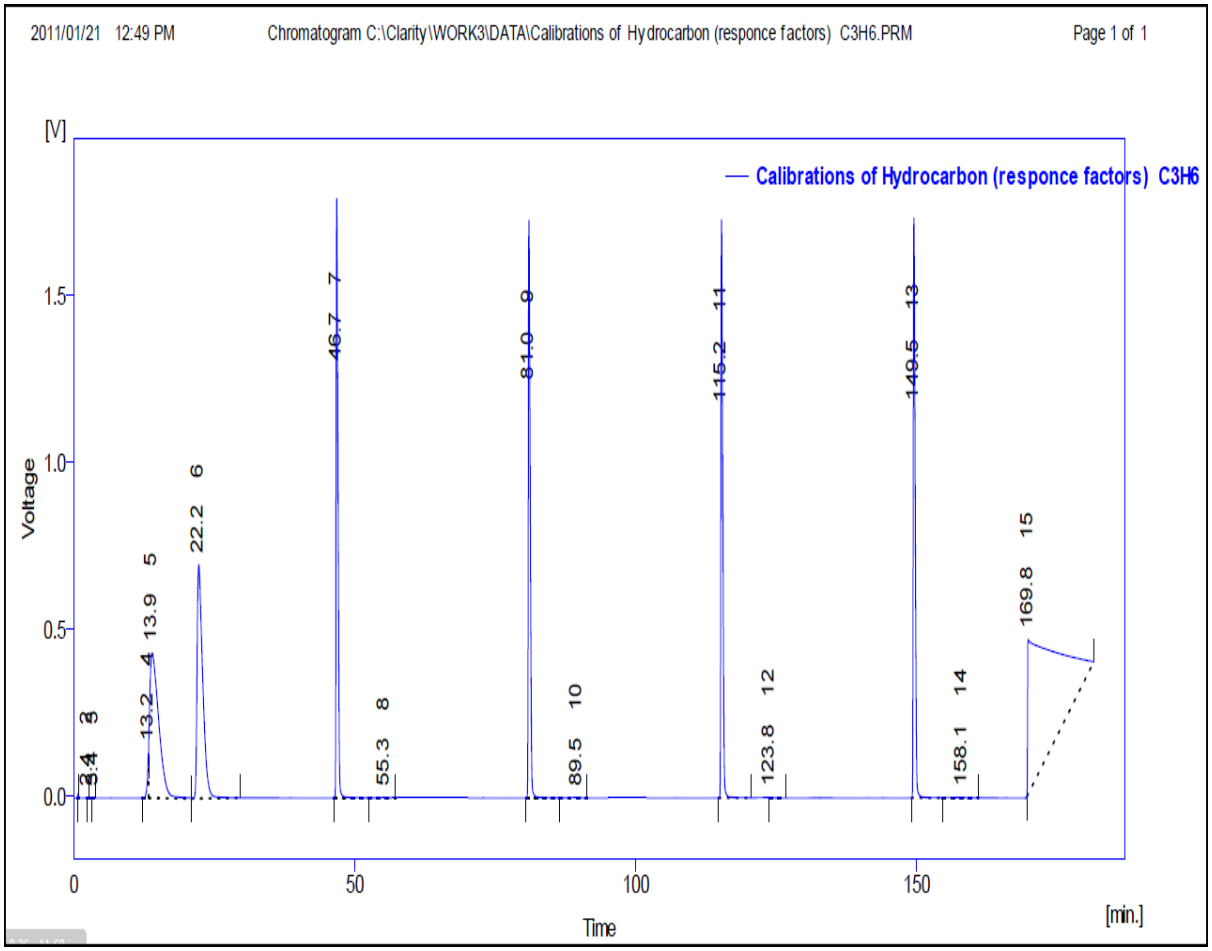


	Reten. Time [min]	Area [mV.s]
1	0.350	0.870
2	8.120	85.614
3	9.990	8088.582
4	10.900	1718.226
	Total	9893.292

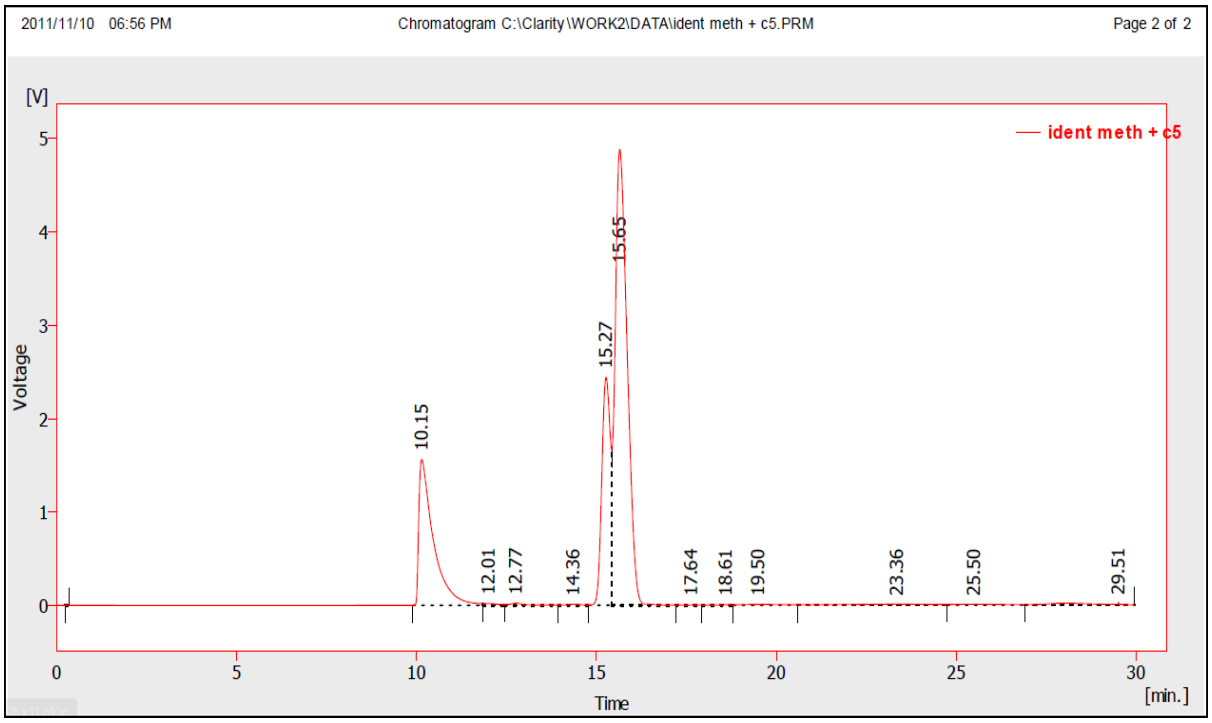


Result Table (Uncal - Calibrations of Hydrocarbons (responce factors) CH4, C2H4 and C2H6 Second run)

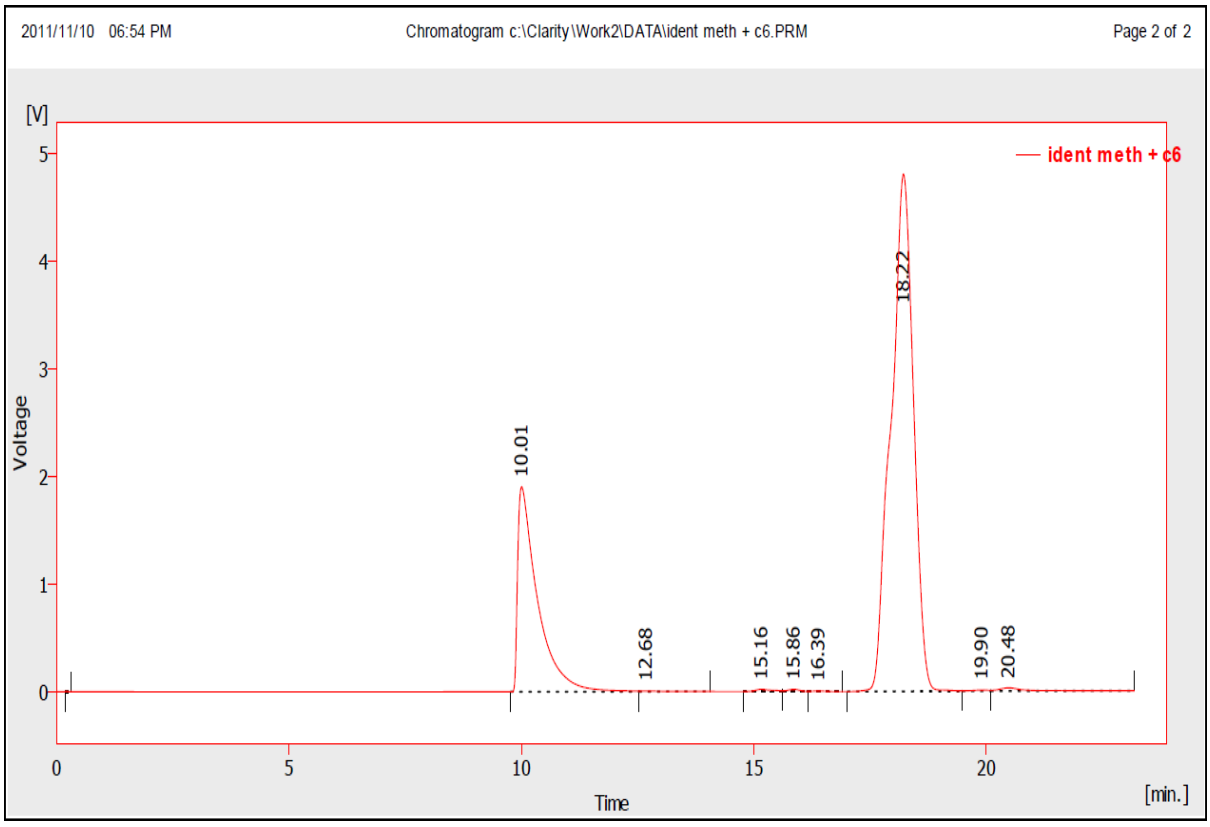
	Reten. Time [min]	Area [mV.s]	Height [mV]	Area [%]	Height [%]	W05 [min]
1	0.620	4047.261	1677.703	62.3	90.8	0.04
2	2.420	703.229	62.226	10.8	3.4	0.18
3	3.427	1749.052	106.806	26.9	5.8	0.26
	Total	6499.542	1846.734	100.0	100.0	


2011/01/21 12:49 PM
Chromatogram C:\Clarity\WORK3\DATA\Calibrations of Hydrocarbon (responce factors) C3H6.PRM
Page 1 of 1
[V]
Calibrations of Hydrocarbon (responce factors) C3H6
Voltage
1.5
1.0
0.5
0.0
0
50
100
150
Time
[min.]
2
3
4
5
6
7
8
9
10
11
12
13
14
15
13.2
13.9
22.2
46.7
55.3
81.0
89.5
115.2
123.8
149.5
158.1
169.8

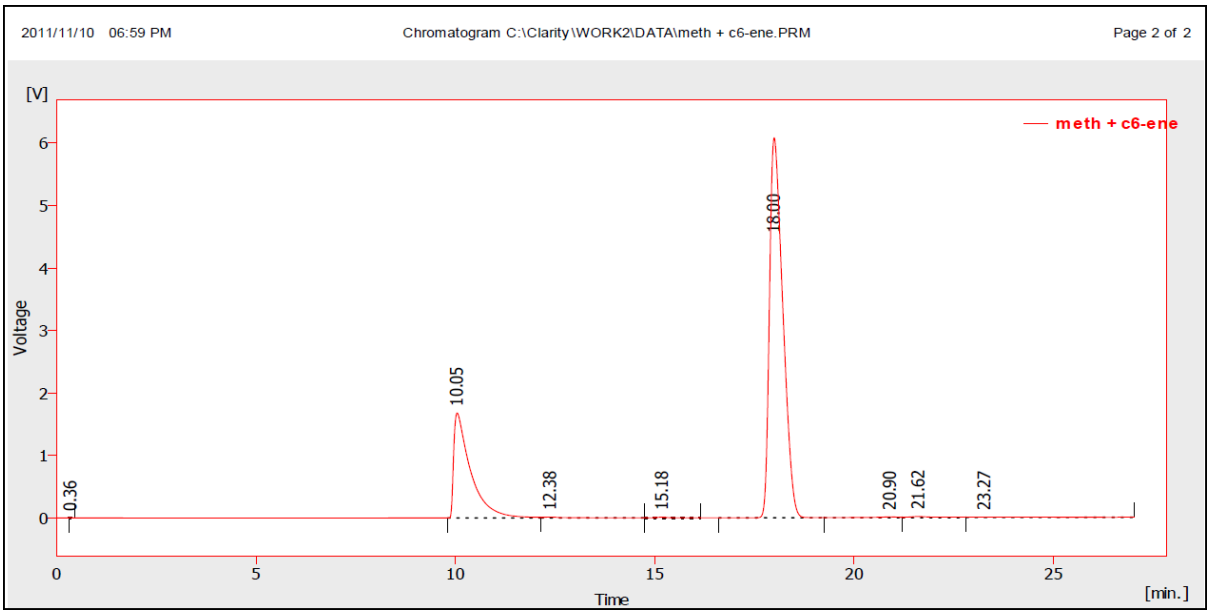
	Reten. Time [min]	Area [mV.s]
1	0.680	25.392
2	2.443	3.603
3	3.437	10.558
4	13.237	1885.995
5	13.893	48627.238
6	22.190	48862.095
7	46.747	41754.515
8	55.270	192.527
9	80.967	41359.610
10	89.530	239.456
11	115.247	41111.740
12	123.823	79.037
13	149.500	41383.051
14	158.090	276.591
15	169.837	159606.359
	Total	425417.766



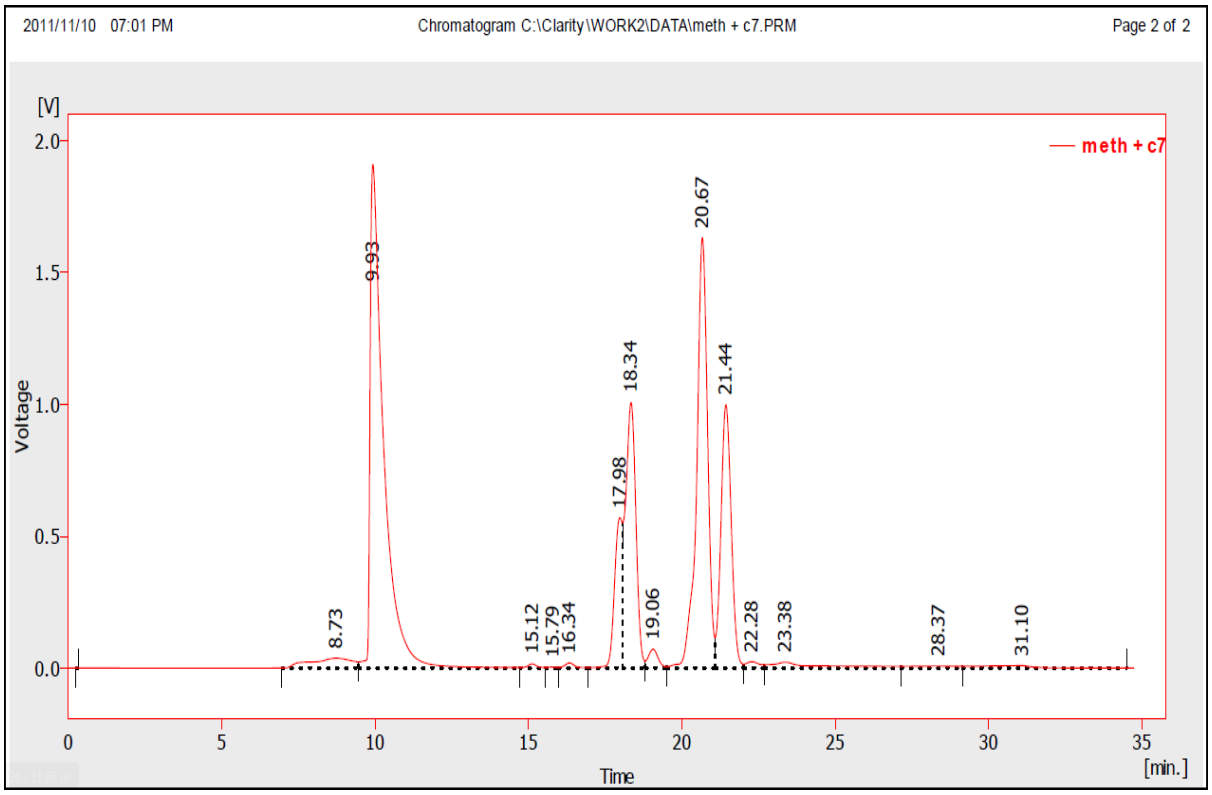
	Reten. Time [min]	Area [mV.s]
1	0.260	0.699
2	10.150	43948.858
3	12.013	509.561
4	12.770	693.851
5	14.363	310.549
6	15.270	39496.348
7	15.650	114661.762
8	17.643	107.491
9	18.607	169.679
10	19.503	640.000
11	23.363	1827.365
12	25.500	864.859
13	29.513	1961.845
	Total	205192.868



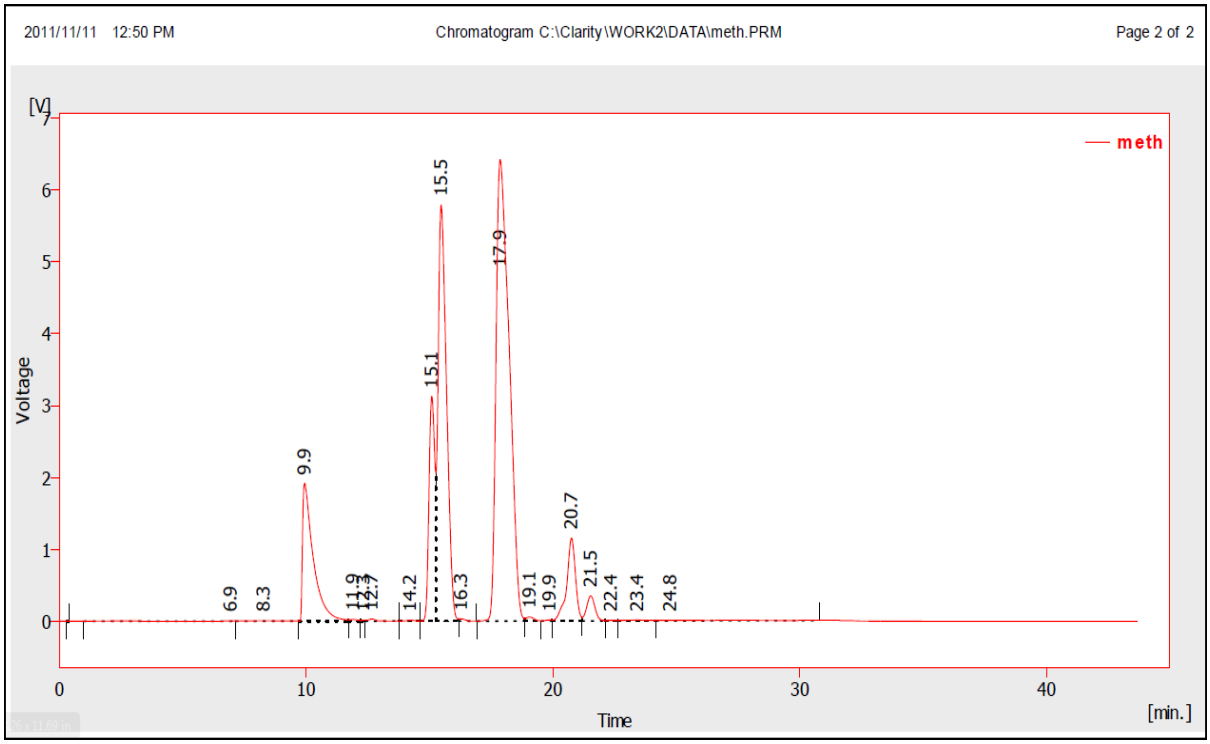
	Reten. Time [min]	Area [mV.s]
1	0.217	0.667
2	10.007	56471.039
3	12.683	190.185
4	15.163	513.581
5	15.857	357.854
6	16.393	84.106
7	18.217	161344.905
8	19.903	273.649
9	20.483	1172.340
	Total	220408.327



	Reten. Time [min]	Area [mV.s]	Height [mV]	Area [%]	Height [%]	W05 [min]
1	0.357	0.753	0.431	0.0	0.0	0.03
2	10.047	49475.872	1679.342	25.5	21.5	0.40
3	12.383	539.592	13.313	0.3	0.2	0.47
4	15.183	187.841	10.551	0.1	0.1	0.27
5	17.997	141274.381	6078.886	72.8	77.7	0.37
6	20.900	596.574	12.616	0.3	0.2	0.57
7	21.617	930.340	18.323	0.5	0.2	0.55
8	23.270	1080.359	6.699	0.6	0.1	3.66
	Total	194085.712	7820.162	100.0	100.0	



	Reten. Time [min]	Area [mV.s]	Height [mV]	Area [%]	Height [%]	W05 [min]
1	0.277	0.765	0.437	0.0	0.0	0.03
2	8.733	3603.360	37.499	2.2	0.6	2.02
3	9.930	58223.611	1908.140	34.8	30.2	0.41
4	15.120	349.881	16.029	0.2	0.3	0.30
5	15.793	80.525	3.677	0.0	0.1	0.43
6	16.337	453.226	19.441	0.3	0.3	0.33
7	17.977	9822.580	569.981	5.9	9.0	0.28
8	18.343	23828.240	1006.069	14.2	15.9	0.45
9	19.060	1613.019	71.449	1.0	1.1	0.37
10	20.670	40616.114	1631.054	24.3	25.8	0.36
11	21.437	23360.921	997.572	14.0	15.8	0.37
12	22.283	746.118	24.128	0.4	0.4	0.68
13	23.377	2616.729	22.342	1.6	0.4	1.08
14	28.367	883.894	7.755	0.5	0.1	2.00
15	31.097	1230.599	9.799	0.7	0.2	2.27
	Total	167429.582	6325.372	100.0	100.0	



	Reten. Time [min]	Area [mV.s]	Height [mV]	Area [%]	Height [%]	W05 [min]
1	0.317	0.542	0.325	0.0	0.0	0.03
2	6.947	1207.609	4.705	0.2	0.0	5.19
3	8.277	622.644	5.107	0.1	0.0	2.34
4	9.937	57998.813	1917.314	10.9	10.1	0.42
5	11.900	521.134	21.745	0.1	0.1	0.50
6	12.323	129.006	11.590	0.0	0.1	0.19
7	12.663	610.172	28.453	0.1	0.2	0.32
8	14.217	254.743	12.633	0.0	0.1	0.32
9	15.087	50648.870	3124.904	9.6	16.5	0.29
10	15.467	138949.178	5788.152	26.2	30.5	0.39
11	16.277	527.516	31.106	0.1	0.2	0.28
12	17.857	237861.869	6419.260	44.9	33.9	0.62
13	19.050	1244.977	55.119	0.2	0.3	0.39
14	19.867	242.770	14.006	0.0	0.1	0.28
15	20.747	28642.162	1151.539	5.4	6.1	0.35
16	21.527	8132.646	347.629	1.5	1.8	0.36
17	22.357	238.951	8.249	0.0	0.0	0.53
18	23.417	747.019	11.584	0.1	0.1	1.32
19	24.757	1096.388	5.276	0.2	0.0	6.62
	Total	529677.008	18958.697	100.0	100.0	

APPENDIX D

FORMULAS FOR CALCULATIONS

% Methanol conversion = $\frac{[MeOH]in-[MeOH]out}{[MeOH]in} \times 100\ \%$

Analyte selectivity (Mol %) = $\frac{[Analyte]}{[MeOH]in-[MeOH]out} \times 100\ \%$

Product distribution (%) = $\frac{[Analyte]}{\sum[analytes]} \times 100\ \%$

Where [ ] is the concentration of an analyte.